

UNIVERSITY COLLEGE OF LONDON

DEPARTMENT OF MATHEMATICS

DOCTORAL THESIS

**Optimal Trading and Inventory
Management in Electronic Markets**

Author:

Maria Alessandra CRISAFI

Supervisor:

Dr Andrea MACRINA

*Thesis submitted in fulfilment of the requirements for the degree of
Doctor of Philosophy*

March 2017

Declaration of Authorship

I, Maria Alessandra CRISAFI, confirm that the work presented in this thesis, titled ‘Optimal Trading and Inventory Management in Electronic Markets’, is my own. Where information has been derived from other sources, I confirm that this has been indicated in the thesis.

Signed: Maria Alessandra Crisafi

Date: 31 March 2017

UNIVERSITY COLLEGE OF LONDON

Abstract

Faculty of Mathematical and Physical Sciences

Department of Mathematics

Doctor of Philosophy

Optimal Trading and Inventory Management in Electronic Markets

by Maria Alessandra CRISAFI

In this thesis three distinct trading scenarios are considered and stochastic optimal control models are proposed to derive the optimal strategy the agent/firm should follow. First, we consider an agent who needs to liquidate a large amount of an asset and can trade in both a ‘lit’ exchange and a dark pool. We find the optimal selling schedule by solving numerically the resulting Hamilton-Jacobi-Bellman (HJB) equation. Next, we consider a customised liquidity pool (CLP) that offers a market-making service, by showing bid and ask prices to its clients. The CLP earns the spread from each transaction and it is subject to an inventory risk deriving from potential unfavourable price movements. The CLP can hedge its position in the ‘lit’ pool by means of limit and/or market orders so to rebalance its position on the asset. Finally, we consider a firm that offers mixed principal-versus-agency trading to its clients, and which earns the spread from the principal portion and a fixed fee for the brokerage service. We find the optimal proportion of principal/agency liquidity that should be displayed to clients and the optimal hedging strategy. We make specific reference to the foreign exchange market and consider the cases of one currency pair and three currency pairs. We provide the pseudo-codes, which have been written for solving numerically the models presented in this thesis, as well as a concise review of the dynamic programming principle (DPP) and the viscosity solution theory, specifically applied to the models discussed herein.

Acknowledgements

First and foremost I would like to express my deepest gratitude towards my supervisor Dr Andrea Macrina. Firstly, for his technical and scientific guidance throughout my PhD studies. Secondly, for his incessant support. Last but not least, for being a friend before being a supervisor. If he hadn't believed in me, I never would have gotten so far. Grazie.

I would like to thank Dr Jamie Walton for sharing his research ideas, and for introducing me to the exciting and fulfilling world of electronic foreign exchange trading. Jamie has been a pivotal player in my career development and no words can express how profoundly grateful I am for his support.

I am grateful to the Head of Department Professor Robb McDonald, and the Senior Learning & Teaching Administrator Dr Mark Roberts for always being available to help and for giving me the opportunity to lecture both undergraduate and graduate-level courses. I also acknowledge the great support I received by the administrative staff of the department of mathematics, UCL.

I would like to acknowledge financial support from both: (i) UCL, which granted me the Graduate Teaching Assistant Scholarship, and (ii) Morgan Stanley, which significantly contributed towards the expenses incurred during my PhD. I wish to clarify that no Morgan Stanley data has been used at any point of this work.

A massive thanks goes to my friends. Caterina, who I started this amazing UK adventure with. Carolina, for her constant presence and guidance. Adam, for being incredibly supportive, both, logistically and emotionally. And my three cousins, Andrea, Giulia and Flavio, for their unconditional love.

Finally, I would like to express all my love and deepest gratitude to my parents. It wasn't easy, but we made it. And we did it together, day after day, in the past 30 years. We'll always be the dream team. And the only team I would ever play for. You've been the pillars which sustained me when I was at my worst, and the hilarious friends I laughed with when I was at my best. I love you and no distance or life-matter will ever change that.

Contents

Declaration of Authorship	2
Abstract	3
Acknowledgements	4
Contents	5
List of Figures	9
1 Introduction	17
1.1 Overview of the thesis	17
1.2 Main contributions	18
1.2.1 Optimal execution	18
1.2.2 Optimal pricing and inventory management	20
1.3 Structure of the thesis	21
2 Reference models	25
2.1 Overview of the chapter	25
2.2 ‘Lit’ pool and its terminology	25
2.2.1 An introduction to optimal execution	26
2.2.1.1 A reference model	27
2.2.1.2 Numerical results and parameters’ analysis	30
2.2.2 An introduction to the market-making problem	33
2.2.2.1 A reference model	34
2.2.2.2 Numerical results and parameters’ analysis	38
2.3 Dark pools	42
2.3.1 Optimal trading in ‘lit’ and dark pools	44
2.3.1.1 A reference model	44
2.3.1.2 Numerical results and parameters’ analysis	46
2.3.2 Dark pools as market makers	49
2.3.2.1 A reference model	50
2.3.2.2 Numerical results and parameters’ analysis	53
2.4 Conclusions	58

3	Optimal execution in ‘lit’ and dark pools	61
3.1	Overview of the chapter	61
3.2	Trading in the ‘lit’ pool	62
3.2.1	Price, inventory and cash dynamics	62
3.2.2	The value function	63
3.2.3	Explicit examples and numerical results	65
3.2.3.1	Geometric Lévy model	65
3.2.3.2	Mean-reverting model	70
3.3	Trading in the dark pool	74
3.3.1	Modified prices, inventory and cash dynamics	75
3.3.2	The value function	76
3.3.3	Explicit examples and numerical results	78
3.3.3.1	Mean-reverting model	78
3.3.3.2	Geometric Lévy model	89
3.4	Conclusions	91
4	The market-making problem in a customised liquidity pool	93
4.1	Overview of the chapter	93
4.2	Market making in CLPs	95
4.2.1	Pricing strategy	96
4.2.2	Hedging strategy	98
4.2.2.1	Limit orders	98
4.2.2.2	Market orders	99
4.2.3	The value function	100
4.3	Explicit examples and numerical results	102
4.3.1	Optimal dark-pool spread	103
4.3.2	Optimal lit-pool posting	106
4.3.3	P&L distribution	108
4.3.4	Stochastic lit-pool spread	109
4.4	Conclusions	111
5	Market making: an application to the eFX spot market	113
5.1	Overview of the chapter	113
5.1.1	The FX spot market	115
5.1.2	Trading spot FX: the CLP perspective	116
5.2	One currency pair	118
5.2.1	Financial problem	118
5.2.2	Mathematical model	119
5.2.2.1	Pricing strategy	121
5.2.2.2	Hedging strategy	122
5.2.3	The value function	123
5.2.4	Numerical results	124
5.2.4.1	Martingale property of the FX rate	125
5.2.4.2	Permanent price impact	128
5.2.4.3	Mean-reversion	129
5.2.5	Price and inventory simulation	130
5.3	Three currency pairs	131

5.3.1	A revision of the state-variables dynamic	133
5.3.2	The value function	136
5.3.3	Numerical results	137
5.3.4	Price and inventory simulation	140
5.4	Conclusions	141
6	Final conclusions	143
6.1	Summary of main results and contributions	143
6.2	Future work	145
7	Viscosity solutions and numerical procedures	147
7.1	Background material	148
7.1.1	Dynamic programming and HJB equation	148
7.1.2	Viscosity solutions	152
7.2	Reconciliation of notation	154
7.2.1	Chapter 2	154
7.2.1.1	Optimal liquidation	154
7.2.1.2	Optimal market making	155
7.2.2	Chapter 3	156
7.2.3	Chapter 4	157
7.3	Proofs for Chapter 3	158
7.3.1	Dark pool optimal control problem	158
7.3.2	Moments estimates	159
7.3.3	Viscosity solution	161
7.4	Proofs for Chapter 4	167
7.4.1	Assumption	167
7.4.2	Viscosity solution	167
7.5	Numerical procedures	176
7.5.1	Chapter 3	176
7.5.2	Chapter 4	178
7.6	Non-equivalence of liquidation strategies	179
	Bibliography	183

List of Figures

2.1	Optimal selling strategy—displayed as a function of the remaining inventory—found by solving the HJB equation (2.6). We set $\sigma = 0.1$, $\beta = 0.1$, $\mu = 0.01$, $x = 30$, $s^b = 8$, $T = 10$. In the left panel we set $\phi = 0.005$. In the right panel we set $\alpha = 0.1$	31
2.2	Optimal selling strategy—displayed as a function of the remaining inventory—found by solving the HJB equation (2.6). We set $\sigma = 0.1$, $x = 30$, $s^b = 8$, $\alpha = 0.1$, $\phi = 0.001$, $T = 10$. In the left panel we set $\mu = 0.01$. In the right panel we set $\beta = 0.1$	32
2.3	Optimal inventory thresholds found by solving the HJB equation (2.16). We set $k = 3$, $\alpha = 2$, $\lambda^+ = \lambda^- = 0.5$, $T = 50$, $\epsilon = 10$. In the left panel we set $\phi = 0.00001$. In the right panel we set $\phi = 0.0001$	39
2.4	Optimal inventory thresholds found by solving the HJB equation (2.16). We set $k = 3$, $\alpha = 2$, $\phi = 0.0001$, $T = 50$, $\epsilon = 10$. In the left panel we set $\lambda^+ = 0.6$, $\lambda^- = 0.4$. In the right panel we set $\lambda^+ = 0.4$, $\lambda^- = 0.6$	39
2.5	Optimal inventory thresholds found by solving the HJB equation (2.16). We set $\alpha = 2$, $\lambda^+ = \lambda^- = 0.5$, $T = 50$, $\epsilon = 10$, $\phi = 0.0001$. In the left panel we set $k = 5$. In the right panel we set $k = 1$	40
2.6	Optimal inventory thresholds found by solving the HJB equation (2.16). We set $k = 3$, $\lambda^+ = \lambda^- = 0.5$, $T = 50$, $\epsilon = 10$, $\phi = 0.0001$. In the left panel we set $\alpha = 5$. In the right panel we set $\alpha = 1$	41
2.7	Optimal inventory thresholds found by solving the HJB equation (2.16). We set $k = 3$, $\lambda^+ = \lambda^- = 0.5$, $\alpha = 2$, $T = 50$, $\phi = 0.0001$. In the left panel we set $\epsilon = 20$. In the right panel we set $\epsilon = 1$	41
2.8	Optimal selling strategy—displayed as a function of the remaining inventory—found by solving the HJB equation (2.22). We set $\sigma = 0.1$, $s = 40$, $\lambda = 0.5$, $\alpha = 0.5$, $T = 10$, $\phi = 0.001$, $\tau = 5$. In the left panel we set $\beta = 0.2$. In the right panel we set $\beta = 0.01$	47
2.9	Optimal selling strategy—displayed as a function of the remaining inventory—found by solving the HJB equation (2.22). We set $\sigma = 0.1$, $s = 40$, $\lambda = 0.5$, $T = 10$, $\phi = 0.001$, $\tau = 5$, $\beta = 0.1$. In the left panel we set $\alpha = 3$. In the right panel we set $\alpha = 0.1$	48
2.10	Optimal selling strategy—displayed as a function of the remaining inventory—found by solving the HJB equation (2.22). We set $\sigma = 0.1$, $s = 40$, $\lambda = 0.5$, $\alpha = 0.5$, $T = 10$, $\alpha = 0.5$, $\tau = 5$, $\beta = 0.1$. In the left panel we set $\phi = 0.01$. In the right panel we set $\phi = 0.0001$	48
2.11	Optimal selling strategy—displayed as a function of the remaining inventory—found by solving the HJB equation (2.22). We set $\sigma = 0.1$, $s = 40$, $\phi = 0.001$, $\alpha = 0.5$, $T = 10$, $\alpha = 0.5$, $\tau = 5$, $\beta = 0.1$. In the left panel we set $\lambda = 1$. In the right panel we set $\lambda = 0.1$	49

- 2.12 Optimal inventory thresholds found by solving the HJB equation (2.33). We set $k = 4$, $\lambda^+ = \lambda^- = 0.5$, $T = 50$, $\epsilon_m = 30$, $\epsilon_\ell = 15$, $\phi = 0.0001$, $\delta^+ = \delta^- = 2$, $p = 0.8$. In the left panel we set $\alpha = 3$. In the right panel we set $\alpha = 1$ 54
- 2.13 Optimal inventory thresholds found by solving the HJB equation (2.33). We set $k = 4$, $T = 50$, $\epsilon_m = 30$, $\epsilon_\ell = 15$, $\phi = 0.0001$, $\alpha = 1$, $\delta^+ = \delta^- = 2$, $p = 0.8$. In the left panel we set $\lambda^+ = 0.7$ and $\lambda^- = 0.3$. In the right panel we set $\lambda^+ = 0.3$ and $\lambda^- = 0.7$ 55
- 2.14 Optimal inventory thresholds found by solving the HJB equation (2.33). We set $k = 4$, $\lambda^+ = \lambda^- = 0.5$, $T = 50$, $\epsilon_m = 30$, $\epsilon_\ell = 15$, $\alpha = 1$, $\phi = 0.0001$, $\delta^+ = \delta^- = 2$, $p = 0.8$. In the left panel we set $k = 6$. In the right panel we set $k = 2$ 55
- 2.15 Optimal inventory thresholds found by solving the HJB equation (2.33). We set $k = 4$, $\lambda^+ = \lambda^- = 0.5$, $T = 50$, $\phi = 0.0001$, $\alpha = 1$, $\delta^+ = \delta^- = 2$, $p = 0.8$. In the left panel we set $\epsilon_m = 35$ and $\epsilon_\ell = 20$. In the right panel we set $\epsilon_m = 6$ and $\epsilon_\ell = 4$ 56
- 2.16 Optimal inventory thresholds found by solving the HJB equation (2.33). We set $k = 4$, $\lambda^+ = \lambda^- = 0.5$, $T = 50$, $\epsilon_m = 30$, $\epsilon_\ell = 15$, $\alpha = 1$, $\delta^+ = \delta^- = 2$, $p = 0.8$. In the left panel we set $\phi = 0.001$. In the right panel we set $\phi = 0.00001$. 57
- 2.17 Optimal inventory thresholds found by solving the HJB equation (2.33). We set $k = 4$, $\lambda^+ = \lambda^- = 0.5$, $T = 50$, $\epsilon_m = 30$, $\epsilon_\ell = 15$, $\phi = 0.0001$, $\alpha = 1$, $\delta^+ = \delta^- = 2$. In the left panel we set $p = 0.95$. In the right panel we set $p = 0.65$ 57
- 3.1 Simulation of Equations (3.1), (3.10), (3.8) and (3.9). We set $\beta = 0.05$, $\mu = 0.01$, $\bar{\mu}^b = 0.01$, $x = 30$, $s^b = 8$, $\lambda^{b,1} = \lambda^{b,2} = 0.5$, $z^{b,i} \sim U[0, 1]$, $r = 0.01$, $T = 10$, $\phi = 0.01$, $\alpha = 1$ 67
- 3.2 Simulation of Equations (3.1), (3.10), (3.8) and (3.9). We set $\beta = 0.05$, $\mu = 0.01$, $\bar{\mu}^b = -0.01$, $x = 30$, $s^b = 8$, $\lambda^{b,1} = \lambda^{b,2} = 0.5$, $z^{b,i} \sim U[0, 1]$, $r = 0.01$, $T = 10$, $\phi = 0.01$, $\alpha = 1$ 68
- 3.3 Optimal mean selling strategy—displayed as a function of the remaining inventory—found by solving the HJB equation (3.12). We set $\beta = 0.1$, $\mu = 0.05$, $\bar{\mu}^b = 0$, $x = 30$, $s^b = 8$, $\lambda^{b,1} = \lambda^{b,2} = 0.1$, $z^{b,i} \sim U[0, 1]$, $r = 0.01$, $T = 10$. In the left panel we set $\phi = 0.001$. In the right panel we set $\alpha = 1$ 69
- 3.4 Optimal mean selling strategy—displayed as a function of the remaining inventory—found by solving the HJB equation (3.12). We set $\alpha = 0.5$, $\bar{\mu}^b = 0.1$, $\phi = 0.001$, $x = 30$, $s^b = 8$, $\lambda^{b,1} = \lambda^{b,2} = 0.1$, $z^{b,i} \sim U[0, 1]$, $r = 0.01$, $T = 10$. In the left panel we set $\mu = 0.05$. In the right panel we set $\beta = 0.1$. . 69
- 3.5 Optimal mean selling strategy—displayed as a function of the remaining inventory—found by solving the HJB equation (3.12). We set $\alpha = 0.5$, $\beta = 0.1$, $\phi = 0.01$, $x = 30$, $s^b = 8$, $\mu = 0.05$, $z^{b,i} \sim U[0, 1]$, $\bar{\mu}^b = 0$, $T = 10$. In the left panel we set $r = 0.01$. In the right panel we set $\lambda^{b,1} = \lambda^{b,2} = 0.1$ 70
- 3.6 Simulation of Equations (3.1), (3.10), (3.13) and (3.9). We set $\beta = 0.05$, $\mu = 0.1$, $x = 30$, $s^b = 5$, $\bar{S} = 8$, $\lambda^{b,1} = \lambda^{b,2} = 0.5$, $z^{b,i} \sim U[0, 1]$, $r = 0.001$, $T = 10$, $\phi = 0.0001$, $\alpha = 0.5$, $\kappa^b = 0.1$ 71
- 3.7 Simulation of Equations (3.1), (3.10), (3.13) and (3.9). We set $\beta = 0.05$, $\mu = 0.1$, $x = 30$, $s^b = 11$, $\bar{S} = 8$, $\lambda^{b,1} = \lambda^{b,2} = 0.5$, $z^{b,i} \sim U[0, 1]$, $r = 0.001$, $T = 10$, $\phi = 0.0001$, $\alpha = 0.5$, $\kappa^b = 0.1$ 72

- 3.8 Optimal selling strategy—displayed as a function of the remaining inventory—
found by solving the HJB equation (3.14). We set $\beta = 0.05$, $\mu = 0.1$, $x = 30$,
 $\bar{S} = 8$, $\lambda^{b,1} = \lambda^{b,2} = 0.5$, $z^{b,i} \sim U[0, 1)$, $r = 0.001$, $T = 10$, $\phi = 0.0001$, $\alpha = 2$.
In the left panel we set $s^b = 6$. In the right panel we set $s^b = 10$ 72
- 3.9 Optimal selling strategy—displayed as a function of the remaining inventory—
found by solving the HJB equation (3.14). We set $\beta = 0.05$, $\mu = 0.1$, $x = 30$,
 $\bar{S} = 8$, $\lambda^{b,1} = \lambda^{b,2} = 0.5$, $z^{b,i} \sim U[0, 1)$, $r = 0.001$, $T = 10$, $\phi = 0.0001$, $\alpha = 1$.
In the left panel we set $\kappa^b = 0.1$. In the right panel we set $\kappa^b = 0.001$ 73
- 3.10 Simulation of Equations (3.23) and (3.24). We set , $z^{b,i}, z^{\Delta,i} \sim U[0, 1)$, $\lambda^{b,1} =$
 $\lambda^{b,2} = \lambda^{\Delta,1} = \lambda^{\Delta,2} = 0.5$, $\bar{\Delta} = 0.2$, $\bar{S} = 40$, $\kappa^b = \kappa^\Delta = 0.0002$, $S_t = 40$,
 $\Delta_t = 0.2$, $T = 100$ 79
- 3.11 Simulation of Equations (3.16), (3.25), (3.23) and (3.24). We set $\beta = 0.001$,
 $\mu = 0.001$, $x = 30$, $s^b = 8$, $\bar{S} = 8$, $\Delta = 1$, $\bar{\Delta} = 1$, $\lambda^{b,1} = \lambda^{b,2} = \lambda^{\Delta,1} = \lambda^{\Delta,2} =$
 0.5 , $z^{b,i}, z^{\Delta,i} \sim U[0, 1)$, $\lambda^y = 0.1$, $z^y \sim U[0, 1]$, $r = 0.02$, $T = 10$, $\phi = 0.001$,
 $\alpha = 2$, $\kappa^b = \kappa^\Delta = 0.1$. In the bottom panels, the black lines depict the
impacted prices while the corresponding blue lines represent the theoretical
unimpacted prices. 81
- 3.12 Optimal mean selling strategy—displayed as a function of the remaining inventory—
found by solving the HJB equation (3.27). We set $\kappa^b = \kappa^\Delta = 0.01$, $\beta = 0.01$,
 $x = 30$, $s^b = 5$, $\Delta = 0.5$, $\bar{S} = 5$, $\bar{\Delta} = 1$, $\lambda^{b,1} = \lambda^{b,2} = \lambda^{\Delta,1} = \lambda^{\Delta,2} = 0.2$,
 $z^{b,i}, z^{\Delta,i} \sim U[0, 1)$, $\mu = 0.01$, $\lambda^y = 0.1$, $z^y \sim U[0, 1]$, $\alpha = 2$, $T = 10$. In the
top panels we set $r = 0.01$, $\phi = 0.001$, $\alpha = 4$ (left), $\alpha = 0.5$ (right). In the
middle panels we set $r = 0.01$, $\alpha = 2$, $\phi = 0.1$ (left), $\phi = 0.0001$ (right). In
the bottom panels we set $\phi = 0.001$, $\alpha = 2$, $r = 0.1$ (left), $r = 0.0001$ (right). 82
- 3.13 Optimal mean selling strategy—displayed as a function of the remaining inventory—
found by solving the HJB equation (3.27). We set $\kappa^\Delta = 0.01$, $\beta = 0.01$, $x = 30$,
 $s^b = 5$, $\Delta = 1$, $\bar{\Delta} = 0.5$, $\lambda^{b,1} = \lambda^{b,2} = \lambda^{\Delta,1} = \lambda^{\Delta,2} = 0.2$, $z^{b,i}, z^{\Delta,i} \sim U[0, 1)$,
 $\mu = 0.01$, $\lambda^y = 0.1$, $z^y \sim U[0, 1]$, $\alpha = 2$, $\phi = 0.001$, $r = 0.01$, $T = 10$. In the
top panels we set $\bar{S} = 3$, $\kappa^b = 0.1$ (left), $\kappa^b = 0.0005$ (right). In the bottom
panels we set $\bar{S} = 7$, $\kappa^b = 0.1$ (left), $\kappa^b = 0.0005$ (right). 83
- 3.14 Optimal mean selling strategy—displayed as a function of the remaining inventory—
found by solving the HJB equation (3.27). We set $\kappa^b = 0.01$, $\beta = 0.01$,
 $x = 30$, $s^b = 5$, $\Delta = 0.5$, $\bar{S} = 5$, $\lambda^{b,1} = \lambda^{b,2} = \lambda^{\Delta,1} = \lambda^{\Delta,2} = 0.2$, $\mu = 0.01$,
 $z^{b,i}, z^{\Delta,i} \sim U[0, 1)$, $\lambda^y = 0.1$, $z^y \sim U[0, 1]$, $\alpha = 2$, $\phi = 0.001$, $r = 0.01$, $T = 10$.
In the top panels we set $\bar{\Delta} = 0.3$, $\kappa^\Delta = 0.1$ (left), $\kappa^\Delta = 0.0005$ (right). In the
bottom panels we set $\bar{\Delta} = 0.7$, $\kappa^\Delta = 0.1$ (left), $\kappa^\Delta = 0.0005$ (right). 85
- 3.15 Optimal mean selling strategy displayed as a function of the remaining inven-
tory. We set $\kappa^b = \kappa^\Delta = 0.01$, $x = 30$, $s^b = 5$, $\Delta = 0.5$, $\bar{S} = 5$, $\bar{\Delta} = 0.5$,
 $\lambda^{b,1} = \lambda^{b,2} = \lambda^{\Delta,1} = \lambda^{\Delta,2} = 0.2$, $z^{b,i}, z^{\Delta,i} \sim U[0, 1)$, $\phi = 0.001$, $\alpha = 2$,
 $\lambda^y = 0.1$, $z^y \sim U[0, 1]$, $r = 0.01$, $\phi = 0.001$, $T = 10$. In the top panels we
set $\beta = 0.01$, $\mu = 0.1$ (left), $\mu = 0.001$ (right). In the bottom panels we set
 $\mu = 0.01$, $\beta = 0.03$ (left), $\beta = 0.001$ (right). 86
- 3.16 Optimal mean selling strategy—displayed as a function of the remaining inventory—
found by solving the HJB equation (3.27). We set $\kappa^b = \kappa^\Delta = 0.01$, $\beta = 0.01$,
 $x = 30$, $s^b = 5$, $\Delta = 0.5$, $\bar{S} = 5$, $\bar{\Delta} = 0.5$, $\mu = 0.01$, $\lambda^y = 0.1$, $z^y \sim U[0, 1]$,
 $z^{b,i}, z^{\Delta,i} \sim U[0, 1)$, $r = 0.01$, $\phi = 0.001$, $\alpha = 2$, $T = 10$. In the top panels
we set $\lambda^{\Delta,1} = \lambda^{\Delta,2} = 0.2$, $\lambda^{b,1} = 0.7$, $\lambda^{b,2} = 0.1$ (left), $\lambda^{b,1} = 0.1$, $\lambda^{b,2} = 0.7$
(right). In the bottom panels we set $\lambda^{b,1} = \lambda^{b,2} = 0.2$, $\lambda^{\Delta,1} = 0.7$, $\lambda^{\Delta,2} = 0.1$
(left), $\lambda^{\Delta,1} = 0.1$, $\lambda^{\Delta,2} = 0.7$ (right) 87

- 3.17 Optimal selling strategy—displayed as a function of the remaining inventory—found by solving the HJB equation (3.27). We set $\kappa^b = \kappa^\Delta = 0.01$, $\beta = 0.01$, $\phi = 0.01$, $x = 30$, $s^b = 5$, $\Delta = 0.5$, $\bar{S} = 5$, $\bar{\Delta} = 0.5$, $\lambda^{b,1} = \lambda^{b,2} = \lambda^{\Delta,1} = \lambda^{\Delta,2} = 0.2$, $z^{b,i}, z^{\Delta,i} \sim U[0, 1]$, $\mu = 0.01$, $z^y \sim U[0, 1]$, $r = 0.01$, $\phi = 0.001$, $\alpha = 2$, $T = 10$. In the left panel we set $\lambda^y = 0.5$. In the right panel we set $\lambda^y = 0.01$ 88
- 3.18 Optimal ‘lit’ and dark-pool strategies—found by solving the HJB equation (3.27)—for an inventory of 30 (left and right panels, respectively). We set $\kappa^b = \kappa^\Delta = 0.01$, $\beta = 0.01$, $\phi = 0.01$, $\bar{S} = 5$, $\bar{\Delta} = 0.5$, $\lambda^{b,1} = \lambda^{b,2} = \lambda^{\Delta,1} = \lambda^{\Delta,2} = 0.2$, $z^{b,i}, z^{\Delta,i} \sim U[0, 1]$, $\mu = 0.01$, $\lambda^y = 0.1$, $z^y \sim U[0, 1]$, $r = 0.01$, $\phi = 0.001$, $\alpha = 2$, $T = 10$. In the top panels, we set $S_t^b > \bar{S}$. In the bottom panels we set $S_t^b < \bar{S}$ 88
- 3.19 Simulation of Equations (3.13) and (3.28). We set $z^{b,i}, z^{\Delta,i} \sim U[0, 1]$, $\lambda^{b,1} = \lambda^{b,2} = 0.5$, $\lambda^{\Delta,1} = \lambda^{\Delta,2} = 0.6$, $\bar{\mu}^b = \bar{\mu}^\Delta = 0$, $\bar{S} = 40$, $S_t = 40$, $\Delta_t = 0.2$, $T = 100$. 89
- 3.20 Simulation of Equations (3.16), (3.25), (3.13) and (3.28). We set $\beta = 0.001$, $\mu = 0.001$, $x = 30$, $s^b = 5$, $\Delta = 0.5$, $\lambda^{b,1} = \lambda^{b,2} = \lambda^{\Delta,1} = \lambda^{\Delta,2} = 0.5$, $z^{b,i}, z^{\Delta,i} \sim U[0, 1]$, $\lambda^y = 0.1$, $z^y \sim U[0, 1]$, $r = 0.02$, $T = 10$, $\phi = 0.001$, $\alpha = 2$, $\bar{\mu}^b = \bar{\mu}^\Delta = 0$. In the bottom panels, the black lines depict the impacted prices while the corresponding blue lines represent the theoretical unimpacted prices. 90
- 3.21 Optimal ‘lit’ and dark-pool strategies—found by solving the HJB equation (3.29)—for an inventory of 30 (left and right panels, respectively). We set $\beta = 0.01$, $x = 30$, $\lambda^{b,1} = \lambda^{b,2} = \lambda^{\Delta,1} = \lambda^{\Delta,2} = 0.2$, $z^{b,i}, z^{\Delta,i} \sim U[0, 1]$, $\mu = 0.01$, $\lambda^y = 0.1$, $z^y \sim U[0, 1]$, $r = 0.01$, $\phi = 0.001$, $\alpha = 2$, $T = 10$. In the left panel we set $\bar{\mu}^b = \bar{\mu}^\Delta = 0.001$. In the right panel we set $\bar{\mu}^b = \bar{\mu}^\Delta = -0.001$. 91
- 4.1 Sample paths for (4.1). We set $\bar{k} = 0.01$ and $\mathbb{K} = \{0.01, 0.02, \dots, 0.1\}$ 96
- 4.2 Optimal inventory thresholds found by solving the HJB equation (4.15). We set $\alpha = 2$, $\mathcal{D} := \{(0.5, 0.5), (0.3, 0.6), (0.6, 0.3)\}$, $\mathcal{I} := \{(0.5, 0.5), (0.6, 0.4), (0.4, 0.6)\}$, $\epsilon_\ell = 3$, $\epsilon_m = 6$, $c = 0.05$, $\lambda^m = 0.5$, $k = 1$, $q^\pm \sim U[1, 10]$, $z \sim U[0, 1]$, $s = 40$, $\mathbb{E}[\bar{k}^\pm] = 0$, $x = y = 0$, $\bar{X} = 100$. In the left panel we set $\phi = 0.01$. In the right panel we set $\phi = 0.0001$ 104
- 4.3 Optimal inventory thresholds found by solving the HJB equation (4.16). We set $\alpha = 2$, $\mathcal{D} := \{(0.5, 0.5), (0.3, 0.6), (0.6, 0.3)\}$, $\mathcal{I} := \{(0.5, 0.5), (0.6, 0.4), (0.4, 0.6)\}$, $\epsilon_\ell = 3$, $\epsilon_m = 6$, $c = 0.05$, $\lambda^m = 0.5$, $k = 1$, $q^\pm \sim U[1, 10]$, $z \sim U[0, 1]$, $s = 40$, $\mathbb{E}[\bar{k}^\pm] = 0$, $x = y = 0$, $\bar{X} = 100$, $\bar{k} = 0.01$, $\ell^{\kappa=0}(z_1) = 0.9$, $\ell^{\kappa=\bar{k}}(z_1) = 0.8$, $\ell^{\kappa=2\bar{k}}(z_1) = 0.6$. In the left panel we set $\phi = 0.01$. In the right panel we set $\phi = 0.0001$ 107
- 4.4 Optimal inventory thresholds found by solving the HJB equation (4.16). We set $\phi = 0.001$, $\mathcal{D} := \{(0.5, 0.5), (0.3, 0.6), (0.6, 0.3)\}$, $\mathcal{I} := \{(0.5, 0.5), (0.6, 0.4), (0.4, 0.6)\}$, $\epsilon_\ell = 3$, $\epsilon_m = 6$, $c = 0.05$, $\lambda^m = 0.5$, $k = 1$, $q^\pm \sim U[1, 10]$, $z \sim U[0, 1]$, $s = 40$, $\mathbb{E}[\bar{k}^\pm] = 0$, $x = y = 0$, $\bar{X} = 100$, $\bar{k} = 0.01$, $\ell^{\kappa=0}(z_1) = 0.9$, $\ell^{\kappa=\bar{k}}(z_1) = 0.8$, $\ell^{\kappa=2\bar{k}}(z_1) = 0.6$. In the left panel we set $\alpha = 6$. In the right panel we set $\alpha = 0.5$ 107
- 4.5 Terminal cash distribution as defined in Section 4.3.2. In the left panel we set $\alpha = 0.5$ and $\phi = 0.00001$. In the right panel we set $\alpha = 6$ and $\phi = 0.01$. . . 108

- 4.6 Optimal inventory thresholds found by solving the HJB equation (4.18). Seasonal pattern. We set $\alpha = 2$, $r = 1$, $\phi = 0.001$, $\mathcal{D} := \{(0.5, 0.5), (0.3, 0.6), (0.6, 0.3)\}$, $\mathcal{I} := \{(0.5, 0.5), (0.6, 0.4), (0.4, 0.6)\}$, $\epsilon_\ell = 3$, $\epsilon_m = 6$, $c = 0.05$, $\lambda^m = 0.5$, $k = 1$, $q^\pm \sim U[1, 10]$, $z \sim U[0, 1]$, $s = 40$, $\mathbb{E}[\bar{k}^\pm] = 0$, $x = y = 0$, $\bar{X} = 100$, $\bar{k} = 0.01$, $\ell^{\kappa=0}(z_1) = 0.9$, $\ell^{\kappa=\bar{k}}(z_1) = 0.8$, $\ell^{\kappa=2\bar{k}}(z_1) = 0.6$, $\mathbb{K} = \{1, 2\}$ 110
- 4.7 Optimal inventory thresholds found by solving the HJB equation (4.18). Mean-reverting pattern. We set $\alpha = 2$, $r_{high} = 6$, $r_{low} = 0.5$, $\phi = 0.001$, $\mathcal{D} := \{(0.5, 0.5), (0.3, 0.6), (0.6, 0.3)\}$, $\mathcal{I} := \{(0.5, 0.5), (0.6, 0.4), (0.4, 0.6)\}$, $\epsilon_\ell = 3$, $\epsilon_m = 6$, $c = 0.05$, $\lambda^m = 0.5$, $k = 1$, $q^\pm \sim U[1, 10]$, $z \sim U[0, 1]$, $s = 40$, $\mathbb{E}[\bar{k}^\pm] = 0$, $x = y = 0$, $\bar{X} = 100$, $\mathbb{K} = \{1, 2\}$, $\bar{k} = 0.01$, $\ell^{\kappa=0}(z_1) = 0.9$, $\ell^{\kappa=\bar{k}}(z_1) = 0.8$, $\ell^{\kappa=2\bar{k}}(z_1) = 0.6$ 111
- 5.1 Optimal principal-liquidity strategy (top panels) and hedging strategy (bottom panels)—displayed as a function of time and inventory—found by solving the HJB equation (5.9). We set $\lambda^\pm = 0.5$, $q^\pm \sim U[0, 20]$, $\eta = 25 \times 10^{-6}$, $\phi = 0.05$, $\gamma = \kappa = 0$, $\xi_1 = 0.5$, $\xi_2 = 0.5$ pips, $\xi_3 = 0.001$, $\epsilon = 5$, $s^{\text{€\$}} = 1.075$, $\Delta^{\text{€\$}} = 2$ pips. In the left panels we set $\hat{\alpha} = 6$. In the right panels we set $\hat{\alpha} = 0.5$. 125
- 5.2 Optimal principal-liquidity strategy (top panels) and hedging strategy (bottom panels)—displayed as a function of time and inventory—found by solving the HJB equation (5.9). We set $\lambda^\pm = 0.5$, $q^\pm \sim U[0, 20]$, $\eta = 25 \times 10^{-6}$, $\hat{\alpha} = 2$, $\gamma = \kappa = 0$, $\xi_1 = 0.5$, $\xi_2 = 0.5$ pips, $\xi_3 = 0.001$, $\epsilon = 5$, $s^{\text{€\$}} = 1.075$, $\Delta^{\text{€\$}} = 2$ pips. In the left panels we set $\phi = 0.1$. In the right panels we set $\phi = 0.001$ 126
- 5.3 Optimal principal-liquidity strategy (top panels) and hedging strategy (bottom panels)—displayed as a function of time and inventory—found by solving the HJB equation (5.9). We set $q^\pm \sim U[0, 20]$, $\eta = 25 \times 10^{-6}$, $\hat{\alpha} = 2$, $\phi = 0.05$, $\gamma = \kappa = 0$, $\xi_1 = 0.5$, $\xi_2 = 0.5$ pips, $\xi_3 = 0.001$, $\epsilon = 5$, $s^{\text{€\$}} = 1.075$, $\Delta^{\text{€\$}} = 2$ pips. In the left panels we set $\lambda^+ = 0.7$ and $\lambda^- = 0.3$. In the right panels we set $\lambda^+ = 0.3$ and $\lambda^- = 0.7$ 127
- 5.4 Optimal principal-liquidity strategy (top panels) and hedging strategy (bottom panels)—displayed as a function of time and inventory—found by solving the HJB equation (5.9). We set $q^\pm \sim U[0, 20]$, $\eta = 25 \times 10^{-6}$, $\hat{\alpha} = 2$, $\phi = 0.05$, $\lambda^\pm = 0.5$, $\kappa = 0$, $\xi_1 = 0.5$, $\xi_2 = 0.5$ pips, $\xi_3 = 0.001$, $\epsilon = 5$, $s^{\text{€\$}} = 1.075$, $\Delta^{\text{€\$}} = 2$ pips. In the left panels we set $\gamma = 0.01$. In the right panels we set $\gamma = 0.0001$ 128
- 5.5 Optimal principal-liquidity strategy (top panels) and hedging strategy (bottom panels)—displayed as a function of time and inventory—found by solving the HJB equation (5.9). We set $q^\pm \sim U[0, 20]$, $\eta = 25 \times 10^{-6}$, $\hat{\alpha} = 2$, $\phi = 0.05$, $\bar{S} = 1.075$, $\lambda^\pm = 0.5$, $\gamma = 0$, $\xi_1 = 0.5$, $\xi_2 = 0.5$ pips, $\xi_3 = 0.001$, $\epsilon = 5$, $\Delta^{\text{€\$}} = 2$ pips. In the left panels we set $\kappa = 0.05$. In the right panels we set $\kappa = 0.005$ 129
- 5.6 Inventory simulation (top panels) and prices simulation (bottom panels). We set $q^\pm \sim U[0, 50]$, $\eta = 25 \times 10^{-6}$, $\hat{\alpha} = 2$, $\phi = 0.05$, $\bar{S} = 1.075$, $\lambda^\pm = 0.5$, $\gamma = 0$, $\xi_1 = 0.5$, $\xi_2 = 0.5$ pips, $\xi_3 = 0.001$, $\epsilon = 5$, $\Delta^{\text{€\$}} = 2$ pips, $\kappa = 0.005$ 130
- 5.7 Optimal principal-liquidity strategy found by solving the HJB equation (5.15). We set $q^\pm \sim U[0, 20]$, $\eta = 25 \times 10^{-6}$, $\hat{\alpha} = 2$, $\phi = 0.05$, $\lambda^\pm = 0.5$, $\xi_1 = 0.5$, $\xi_2 = 0.5$ pips, $\xi_3 = 0.001$, $\epsilon^{\text{€\$}, \text{£\$}} = 5$, $\epsilon^{\text{€£}} = 10$, $\Delta^{\text{€\$}} = \Delta^{\text{£\$}} = 2$ pips, $\Delta^{\text{€£}} = 3$ pips. 138

5.8	Optimal hedging strategy found by solving the HJB equation (5.15). Top panels: $t = 0$. Bottom panels: $t \rightarrow T$	139
5.9	Optimal hedging strategy found by solving the HJB equation (5.15). Top panels: $t = 0$. Bottom panels: $t \rightarrow T$	139
5.10	Price simulation (top panels and bottom-left panel) and inventory simulation (bottom-right panel).	140

*To my parents: The best people I've had the privilege to
meet.*

Chapter 1

Introduction

1.1 Overview of the thesis

This thesis can be collocated within the extensive literature of algorithmic and high-frequency trading. The increasing power of the machine, together with new market needs, has determined a substantial increase in trading speed. Such trading activity, which may take place at a millisecond level, is now mostly performed by computers. At the basis of such execution rules there are complex algorithms, which originate from mathematical models. Industry practitioners typically have extensive market knowledge and convey such information into a modest number of mathematical equations that output instructions, which form the trading strategies followed by the firm. Depending on the firm's activity, whether it be betting on future price-movements direction or offering two-way quotes to clients, financial analysis endeavours to maximise the firm's net earnings, while managing the risk taken. An analysis of the impact of high-frequency trading has been studied in, e.g., Cartea et al. [25], who find that traders belonging to such a class increase price impact as well as market noise, traded volume and market liquidity.

In this context, we propose two classes of mathematical models which can be utilised depending on the trading situations the agent (or firm) may face. For each class of models we treat, we proceed as follows: We define the stochastic differential equations, which model the evolution of the surrounding environment,

and we describe the set of actions the agent may take to intervene on the financial system. We make use of the optimisation techniques provided by stochastic optimal control theory to single out the best admissible strategy and we plot the results. We analyse how the results vary when different values of the model parameters are employed, and we discuss the financial validity of the derived results. In Section 7.1 we collect the main mathematical tools applied throughout the thesis.

One of the important contributions of this thesis is to provide market practitioners with new understanding and novel tools. As such, the thesis also aims at capturing real market dynamics, which take place in modern trading floors. Therefore, mathematical assumptions are made, while keeping practical considerations in mind at all times.

1.2 Main contributions

The original work presented in this thesis revolves around two main research streams: (i) optimal execution and (ii) optimal pricing and inventory management. In this section we contextualise this work within the current literature and we make specific references to the proposed innovations and the new contributions we made.

1.2.1 Optimal execution

Agents who need to perform an ‘optimal execution’ typically trade for underlying economic reasons. They trade in one direction only at any given time and are subject to (unfavourable) price slippage. Since the rise of algorithmic and high frequency trading, the need for clear and predetermined trading schedules has become essential to guarantee minimal market impact and effective execution by the due-date the agent may have. The general agreement is that slicing a “parent order” (i.e. the whole amount which needs to be executed) into “child orders” is optimal when it comes to large executions. This is so to minimise the turmoil in the market, which may encourage other agents to trade in the

same direction, further impacting the market price. Additionally, it gives the chance for the order book to be refilled, in order for market participants to trade at better prices. The main question is how such parent orders should be sliced. With no information available and a set terminal date, trading at a constant rate looks like a reasonable approximation of an optimal strategy. On the other hand, depending on market conditions and the benchmark of the agent, the trading speed may take visibly different shapes, making the constant-rate liquidation strategy largely sub-optimal. Pioneers of this research field are Almgren and Chriss [2] and Bertsimas and Lo [10]. A great deal of research has developed since then and we refer in particular to the book by Cartea et al. [23] and Guéant et al. [43] and the references therein. In particular, the benchmark of the agent substantially changes the shape of the optimal policy. We find, e.g., (i) the work by Lorenz and Almgren [61] where agents target a mean-variance criterion, (ii) the papers by Cartea and Jaimungal [21], Frei and Westray [39] and Guéant and Royer [46] on targeting VWAP¹, (iii) the work by Løkka [62] in which a maximisation of a CARA² utility function is considered, et cetera.

A related research stream, i.e. optimal execution in situations where multiple venues are available to market participants, has also been the object of recent studies. In particular Kratz and Schöneborn [57, 58] introduced dark pools as a liquidating venue in a setting applicable to order-driven markets. Horst and Naujokat [52] studied a similar problem, in that liquidation was performed through passive orders (which share similarities with the dark-pool order-matching structure) and aggressive orders.

Main Contributions: Our work on optimal execution falls in the latter category and we consider a situation where both ‘lit’ and dark pools are available to market participants. Although the topic is not original in itself, we propose several modifications and extensions to the state-of-the-art literature by analysing the effects of, e.g., permanent price impact³ in a continuous-time model, which

¹Volume Weighted Average Price.

²Constant Absolute Risk Aversion.

³Permanent price impact may occur more often in less liquid markets, in which it takes more time for the liquidity taken by a market order to be refilled via submission of fresh limit orders. Furthermore, it may happen due to trades originated by a new flow of price-sensitive information. Finally, large orders are more likely to cause permanent market impact compared to small-sized orders.

has not been discussed elsewhere in the aforementioned works. Next we propose a model for the whole top of the book, by giving a structure to both the lit-pool best bid price and the spread. Additionally, we consider partial order execution in the dark pool. Finally, we work with more structured price dynamics and do not require for the latter to be martingales. With this last assumption, we consider the possibility for the agent to have a market view and schedule his trading accordingly. These results are presented in Chapter 3.

1.2.2 Optimal pricing and inventory management

As noted by Carmona and Webster [17], research on optimal market making can be associated to two different schools of thought. On the one hand, we find inventory-risk models in which market makers construct their posting strategy in accordance with their risk aversion and the current distance from their preferred inventory position. Such market makers rarely, if ever, bet on future price movements. They offer bid and ask quotes and trade in either direction with their clients. As a result of such trades, and assuming the price remains constant, market makers earn the spread from each transaction. Price updates today are at a millisecond level and thus it can happen that the market maker trades (out of a long position) at a lower price than the one they entered at. Such a trade results in a loss if the charged spread was not wide enough to cover such a movement. Therefore, by offering liquidity, the market maker is subject to an inventory risk, which can be mitigated by adjusting his quotes and/or crossing the spread to actively hedge out his position. Pioneers of this line of research are Garman [40] and Amihud and Mendelson [3, 4].

On the other hand, a second line of research has its focus on adverse selection, asymmetric information, client alpha and price direction. Such optimal quoting problems have been extensively studied since the late '80s (cfr. Kyle [59]). The goal was to find the optimal bid and ask quotes to trade a security, given partial information about its future value.

In the context of an order driven market, such a problem has recently been studied by Guilbaud and Pham [47]. They assume that a market maker posts limit

orders on both sides of the book and submits market orders when its inventory becomes critically small or large.

Main Contributions: The research presented in this thesis can be positioned in the framework of inventory-risk. We consider a firm which offers quotes to its clients. It also intersects the more recent research on order-driven markets in that such a firm can hedge out its position by means of limit and market orders. At the time of this writing we are not aware of other similar works. We find the optimal pricing and hedging strategies the firm should follow, and we present our results in Chapter 4. In the same context, we provide an application of the above framework to the foreign exchange market in which one and three currency pairs are traded. We propose a mixed principal and agency execution offered by a firm to its clients. The foreign exchange literature is very limited in itself and currency-pair trading in an order-driven market is rather unexplored territory as of now. We find the optimal principal versus agency proportion of liquidity that should be offered to clients as well as the hedging strategy the firm should follow. In this last application, we further (implicitly) consider an element of price discovery and adverse selection when, e.g., we allow for features such as permanent impact and mean reversion of the price process. These additional features position the work presented in Chapter 5 in the intersection of the two research lines discussed above.

1.3 Structure of the thesis

This thesis consists of six main chapters. The original work is presented in Chapter 2, in particular Section 2.3.2, and in Chapters 3, 4, 5 and 6. The remainder of Chapter 2 gives the reader an overview of the problems at hand, and in Chapter 7 we collect the main mathematical tools utilised throughout the thesis. While we provide proofs specific to the original models presented here, such results are not original in the sense that standard techniques are applied, and thus we do not wish to refer to them as being ‘original’ work. This thesis is structured as follows:

In Chapter 2 we provide four reference models for both optimal execution and optimal market making, with and without the presence of a dark pool as an alternative trading venue. We start the chapter by refreshing some order-driven market terminology and, in Section 2.2, we introduce the optimal-execution and market-making problems when only a lit pool is available to market participants. In the optimal-execution case, the goal is to find the optimal trading schedule of an agent who wishes to execute a sizeable amount of shares over a finite period of time. We provide a reference model and we show the optimal strategy, which we obtain numerically. Next, we introduce the market-making problem faced by an agent who submits limit orders on both sides of the book and is subject to an inventory risk (associated with future price movements) throughout the activity. The agent can hedge his position by crossing the spread via the submission of market orders. The optimal strategy is shown and its features are discussed. Next we move to Section 2.3 where we assume the presence of a dark pool, and we revisit the optimal-liquidation and optimal market-making problems within this new setting. In the optimal execution case, the agent can post simultaneously in both venues. With regard to the market-making problem, we switch our vantage point and assume that a firm (which shares similarities with modern dark pools) offers tailored prices which are only visible to its clients. Such a firm, which is also subject to an inventory risk, can hedge its position in a standard exchange by submitting both limit and/or market orders. This latter problem (cfr. Section 2.3.2) is a novelty in the literature and as-such is part of the original work presented in this thesis. The models analysed in this chapter do not aim at capturing realistic market features, for they are only meant to provide the reader with the basic tools and concepts that will be largely utilised later in the thesis. In light of such a goal, the mathematical complexity has been reduced to a minimum.

In Chapter 3 we take the perspective of an agent who wishes to liquidate or acquire a substantial number of shares. We consider structured price dynamics and, in Section 3.2, we start by analysing the situation where the agent is only allowed to trade in a ‘lit’ pool. When mentioning a ‘lit’ market, we refer to an accessible venue with full transparency and a limit order book publicly available for trading. In such a venue the execution is certain, since we assume the agent

trades by means of market orders only. We find the optimal trading schedule of the agent and compare it with the one shown in Chapter 2. In Section 3.3, we consider an optimal simultaneous execution in ‘lit’ and dark pools. In the latter venue the liquidity is hidden and trades take place at the ‘lit’-pool mid-price. Here anonymity is preserved, and price impact is avoided. As a shortcoming, execution is not guaranteed, for it is subject to the existence of a trading counterparty. We take as a reference model the work by Kratz and Schöneborn [57] and we consider the following modifications: (i) more realistic price dynamics which incorporate empirically observed market features, (ii) presence of permanent price impact when trading in the ‘lit’ pool, and (iii) optionality of partially filled orders submitted to the dark pool. We show, and provide a financial interpretation to, the optimal trading schedule in each venues. This chapter is based on Crisafi and Macrina [30].

In Chapter 4 we consider a firm which provides two-way liquidity to its clients and optimally chooses the spread it charges for offering such a service. Such a spread is also a function of the order size, since we assume that larger orders should be executed at a wider spread. We consider a jump process for the ‘lit’ pool mid-price and a continuous-time Markov chain with a discrete state space for the spread process. The firm is subject to an inventory risk, which can be mitigated by skewing the quotes offered. In addition, the firm can resort to the ‘lit’ exchange to actively exit its position. In particular, the firm can post limit orders in the standard exchange, of which execution is uncertain, but from which the firm benefits due to advantageous prices. The firm may also cross the spread and post expensive market orders. Limit orders posted for hedging purposes need not to be placed on top of the book. We numerically solve the derived system of quasi-variational inequalities and we graphically show the optimal strategy of the firm. Finally, we comment on the empirical terminal-cash distribution, which we obtain by Monte Carlo simulations. This chapter is based on Crisafi and Macrina [31].

In Chapter 5 we further extend the framework presented in Chapter 4 by including the possibility for the firm to execute only a portion of the client’s order principally, i.e. as a market maker, while trading the remaining part in the

standard exchange on behalf of the client. Analogous to Chapter 4 the firm is subject to an inventory risk, which can be mitigated by (i) skewing its prices, (ii) offering asymmetric percentages of principal liquidity and (iii) crossing the spread in the standard exchange via market orders. We consider the foreign exchange market and present models for trading one and three currency pairs. We show the optimal principal strategy, that is, the optimal portion of order to be executed principally, and the hedging strategy of the firm.

In Chapter 6 we summarise the results obtained in this work and suggest further directions this research may take. Finally, in Chapter 7, we provide a brief description of the viscosity solution theory and we give the pseudocodes we use to numerically solve the HJB equations stated in the thesis.

Chapter 2

Reference models

2.1 Overview of the chapter

In this chapter we provide an introduction to the optimal execution and the optimal market making problems. We start by describing the functioning of ‘lit’ pools, namely (i) the different types of order that can be sent to such pools, and (ii) the different types of agent that trade regularly within those venues. We then provide reference models for the aforementioned trading situations, which are the object of study of this thesis. We finally introduce the concept of dark pools, their main features and the associated reference models for both trade execution and market making.

In what follows we consider a probability space $(\Omega, \mathcal{F}, \mathbb{P})$ equipped with a filtration $\{\mathcal{F}_u\}_{0 \leq u \leq T}$ satisfying the usual conditions, such that all the processes specified below are taken to be $\{\mathcal{F}_u\}$ -adapted.

2.2 ‘Lit’ pool and its terminology

Market participants can send passive or aggressive orders to the ‘lit’ pool. *Passive orders* (or *limit orders*) specify the quantity and the price at which the posting agent wants to buy or sell. Such orders are recorded in the limit order book (LOB) until they are executed or cancelled. The highest price at which an

investor is willing to buy (or, equivalently, a limit buy order is posted) is called the *best bid price*, and the lowest price at which an investor is willing to sell (or, equivalently, a limit sell order is posted) is called the *best ask price*. The difference between the best ask and the best bid prices is called *spread* and their arithmetic average is called *mid-price*. The latter is a theoretical quantity and is not a tradable price in most standard exchanges (exceptions include mid-matching orders for foreign exchange trading in electronic crossing networks). Limit orders are filled by *aggressive orders* (or *market orders*), which only specify quantities that wish to be traded, and are to be executed at the best available LOB prices. In particular, market buy (sell) orders are matched with limit sell (buy) orders. Most exchanges follow the price-priority rule. That is, limit orders at a more favourable price are executed first. When multiple limit orders are posted at the same price, the first-in-first-out rule applies (time priority). Investors who post limit orders are called *liquidity providers*, while investors who submit market orders are called *liquidity takers*. A market order is expensive and the agent pays the spread, while the latter can be earned through limit orders. On the other hand, a market order benefits from sure execution (provided that there is enough liquidity in the LOB), while a limit order may not be executed. *Crossing the spread* is an alternative definition of submitting market orders and *walking the book* is the action of moving the best price available via aggressive trading. Such a movement is called *price impact* (or *slippage*), which can be temporary and/or permanent. We distinguish between two main classes of market participants that operate in ‘lit’ pools. *Buy-side* agents, who trade only in one direction at any given time, and *sell-side* agents or *market makers*, who post limit orders on both sides of the LOB to earn the spread. The former agents need to solve an optimal execution problem to find their optimal trading schedule, while the latter need a model for optimal market making. In what follows, we provide reference models for both types of agent.

2.2.1 An introduction to optimal execution

The current literature on optimal execution in an order-driven market is vast and interesting. Research in the field has its roots in the papers by Almgren

and Chriss [2], and Bertsimas and Lo [10]. More recent contributions include, e.g., Pemy and Zhang [72], Pemy et al. [73], Gatheral and Schied [41], Brigo and Di Graziano [12], Moazeni et al. [67], and Cartea et al. [22]. Cartea and Jaimungal [20] consider a continuous-time, jump-diffusion mid-price model and explicitly take into account the impact of the market activity on the mid-price. In the same context, we also mention the works by Guéant et al. [44], and Bayraktart and Ludkovsky [7], who treat optimal liquidation via limit orders. Microstructural features of optimal trading in LOBs are, for example, treated in (i) Cartea and Jaimungal [19], who model the spot price via a hidden Markov chain to capture the switches between price regimes, (ii) Cartea et al. [24], who model the deviation of mid-price from its long-term mean via a jump-diffusion process, and (iii) Obizhaeva and Wang [69] and Alfonsi et al. [1], who propose trading strategies by modelling the LOB's depth.

Here we describe a simple model based on Cartea et al. [23], which serves as a building block for the next chapters. We consider an agent who wants to execute a sizeable trade by means of aggressive orders in a 'lit' pool. We assume that there is enough liquidity in the LOB to match their market orders at any point in time. They execute existing limit orders and impacts the best price, making their subsequent trades less profitable. The agent's trades are subject to both permanent and temporary price impacts. For explanation purposes, we restrict our attention to optimal liquidation, while keeping in mind that optimal acquisition is analogous. The goal is to find the optimal selling schedule that maximises their performance criterion.

2.2.1.1 A reference model

In this section we provide a base model that is useful for comparison with the ones proposed in the following chapters. We assume that the agent trades on a continuous-time basis between a starting time $t \geq 0$ and a terminal date T , and we denote by $\nu := \{\nu_u\}$ their selling rate. The LOB best bid price is subject to both a permanent and a temporary price impact derived by the agent's trades.

In particular, the permanently impacted best bid price satisfies

$$dS_u^b = -\mu\nu_u du + \sigma dW_u, \quad (2.1)$$

where $\{W_u\}$, for $u \geq t$, is a standard Brownian motion, the initial price level is $S_t^b = s^b$ and $\mu \geq 0$. An assumption that is usually made, see e.g. Almgren and Chriss [10], is that the investor will get the trade orders executed at a price that includes an instantaneous impact commensurate to the liquidation rate ν . This feedback effect is commonly referred to as *temporary impact*. The temporarily impacted best bid price \hat{S}_u^b is given by

$$\hat{S}_u^b = S_u^b - \beta\nu_u, \quad (2.2)$$

where $\beta \geq 0$. The temporary price impact happens when the quantity posted at the best-price level is not sufficient to fill the the incoming aggressive order. Hence, by (potentially) exhausting multiple book levels, the resulting price received by the agent may be less than the current best bid price.

Finally, the agent's inventory evolves according to

$$dX_u = -\nu_u du, \quad (2.3)$$

and starts at an initial size $X_t = x \geq 0$. The agent has a performance criterion that they wish to maximise by optimally choosing their trading schedule (i.e. the process $\nu_u, \forall u \in [t, T]$). Such a criterion can include a variety of components in order to reflect the preferences specific to that particular agent. In this context we assume that the agent wants to maximise their total revenues subject to: (i) a running penalty for holding the inventory throughout the whole liquidation period, and (ii) a penalty for failing to liquidate their entire inventory by T . The former penalty models the urgency of the agent for liquidating the inventory, while the latter penalty can be interpreted as the reluctancy of the agent to terminate the trading period with a non-zero inventory. Further details are given below. We write for the value function

$$V(t, \mathbf{x}) = \sup_{\nu} \mathbb{E}_{t, \mathbf{x}} \left[\int_t^{\tau} (\hat{S}_u^b \nu_u - \phi X_u^2) du + (S_{\tau}^b - \alpha X_{\tau}) X_{\tau} \right], \quad (2.4)$$

where α and ϕ are non negative constants, and $\mathbf{x} := (x, s^b)$ is a vector of state variables¹. The stopping time τ , defined by

$$\tau := \inf\{u \geq t \mid X_u \leq 0\} \wedge T, \quad (2.5)$$

indicates the first time the inventory is depleted or the terminal date, whichever comes first. That is, the agent stops trading as soon as their inventory reaches zero, if that happens before T . Equation (2.4) will be used throughout the thesis, hence it is worth commenting on the meaning of each of its components. The quantity $\hat{S}_u^b \nu_u$ models the instantaneous revenues due to the sale of the shares. Indeed, the rate of trading ν_u is multiplied by the temporary impacted bid price. This reflects the fact that there may not be enough liquidity posted on the first level of the book to satisfy the order of size ν_u and thus the agent's aggressive order may exhaust multiple levels. The higher the rate of trading, the higher the number of levels taken from the book. This is incorporated in the functional form of \hat{S}_u^b in (2.2). The quantity ϕX_u^2 models the running penalty for holding the inventory. In other words, ϕ is a measure of the urgency of the agent. The higher ϕ , the sooner the agent wants to liquidate their inventory. The quantity $S_\tau^b X_\tau$ represents the terminal theoretical value of the shares at time τ . Such quantity is different from zero only if $\tau = T$ and $X_T > 0$. In fact, if $\tau < T$, then $X_\tau = 0$ —by definition of the stopping time τ —and the liquidation task is over. The analogous holds for the quantity $-\alpha X_\tau^2$, which is non-zero only if $\tau = T$ and $X_T > 0$. Such a quantity models the terminal penalty for holding the inventory. We interpret it as the ‘disappointment’ of the agent who failed to liquidate their whole inventory. We would like to remark that the expression $(S_\tau^b - \alpha X_\tau)$ is not necessarily to be intended as the price at which the remaining shares are evaluated, since that could easily be negative for X_τ and α sufficiently large.

Standard techniques from dynamic programming principle² (DPP) suggest that the value function $V(t, \mathbf{x})$ should satisfy the following Hamilton-Jacobi-Bellman

¹Throughout the thesis we refer to the vector of state variables by the notation \mathbf{x} , which may take different meanings within different models, depending on the state variables considered for the particular model. We always state explicitly the components of the vector \mathbf{x} .

²See, e.g., Pham [75].

(HJB) partial differential equation:

$$\sup_v \left\{ (s^b - \beta v)v - \phi x^2 + \frac{\partial V}{\partial t}(t, \mathbf{x}) - \mu v \frac{\partial V}{\partial s^b}(t, \mathbf{x}) + \frac{1}{2} \sigma^2 \frac{\partial^2 V}{(\partial s^b)^2}(t, \mathbf{x}) - v \frac{\partial V}{\partial x}(t, \mathbf{x}) \right\} = 0, \quad (2.6)$$

with terminal condition $V(\tau, \mathbf{x}) = (s^b - \alpha x)x$ and boundary condition $V(u, 0, s^b) = 0$.

Remark 2.1. The HJB equation (2.6) is a special case of the more general model discussed in the appendix, Section 7.1. The steps for its derivation are provided in details therein. The above applies to all the HJB equations presented in this thesis.

The functional form of the terminal condition (used to formulate an appropriate ansatz), together with the linearity of the impact functions (i.e. $\beta \nu_u$ and $\mu \nu_u$) and the continuous price process dynamics result in the possibility of finding a closed-form solution for Equation (2.6). An explicit expression for the optimal strategy $\{\nu_u\}$ and the remaining inventory $\{X_u\}$ deriving from (2.6) are given by³:

$$\nu_u = \gamma \frac{\zeta e^{\gamma(T-u)} + e^{-\gamma(T-u)}}{\zeta e^{\gamma T} - \zeta e^{-\gamma T}} x, \quad X_u = \gamma \frac{\zeta e^{\gamma(T-u)} - e^{-\gamma(T-u)}}{\zeta e^{\gamma T} - \zeta e^{-\gamma T}} x, \quad (2.7)$$

where

$$\gamma = \sqrt{\frac{\phi}{\beta}}, \quad \zeta = \frac{\alpha - \frac{\mu}{2} + \sqrt{\beta \phi}}{\alpha - \frac{\mu}{2} - \sqrt{\beta \phi}}, \quad (2.8)$$

and x is the initial inventory level. Equation (2.7) is a deterministic function of time and of the model parameters. In what follows, for consistency with the remainder of the thesis, we graphically show the optimal strategy for various parameters' values and comment on their roles.

2.2.1.2 Numerical results and parameters' analysis

In this section we show how the trading schedule changes when the model parameters vary.

³We refer to Cartea et al. [23], pages 144-146, for the details of the steps sufficient to achieve a closed-form solution of (2.6).

Remark 2.2. We numerically solve Equation (2.6)—which describes the local behaviour of the value function—and plot the optimal strategy of the agent. We then double-check the validity of our algorithm with Equation (2.7).

First, we find the optimal rate of trading v by applying first order conditions to Equation (2.6). Then we substitute the resulting expression for v in the HJB equation, in order to eliminate the sup operator (the method is standard and widely used in, e.g. Cartea et al [23]). Finally, we employ a standard finite difference method to solve the resulting, highly non-linear, PDE. We define time and space grids, and apply the terminal and boundary conditions to the relevant grid points. We then proceed backwards in time to determine further points in the grid via a discretisation of the HJB equation (2.6). We thus are able to approximate the value function and the optimal strategy of the agent. This method is used throughout this chapter and we refer to the above high-level view of the methodology for all the numerical results shown herein. Boundary and terminal conditions are stated below each HJB equation, and parameters values are reported below each plot.

Throughout this section, we consider an equally-spaced time grid $[0,10]$ with intervals of 0.01, an equally-spaced price grid $[0,10]$ with intervals of 0.1 and an equally-spaced inventory grid $[0, 30]$, with intervals of 1.

We start by analysing the role of α and ϕ .

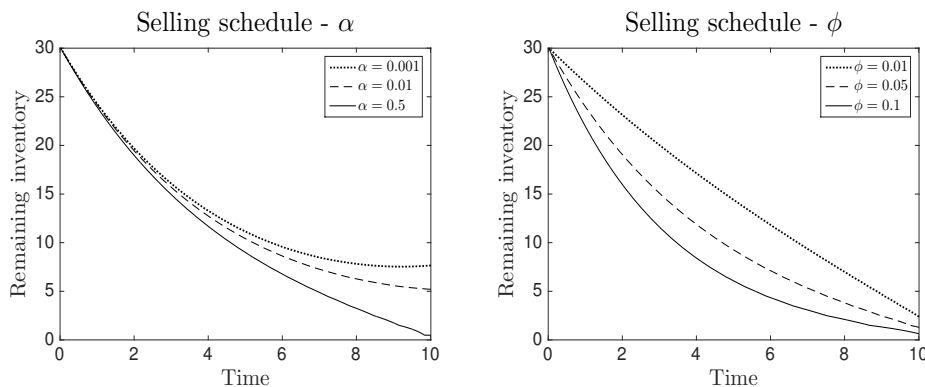


FIGURE 2.1: Optimal selling strategy—displayed as a function of the remaining inventory—found by solving the HJB equation (2.6). We set $\sigma = 0.1$, $\beta = 0.1$, $\mu = 0.01$, $x = 30$, $s^b = 8$, $T = 10$. In the left panel we set $\phi = 0.005$. In the right panel we set $\alpha = 0.1$

In Figure 2.1 we plot the evolution of the inventory for different values of α (left panel) and ϕ (right panel). As α increases, the agent is motivated to liquidate a bigger portion of their inventory by T . Higher values of ϕ incentivise the investor to liquidate faster at the beginning, as a consequence of the higher reductions of the value function when holding a large inventory throughout the whole period.

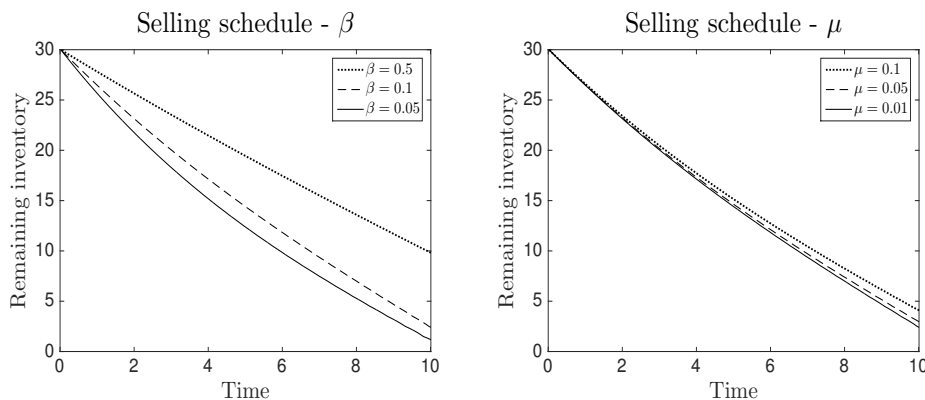


FIGURE 2.2: Optimal selling strategy—displayed as a function of the remaining inventory—found by solving the HJB equation (2.6). We set $\sigma = 0.1$, $x = 30$, $s^b = 8$, $\alpha = 0.1$, $\phi = 0.001$, $T = 10$. In the left panel we set $\mu = 0.01$. In the right panel we set $\beta = 0.1$

In Figures 2.2 we show how the optimal selling schedule changes, when different values of the temporary (left panel) and permanent (right panel) impacts are considered. When the impacts decrease, the agent liquidates a bigger portion of their inventory by the terminal date T . This confirms the intuition that the agent refrains from placing large orders (when the market impact is high) as to avoid slippage: a feature that makes their trades progressively less profitable.

Our conclusion on the above reference model on optimal liquidation can be summarised as follows. The agent wishes to liquidate their inventory by T , though there is no obligation to do so. This feature is modelled by the parameters α and ϕ , which penalise the agent for holding inventory (at maturity and throughout the whole period, respectively). The agent's liquidation urgency is modelled by the parameters α and ϕ . In particular, we observe the following: (i) the higher α , the smaller the remaining inventory at T , and (ii) the higher ϕ , the faster the liquidation during the initial period. On the other hand, higher price impacts reduce the selling rate of the agent by making the liquidation process more expensive. A variation of the above model consists in constraining the inventory to

be zero by T , i.e. by setting $x = -\int_t^T \nu_u du$. This gives rise to a singular terminal condition where $\lim_{t \rightarrow T} V(t, \mathbf{x}) = 0 \mathbb{1}_{\{x=0\}} - \infty \mathbb{1}_{\{x \neq 0\}}$. Within this alternative model, the coefficients μ and β have no impact on the amount of inventory liquidated by T , while ϕ determines the selling impatience within the considered time frame. A very similar feature is obtained, in the present framework, by setting a sufficiently large α (see Figure 2.1—left panel—for $\alpha = 0.5$). In fact, from Equation (2.7), we have $\lim_{\alpha \rightarrow +\infty} X_u = \sinh(\gamma(T-u)x / \sinh(\gamma T))$. Hence, for $u = T$, we have $X_T = 0$, which means that no remaining inventory is held at time T . This is not surprising, since by setting $\alpha = +\infty$, we have recovered the aforementioned singular terminal condition, i.e. $\lim_{t \rightarrow T} V(t, \mathbf{x}) = 0 \mathbb{1}_{\{x=0\}} - \infty \mathbb{1}_{\{x \neq 0\}}$.

2.2.2 An introduction to the market-making problem

As opposed to the agent whose goal is to find the optimal strategy to buy or sell a large amount of an asset, a market maker does not trade in one direction only. They post limit orders on both sides of the book, thus selling at the higher rate and buying at the lower rate. Throughout their activity, the market maker may hold an inventory (which may be negative in the case of short-selling), which is associated to a risk coming from future price uncertainty as well as better information that the market-maker's counterparties may have. If the inventory surpasses a (optimal) threshold, we assume that the market maker themselves crosses the spread—by submitting aggressive orders—until the inventory is rebalanced and set within the acceptable level. At the end of the trading period, say T , the market maker wishes to have a neutral position (equivalently, a zero inventory) and is subject to a penalty proportional to the amount of asset held at T . Previous work on market making includes Amihud and Mendelson [3] who, based on Garman [42], relate the bid-ask prices to the share holding of a risk-neutral agent. They find a relationship between the optimal quotes and the distance from the “preferred” inventory position. Stoll [83] considers a two-period model in which a risk-averse agent supplies liquidity and maximises their expected utility. Ho and Stoll [51] utilise the DPP to obtain the optimal quotes which maximise the terminal wealth in a single-dealer market. The recent evolution in financial markets, arising with algorithmic and high-frequency trading, has

shifted the optimal market-making problem to trading in an order-driven market, where optimal quotes and trading strategies are computed and performed by electronic machines. For example, Avellaneda and Stoikov [5] consider a market-making problem in a limit order book. They consider the maximisation of the agent's utility function in both the finite and the infinite-time cases. They model the arrival of buy and sell orders by Poisson processes and the dynamics of the mid-price by an arithmetic Brownian motion. This type of problem has been investigated elsewhere, too. The works by Cartea and Jaimungal [20] on risk metrics and by Cartea et al. [18] consider ambiguity and Hawkes processes⁴, respectively. Guéant et al. [45] deal with the inventory risk and reduce a complex optimisation problem to a system of ODEs. Guilbaud and Pham [47] consider a market maker who continuously submits limit orders at the best quoted (or slightly better) prices and resorts to market orders when the inventory becomes too large. They numerically solve a finite-time impulse-control problem and find the optimal order sizes and quotes to be posted in the standard exchange.

As a reference model we here consider a mixture of (i) the market making problem treated in Cartea et al. [23], and (ii) a simplified version of the Guilbaud and Pham [47] framework. In particular, the following two modifications with respect to Cartea et al. [23] are employed: (i) the market maker does not choose the limit price and only posts on top of the book, and (ii) they can hedge their inventory through market orders. Compared to Guilbaud and Pham [47], we have: (i) unit-sized orders, (ii) continuous price process and constant market spread, and (iii) the market maker can only post on top of the book. The model described in Section 2.2.2.1 is for introduction purposes only and does not wish to be realistic. The modifications with respect to Cartea et al. [23] and Pham [47] are only made for simplicity of exposition. For example, the assumption regarding a constant half spread is unrealistic (in normal market conditions) and will, in fact, be removed in Chapter 4.

2.2.2.1 A reference model

We assume that the market maker trades within t and T , and continuously posts unit-sized limit buy and sell orders on top of the book. Such orders are assumed

⁴Hawkes processes are self-exciting processes introduced by Hawkes [49].

to be immediate-or-cancel (IOC) orders, that is either they are immediately executed, or the market maker cancels them and posts new orders at the (possibly updated) best bid and ask prices. We assume that the mid-price follows an arithmetic Brownian motion

$$dS_u = \sigma dW_u, \quad (2.9)$$

with initial state level $S_t = s$. We assume that the market has a constant half spread k , such that the best ask and bid prices are defined by

$$S_u^a = S_u + k \quad \text{and} \quad S_u^b = S_u - k, \quad (2.10)$$

respectively. We assume that the market-maker's inventory satisfies the following stochastic differential equation

$$dX_u = dN_u^- - dN_u^+, \quad (2.11)$$

where $X_t = x$ and $\{N_u^\pm\}$ are independent Poisson processes with intensities λ^\pm . The process $\{N_u^-\}$ models incoming market sell orders which fill the market maker's limit buy orders, while the process $\{N_u^+\}$ models incoming market buy orders which fill limit sell orders posted by the market maker.

Remark 2.3. The difference of two independent Poisson-distributed random variables is well-known to be distributed according to the Skellam distribution (Skellam [80]). As such, we could have written Equation (2.11) by a Skellam process for the sake of compactness. We chose the current non-compact formulation for ease of interpretation and for ease of comparison with the current relevant literature (e.g. Cartea et al. [23]).

Finally, we define the cash process by

$$dY_u = (S_u + k)dN_u^+ - (S_u - k)dN_u^-, \quad (2.12)$$

with initial state level $Y_t = y$. The inventory and cash equations are to be interpreted as follows. When the Poisson process $\{N_u^+\}$ jumps, a limit sell order is executed by an incoming aggressive buy order. The market-maker's inventory is reduced by one unit and their cash is increased by the amount $S_u + k$. The

analogous holds when $\{N_u^-\}$ jumps. We emphasise that this is not an optimal posting problem, i.e., the market maker does not choose the prices at which they post their limit orders. We remove such an assumption in Chapter 4.

At any time the market maker can choose whether they want to cross the spread in order to reduce their inventory. If, at time τ , a unit-sized market sell order is placed, the inventory and the cash amounts are modified as follows: $X_\tau = X_{\tau^-} - 1$, and $Y_\tau = Y_{\tau^-} + S_\tau - k$. If a market buy order is optimal, the inventory and the cash amounts become: $X_\tau = X_{\tau^-} + 1$ and $Y_\tau = Y_{\tau^-} - S_\tau - k$. Such expressions can be written concisely as

$$X_\tau = X_{\tau^-} + \xi_\tau \quad \text{and} \quad Y_\tau = Y_{\tau^-} - \xi_\tau(S_\tau + k\xi_\tau), \quad (2.13)$$

where $\xi_\tau \in \{-1, 1\}$.

Remark 2.4. Equations (2.11), (2.12) and (2.13) can be compactly written by

$$\begin{aligned} dX_u &= dN_u^- - dN_u^+ + \sum_i \delta(u - \tau_i) \xi_{\tau_i}, \\ dY_u &= (S_u + k)dN_u^+ - (S_u - k)dN_u^- - \sum_i \delta(u - \tau_i) \xi_{\tau_i} (S_{\tau_i} + k\xi_{\tau_i}), \end{aligned} \quad (2.14)$$

where $\delta(\cdot)$ is the Dirac delta function. More details can be found in Remark 7.1. In the remainder of the thesis we will use the non-compact notation, although we acknowledge that this remark applies to all the state-variables dynamics which can be subject to discretionary impulses.

Every time the market maker sends (expensive) aggressive orders, they reveal to other market participants the sign of their inventory. That is, a market sell order is a sign of holding a positive inventory, which they want to liquidate, and vice versa. The potential information leakage may push the price against the market-maker's inventory and therefore we find it suitable to add an additional fixed penalty $\epsilon > 0$, to which the market maker is subject to when they cross the spread. We choose a constant penalty for tractability of the model. Alternative specifications may include a penalty commensurate to the order size, as well as a time-dependent penalty (as opposed to an instantaneous penalty), of

which effect may decay with time. In the current setting, the former specification does not make a difference since orders are assumed to be unit-sized. The latter specification would be more appropriate if hedging was performed on a continuous-time basis as it would have an interpretation analogous to the one pertaining to permanent price impact.

Within the present model, the market maker aims to maximise their terminal cash subject to both terminal and running penalties for holding a non-zero inventory. their optimal strategy consists of a double sequence of stopping times τ_i and random variables⁵ ξ_i , for $i = 0, 1, 2, \dots$, which maximises their performance criterion:

$$V(t, \mathbf{x}) = \sup_{(\tau_i, \xi_i)_{i \geq 0}} \mathbb{E}_{t, \mathbf{x}} \left[Y_T + X_T(S_T - \alpha X_T) - \phi \int_t^T X_u^2 du - \sum_{t \leq \tau_i < T} \epsilon \right], \quad (2.15)$$

where $\mathbf{x} := (x, y, s)$ is the vector of state variables, corresponding to the inventory, the cash and the mid-price processes. This is an optimal impulse-control problem and the value function solves the following HJB quasi variational inequality (QVI)

$$\begin{aligned} \min \left\{ \phi x^2 - \frac{\partial V}{\partial t}(t, \mathbf{x}) - \lambda^+ [V(t, x-1, y+s+k, s) - V(t, \mathbf{x})] \right. \\ \left. - \frac{1}{2} \sigma^2 \frac{\partial^2 V}{\partial s^2}(t, \mathbf{x}) - \lambda^- [V(t, x+1, y-s+k, s) - V(t, \mathbf{x})]; \right. \\ \left. V(t, \mathbf{x}) - \mathcal{M}V(t, \mathbf{x}) \right\} = 0, \end{aligned} \quad (2.16)$$

with terminal condition $V(T, \mathbf{x}) = y + (s - \alpha x)x$ —see, e.g., Pham [75] for details.

The operator $\mathcal{M}V(t, \mathbf{x})$ in (2.16) is defined by

$$\mathcal{M}V(t, \mathbf{x}) = \sup_{e \in \{-1, +1\}} V(t, x+e, y-e(s+ke), s) - \epsilon. \quad (2.17)$$

Remark 2.5. The reason why Equation (2.16) is referred-to as an inequality is explained in Section 7.1, Remark 7.2.

The result of the above optimisation thus only consists of the thresholds which indicate—to the market maker—the inventory level at which it is optimal for

⁵We let ξ_i be the shorthand notation of ξ_{τ_i} .

them to cross the spread and post aggressive orders to rebalance their position (also known as *hedging*).

2.2.2.2 Numerical results and parameters' analysis

Next we study the behaviour of the optimal strategy for various values of parameters. The graphs of the present section show the optimal inventory thresholds for the entire trading period. The region between the two lines (labelled "Limit orders") shows the range of inventory for which it is optimal for the market maker to keep posting limit orders. As maturity is approached, the region shrinks due to the penalty to which the market maker is subject to, if they reach T with a non-zero inventory. If the inventory falls in the region above the upper line, then it is optimal to post market sell orders until the inventory is back in the limit-order region. If the inventory falls below the bottom line, the market maker starts posting aggressive buy orders. The market-order regions widen when the maturity is approached. This is due to the necessity to liquidate as much inventory as possible before T .

We can use an ansatz to reduce the number of state variables of Equation (2.16) and, in-particular, we set $V(t, x, s, y) = y + xs + h(t, x)$ and substitute it into Equation (2.16). We thus find, and numerically solve, the PDE satisfied by the function $h(t, x)$. (See (i) Cartea et al. [23], and (ii) Chapter 4, Section 4.3, of the present work for details and examples of such substitution, respectively). We use an explicit finite difference method to approximate the solution of Equation (2.16) and the optimal strategy of the market maker. Throughout this section, we consider an equally-spaced time grid $[0, 50]$ with intervals of 1 and an equally-spaced inventory grid $[-150, 150]$, with intervals of 0.1. The terminal condition is stated below HJB equation (2.16) and parameters' values are stated below each plot.

The parameter ϕ models the running penalty for holding the inventory. The higher the penalty, the sooner the market maker resorts to aggressive orders, so to rebalance their position on the asset. The numerical results confirm the

intuition, and Figure 2.3 shows that the limit-order region widens for a lower value of ϕ .

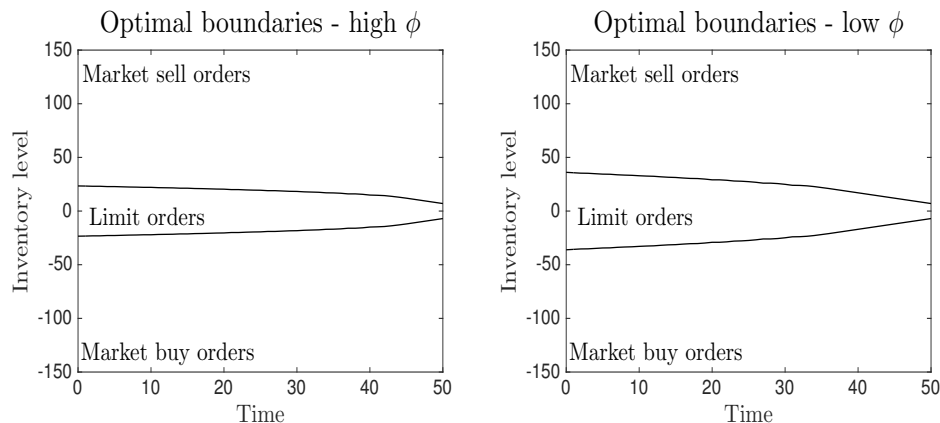


FIGURE 2.3: Optimal inventory thresholds found by solving the HJB equation (2.16). We set $k = 3$, $\alpha = 2$, $\lambda^+ = \lambda^- = 0.5$, $T = 50$, $\epsilon = 10$. In the left panel we set $\phi = 0.00001$. In the right panel we set $\phi = 0.0001$.

In Figure 2.4 we choose different values for the arrival-rates of buyers and sellers, who fill the market-maker's limit orders. We note that we lose the symmetry—around the line $X_u = 0$ —featured in Figure 2.3 and that the optimal boundaries are now skewed. In the left panel, buyers come more frequently than sellers and thus the optimal threshold at which the market maker starts posting aggressive buy orders is closer to zero. The opposite holds when the arrival-rate of the sellers is higher than the one of the buyers (right panel).

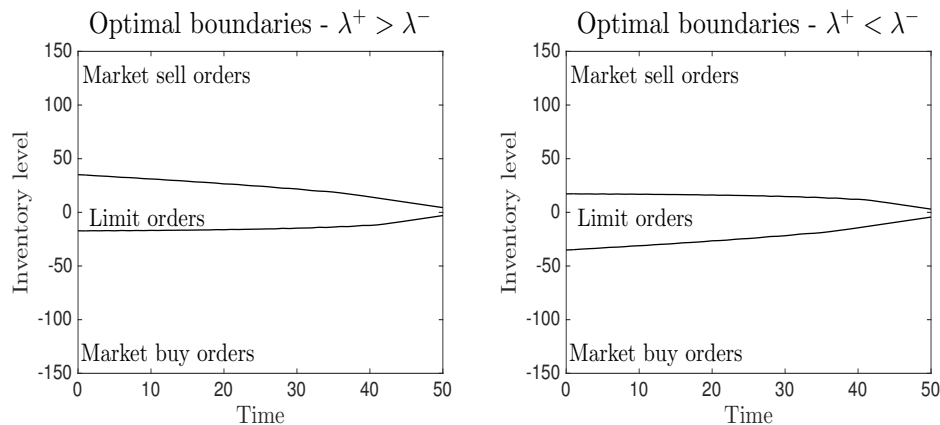


FIGURE 2.4: Optimal inventory thresholds found by solving the HJB equation (2.16). We set $k = 3$, $\alpha = 2$, $\phi = 0.0001$, $T = 50$, $\epsilon = 10$. In the left panel we set $\lambda^+ = 0.6$, $\lambda^- = 0.4$. In the right panel we set $\lambda^+ = 0.4$, $\lambda^- = 0.6$.

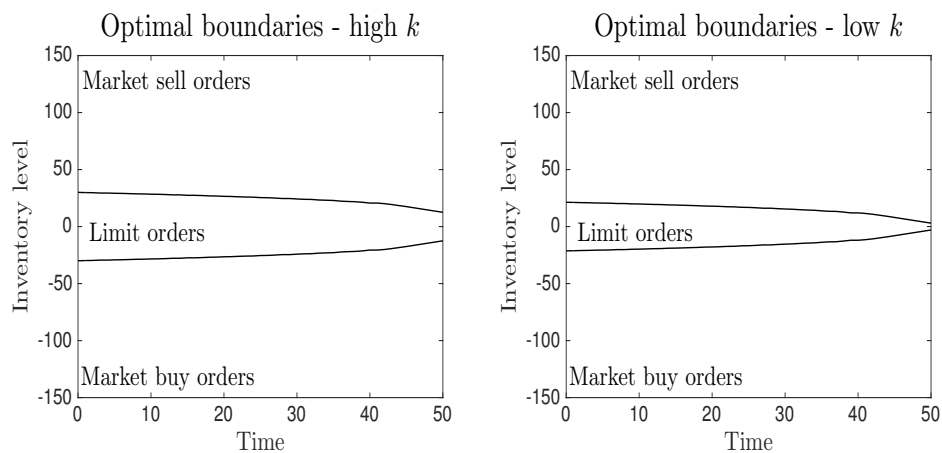


FIGURE 2.5: Optimal inventory thresholds found by solving the HJB equation (2.16). We set $\alpha = 2$, $\lambda^+ = \lambda^- = 0.5$, $T = 50$, $\epsilon = 10$, $\phi = 0.0001$. In the left panel we set $k = 5$. In the right panel we set $k = 1$.

The role of the parameter k is two-fold as it appears in both the earnings coming from limit orders as well as the costs for submitting market orders. In fact, when a passive order is posted (and executed), the submitting agent earns the spread, which is paid by the counterparty, who sent an aggressive order to the same market venue. We want to address the question of what a market maker should do when the spread widens. According to the numerical results, a higher spread incentivises the market maker to refrain from posting aggressive orders while keeping posting passive orders. This behaviour has two interpretations. (i) The earnings obtained through limit orders compensate both the running and the terminal penalties for holding the inventory. (ii) The submission of aggressive orders is very expensive in the scenario of a high spread k , and it offsets the benefits coming from reducing the inventory. Such a feature is shown in Figure 2.5, where for high k (left panel) the limit-order region is wider compared to the case where k is low (right panel).

Figure 2.6 shows the role of the parameter α , which models the penalty for holding a non-zero inventory at the end of the trading period. A higher α (left panel) incentivises the market maker to resort to aggressive orders sooner—by shrinking the limit-orders region—versus lower values of α (right panel).

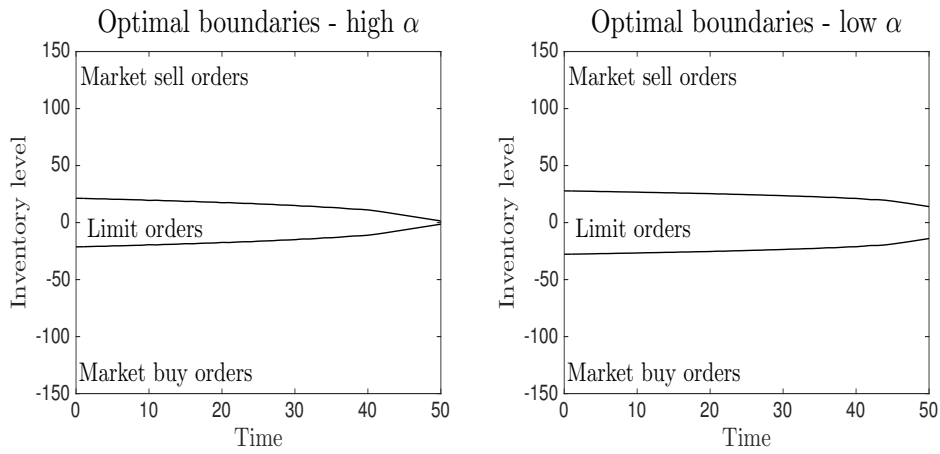


FIGURE 2.6: Optimal inventory thresholds found by solving the HJB equation (2.16). We set $k = 3$, $\lambda^+ = \lambda^- = 0.5$, $T = 50$, $\epsilon = 10$, $\phi = 0.0001$. In the left panel we set $\alpha = 5$. In the right panel we set $\alpha = 1$.

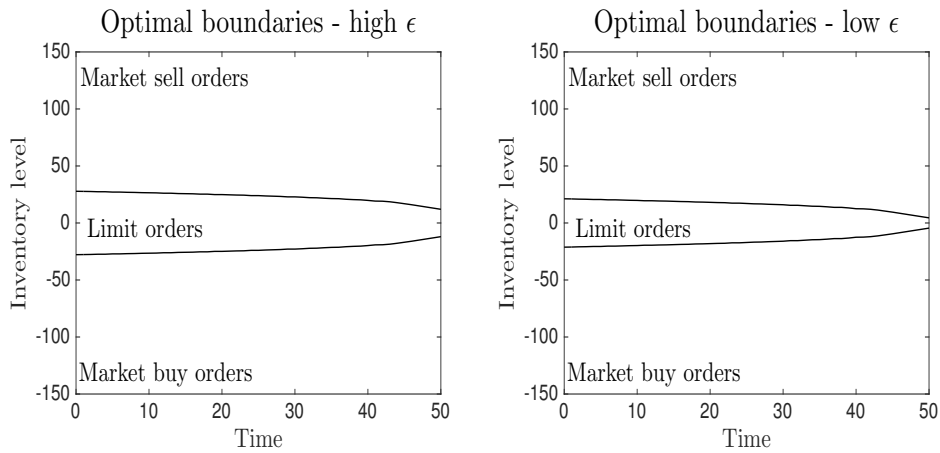


FIGURE 2.7: Optimal inventory thresholds found by solving the HJB equation (2.16). We set $k = 3$, $\lambda^+ = \lambda^- = 0.5$, $\alpha = 2$, $T = 50$, $\phi = 0.0001$. In the left panel we set $\epsilon = 20$. In the right panel we set $\epsilon = 1$.

Finally, we show that as ϵ (that is, the penalty for crossing the spread) increases, the market maker refrains from posting aggressive orders. Figure 2.7 shows this feature, and we can see a shrunk limit-order region for low values of ϵ (right panel).

We conclude this section by summarising the insights provided by such a reference model. The market maker earns the spread by posting limit orders and is subject to an inventory risk, derived by potential unfavourable price movements (e.g. the price decreases when they have a positive inventory and vice versa).

We note that the shape and the width of the optimal thresholds derive from such a tradeoff. The optimal strategy of the market maker consists of posting limit orders on both sides of the book, as long as the inventory does not surpass the critical boundaries. In the event that the inventory crosses one of the thresholds, the market maker posts aggressive buy or sell orders (when the inventory is negative or positive, respectively), until their holdings are back within an acceptable level. While the main purpose of this model is to construct a common ground for the discussion presented in the following chapters, we acknowledge that in the literature, see e.g. Cartea et al. [23, 24], optimal market-making problems are closely related to optimal-posting problems, where the market maker can choose the price at which their limit orders are posted. Such feature is included later in the thesis, in Chapter 4.

2.3 Dark pools

Dark pools are alternative trading venues where buy and sell orders are not displayed publicly. The introduction of dark pools was motivated by the existence of big institutional investors who wanted to trade large amounts of an asset with no impact on the market price, while also maintaining anonymity so to avoid information leakage. There are different types of dark pools and one way of distinguishing among them is to consider the amount of principal liquidity offered to the clients (see, e.g., Zhu [87]). There are dark pools which limit their activity to just offering the platform for trading, subject to the payment of a fee. Such pools match buyers and sellers at the ‘lit’-pool mid-price and are known as *crossing networks*. There is no guarantee of execution of orders sent to such types of dark pools, for each trade is subject to the availability of a counterparty. On the other hand, there are dark pools which trade principally with their clients and in-effect act as market makers. They guarantee anonymity to their clients and, loosely speaking, offer a tighter spread than the one available in ‘lit’ pools in order to be competitive and win more business. Analogously to ‘lit’-pool market makers, they charge the spread for client’s transactions and are subject to an inventory risk. In between these two categories, there are dark pools which trade both principally and as agents, possibly within the same

transaction. They earn the spread from the principal portion and a commission fee from the brokerage service. The firms belonging to latter two categories are commonly referred to as CLP or *broker-dealer firms*. The new European regulation due to take effect in January 2018—known as MiFID ii—will substantially reduce the anonymity granted to dark pool’s clients. In particular, monthly size caps will be implemented so to limit the opaque activity of market participants. Furthermore, reporting, clearing and transparency obligations will be in place for instruments that are less regulated to date. Although the new regulation will impact dark pools, the models presented in this thesis will still be relevant for the following reasons: (i) agents will still be able to trade within multiple venues, (ii) anonymity and opaqueness enter only marginally in the discussion and in the model design, and (iii) we propose flexible setups that provide high potentials for customisation.

To the best of our knowledge, at the time this thesis is being written, there are no references available for trading in CLPs. On the contrary, optimal execution within dark pools that limit their activity to third-parties orders’ match has been extensively studied in, e.g., Kratz and Schöneborn [57, 58]. In the next section, we outline a simplified model, inspired by Cartea et al. [23], as a reference for the class of models presented in Chapter 3. Next, we provide a toy model for the case in which the dark pool (CLP) operates as principal and provides liquidity to its clients. The last reference model is part of the original work presented in this thesis and we refer to Crisafi and Macrina [31]. A larger class of such models is thoroughly discussed in Chapter 4.

Research on dark-pool trading includes the early work by Hendershott and Mendelson [50], who extend the Kyle [59] model to capture the dynamics of the interplay between investors, dark pools and standard exchanges, followed by Degryse et al. [34], Buti et al. [14] and Daniëls et al. [32]. The works by Ye [86] and Zhu [87] examine the effects—on price discovery—of the migration of order flows from exchanges to dark pools. Increase in overall trading volume is shown in Buti et al. [15].

Kratz and Schöneborn [57] consider continuous-time trading in the dark pool within the classical field of optimal liquidation. They model the LOB mid-price

by an exogenous square-integrable martingale and regard the dark pool as a complete-or-zero-execution venue where the arrival of trading counterparties is modelled by a Poisson process. In this context, we also refer to work by Horst and Naujokat [52], in which the authors find the optimal strategy when trading in an illiquid market. The agent under consideration seeks to minimise the deviation from a given target, while submitting market orders in the standard exchange and “passive orders” in a dark pool.

2.3.1 Optimal trading in ‘lit’ and dark pools

We consider an agent who wants to liquidate a sizeable amount of an asset by means of both, (i) aggressive orders in the ‘lit’ pool, and (ii) dark-pool orders. The agent trades continuously in both venues and wishes to maximise their revenues while (i) minimising the price impact, and (ii) reaching the terminal date with as few shares as possible. The goal is to find the optimal selling schedule in both venues, which maximises the performance criterion of the agent.

2.3.1.1 A reference model

We assume that the ‘lit’-pool mid-price follows an arithmetic Brownian motion

$$dS_u = \sigma dW_u. \quad (2.18)$$

Trades in the ‘lit’ pool take place at the instantaneously impacted price $\hat{S}_u = S_u - \beta\nu_u$, where $\nu := \{\nu_u\}$ is the agent’s rate of trading in the ‘lit’ pool. The agent simultaneously posts sell orders in the dark pool, which may or may not be executed, depending on the availability of a trade counterparty. We assume that the execution price in the dark pool is the ‘lit’-pool mid-price. We model the arrival of dark-pool counterparties by a Poisson process $\{N_u\}$ with constant intensity λ . We define the agent’s inventory process by

$$dX_u = -\nu_u du - \eta_u dN_u, \quad (2.19)$$

where $\eta := \{\eta_u\}$ is a predictable process, which models the size of the orders placed in the dark pool at each time $u \in [t, T]$. We further define the cash process of the agent by

$$dY_u = \nu_u \hat{S}_u du + \eta_u S_u dN_u. \quad (2.20)$$

The constant-intensity assumption is an unrealistic one. Market generally sees activity bursts followed by periods of relative calmness. On the other hand, a random intensity would reduce the tractability of the model. The agent aims to maximise their expected terminal cash, subject to both terminal and running penalties for holding a positive inventory. We define the value function by

$$V(t, \mathbf{x}) = \sup_{\nu, \eta} \mathbb{E}_{t, \mathbf{x}} \left[Y_\tau + X_\tau (S_\tau - \alpha X_\tau) - \phi \int_t^\tau X_u^2 du \right], \quad (2.21)$$

where α and ϕ are non-negative constants and $\mathbf{x} := (x, y, s)$ is a vector of state variables. The stopping time τ is defined by Equation (2.5), and it is needed since the agent may terminate their liquidation task well before the terminal date T (provided there is enough liquidity available in the dark pool). The value function $V(t, \mathbf{x})$ satisfies the HJB equation

$$\sup_{v, n} \left\{ -\phi x^2 + \frac{\partial V}{\partial t}(t, \mathbf{x}) + \lambda [V(t, x - n, y + ns, s) - V(t, \mathbf{x})] \right. \\ \left. + \frac{1}{2} \sigma^2 \frac{\partial^2 V}{\partial s^2}(t, \mathbf{x}) - v \frac{\partial V}{\partial x}(t, \mathbf{x}) + v(s - \beta v) \frac{\partial V}{\partial y}(t, \mathbf{x}) \right\} = 0, \quad (2.22)$$

with terminal and boundary conditions given by $V(\tau, \mathbf{x}) = y + x(s - \alpha x)$ and $V(u, 0, y, s) = y$, respectively. A closed-form solution, together with the techniques to obtain it, is provided in Cartea et al. [23], pages 178-181. In particular, the optimal strategy $(\{\nu_u\}, \{\eta_u\})$ is given by

$$\nu_u = -\frac{X_u \left(\zeta^- - \zeta^+ \bar{\zeta} e^{-\gamma(T-u)} \right)}{\beta \left(1 - \bar{\zeta} e^{-\gamma(T-u)} \right)}, \quad \eta_u = X_u, \quad (2.23)$$

and the remaining inventory is given by

$$X_u = e^{\zeta^- u/\beta} x \frac{1 - \bar{\zeta} e^{-\gamma(T-u)}}{1 - \bar{\zeta} e^{-\gamma T}}, \quad (2.24)$$

where

$$\zeta^\pm = \frac{\beta\lambda}{2} \pm \sqrt{\frac{\beta^2\lambda^2}{4} + \beta\phi} \quad \text{and} \quad \bar{\zeta} = \frac{\alpha + \zeta^-}{\alpha + \zeta^+}. \quad (2.25)$$

Here, for consistency with the remainder of the thesis, we graphically show the optimal trading schedule and comment on the roles played by the model's parameters.

2.3.1.2 Numerical results and parameters' analysis

In this section we provide a numerical analysis of the agent's optimal liquidation strategy, and how it changes when the model parameters vary. In the plots below we show the inventory trajectories over time. In each plot, the dotted line shows the inventory evolution if no dark-pool execution takes place throughout the whole period. The solid line shows the effect of one dark-pool execution at time $\tau = 5$. We note that, within this model, the agent places a small portion of the inventory in the 'lit' pool and *all* the remaining shares in the dark pool. That is, the liquidation task ends as soon as the first dark-pool execution takes place. We note that the optimal strategy ceases to be convex. In fact the agent hopes to liquidate as much as possible in the dark pool, and thus starts by placing small orders in the 'lit' pool. The speed of the 'lit'-pool trading rate increases towards the end of the trading period due to the terminal penalty for holding the inventory.

Throughout this section, we consider an equally-spaced time grid $[0,10]$ with intervals of 0.01 and an equally-spaced inventory grid $[0, 30]$, with intervals of 1. The terminal and boundary conditions are stated below HJB equation (2.22) and parameters' values are stated below each plot.

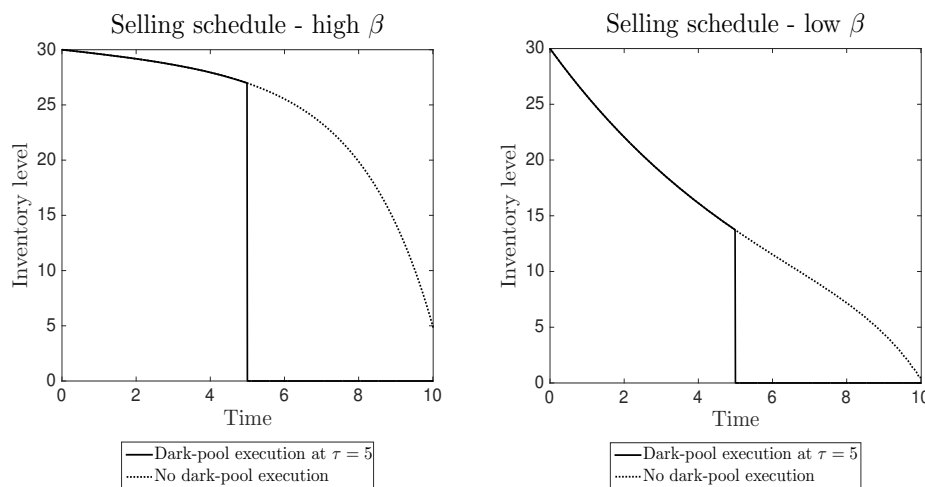


FIGURE 2.8: Optimal selling strategy—displayed as a function of the remaining inventory—found by solving the HJB equation (2.22). We set $\sigma = 0.1$, $s = 40$, $\lambda = 0.5$, $\alpha = 0.5$, $T = 10$, $\phi = 0.001$, $\tau = 5$. In the left panel we set $\beta = 0.2$. In the right panel we set $\beta = 0.01$.

In Figure 2.8 we see that β , i.e. the coefficient of the instantaneous price impact, dramatically changes the shape of the selling schedule. A low β (right panel) induces a faster liquidation in the ‘lit’ pool since the reduced impact makes the dark pool less attractive to the investor. The trading speed reflects such feature and increases in the case of low temporary price impact (left panel). Furthermore, we note that the liquidation task is almost fully achieved even in the case of no dark-pool executions (right panel, dotted line). This is not the case for a high β . In fact, the agent fails to liquidate a relevant portion of their inventory by T , if no liquidity is available in the dark pool (left panel, dotted line).

Next, we analyse the role of the terminal penalty for holding a non-zero inventory at T . The value function of the agent decreases proportionally to the square of the terminal inventory, and therefore a higher penalty increases the trading speed of the agent, so that the trading period can be concluded with a smaller inventory. Our intuition is confirmed in Figure 2.9, where we note that a higher α incentivises the agent to hold as few units of the asset as possible at T (left panel). We further note that the selling speed increases more towards the end of the trading period, rather than consistently between t and T . This is due to the presence of the dark pool, since the agent wishes to liquidate as much as possible in the alternative venue.

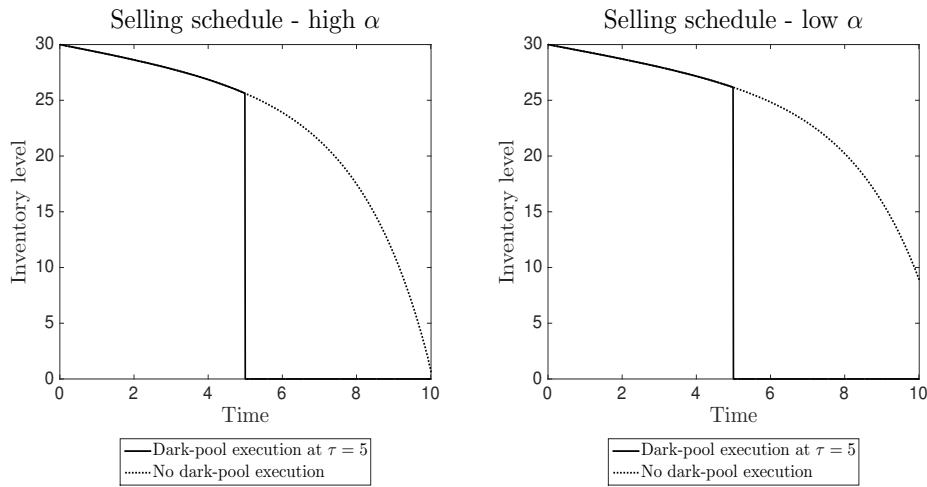


FIGURE 2.9: Optimal selling strategy—displayed as a function of the remaining inventory—found by solving the HJB equation (2.22). We set $\sigma = 0.1$, $s = 40$, $\lambda = 0.5$, $T = 10$, $\phi = 0.001$, $\tau = 5$, $\beta = 0.1$. In the left panel we set $\alpha = 3$. In the right panel we set $\alpha = 0.1$.

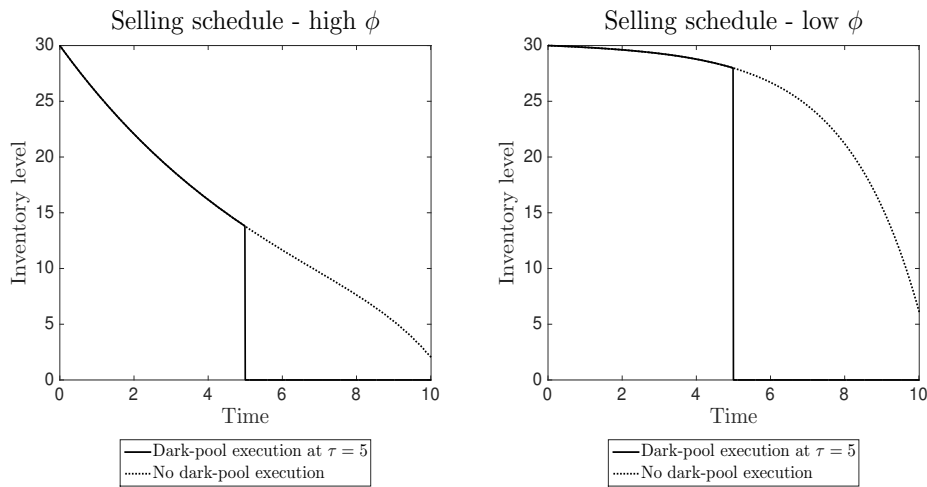


FIGURE 2.10: Optimal selling strategy—displayed as a function of the remaining inventory—found by solving the HJB equation (2.22). We set $\sigma = 0.1$, $s = 40$, $\lambda = 0.5$, $\alpha = 0.5$, $T = 10$, $\alpha = 0.5$, $\tau = 5$, $\beta = 0.1$. In the left panel we set $\phi = 0.01$. In the right panel we set $\phi = 0.0001$.

In Figure 2.10 we show how the selling schedule changes when we vary the parameter ϕ of the quadratic running penalty for the inventory holding. We note that a high ϕ increases the trading speed of the agent in the ‘lit’ pool from the beginning of the trading period.

The last parameter we focus on is λ , which models the arrival intensity of trading counterparties in the dark pool. In the right panel of Figure 2.11 we note that a low λ (that is, there is little to no liquidity in the dark pool) induces a faster

liquidation in the ‘lit’ pool. In particular, as $\lambda \rightarrow 0$, the trading trajectories approach the ones obtained when trading in the ‘lit’ pool only.

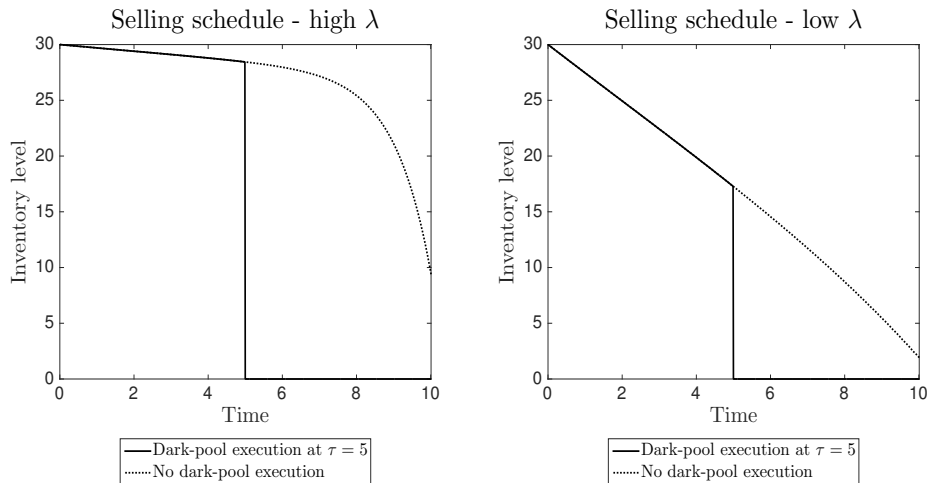


FIGURE 2.11: Optimal selling strategy—displayed as a function of the remaining inventory—found by solving the HJB equation (2.22). We set $\sigma = 0.1$, $s = 40$, $\phi = 0.001$, $\alpha = 0.5$, $T = 10$, $\alpha = 0.5$, $\tau = 5$, $\beta = 0.1$. In the left panel we set $\lambda = 1$. In the right panel we set $\lambda = 0.1$.

We can summarise our findings as follows. The trading trajectories in the ‘lit’ pool cease to be convex (i.e. the agent reduces their speed of trading in the ‘lit’ pool at the beginning of the period) since the agent is keen to liquidate as much of their inventory as possible in the dark pool so as to avoid price impact. One of the main features of the optimal selling strategy, which we derive by solving the HJB Equation (2.22), is that the agent always places an optimal portion of the asset in the ‘lit’ pool and *all* the remaining inventory in the dark pool at all times. In Chapter 3, where we propose price dynamics with more structure, we present cases where this feature ceases to be true. Finally, we note that the permanent price impact is not treated in the present model. Its effects are studied in Chapter 3.

2.3.2 Dark pools as market makers

In this section we explore the optimal trading strategies of a dark pool that plays the role of a market maker. Here, we use the terms *dark pool*, *CLP* and *broker-dealer firm* interchangeably. As opposed to the previous section, where

the dark-pool activity was limited to matching third-party orders, here the CLP offers liquidity to buyers and sellers, and we refer to such activity by saying that the CLP trades *principally*. Within this basic model, we assume that the CLP trades 100% principally, thus transferring internally the whole inventory risk. This assumption is removed in Chapter 5.

The CLP provides bid and ask quotes to its clients and earns the spread from each transaction. We assume that the spread offered by the CLP is tighter than the one shown in the ‘lit’ pool. Clients are incentivised to trade in the CLP, since they are offered advantageous prices, while also preserving their anonymity. Furthermore, such a feature increases the competitiveness of the venue compared to similar liquidity providers. The assumption that the dark-pool spread lies within the ‘lit’-pool one at any time is an unrealistic one. In fact, this does not need to be the case, and it is not true when the CLP holds a non-zero inventory. In the simplified model presented below, this is not an issue since we consider both the dark-pool quotes and the ‘lit’-pool spread to be constants. Such assumptions are removed in Chapter 4.

Throughout its activity, the CLP is subject to an inventory risk, which can be reduced by submitting limit and/or market orders in the ‘lit’ pool. We sometimes refer to such activity as *hedging*. We assume that the CLP is subject to a penalty every time it resorts to the ‘lit’ venue, so to model the potential information leakage the CLP would suffer. In particular, publicly displaying its orders on a regular exchange may give insights to other market participants into the dark-pool inventory and, thus, the market trend.

In the next section we provide a simplified version of the model presented in Chapter 4 and we show the optimal inventory thresholds, which provide the dark-pool trading strategy.

2.3.2.1 A reference model

We assume that the CLP trades within the time interval $[t, T]$, and executes unit-sized buy and sell orders submitted by its clients⁶. We assume that the

⁶A unit-size order can be interpreted/changed to one lot or a fixed size with no added complexity. We prefer to keep it to one, to reduce the numbers of parameters to a minimum.

‘lit’-pool mid-price follows an arithmetic Brownian motion

$$dS_u = \sigma dW_u, \quad (2.26)$$

starting at $S_t = s$. We further assume that the market has a constant half spread k , such that the ‘lit’-pool best ask and bid prices are defined by

$$S_u^a = S_u + k \quad \text{and} \quad S_u^b = S_u - k, \quad (2.27)$$

respectively. Equations (2.26) and (2.27) are far from capturing realistic market dynamics. We choose them for tractability purposes, bearing in mind this model is for reference purpose only. We let the CLP’s inventory start at the value $x \in \mathbb{R}$ and satisfy the following stochastic differential equation

$$dX_u = dN_u^- - dN_u^+, \quad (2.28)$$

where $\{N_u^\pm\}$ are independent Poisson processes with intensities λ^\pm . The CLP offers bid and ask quotes pegged to the ‘lit’-pool mid-price. That is, it executes orders from buyers at a price $S_u + \delta^+$ and orders from sellers at a price $S_u - \delta^-$, where δ^+ and δ^- are positive constants, not greater than k . We define the cash process of the CLP by

$$dY_u = (S_u + \delta^+)dN_u^+ - (S_u - \delta^-)dN_u^-, \quad (2.29)$$

with initial state level $Y_t = y$.

At each time the CLP can choose whether it wishes to reduce its inventory by means of market or limit orders. If at time τ^m a market order is placed, the inventory and the cash processes are subject to the following impulses

$$X_{\tau^m} = X_{\tau^m-} + \xi_\tau \quad \text{and} \quad Y_{\tau^m} = Y_{\tau^m-} - \xi_\tau^m (S_{\tau^m} + k\xi_{\tau^m}), \quad (2.30)$$

where $\xi_{\tau^m} \in \{-1, 1\}$, for a sell and buy market order, respectively. On the other hand, if at time τ^ℓ a IOC limit order is placed, the inventory and the cash processes are subject to the following impulse

$$X_{\tau^\ell} = X_{\tau_-^\ell} + \eta_{\tau^\ell} z_{\tau^\ell} \quad \text{and} \quad Y_{\tau^\ell} = Y_{\tau_-^\ell} - \eta_{\tau^\ell} (S_{\tau^\ell} - k\eta_{\tau^\ell}) z_{\tau^\ell}, \quad (2.31)$$

where $\eta_{\tau^\ell} \in \{-1, 1\}$, for a sell and buy market order, respectively, and z_{τ^ℓ} is a collection of i.i.d. $\{0, 1\}$ -valued random variables which model the limit-order execution percentage. When $z = 1$ the limit order posted by the CLP gets executed, otherwise it gets cancelled. In a more structured model the probability mass function of the random variables z_{τ^ℓ} should be related to the depth of the book at which the CLP posts its limit orders. In the present framework we assume that limit orders are always posted at the best prices available in the ‘lit’ market (which has a constant spread), and therefore we set $\mathbb{P}[z = 1] = p$, where p is a positive constant.

Similarly to Section 2.2.2.1, every time the CLP sends orders to the ‘lit’ pool, it leaks information to other market participants. This feature is modelled by fixed penalties $\epsilon^m > \epsilon^\ell > 0$ for market and limit orders, respectively, to which the CLP is subject to. We assume that the market-order penalty is larger than the limit-order one since, by crossing the spread, the CLP reveals a higher degree of execution urgency to other market participants. Furthermore, an aggressive order produces a higher price impact (against the market-maker inventory) compared to a limit-order.

The optimal strategy of the CLP is a pair of double sequences of stopping times τ_i^m and τ_j^ℓ and random variables ξ_i and η_j , for $i, j = 0, 1, 2, \dots$, which maximise its expected terminal cash Y_T while minimising the risk of holding the inventory throughout the whole trading period. We thus plot the optimal inventory thresholds which indicate—to the market maker—the inventory level at which it is optimal for them to cross the spread and post ‘lit’ pool orders. We define the value function by

$$V(t, \mathbf{x}) = \sup_{M_i, L_j} \mathbb{E}_{t, \mathbf{x}} \left[Y_T + X_T (S_T - \alpha X_T) - \phi \int_t^T X_u^2 du - \sum_{t \leq \tau_i^m < T} \epsilon^m - \sum_{t \leq \tau_j^\ell < T} \epsilon^\ell \right], \quad (2.32)$$

where $\mathbf{x} := (x, y, s)$, $M_i : (\tau_i^m, \xi_i)_{i \geq 0}$ and $L_j : (\tau_j^\ell, \eta_j)_{j \geq 0}$. This is a double-obstacle impulse-control problem and the value function solves the following QVI:

$$\min \left\{ \begin{aligned} & \phi x^2 - \frac{\partial V}{\partial t}(t, \mathbf{x}) - \lambda^+ [V(t, x-1, y+s+\delta^+, s) - V(t, \mathbf{x})] \\ & - \frac{1}{2} \sigma^2 \frac{\partial^2 V}{\partial s^2}(t, \mathbf{x}) - \lambda^- [V(t, x+1, y-s+\delta^-, s) - V(t, \mathbf{x})]; \end{aligned} \right. \quad (2.33)$$

$$\left. \begin{aligned} & V(t, \mathbf{x}) - \mathcal{M}V(t, \mathbf{x}); V(t, \mathbf{x}) - \mathcal{L}V(t, \mathbf{x}) \end{aligned} \right\} = 0,$$

with terminal condition $V(T, \mathbf{x}) = y + (s - \alpha x)x$. The operators $\mathcal{M}V(t, \mathbf{x})$ and $\mathcal{L}V(t, \mathbf{x})$ in Equation (2.33) are defined by

$$\mathcal{M}V(t, \mathbf{x}) = \sup_{e \in \{-1, +1\}} V(t, x+e, y-e(s+ke), s) - \epsilon^m, \quad (2.34)$$

and

$$\mathcal{L}V(t, \mathbf{x}) = \sup_{n \in \{-1, +1\}} \mathbb{E}^{(z)} [V(t, x+nz, y-n(s-kn)z, s)] - \epsilon^\ell, \quad (2.35)$$

where the expectation in Equation (2.35) is taken with respect to the random variable z , which represents what percentage of a limit order is filled in the ‘lit’ pool. The result of the above optimisation consists of the thresholds for the CLP’s inventory at which it is optimal to post (passive or aggressive) orders in the ‘lit’ pool.

2.3.2.2 Numerical results and parameters’ analysis

In this section we show the optimal boundaries found by solving the quasi variational inequality in Equation (2.33). We find the critical thresholds that define the strategy of the CLP. In the plots that follow, we show the optimal boundaries and we see that no ‘lit’-pool orders are submitted by the CLP as long as its inventory lies within the central region, labelled “Market making”. If the inventory falls outside the central region, the CLP starts submitting limit buy or sell orders in the ‘lit’ pool when the inventory is negative or positive, respectively. Market orders are the last resort means of trading and are submitted when the

inventory surpasses the upper line for sell orders and the bottom line for buy orders. We note that the boundaries shrink as we approach T as a result of the terminal penalty for holding the inventory, which we model by α . In what follows we look at the role played by the model's parameter.

In Figure 2.12 we note that a high α (left panel) incentivises the CLP to resort faster to hedging, compared to the case of low α (right panel). In particular, the CLP resorts to market orders for lower inventory levels. Market orders are expensive but benefit from sure execution and thus are preferred when the penalty for holding the inventory is higher. When α is low, the aggressive-orders boundaries widen in favour of passive orders.

We can use the ansatz $V(t, x, s, y) = y + xs + h(t, x)$ in order to reduce the number of state variables of Equation (2.33). We thus find, and numerically solve, the PDE satisfied by the function $h(t, x)$. We use an explicit finite difference method to approximate the solution of Equation (2.33) and the optimal strategy of the agent. Throughout this section, we consider an equally-spaced time grid $[0, 50]$ with intervals of 1 and an equally-spaced inventory grid $[-200, 200]$, with intervals of 0.1. The terminal condition is stated below HJB equation (2.16) and parameters' values are stated below each plot.

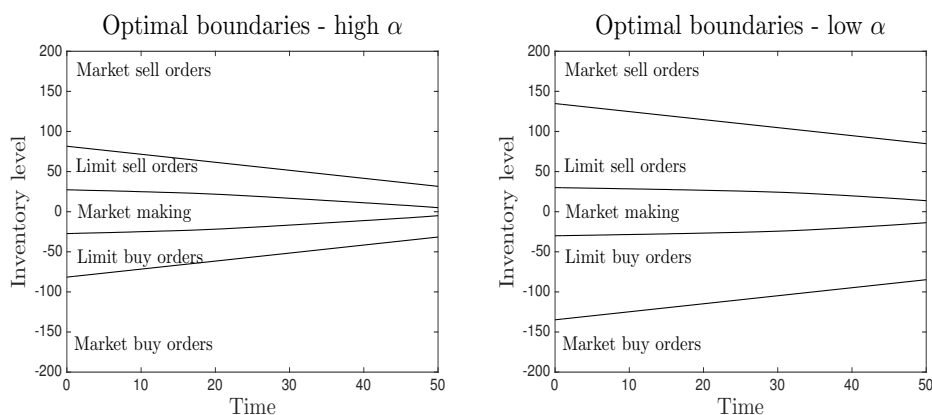


FIGURE 2.12: Optimal inventory thresholds found by solving the HJB equation (2.33). We set $k = 4$, $\lambda^+ = \lambda^- = 0.5$, $T = 50$, $\epsilon_m = 30$, $\epsilon_\ell = 15$, $\phi = 0.0001$, $\delta^+ = \delta^- = 2$, $p = 0.8$. In the left panel we set $\alpha = 3$. In the right panel we set $\alpha = 1$.

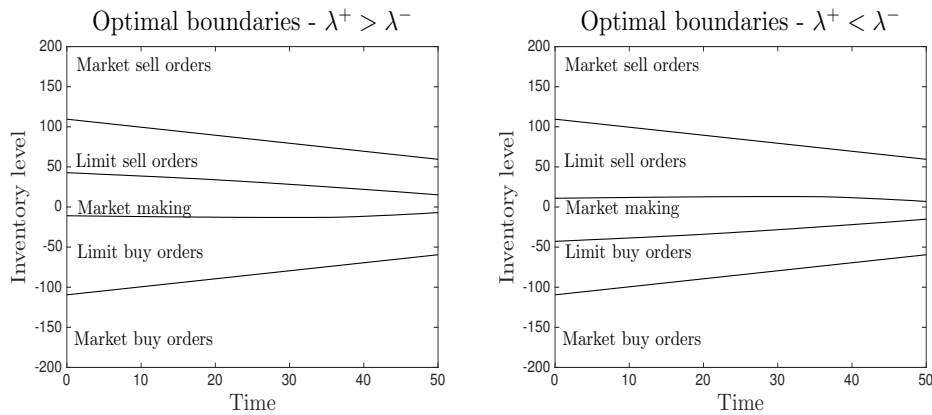


FIGURE 2.13: Optimal inventory thresholds found by solving the HJB equation (2.33). We set $k = 4$, $T = 50$, $\epsilon_m = 30$, $\epsilon_\ell = 15$, $\phi = 0.0001$, $\alpha = 1$, $\delta^+ = \delta^- = 2$, $p = 0.8$. In the left panel we set $\lambda^+ = 0.7$ and $\lambda^- = 0.3$. In the right panel we set $\lambda^+ = 0.3$ and $\lambda^- = 0.7$.

In Figure 2.13 the market-making boundaries are skewed upward (resp. downward) when the arrival rate of buyers is higher (resp. lower) than the one of sellers. In the right panel the inventory is expected to increase on average and thus the CLP resorts to the ‘lit’ pool faster in the case of positive inventory, compared to the case of negative inventory. In the left panel the opposite holds since buyers are expected to arrive at a higher rate than sellers. The CLP incorporates its beliefs on the market trend, and it is thus incentivised to take its hedging decisions consistently with the arrival rate of buyers and sellers.

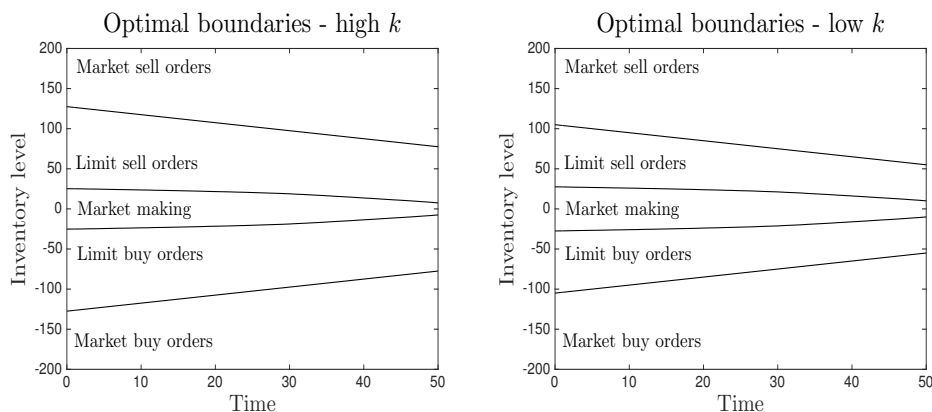


FIGURE 2.14: Optimal inventory thresholds found by solving the HJB equation (2.33). We set $k = 4$, $\lambda^+ = \lambda^- = 0.5$, $T = 50$, $\epsilon_m = 30$, $\epsilon_\ell = 15$, $\alpha = 1$, $\phi = 0.0001$, $\delta^+ = \delta^- = 2$, $p = 0.8$. In the left panel we set $k = 6$. In the right panel we set $k = 2$.

The half spread k plays an important role since a higher k results in more expensive aggressive ‘lit’-pool orders and more advantageous ‘lit’-pool passive orders. These properties make limit orders preferred to market orders and thus the CLP crosses the spread for higher levels of the inventory. Figure 2.14 shows that for a high spread (left panel) the boundaries widen, while for a low spread (right panel), the boundaries shrink.

In Figure 2.15 we show that low values of the penalties ϵ^m and ϵ^ℓ (right panel) encourage the CLP to resort sooner to the ‘lit’ pool for its hedging activity. This confirms the intuition that, being risk averse, the CLP resorts to the ‘lit’ pool sooner, provided the hedging is less penalising.

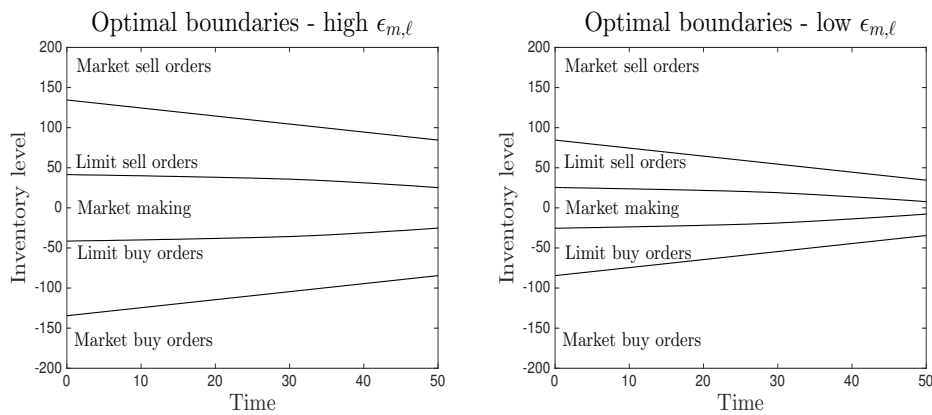


FIGURE 2.15: Optimal inventory thresholds found by solving the HJB equation (2.33). We set $k = 4$, $\lambda^+ = \lambda^- = 0.5$, $T = 50$, $\phi = 0.0001$, $\alpha = 1$, $\delta^+ = \delta^- = 2$, $p = 0.8$. In the left panel we set $\epsilon_m = 35$ and $\epsilon_\ell = 20$. In the right panel we set $\epsilon_m = 6$ and $\epsilon_\ell = 4$.

The parameter ϕ models the running penalty for holding the inventory. In the left panel of Figure 2.16 we note that the market-making region is consistently shrunk compared to the right panel. This implies that the CLP reduces the amount of inventory it is willing to hold at every point in time, in favour of hedging, as the inventory causes higher reductions of the value function.

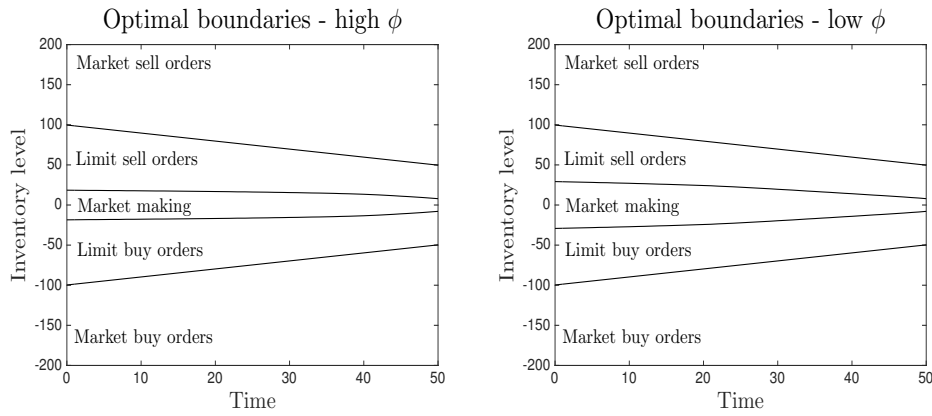


FIGURE 2.16: Optimal inventory thresholds found by solving the HJB equation (2.33). We set $k = 4$, $\lambda^+ = \lambda^- = 0.5$, $T = 50$, $\epsilon_m = 30$, $\epsilon_\ell = 15$, $\alpha = 1$, $\delta^+ = \delta^- = 2$, $p = 0.8$. In the left panel we set $\phi = 0.001$. In the right panel we set $\phi = 0.00001$.

The parameter p models the probability of execution of the limit orders submitted to the ‘lit’ pool by the CLP. A higher p increases the likelihood of reducing the inventory by means of limit orders, which are less expensive and, thus, preferred. Figure 2.17 shows that in the case of a high probability of execution p (left panel), the market-orders regions shrink as the CLP is confident it can rebalance its inventory by means of limit orders. The opposite holds in case of a low p .

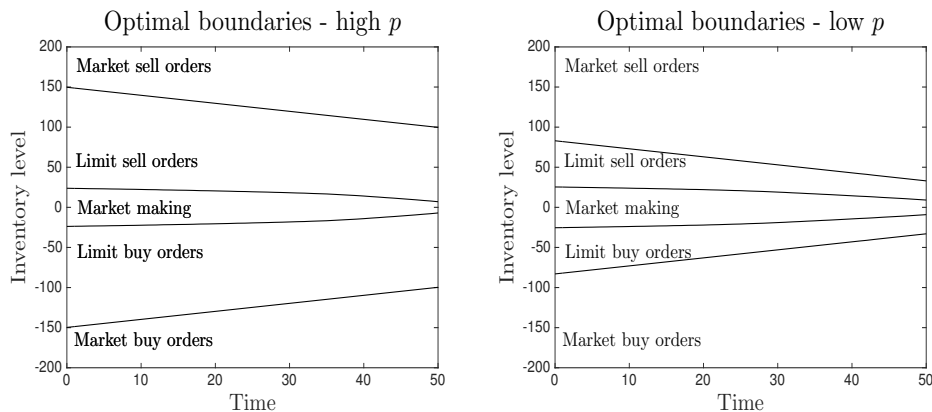


FIGURE 2.17: Optimal inventory thresholds found by solving the HJB equation (2.33). We set $k = 4$, $\lambda^+ = \lambda^- = 0.5$, $T = 50$, $\epsilon_m = 30$, $\epsilon_\ell = 15$, $\phi = 0.0001$, $\alpha = 1$, $\delta^+ = \delta^- = 2$. In the left panel we set $p = 0.95$. In the right panel we set $p = 0.65$.

2.4 Conclusions

In the present chapter, we have considered both optimal execution and optimal market making, with and without the presence of a dark pool (or CLP) as an additional venue.

In the case of optimal execution, we note that the presence of a dark pool considerably changes the optimal strategy of the agent. In fact, they place a small portion of their inventory in the ‘lit’ pool and the remaining inventory in the dark pool at every point in time. That is, the ‘lit’-pool trading speed is reduced compared to scenarios where only a standard exchange is available to the agent. This is in line with the feature that the dark pool offers more favourable trading prices (i.e. mid-price trading rather than buying at the best ask price and sell at the best bid price). In the presented model, the liquidation task ends as soon as the first dark-pool execution takes place. This behaviour of the optimal strategy (i.e. placing all the remaining inventory in the dark pool) is due to the dynamics of the mid-price, which we choose to be a martingale. In Chapter 3, where this assumption is removed and more realistic dynamics for the mid-price are chosen (e.g. a mean-reverting jump process), the aforementioned strategy ceases to be optimal, since the agent takes advantage of the expected movements of the market price.

When the dark pool (here, CLP) plays the role of a market maker by providing principal liquidity to its clients, it sets bid and ask quotes and resorts to the ‘lit’ pool to reduce its risk of holding the inventory. It first posts limit orders, which are less expensive but their execution is uncertain, and ultimately market orders. We show that the optimal thresholds crucially depend on the model parameters and, in particular, on the degree of risk that the CLP is willing to take. In Chapter 4 we consider additional state and control variables. We allow the CLP to choose both (i) the spread it charges to its client, and (ii) the depth of the LOB at which it posts passive orders (i.e. the CLP need not to post on top of the book). Furthermore, we drop the unrealistic assumption of a constant ‘lit’-pool spread.

In Chapter 5 we provide an application of the above framework to the electronic foreign exchange (eFX) market. We slightly modify some of the assumptions made in Chapter 4, so to make the model consistent with the specific features of the eFX market.

Chapter 3

Optimal execution in ‘lit’ and dark pools

3.1 Overview of the chapter

In this chapter we study an optimal execution problem from the perspective of an investor, when both dark and ‘lit’ pools are available to market participants. We assume that an agent seeks to execute a sizeable amount of a liquidly-traded asset over a finite period of time $[t, T]$, where the initial time t lies in the interval $[0, T]$. The ultimate goal is to find the optimal trading schedule which maximises the performance criterion of the agent. This chapter is based on Crisafi and Macrina [30].

In Section 3.2 we propose a class of models and we numerically solve an optimal execution problem when only the ‘lit’ pool is available to the agent. We show that the optimal trading trajectories are closely related to the price dynamics assumed.

In Section 3.3 we add the possibility for the agent to trade simultaneously in both ‘lit’ and dark pools and we compare the results to the ones obtained in the reference model presented in Section 2.3.1. We find, e.g., that the choice of the optimal strategy depends on the price dynamics assumed (i.e. it depends on the current and expected market conditions). In Section 2.3.1 the strategy was

independent from the price since no information was available on future price movements (i.e. the price was a martingale). We believe this is not realistic since agents may have their own expectations on the market’s evolution and thus wish to incorporate this feature in the model.

Throughout the present chapter we use standard finite difference methods to solve—backward in time—the HJB equations stated herein. We thus obtain and plot the numerical solution. The algorithm and techniques used are described in detail in Section 7.5.1. Furthermore, the values of the parameters used are reported under each plot, for reproducibility purposes.

3.2 Trading in the ‘lit’ pool

We assume that the agent trades in the ‘lit’ pool by means of aggressive orders only. Such urgency may be motivated by a need for immediate liquidity as well as some private information the agent may have. In order to precisely determine the liquidation price received by the agent, a model of all LOB levels should be considered. This would reduce the model’s tractability and thus we assume that—as far as an optimal liquidation strategy is concerned—it suffices to model the best bid price¹. We remark that the effect of exhausting distinct book levels can be achieved by a temporary price impact function, as seen in Chapter 2.

3.2.1 Price, inventory and cash dynamics

We fix a probability space $(\Omega, \mathcal{F}, \mathbb{P})$ equipped with a filtration $\{\mathcal{F}_u\}_{0 \leq u \leq T}$ satisfying the usual conditions. In what follows, we assume that the task is to liquidate an amount $X_t = x$ of shares, where $0 \leq x < \infty$, and write for the inventory dynamics

$$dX_u = -\nu_u du, \tag{3.1}$$

where the rate of trading $\nu := \{\nu_u\}$ takes value in a compact set $\mathcal{V} = [0, N] \subset [0, \infty)$ and is the control process of the stochastic optimal control problem presented in Section 3.2.2. In the short run, we assume that the best bid price at

¹Or the best ask price in the case of an optimal acquisition.

time $u \in [t, T]$ depends on its initial state and on the cumulated market activity up to time u . We introduce two compensated compound Poisson processes defined by

$$\tilde{J}_u^{b,i} = J_u^{b,i} - \lambda^{b,i} u \mathbb{E}[z_1^{b,i}] = \sum_{j=1}^{N_u^{b,i}} z_j^{b,i} - \lambda^{b,i} u \mathbb{E}[z_1^{b,i}],$$

where $i = 1, 2$. In the above notation, $\{N_u^{b,i}\}$ are independent Poisson processes with intensity $\lambda^{b,i}$. The jump sizes are modelled by sequences of i.i.d. random variables $z_j^{b,i}$, where $j=1, 2, \dots$. We model the best bid price process by

$$dS_u^b = \mu^b(u, S_{u-}^b, \nu_u) du + \sum_{i=1}^2 h_i^b(u, S_{u-}^b) d\tilde{J}_u^{b,i}, \quad (3.2)$$

with initial value $S_t^b = s^b$. The functions μ^b and h_i^b can be chosen such that the best bid price is always non-negative, or in ways that reproduce market features. In Equation (3.2) we consider positive jumps which model the incoming limit buy orders at a more favourable price, and negative jumps to account for cancellations of limit buy orders and market sell orders which walk the LOB. The price model in Equation (3.2) has been inspired by the financial considerations made in Cont et al [28]. Explicit examples will be provided in Section 3.2.3. Although we view the optimisation problem from the perspective of liquidating orders, the model proposed in Equations (3.1) and (3.2) can be adapted to the case of optimal acquisition. Last, we define the cash (wealth) process by

$$dY_u = \mu^y(u, S_u^b, \nu_u) du,$$

with initial value $Y_t = y$. The function μ^y models the instantaneous gains made by the investor through selling shares, possibly taking into account the temporary price impact of trades. We consider a general function μ^y so to account for different ways of calculating profits and losses (P&L).

3.2.2 The value function

We introduce a stopping time τ ,

$$\tau := \inf \{u \geq t \mid X_u \leq 0\} \wedge T, \quad (3.3)$$

that describes the first time the inventory is depleted, if such an event occurs before the terminal date T . For notational simplicity, in this section we define the space $\mathcal{O} = [0, x] \times \mathbb{R}^2$ and let the vector of the state variables be defined by $\mathbf{X}_u = (X_u, S_u^b, Y_u) \in \mathcal{O}$, with initial values at time t given by $\mathbf{x} = (x, s^b, y) \in \mathcal{O}$. We propose a general objective function of the form

$$V(t, \mathbf{x}) = \sup_{\nu \in \mathcal{V}} \mathbb{E}_{t, \mathbf{x}} \left[\int_t^\tau e^{-r(u-t)} f(u, \mathbf{X}_u, \nu_u) du + e^{-r(\tau-t)} g(\mathbf{X}_\tau) \right], \quad (3.4)$$

where $r \geq 0$ is a discount rate (also used in, e.g., Pemy and Zhang [72], and Bian et al. [11]) and $E_{t, \mathbf{x}}[\cdot]$ is the expectation given the initial state of the system $(t, \mathbf{x}) \in [0, T] \times \mathcal{O}$. We consider a discount factor to model the potential preference of the agent for an immediate execution. We emphasise that while r may be the risk-free interest rate, it doesn't have to be so. The function $f : [0, T] \times \mathcal{O} \times \mathcal{V} \rightarrow \mathbb{R}$ may have several interpretations. For example it may represent the gains made from the shares sale (e.g. $S_u^b \nu_u$), or correspond to a penalty for holding the inventory (e.g. $-\phi X_u^2$, where $\phi > 0$). The function $g : \mathcal{O} \rightarrow \mathbb{R}$ may be the terminal reward obtained by a block trade liquidation of the remaining inventory at time T (e.g. $S_T^b X_T$). However, g may also represent a penalty resulting from failing to liquidate the whole inventory (e.g. $-\alpha X_T^2$, where $\alpha > 0$). Explicit examples are provided in Section 3.2.3.

We let $\mathbf{p} := (p_1, p_2, p_3) \in \mathbb{R}^3$, and we define the operator \mathcal{H} by

$$\mathcal{H}(t, \mathbf{x}, \mathbf{p}) = \sup_{v \in \mathcal{V}} \left\{ f(t, \mathbf{x}, v) - v p_1 + \mu^b(t, s^b, v) p_2 + \mu^y(t, s^b, v) p_3 \right\}. \quad (3.5)$$

Also, for polynomially bounded (\mathcal{PB}) functions $\varphi \in \mathcal{C}^{1,1}([0, T] \times \mathcal{O})$, we let \mathcal{B}_b be defined by

$$\begin{aligned} \mathcal{B}_b(t, \mathbf{x}, \varphi) = & \sum_{i=1}^2 \lambda^{b,i} \mathbb{E}^{(z^{b,i})} \left[\varphi(t, x, s^b + h_i^b(t, s^b) z^{b,i}, y) - \varphi(t, \mathbf{x}) \right. \\ & \left. - h_i^b(t, s^b) z^{b,i} \frac{\partial \varphi}{\partial s^b}(t, \mathbf{x}) \right], \end{aligned} \quad (3.6)$$

where $\mathbb{E}^{(z^{b,i})}$ is the expectation taken with respect to the random variable $z^{b,i}$. Standard arguments from dynamic programming suggest that the value function of the optimal control problem (3.4) satisfies the following HJB partial integro differential equation (PIDE)²:

$$rV(t, \mathbf{x}) - \frac{\partial V}{\partial t}(t, \mathbf{x}) - \mathcal{H}(t, \mathbf{x}, D_{\mathbf{x}}V) - \mathcal{B}_b(t, \mathbf{x}, V) = 0, \quad (3.7)$$

on $[0, T) \times \mathcal{O}$, where $D_{\mathbf{x}}V$ denotes the gradient vector of the function V and with terminal condition $V(\tau, \mathbf{x}) = g(\mathbf{x})$ and boundary condition $V(u, 0, s, y) = y$. The meaning of the boundary condition is that if there are no shares to liquidate, the agent does not take any action and they are left with their current cash holdings. The same holds at time τ , if $X_\tau = 0$. Since one cannot guarantee the smoothness of $V(t, \mathbf{x})$ on the whole domain, one cannot discuss the solution of the HJB PIDE in the classical sense. We show the viscosity property of the value function in Chapter 7.

3.2.3 Explicit examples and numerical results

In this section we propose two explicit examples of the price dynamics. We consider a specific form of the cash dynamics and of the performance criterion, and we numerically find the optimal inventory trajectories.

3.2.3.1 Geometric Lévy model

We propose an exponential model for the best bid price process, so to ensure its positivity at every point in time:

$$\frac{dS_u^b}{S_{u^-}^b} = (\bar{\mu}^b - \mu\nu_u)du + dJ_u^{b,1} - dJ_u^{b,2}. \quad (3.8)$$

In (3.8) we have let $\mu^b(t, s^b, v) = (\bar{\mu}^b - \mu v)s^b$ and $h_i^b(t, s^b) = s^b(\mathbb{1}_{\{i=1\}} - \mathbb{1}_{\{i=2\}})$. Furthermore, the processes $\{J_u^{b,1}\}$ and $\{J_u^{b,2}\}$ are defined as in Equation (3.2), and we let the random variables $z_j^{b,i}$ be sequences of non-negative independent and

²We refer to Section 7.1 for details on its derivation.

uniformly distributed random variables³. In Equation (3.8) we interpret $dJ^{b,1}$ as the change in the best bid price due to the submission of limit buy orders at a more favourable price, whereas $dJ^{b,2}$ models the changes due to: (i) incoming market sell orders which walk the book, and (ii) the effect of cancellations of limit buy orders posted at the best price.

We introduce a permanent price impact (parametrised by $\mu \geq 0$), deriving from the lit-pool orders submitted by the agent. We further consider a constant drift coefficient, $\bar{\mu}^b \in \mathbb{R}$. The inventory evolution of the investor is here described by Equation (3.1), and we model the temporarily impacted best bid price \hat{S}_u^b by

$$\hat{S}_u^b = S_u^b - \beta \nu_u, \quad (3.9)$$

where $\beta > 0$, and the cash process by

$$dY_u = \nu_u \hat{S}_u^b du, \quad (3.10)$$

where we have set $\mu^y(t, s^b, v) = v s^b$. Next we consider an investor who wants to optimally liquidate their portfolio by placing aggressive sell orders in the ‘lit’ market. For this purpose, we consider the following value function:

$$V(t, \mathbf{x}) = \sup_{\nu \in \mathcal{V}} \mathbb{E}_{t, \mathbf{x}} \left[e^{-r(\tau-t)} (Y_\tau + X_\tau (S_\tau^b - \alpha X_\tau)) - \phi \int_t^\tau e^{-r(u-t)} X_u^2 du \right], \quad (3.11)$$

where we have set $f(t, \mathbf{x}, v) = -\phi x^2$ and $g(\mathbf{x}) = y + x(s^b - \alpha x)$. The interpretation of Equation (3.11) is analogous to the one presented in Chapter 2: the agent seeks to maximise their terminal cash subject to both (i) a terminal penalty (parametrised by α) for failing to liquidate the whole inventory, and (ii) a running penalty (parametrised by ϕ) for holding the inventory throughout the

³We notice that, in order to guarantee the positivity of the price process, we shall ensure that $z^{b,1} > -1$ and $z^{b,2} < 1$.

whole period. The value function solves the following HJB PIDE

$$\begin{aligned} \sup_{\mathbf{v} \in \mathcal{Z}} \left\{ rV(t, \mathbf{x}) - \phi x^2 + \frac{\partial V}{\partial t}(t, \mathbf{x}) + (\bar{\mu}^b - \mu v) s^b \frac{\partial V}{\partial s^b}(t, \mathbf{x}) - v \frac{\partial V}{\partial x}(t, \mathbf{x}) \right. \\ \left. + v(s^b - \beta v) \frac{\partial V}{\partial y}(t, \mathbf{x}) + \lambda^{b,1} \mathbb{E}^{(z^{b,1})} [V(t, x, s^b(1 + z^{b,1}), y) - V(t, \mathbf{x})] \right. \\ \left. + \lambda^{b,2} \mathbb{E}^{(z^{b,2})} [V(t, x, s^b(1 - z^{b,2}), y) - V(t, \mathbf{x})] \right\} = 0, \end{aligned} \quad (3.12)$$

with terminal condition $V(\tau, \mathbf{x}) = y + x(s^b - \alpha x)$ and boundary condition $V(u, 0, s^b, y) = y$. The expectations in Equation (3.12) are taken with respect to the random variables $z^{b,1}$ and $z^{b,2}$, respectively. In what follows, we plot the optimal strategy obtained by numerically solving Equation (3.12) and we provide a detailed analysis of the model's parameters.

In Figures 3.1 and 3.2 we plot a hundred simulated paths for: (i) the inventory evolution (top left panel), (ii) the cash process (top right panel), (iii) the unimpacted best bid price (bottom left panel), and (iv) the impacted best bid price (bottom right panel).

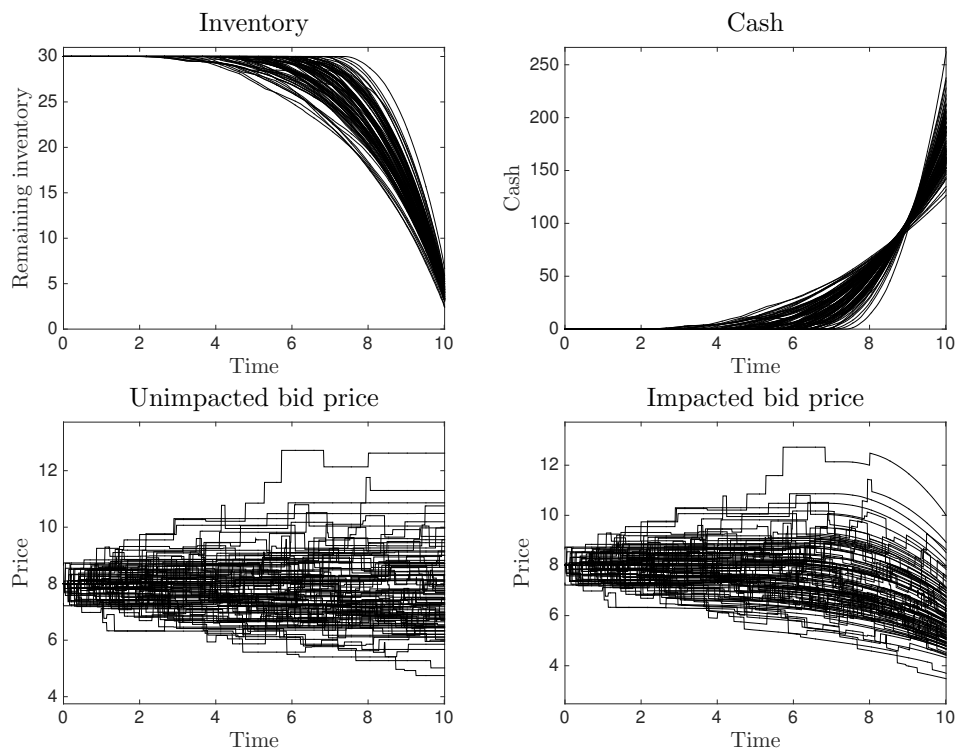


FIGURE 3.1: Simulation of Equations (3.1), (3.10), (3.8) and (3.9). We set $\beta = 0.05$, $\mu = 0.01$, $\bar{\mu}^b = 0.01$, $x = 30$, $s^b = 8$, $\lambda^{b,1} = \lambda^{b,2} = 0.5$, $z^{b,i} \sim U[0, 1)$, $r = 0.01$, $T = 10$, $\phi = 0.01$, $\alpha = 1$.

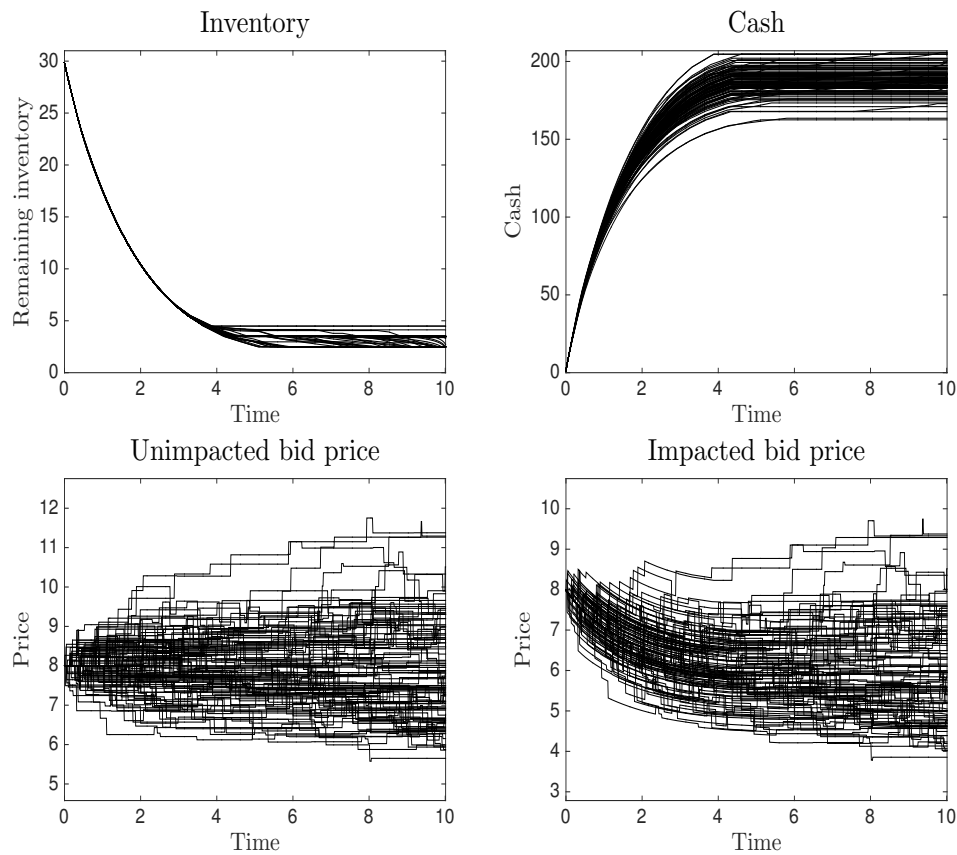


FIGURE 3.2: Simulation of Equations (3.1), (3.10), (3.8) and (3.9). We set $\beta = 0.05$, $\mu = 0.01$, $\bar{\mu}^b = -0.01$, $x = 30$, $s^b = 8$, $\lambda^{b,1} = \lambda^{b,2} = 0.5$, $z^{b,i} \sim U[0, 1)$, $r = 0.01$, $T = 10$, $\phi = 0.01$, $\alpha = 1$.

In Figure 3.1 we consider an upward trend (i.e. $\bar{\mu}^b > 0$), while in Figure 3.2 we consider a downward trend (i.e. $\bar{\mu}^b < 0$) for the best bid price process.

Contrary to the models presented in Chapter 2, where the optimal strategy only depends on the inventory level, here it also depends on the current price level. As such, for the parameters' analysis, we only plot the mean strategy, as similarly done in Cartea et al. [23].

In Figure 3.3 we show how the optimal trading speed changes when we vary the parameters α (left panel) and ϕ (right panel). As expected, a higher terminal penalty coefficient α encourages the agent to liquidate a bigger portion of their inventory by T , while the running penalty ϕ increases the initial speed of trading.

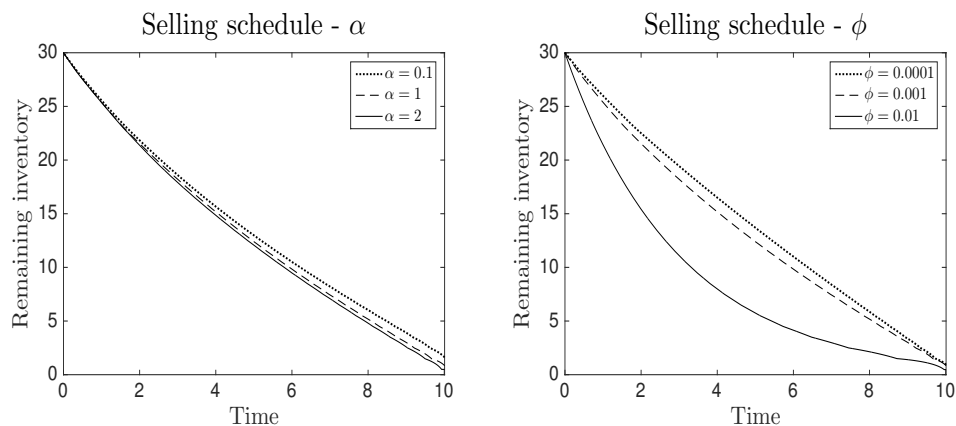


FIGURE 3.3: Optimal mean selling strategy—displayed as a function of the remaining inventory—found by solving the HJB equation (3.12). We set $\beta = 0.1$, $\mu = 0.05$, $\bar{\mu}^b = 0$, $x = 30$, $s^b = 8$, $\lambda^{b,1} = \lambda^{b,2} = 0.1$, $z^{b,i} \sim U[0, 1)$, $r = 0.01$, $T = 10$. In the left panel we set $\phi = 0.001$. In the right panel we set $\alpha = 1$.

In Figure 3.4 we plot the effects of the temporary and permanent price impacts—left and right panels, respectively—on the selling schedule of the agent. When the coefficient of the temporary price impact β is low (left panel, upper line), the agent reduces their trading speed at the beginning of the period, so to benefit from the submartingale property of the best bid price, which is assumed to increase on average according to the positive drift parameter $\bar{\mu}^b$. The agent accelerates their trading towards the end of the period, due to the terminal penalty α . Such an acceleration is less detrimental than in the case of low instantaneous impact. The analogous holds for the permanent price impact μ .

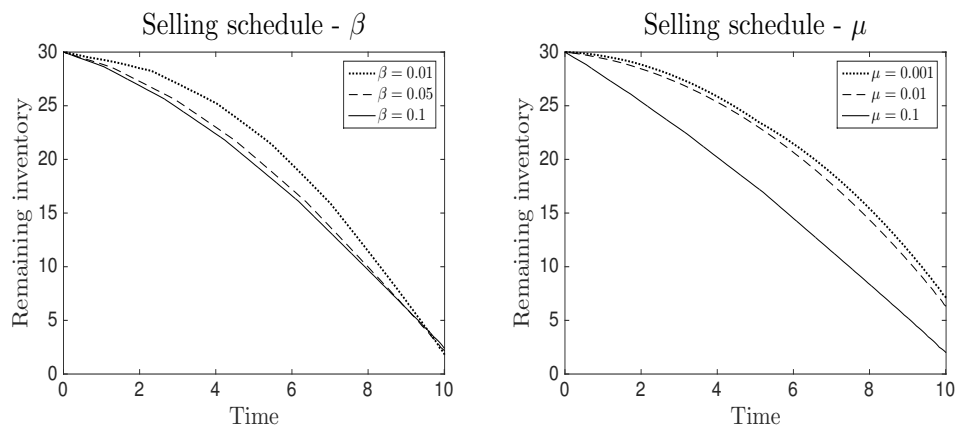


FIGURE 3.4: Optimal mean selling strategy—displayed as a function of the remaining inventory—found by solving the HJB equation (3.12). We set $\alpha = 0.5$, $\bar{\mu}^b = 0.1$, $\phi = 0.001$, $x = 30$, $s^b = 8$, $\lambda^{b,1} = \lambda^{b,2} = 0.1$, $z^{b,i} \sim U[0, 1)$, $r = 0.01$, $T = 10$. In the left panel we set $\mu = 0.05$. In the right panel we set $\beta = 0.1$.

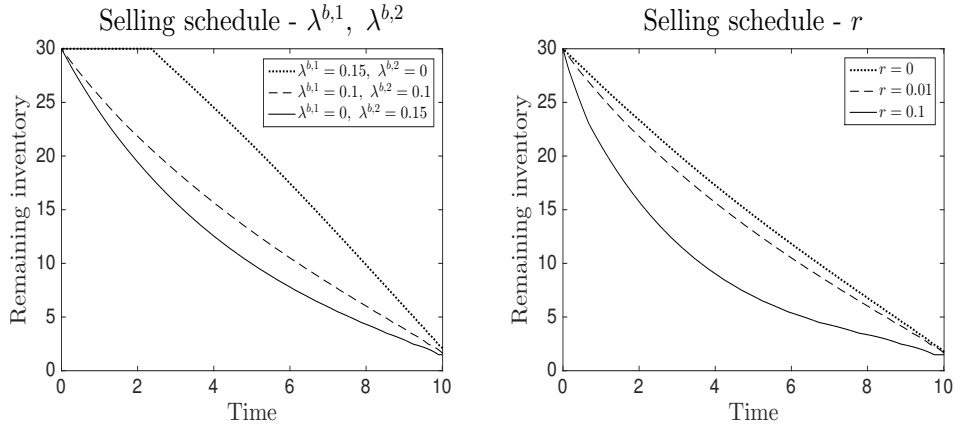


FIGURE 3.5: Optimal mean selling strategy—displayed as a function of the remaining inventory—found by solving the HJB equation (3.12). We set $\alpha = 0.5$, $\beta = 0.1$, $\phi = 0.01$, $x = 30$, $s^b = 8$, $\mu = 0.05$, $z^{b,i} \sim U[0, 1)$, $\bar{\mu}^b = 0$, $T = 10$. In the left panel we set $r = 0.01$. In the right panel we set $\lambda^{b,1} = \lambda^{b,2} = 0.1$.

In the left panel of Figure 3.5 we consider different intensities for the jump processes in the price dynamics. When the latter is a submartingale (upper line) the agent liquidates slower so to benefit from the increasing market trend. On the contrary, when the best bid price is a supermartingale, the agent increases their trading rate (bottom line). The dashed line represents the optimal selling schedule when the price is a martingale. In the right panel we display the effect of the discount rate r . Such a rate may model the urgency of the agent for their liquidation task. We note that while the terminal quantity liquidated does not change when we vary r , the initial speed increases for higher values of r . This is coherent with our modelling assumption that a faster liquidation increases the value function of the agent.

3.2.3.2 Mean-reverting model

Here we modify the best bid price dynamics and model it by a mean-reverting process—coherently with its observed market features—while leaving the other state variables unchanged. The shortcoming of this model is that the price may become negative. We now let the best bid price evolve according to

$$dS_u^b = [\kappa^b(\bar{S} - S_{u-}^b) - \mu\nu_u]du + dJ_u^{b,1} - dJ_u^{b,2}, \quad (3.13)$$

In (3.13) we have set $\mu^b(t, s^b, v) = [\kappa^b(\bar{S} - s^b) - \mu v]$ and $h_i^b(t, s^b) = \mathbb{1}_{\{i=1\}} - \mathbb{1}_{\{i=2\}}$, where $\kappa^b > 0$ is the speed of mean reversion and $\bar{S} > 0$ is its long term mean. For simplicity we consider the same optimisation problem in Equation (3.11) and the value function now satisfies

$$\sup_{v \in \mathcal{Z}} \left\{ \frac{\partial V}{\partial t}(t, \mathbf{x}) - rV(t, \mathbf{x}) - \phi x^2 + [\kappa^b(\bar{S} - s^b) - \mu v] \frac{\partial V}{\partial s^b}(t, \mathbf{x}) - v \frac{\partial V}{\partial x}(t, \mathbf{x}) \right. \\ \left. + v(s^b - \beta v) \frac{\partial V}{\partial y}(t, \mathbf{x}) + \lambda^{b,1} \mathbb{E}^{(z^{b,1})} [V(t, x, s^b + z^{b,1}, y) - V(t, \mathbf{x})] \right. \\ \left. + \lambda^{b,2} \mathbb{E}^{(z^{b,2})} [V(t, x, s^b - z^{b,2}, y) - V(t, \mathbf{x})] \right\} = 0, \quad (3.14)$$

with terminal and boundary conditions given by $V(\tau, \mathbf{x}) = y + x(s^b - \alpha x)$ and $V(u, 0, s^b, y) = y$, respectively. In Figures 3.6 and 3.7 we plot a hundred simulated paths for: (i) the inventory evolution (top left panel), (ii) the cash process (top right panel), (iii) the unimpacted best bid price (bottom left panel), and (iv) the impacted best bid price (bottom right panel). In Figure 3.6 we set $S_t^b < \bar{S}$, while in Figure 3.7 we set $S_t^b > \bar{S}$.

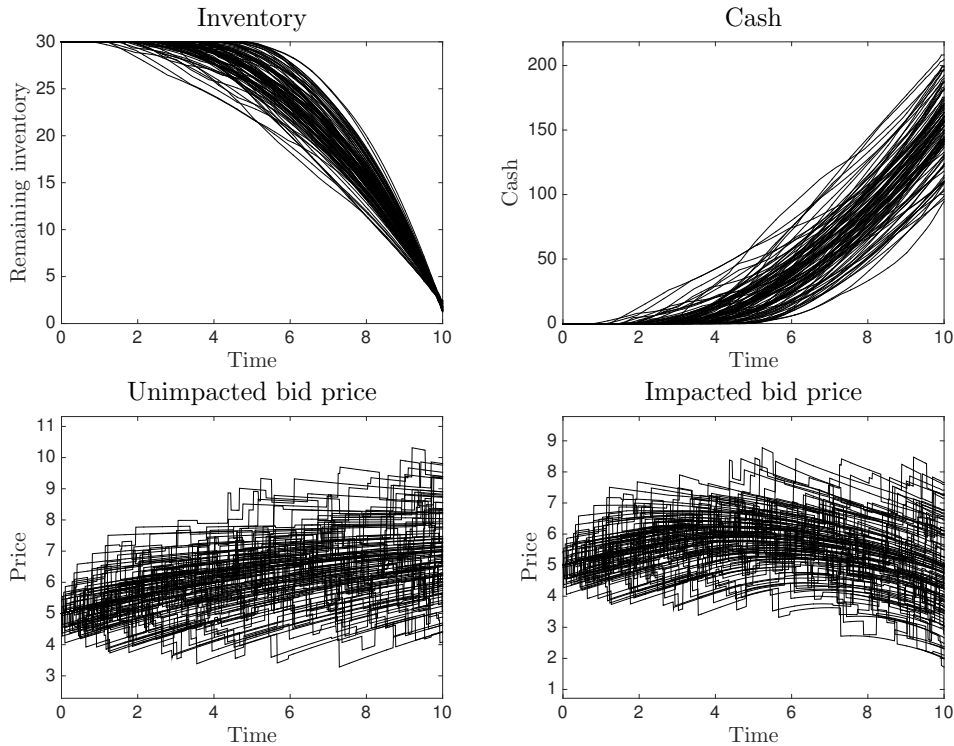


FIGURE 3.6: Simulation of Equations (3.1), (3.10), (3.13) and (3.9). We set $\beta = 0.05$, $\mu = 0.1$, $x = 30$, $s^b = 5$, $\bar{S} = 8$, $\lambda^{b,1} = \lambda^{b,2} = 0.5$, $z^{b,i} \sim U[0, 1]$, $r = 0.001$, $T = 10$, $\phi = 0.0001$, $\alpha = 0.5$, $\kappa^b = 0.1$.

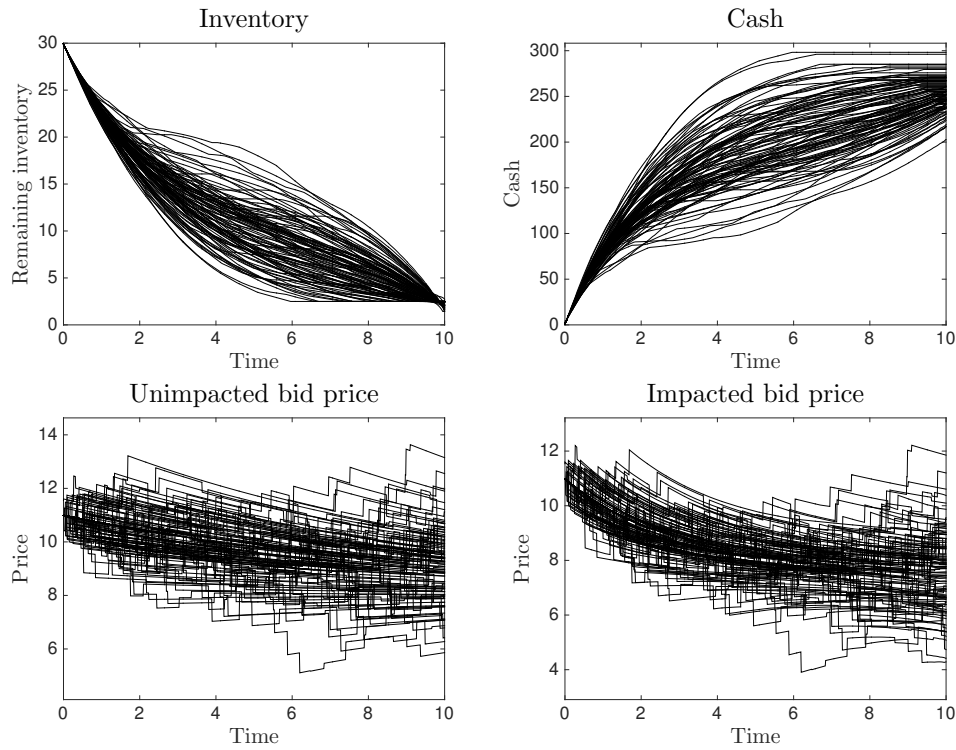


FIGURE 3.7: Simulation of Equations (3.1), (3.10), (3.13) and (3.9). We set $\beta = 0.05$, $\mu = 0.1$, $x = 30$, $s^b = 11$, $\bar{S} = 8$, $\lambda^{b,1} = \lambda^{b,2} = 0.5$, $z^{b,i} \sim U[0, 1]$, $r = 0.001$, $T = 10$, $\phi = 0.0001$, $\alpha = 0.5$, $\kappa^b = 0.1$.

The majority of the model parameters share the same features outlined in Section 3.2.3.1, and thus we here only look at the role of the mean-reversion speed and the long-term mean, and plot the mean strategy of the agent.

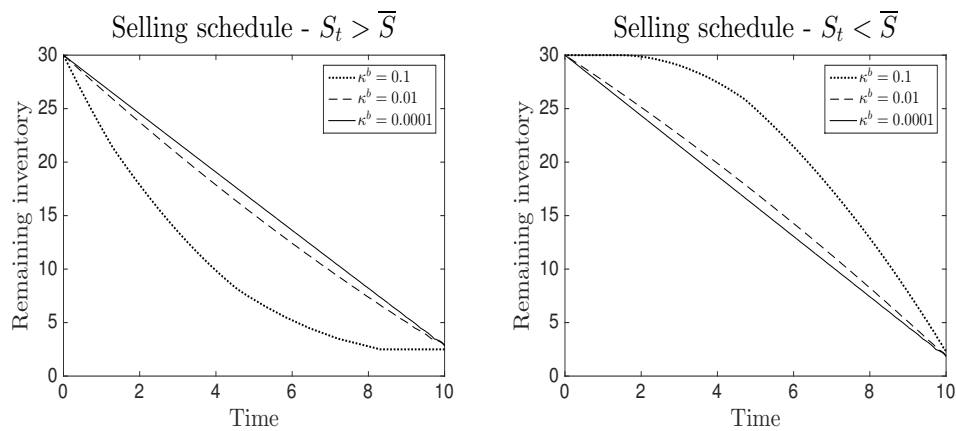


FIGURE 3.8: Optimal selling strategy—displayed as a function of the remaining inventory—found by solving the HJB equation (3.14). We set $\beta = 0.05$, $\mu = 0.1$, $x = 30$, $\bar{S} = 8$, $\lambda^{b,1} = \lambda^{b,2} = 0.5$, $z^{b,i} \sim U[0, 1]$, $r = 0.001$, $T = 10$, $\phi = 0.0001$, $\alpha = 2$.

In the left panel we set $s^b = 6$. In the right panel we set $s^b = 10$.

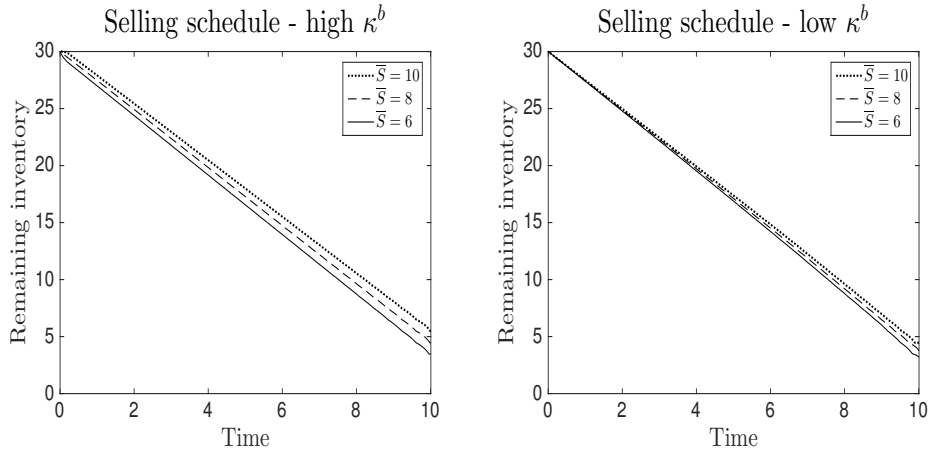


FIGURE 3.9: Optimal selling strategy—displayed as a function of the remaining inventory—found by solving the HJB equation (3.14). We set $\beta = 0.05$, $\mu = 0.1$, $x = 30$, $\bar{S} = 8$, $\lambda^{b,1} = \lambda^{b,2} = 0.5$, $z^{b,i} \sim U[0, 1]$, $r = 0.001$, $T = 10$, $\phi = 0.0001$, $\alpha = 1$. In the left panel we set $\kappa^b = 0.1$. In the right panel we set $\kappa^b = 0.001$.

In Figure 3.8 we show different trading trajectories for different values of the speed of mean reversion. First we note that the trading speed in the left panel is higher than the one appearing in the right panel. This is due to the price sensitivity of the policy and, in particular, to a higher starting price in the left panel compared to the one in the right panel. Furthermore, we note that if the current price is above its long-term average (left panel), the agent liquidates faster when the speed of mean reversion is higher (solid line). This result incorporates (i) the opportunity to liquidate at a more favourable price (which is short-lived compared to the case of low κ^b —dotted line), and (ii) the lower terminal value of the remaining portfolio, given by the asset price being, on average, closer to its long-term mean. Analogous considerations can be made for the case of a starting price lower than the long-term mean of the asset (right panel). That is, a higher speed of mean reversion discourages the investor to liquidate faster as the price is going to quickly mean-revert to a higher value.

Figure 3.9 shows the optimal strategy for different values of the long-term mean of the asset’s price, while also considering both the cases of high and low speed of mean reversion. In both panels, in agreement with the considerations made for Figure 3.8, higher values of the long-term mean \bar{S} reduce the liquidation speed. Such difference is more evident for higher values of the mean-reversion speed (left panel). In particular, as $\kappa^b \rightarrow 0$, the three inventory evolutions converge to

a unique path. This is trivial since, if we set $\kappa^b = 0$, the best bid price is not affected by the parameter \bar{S} .

3.3 Trading in the dark pool

We here propose a more flexible setup than the continuous-time model elaborated by Kratz and Schöneborn [57] and we outline here our main contributions to the literature.

1. We do not require for the price process to be a martingale.
2. We incorporate the permanent price impact in our model (Kratz and Schöneborn [58] include price impact in a discrete-time model).
3. We allow for partial execution in the dark pool.
4. We consider a general objective function and a general terminal bequest function to account for: (i) different preferences of agents, (ii) various ways of calculating P&L, and (iii) minimisation/maximisation of various performance measures (e.g. implementation shortfall⁴).

As a shortcoming deriving from a more complex structure, we lose the opportunity of finding a closed-form solution and need to resort to numerical techniques for describing the optimal selling schedule. Another difference which is worth noticing is that we do not constrain the inventory to be fully liquidated by T . While it may be an interesting problem to look at, we believe that practical market considerations should be set as a priority and fully liquidating a large inventory under strongly averse conditions may not necessarily be the optimal choice and/or economically justified. We therefore prefer to keep the terminal penalty for failing to liquidate the whole inventory, so to account for various urgencies that agents may experience. We believe that current market conditions should contribute to the choice of the optimal portion to liquidate and they should, therefore, affect the trading schedule.

⁴The implementation shortfall (IS) is defined in, e.g., Almgren and Chriss [2] by the difference between the theoretical and realised gain. That is $IS = X_t S_t^b - \int_t^T \nu_u S_u^b du$.

As mentioned earlier in this work, we assume that trades in the dark pool get executed at the lit-pool mid-price, for which we still need a model. We decide to model the spread process $\{\Delta_u\}$ —from which the mid price $S_u^m = S_u^b + \Delta_u/2$ derives—for the following reasons:

1. By providing a flexible model, one can choose dynamics that guarantee the positivity of the spread process at all times.
2. Market liquidity (understood as the spread's width) can be easily incorporated in the model and its effects on the optimal strategy can be better understood.
3. By modelling the spread we can capture market features such as, e.g., the high bid-ask correlation and the mean reversion of the market spread.

In the next sections we present the optimal control problem and we provide explicit examples which depict the flexibility of our model.

3.3.1 Modified prices, inventory and cash dynamics

The market spread is determined by both the best bid and the best ask prices movements. In particular, when the bid price experiences a positive jump (increases), the spread should decrease in the same instant, given that the ask price has not jumped. Analogously, a downward jump of the best bid price should increase the spread. The opposite holds for jumps in the best ask price. Furthermore, as the lit-pool trades of the agent permanently impact the best bid price downward, such impact should also be reflected in the spread process. We thus choose for the latter the following dynamics

$$d\Delta_u = \mu^\Delta(u, \Delta_{u-}, \nu_u) du + \sum_{i=1}^2 h_i^\Delta(u, \Delta_{u-}) d\tilde{J}_u^{\Delta,i} + \sum_{i=1}^2 h_i^{b,\Delta}(u, S_{u-}^b, \Delta_{u-}) d\tilde{J}_u^{b,i}, \quad (3.15)$$

with initial value $\Delta_t = \Delta$. In the above notation, the processes $\{J_u^{b,i}\}$ are defined as in Equation (3.2) and we further introduce the compensated compound Poisson processes

$$\tilde{J}_u^{\Delta,i} = J_u^{\Delta,i} - \lambda^{\Delta,i} u \mathbb{E}[z_1^{\Delta,i}] = \sum_{j=1}^{N_u^{\Delta,i}} z_j^{\Delta,i} - \lambda^{\Delta,i} u \mathbb{E}[z_1^{\Delta,i}],$$

where $i = 1, 2$ and $\{N_u^{\Delta,i}\}$ are independent Poisson processes with intensity $\lambda^{\Delta,i}$. The jump sizes are modelled by sequences of i.i.d. random variables $z_j^{\Delta,i}$, where $j=1,2,\dots,$.

The purpose of this section is to find the optimal trading strategy in both ‘lit’ and dark venues at any time $u \in [t, T)$. We denote the optimal order size in the dark pool by $\{\eta_u\}$, and we define the vector-valued control process by $\boldsymbol{\nu} = \{\boldsymbol{\nu}_u\} := (\nu_u, \eta_u)$, where $\{\nu_u\}$ is progressively measurable and $\{\eta_u\} \in [0, X_u]$ is predictable. Next, we modify the inventory and the cash dynamics since they now also depend on the dark pool activity. Along the lines of Horst and Naujokat [52], we model the dark-pool execution part by a jump process. We thus write

$$dX_u = -\nu_u du - \eta_u dJ_u^y, \quad (3.16)$$

and

$$dY_u = \mu^y(u, S_u^b, \nu_u) du + h^y(u, S_{u-}^b, \Delta_{u-}, \eta_u) dJ_u^y. \quad (3.17)$$

In the above, we define $J_u^y := \sum_{j=1}^{N_u^y} z_j^y$, where $\{N_u^y\}$ is a Poisson process with intensity λ^y and z_j^y , for $j = 1, 2, \dots$, are i.i.d. random variables supported in $[0, 1]$, which model the executed portion of the order submitted to the dark pool.

3.3.2 The value function

To simplify the notation, we here introduce the space $\mathcal{O} := [0, x] \times \mathbb{R}^3$ and we define a vector of state variables $\mathbf{X}_u = (X_u, S_u^b, \Delta_u, Y_u) \in \mathcal{O}$ with initial values $\mathbf{x} = (x, s^b, \Delta, y) \in \mathcal{O}$. Next we consider a generalised optimisation problem of the form

$$V(t, \mathbf{x}) = \sup_{\nu \in \mathcal{Z}} \mathbb{E}_{t, \mathbf{x}} \left[\int_t^\tau e^{-r(u-t)} f_1(u, \mathbf{X}_u, \nu_u) du + e^{-r(\tau-t)} g_1(\mathbf{X}_\tau) \right], \quad (3.18)$$

where τ is defined by Equation (3.3), $\mathcal{Z} := \mathcal{V} \times \mathcal{N}$ and $\mathbb{E}_{t, \mathbf{x}}[\cdot]$ is the expectation given the initial state of the system $(t, \mathbf{x} \in [0, T) \times \mathcal{O})$. The function f_1 may play the role of a running gain and/or penalty criterion. We include the lit-pool trading rate ν in f_1 as it may reflect a penalisation for the information leakage to which publicly-displayed orders are subject to. The function g_1 is a terminal bequest function which can include (i) the terminal cash, and (ii) the theoretical monetised value as well as a terminal penalty for the remaining inventory at time τ . For $\mathbf{p} \in \mathbb{R}^4$ with components (p_1, p_2, p_3, p_4) , we define the operator \mathcal{H}_1 by

$$\mathcal{H}_1(t, \mathbf{x}, \mathbf{p}) = \sup_{v \in \mathcal{V}} \left\{ f_1(t, \mathbf{x}, v) - vp_1 + \mu^b(t, s^b, v)p_2 + \mu^\Delta(t, \Delta, v)p_3 + \mu^y(t, s^b, \Delta, v)p_4 \right\},$$

and further the operators $\mathcal{B}_{b, \Delta}(t, \mathbf{x}, \varphi)$, $\mathcal{B}_\Delta(t, \mathbf{x}, \varphi)$ and $\mathcal{B}_y(t, \mathbf{x}, \varphi)$ by

$$\begin{aligned} \mathcal{B}_{b, \Delta}(t, \mathbf{x}, \varphi) = & \sum_{i=1}^2 \lambda^{b, i} \mathbb{E}^{(z^{b, i})} \left[\varphi(t, x, s^b + h_i^b(t, s^b) z^{b, i}, \Delta + h_i^{b, \Delta}(t, s^b, \Delta) z^{b, i}, y) \right. \\ & \left. - \varphi(t, \mathbf{x}) - h_i^b(t, s^b) z^{b, i} \frac{\partial \varphi}{\partial s^b}(t, \mathbf{x}) - h_i^{b, \Delta}(t, s^b, \Delta) z^{b, i} \frac{\partial \varphi}{\partial \Delta}(t, \mathbf{x}) \right], \end{aligned} \quad (3.19)$$

$$\begin{aligned} \mathcal{B}_\Delta(t, \mathbf{x}, \varphi) = & \sum_{i=1}^2 \lambda^{\Delta, i} \mathbb{E}^{(z^{\Delta, i})} \left[\varphi(t, x, s^b, \Delta + h_i^\Delta(t, \Delta) z^{\Delta, i}, y) - \varphi(t, \mathbf{x}) \right. \\ & \left. - h_i^\Delta(t, \Delta) z^{\Delta, i} \frac{\partial \varphi}{\partial \Delta}(t, \mathbf{x}) \right] \end{aligned} \quad (3.20)$$

and

$$\mathcal{B}_y(t, \mathbf{x}, \varphi) = \sup_{n \in \mathcal{N}} \lambda^y \mathbb{E}^{(z^y)} \left[\varphi(t, x - nz^y, s^b, \Delta, y + h^y(t, s^b, \Delta, n)z^y) - \varphi(t, \mathbf{x}) \right], \quad (3.21)$$

Standard dynamic programming arguments suggest that the HJB equation associated to the optimisation problem in (3.18) is a PIDE of the form

$$\begin{aligned} rV(t, \mathbf{x}) - \frac{\partial V}{\partial t}(t, \mathbf{x}) - \mathcal{H}_1(t, \mathbf{x}, D_{\mathbf{x}}V) - \mathcal{B}_{b, \Delta}(t, \mathbf{x}, V) - \mathcal{B}_{\Delta}(t, \mathbf{x}, V) \\ - \mathcal{B}_y(t, \mathbf{x}, V) = 0, \end{aligned} \quad (3.22)$$

on $[0, T) \times \mathcal{O}$, with terminal condition $V(\tau, \mathbf{x}) = g_1(\mathbf{x})$ and boundary condition $V(u, 0, s^b, \Delta, y) = y$. In Chapter 7 we show that $V(t, \mathbf{x})$ is the unique continuous viscosity solution of Equation (3.22).

3.3.3 Explicit examples and numerical results

We now look at the same examples presented in Section 3.2.3, only this time we start with the mean-reverting model, which is the one that is widely known to better reflect empirical market features.

3.3.3.1 Mean-reverting model

As well-known by practitioners and as also taken into account in much of the current literature (see e.g. Cartea et al. [24], and Fodra and Pham [38]), the LOB prices—and, thus, the market spread—mean-revert quickly to their long-term mean. Thus we choose the following dynamics for the best bid price and the spread processes:

$$dS_u^b = [\kappa^b(\bar{S} - S_{u-}^b) - \mu\nu_u]du + dJ_u^{b,1} - dJ_u^{b,2}, \quad (3.23)$$

$$d\Delta_u = [\kappa^\Delta(\bar{\Delta} - \Delta_{u-}) + \mu\nu_u]du + dJ_u^{\Delta,1} - dJ_u^{\Delta,2} - dJ_u^{b,1} + dJ_u^{b,2}, \quad (3.24)$$

where we have set $\mu^b(t, s^b, v) = [\kappa^b(\bar{S} - s^b) - \mu v]$, $h_i^b(t, s^b) = \mathbb{1}_{\{i=1\}} - \mathbb{1}_{\{i=2\}}$, $\mu^\Delta(t, \Delta, v) = [\kappa^\Delta(\bar{\Delta} - \Delta) + \mu v]$, $h_i^\Delta(t, \Delta) = \mathbb{1}_{\{i=1\}} - \mathbb{1}_{\{i=2\}}$ and $h_i^{b,\Delta}(t, s^b, \Delta) = \mathbb{1}_{\{i=2\}} - \mathbb{1}_{\{i=1\}}$. We let \bar{S} and $\bar{\Delta}$ be the long-term means and κ^b and κ^Δ are the speeds of mean reversion of $\{S_u^b\}$ and $\{\Delta_u\}$, respectively. In Equation (3.23) we

interpret $dJ^{b,1}$ to be the change in the best bid price due to the submission of limit buy orders at a more favourable price, whereas $dJ^{b,2}$ models the changes due to incoming market sell orders which walk the book and the effect of cancellations of limit buy orders posted at the best price. As we stated earlier in this work, when the best bid price jumps upward by means of $dJ^{b,1}$, the spread process should simultaneously jump downward and this is the reason why $dJ^{b,1}$ also appears in Equation (3.24). The analogous holds for $dJ^{b,2}$. The remaining compound Poisson processes that appear in the spread dynamics are associated to the movements of the best ask price, which jumps upward thanks to market buy orders that walk the book, and jumps downward when a limit sell order is posted at a price lower than the current best ask price. Finally, we note that the trading rate in the ‘lit’ pool appears in the drift of the spread dynamics since, by pushing the best bid price down, it simultaneously widens the spread. The top of the book (TOB) simulation in Figure 3.10 depict very similar features to those shown in real data.

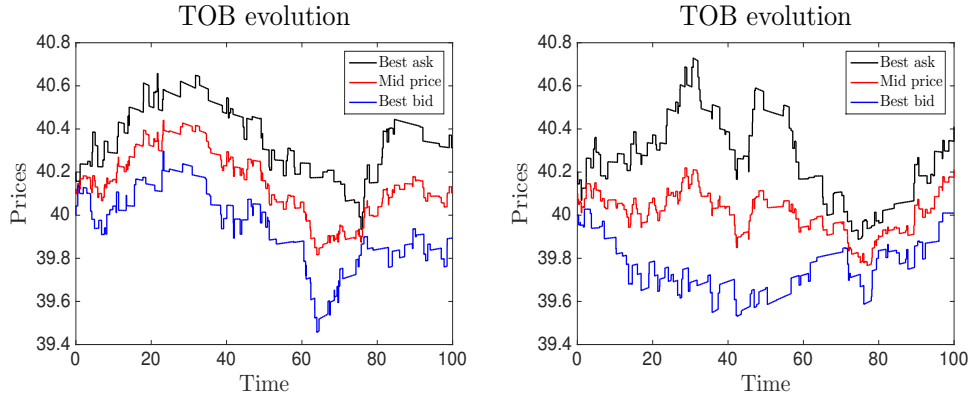


FIGURE 3.10: Simulation of Equations (3.23) and (3.24). We set $z^{b,i}, z^{\Delta,i} \sim U[0, 1)$, $\lambda^{b,1} = \lambda^{b,2} = \lambda^{\Delta,1} = \lambda^{\Delta,2} = 0.5$, $\bar{\Delta} = 0.2$, $\bar{S} = 40$, $\kappa^b = \kappa^{\Delta} = 0.0002$, $S_t = 40$, $\Delta_t = 0.2$, $T = 100$.

Next, we consider an investor who wants to optimally liquidate their portfolio by placing sell orders in both the ‘lit’ market and the dark pool. The inventory process of the investor is here modelled by (3.16), while we model the cash process by

$$dY_u = \nu_u \hat{S}_u^b du + \eta_u S_u^m dJ_u^y, \quad (3.25)$$

where we define, for $\beta > 0$, $\hat{S}_u^b = S_u^b - \beta \nu_u$. In Equation 3.25 we have set $\mu^y(u, s^b, \nu) = \nu s^b$ and $h^y(u, s^b, \Delta, \eta) = \eta s^m = \eta(s^b + \Delta/2)$. Equation 3.25 can

be interpreted as follows. The quantity $\nu_u \hat{S}_u^b$ represents the revenues deriving from selling the shares at the impacted bid price in the 'lit' pool. The quantity $\eta_u S_u^m$ represents the order sent to the dark pool evaluated at the mid-price, which increases the cash process of the agent, only if it is executed (and for the quantity executed). The execution in the dark pool is modelled by the compound Poisson process J_u^y .

The maximised expected return derived by the shares sale is obtained by solving the optimisation problem

$$V(t, \mathbf{x}) = \sup_{\nu \in \mathcal{Z}} \mathbb{E}_{t, \mathbf{x}} \left[e^{-r(\tau-t)} (Y_\tau + X_\tau (S_\tau^m - \alpha X_\tau)) - \phi \int_t^\tau e^{-r(u-t)} X_u^2 du \right], \quad (3.26)$$

where we have set $f_1(t, \mathbf{x}, v) = -\phi x^2$ and $g_1(\mathbf{x}) = y + x(s^m - \alpha x)$, where τ is defined by Equation (3.3) and $\phi \in \mathbb{R}_+ \cup 0$. In the considered performance criterion, we allow for a maximisation of the terminal cash Y_τ together with the terminal theoretical value of the portfolio $S_\tau^m X_\tau$ (i.e. the remaining shares evaluated at the mid-price), and a penalty for a non-zero inventory level at time τ given by $-\alpha X_\tau^2$, where $\alpha > 0$. The integral term, as in Cartea et al. [18, 20], penalises for the inventory holding over the whole period in which the strategy is applied. The associated HJB PIDE is given by

$$\begin{aligned} \sup_{v \in \mathcal{Z}} \left\{ \frac{\partial V}{\partial t}(t, \mathbf{x}) - rV(t, \mathbf{x}) - \phi x^2 + [\kappa^b (\bar{S} - s^b) - \mu v] \frac{\partial V}{\partial s^b}(t, \mathbf{x}) \right. \\ \left. + [\kappa^\Delta (\bar{\Delta} - \Delta) + \mu v] \frac{\partial V}{\partial \Delta}(t, \mathbf{x}) + v(s^b - \beta v) \frac{\partial V}{\partial y}(t, \mathbf{x}) - v \frac{\partial V}{\partial x}(t, \mathbf{x}) \right. \\ \left. + \lambda^y \mathbb{E}^{(z^y)} \left[V(t, x - nz^y, s^b, \Delta, y + nz^y(s^b + \Delta/2)) - V(t, \mathbf{x}) \right] \right. \\ \left. + \lambda^{b,1} \mathbb{E}^{(z^{b,1})} \left[V(t, x, s^b + z^{b,1}, \Delta - z^{b,1}, y) - V(t, \mathbf{x}) \right] \right. \\ \left. + \lambda^{b,2} \mathbb{E}^{(z^{b,2})} \left[V(t, x, s^b - z^{b,2}, \Delta + z^{b,2}, y) - V(t, \mathbf{x}) \right] \right. \\ \left. + \lambda^{\Delta,1} \mathbb{E}^{(z^{\Delta,1})} \left[V(t, x, s^b, \Delta + z^{\Delta,1}, y) - V(t, \mathbf{x}) \right] \right. \\ \left. + \lambda^{\Delta,2} \mathbb{E}^{(z^{\Delta,2})} \left[V(t, x, s^b, \Delta - z^{\Delta,2}, y) - V(t, \mathbf{x}) \right] \right\} = 0, \quad (3.27) \end{aligned}$$

with terminal condition $V(\tau, \mathbf{x}) = y + (s^b + \Delta/2 - \alpha x)x$ and boundary condition $V(u, 0, s^b, \Delta, y) = y$.

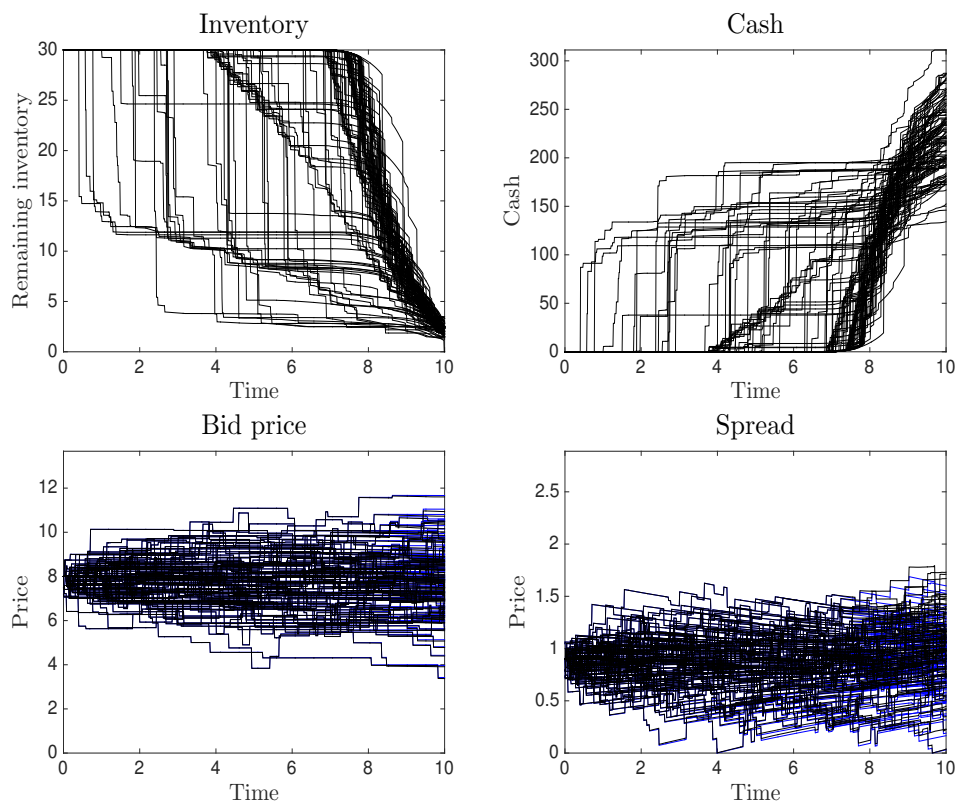


FIGURE 3.11: Simulation of Equations (3.16), (3.25), (3.23) and (3.24). We set $\beta = 0.001$, $\mu = 0.001$, $x = 30$, $s^b = 8$, $\bar{S} = 8$, $\Delta = 1$, $\bar{\Delta} = 1$, $\lambda^{b,1} = \lambda^{b,2} = \lambda^{\Delta,1} = \lambda^{\Delta,2} = 0.5$, $z^{b,i}, z^{\Delta,i} \sim U[0, 1]$, $\lambda^y = 0.1$, $z^y \sim U[0, 1]$, $r = 0.02$, $T = 10$, $\phi = 0.001$, $\alpha = 2$, $\kappa^b = \kappa^\Delta = 0.1$. In the bottom panels, the black lines depict the impacted prices while the corresponding blue lines represent the theoretical unimpacted prices.

First, we plot a hundred simulations of the state variables of the model and, in Figure 3.11, we show: (i) the inventory evolution (top left panel), (ii) the cash evolution (top right panel), (iii) the best bid price (bottom left panel), and (iv) the spread (bottom right panel). For the parameters' analysis, we plot the mean strategy and we consider three different scenarios for the dark-pool liquidity: (i) no execution takes place in the dark pool throughout the entire trading period (upper/dotted line), (ii) partial execution (middle/dashed line), and (iii) full execution (bottom/solid line). We let the dark-pool executions, if any, take place at $\tau_1 = 4$ and $\tau_2 = 7$. Furthermore, we let the partial execution to account for 50% of the order posted. We emphasise that τ_1 and τ_2 , as well as the execution portion in the dark pool, are fixed arbitrarily—for the sake of illustration only—after a complete solution has been found. The reason for this choice is to make comparison between graphs rather straightforward.

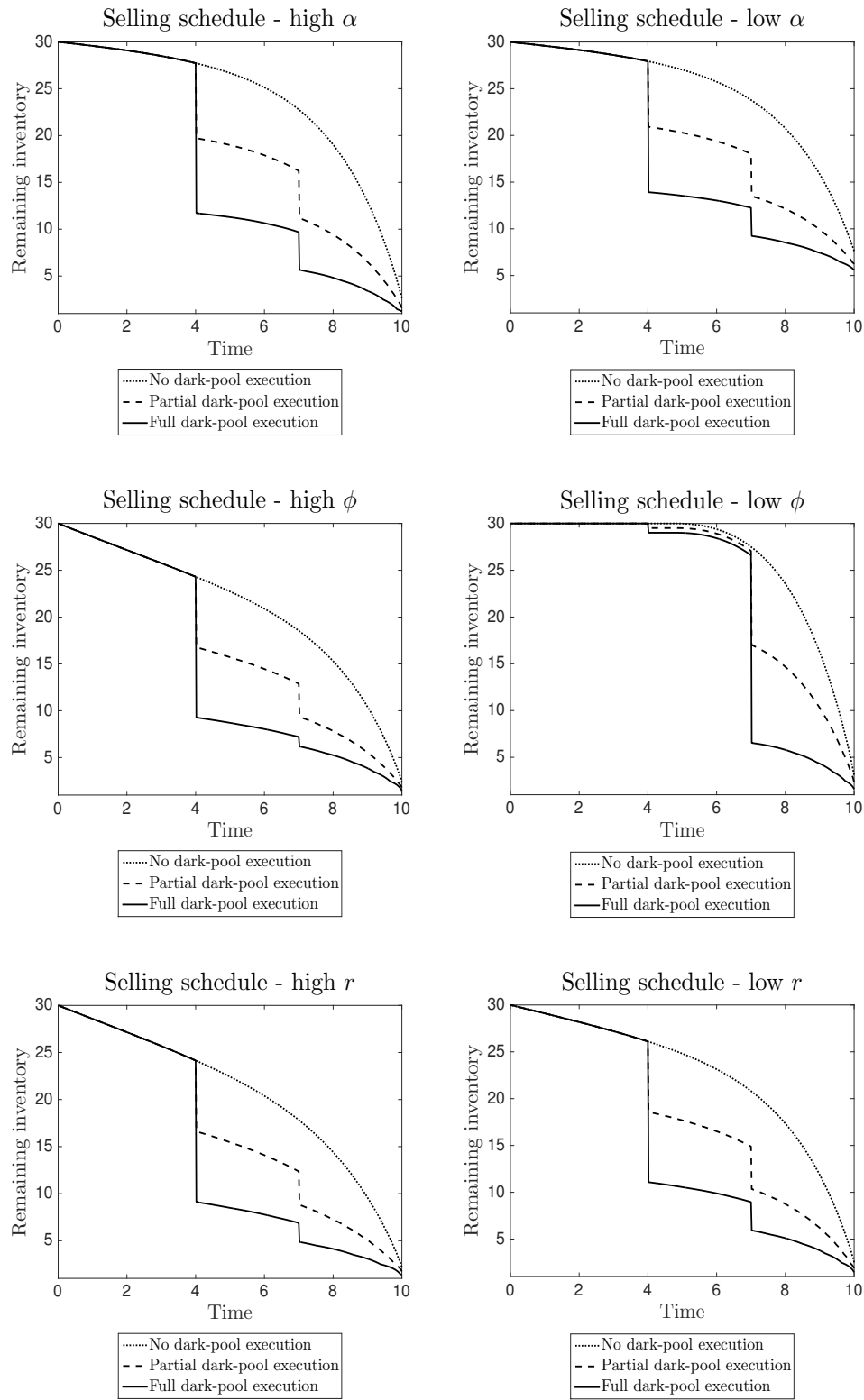


FIGURE 3.12: Optimal mean selling strategy—displayed as a function of the remaining inventory—found by solving the HJB equation (3.27). We set $\kappa^b = \kappa^\Delta = 0.01$, $\beta = 0.01$, $x = 30$, $s^b = 5$, $\Delta = 0.5$, $\bar{S} = 5$, $\bar{\Delta} = 1$, $\lambda^{b,1} = \lambda^{b,2} = \lambda^{\Delta,1} = \lambda^{\Delta,2} = 0.2$, $z^{b,i}, z^{\Delta,i} \sim U[0, 1]$, $\mu = 0.01$, $\lambda^y = 0.1$, $z^y \sim U[0, 1]$, $\alpha = 2$, $T = 10$. In the top panels we set $r = 0.01$, $\phi = 0.001$, $\alpha = 4$ (left), $\alpha = 0.5$ (right). In the middle panels we set $r = 0.01$, $\alpha = 2$, $\phi = 0.1$ (left), $\phi = 0.0001$ (right). In the bottom panels we set $\phi = 0.001$, $\alpha = 2$, $r = 0.1$ (left), $r = 0.0001$ (right).

In Figures 3.12 we see that higher values of the terminal penalty α increase the total portion of inventory liquidated by T , while higher value of the parameter ϕ and r increase the liquidation speed throughout the whole period, while leaving the terminal-inventory level almost unchanged. As noted earlier, α penalises only for the terminal holdings, while ϕ penalises for the current holdings, and r increases the reward for the shares liquidated earlier.

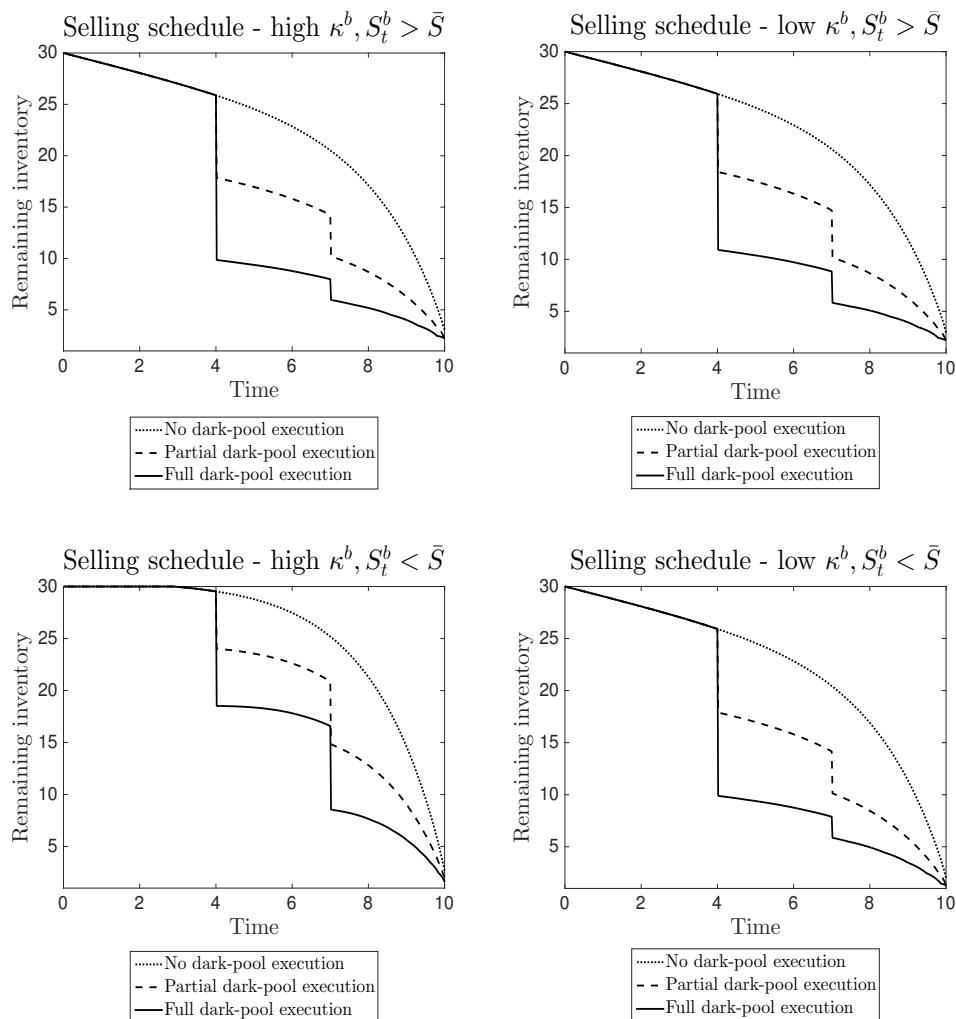


FIGURE 3.13: Optimal mean selling strategy—displayed as a function of the remaining inventory—found by solving the HJB equation (3.27). We set $\kappa^\Delta = 0.01$, $\beta = 0.01$, $x = 30$, $s^b = 5$, $\Delta = 1$, $\bar{\Delta} = 0.5$, $\lambda^{b,1} = \lambda^{b,2} = \lambda^{\Delta,1} = \lambda^{\Delta,2} = 0.2$, $z^{b,i}, z^{\Delta,i} \sim U[0, 1]$, $\mu = 0.01$, $\lambda^y = 0.1$, $z^y \sim U[0, 1]$, $\alpha = 2$, $\phi = 0.001$, $r = 0.01$, $T = 10$. In the top panels we set $\bar{S} = 3$, $\kappa^b = 0.1$ (left), $\kappa^b = 0.0005$ (right). In the bottom panels we set $\bar{S} = 7$, $\kappa^b = 0.1$ (left), $\kappa^b = 0.0005$ (right).

The speed of mean reversion of the best bid price (i.e. κ^b) has a different impact on the selling schedule, depending on the initial value of the bid price S_t^b and,

in particular, whether it is higher or lower than its long-term mean \bar{S} . In the top panels of Figure 3.13 we set $S_t^b > \bar{S}$, which implies that, on average, the price is going to decrease to get closer to its long-term mean. The agent is thus incentivised to liquidate faster at the beginning since the price is higher than it is supposed to be. This feature is more evident when the speed of mean reversion κ^b is higher. In fact, the price reverts faster and the agent increases their liquidation speed so to exploit the opportunity of selling at a higher price.

In the bottom panels of Figure 3.13, the starting price is lower than its long-term mean, i.e. $S_t^b < \bar{S}$, and thus the agent waits for it to revert, so to liquidate at a more favourable price. As opposed to the previous case, a higher κ^b reduces the liquidation speed. This is rather intuitive: the agent is willing to wait for the price to increase, which, on average, takes less time than the case of low κ^b .

In Figure 3.14 we analyse the role of the speed of mean reversion κ^Δ of the spread process. Before entering into details, we make a few considerations on how the spread affects the agent's trading strategy. First and foremost, we acknowledge that the spread is a measure of the market liquidity. In particular, a tighter spread models a highly liquid market, while less liquid markets usually have wider spreads. Also, in liquid markets, the spread mean-reverts faster than in an illiquid market, where trades have higher permanent impact. Finally, a wider spread makes the trading in the dark pool more advantageous, than the case of a tighter spread. We thus expect larger trades in the dark pool when the spread is higher.

In the top panels of Figure 3.14, we set $\Delta_t > \bar{\Delta}$ and, therefore, the spread is expected to decrease by reverting to its long-term mean $\bar{\Delta}$. For high values of the speed of mean reversion κ^Δ , the agent increases their liquidation speed in both venues, compared to the case of low κ^Δ . In fact, when the speed of mean reversion is low, the benefits of a fast liquidation decrease (top right panel). In the bottom panels, we set $\Delta_t < \bar{\Delta}$ and thus the spread is expected to increase. For a high speed of mean reversion (bottom left panel), the agent dramatically reduces their dark-pool posting as they are encouraged to wait for a larger spread. The opposite holds when the spread is expected to revert slowly (bottom right panel).

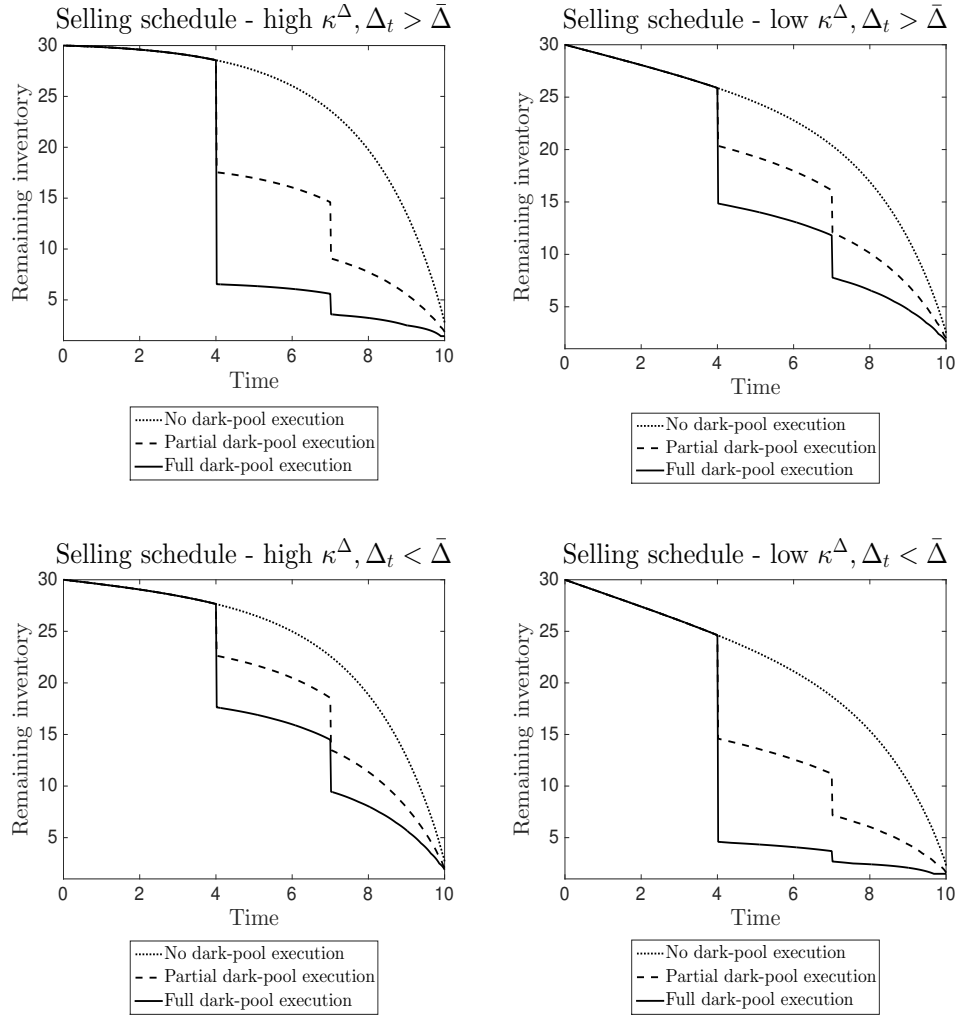


FIGURE 3.14: Optimal mean selling strategy—displayed as a function of the remaining inventory—found by solving the HJB equation (3.27). We set $\kappa^b = 0.01$, $\beta = 0.01$, $x = 30$, $s^b = 5$, $\Delta = 0.5$, $\bar{S} = 5$, $\lambda^{b,1} = \lambda^{b,2} = \lambda^{\Delta,1} = \lambda^{\Delta,2} = 0.2$, $\mu = 0.01$, $z^{b,i}, z^{\Delta,i} \sim U[0, 1)$, $\lambda^y = 0.1$, $z^y \sim U[0, 1]$, $\alpha = 2$, $\phi = 0.001$, $r = 0.01$, $T = 10$. In the top panels we set $\bar{\Delta} = 0.3$, $\kappa^\Delta = 0.1$ (left), $\kappa^\Delta = 0.0005$ (right). In the bottom panels we set $\bar{\Delta} = 0.7$, $\kappa^\Delta = 0.1$ (left), $\kappa^\Delta = 0.0005$ (right).

In Figure 3.15 we analyse the role of both the permanent and the temporary price impacts.

As expected, higher impacts reduce the quantity we post in the ‘lit’ pool (left panels) while lower impacts encourage the lit-pool posting (right panels).

This is in agreement with the results previously obtained.

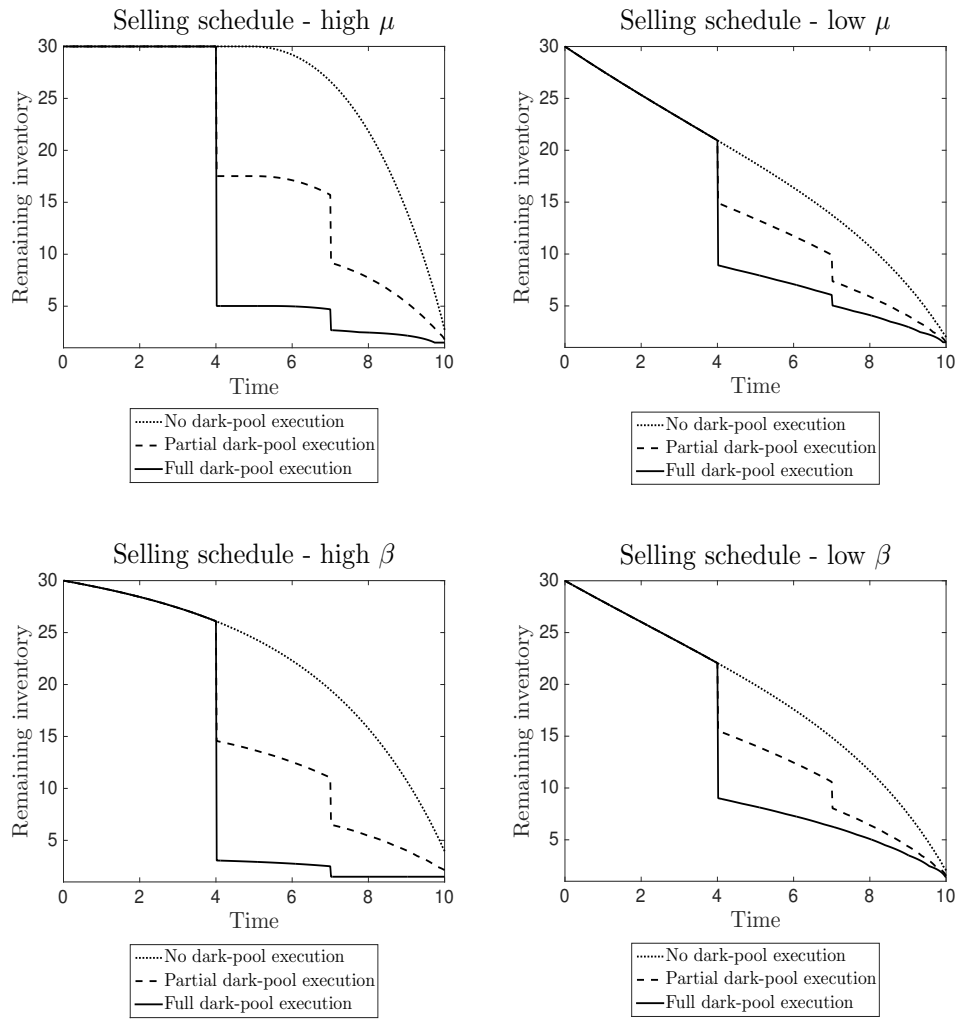


FIGURE 3.15: Optimal mean selling strategy displayed as a function of the remaining inventory. We set $\kappa^b = \kappa^\Delta = 0.01$, $x = 30$, $s^b = 5$, $\Delta = 0.5$, $\bar{S} = 5$, $\bar{\Delta} = 0.5$, $\lambda^{b,1} = \lambda^{b,2} = \lambda^{\Delta,1} = \lambda^{\Delta,2} = 0.2$, $z^{b,i}, z^{\Delta,i} \sim U[0,1]$, $\phi = 0.001$, $\alpha = 2$, $\lambda^y = 0.1$, $z^y \sim U[0,1]$, $r = 0.01$, $\phi = 0.001$, $T = 10$. In the top panels we set $\beta = 0.01$, $\mu = 0.1$ (left), $\mu = 0.001$ (right). In the bottom panels we set $\mu = 0.01$, $\beta = 0.03$ (left), $\beta = 0.001$ (right).

Figure 3.16 shows the optimal selling schedule for different values of the arrival rates of the jump processes in both the best bid price and the spread processes. We show that the agent's trading schedule crucially depends on both the price dynamics and the market liquidity. In particular, a trading acceleration in both venues is optimal when the spread is subject to more downwards jumps rather than upwards jumps. The opposite holds for the case of more frequent upwards jumps.

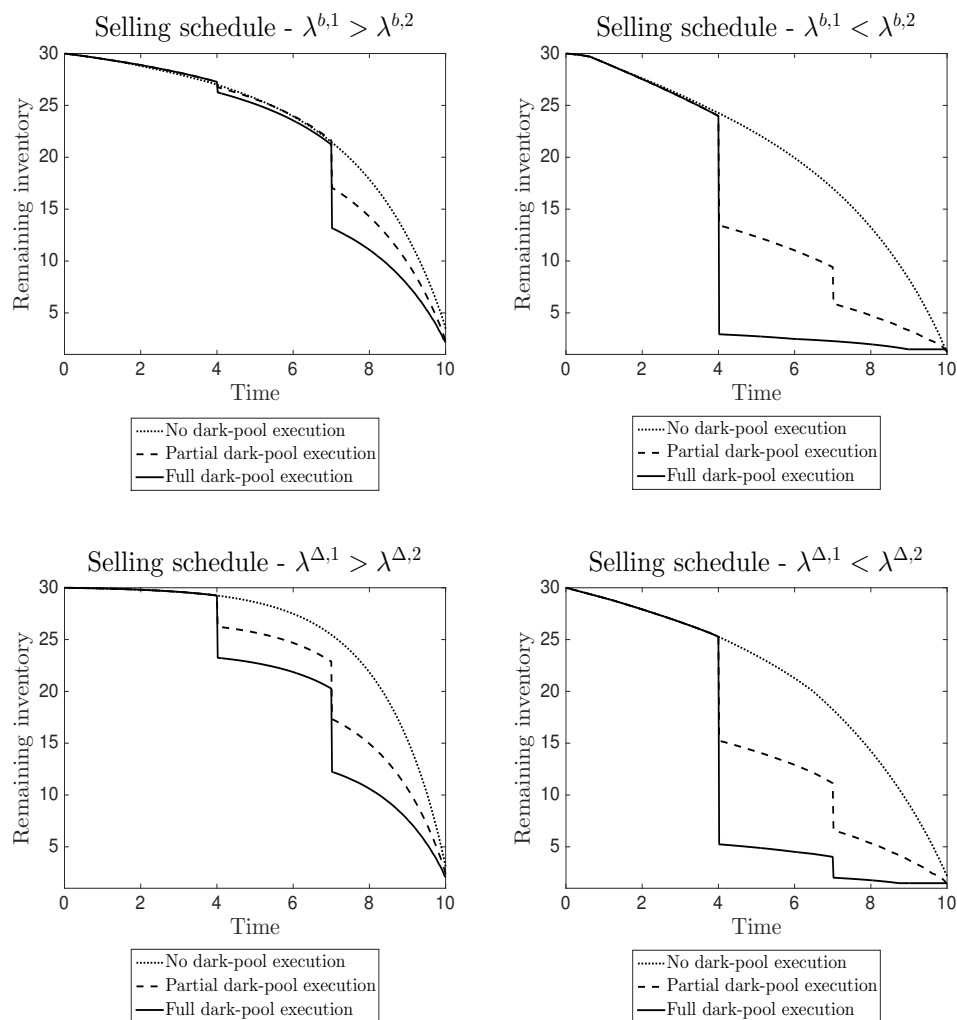


FIGURE 3.16: Optimal mean selling strategy—displayed as a function of the remaining inventory—found by solving the HJB equation (3.27). We set $\kappa^b = \kappa^\Delta = 0.01$, $\beta = 0.01$, $x = 30$, $s^b = 5$, $\Delta = 0.5$, $\bar{S} = 5$, $\bar{\Delta} = 0.5$, $\mu = 0.01$, $\lambda^y = 0.1$, $z^y \sim U[0, 1]$, $z^{b,i}, z^{\Delta,i} \sim U[0, 1]$, $r = 0.01$, $\phi = 0.001$, $\alpha = 2$, $T = 10$. In the top panels we set $\lambda^{\Delta,1} = \lambda^{\Delta,2} = 0.2$, $\lambda^{b,1} = 0.7$, $\lambda^{b,2} = 0.1$ (left), $\lambda^{b,1} = 0.1$, $\lambda^{b,2} = 0.7$ (right). In the bottom panels we set $\lambda^{b,1} = \lambda^{b,2} = 0.2$, $\lambda^{\Delta,1} = 0.7$, $\lambda^{\Delta,2} = 0.1$ (left), $\lambda^{\Delta,1} = 0.1$, $\lambda^{\Delta,2} = 0.7$ (right)

Figure 3.17 shows the optimal selling schedule for different values of the arrival rate of the dark-pool executions, λ^y . Higher values of λ^y act as a deterrent for lit-pool trading, as dark-pool executions are more likely than in the case of low λ^y . We note that the lit-pool liquidation speed decreases for high λ^y (left panel) while it increases for low λ^y (right panel). This confirms both our intuition and the results previously obtained in Figure 2.11.

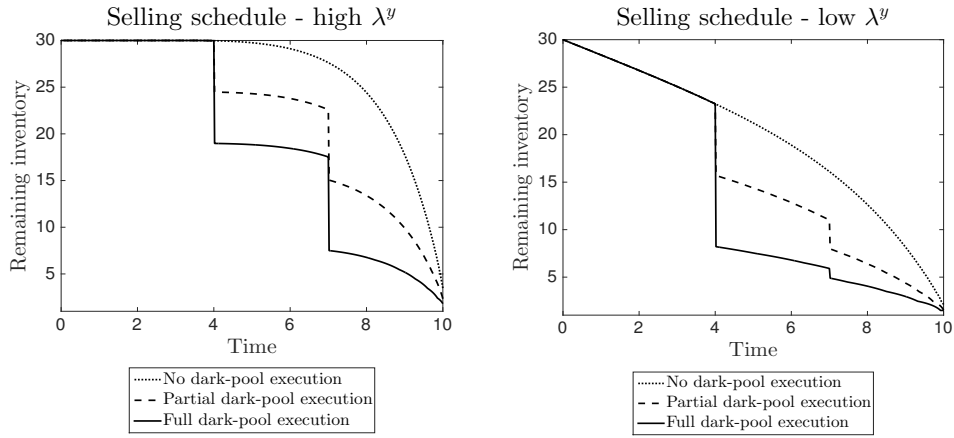


FIGURE 3.17: Optimal selling strategy—displayed as a function of the remaining inventory—found by solving the HJB equation (3.27). We set $\kappa^b = \kappa^\Delta = 0.01$, $\beta = 0.01$, $\phi = 0.01$, $x = 30$, $s^b = 5$, $\Delta = 0.5$, $\bar{S} = 5$, $\bar{\Delta} = 0.5$, $\lambda^{b,1} = \lambda^{b,2} = \lambda^{\Delta,1} = \lambda^{\Delta,2} = 0.2$, $z^{b,i}, z^{\Delta,i} \sim U[0, 1]$, $\mu = 0.01$, $z^y \sim U[0, 1]$, $r = 0.01$, $\phi = 0.001$, $\alpha = 2$, $T = 10$. In the left panel we set $\lambda^y = 0.5$. In the right panel we set $\lambda^y = 0.01$.

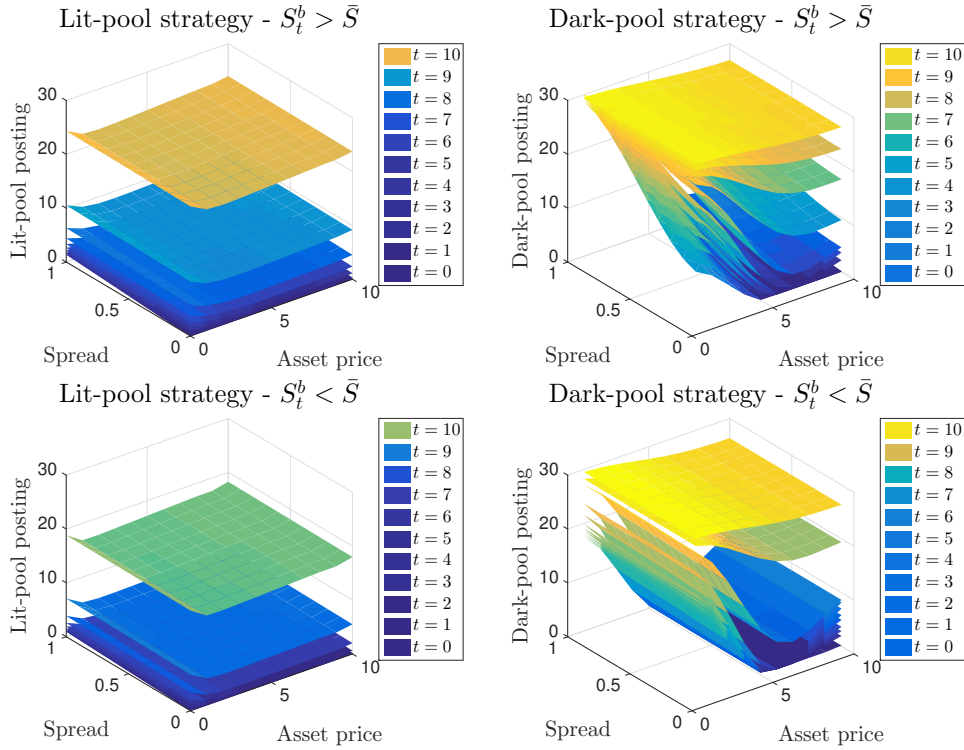


FIGURE 3.18: Optimal ‘lit’ and dark-pool strategies—found by solving the HJB equation (3.27)—for an inventory of 30 (left and right panels, respectively). We set $\kappa^b = \kappa^\Delta = 0.01$, $\beta = 0.01$, $\phi = 0.01$, $\bar{S} = 5$, $\bar{\Delta} = 0.5$, $\lambda^{b,1} = \lambda^{b,2} = \lambda^{\Delta,1} = \lambda^{\Delta,2} = 0.2$, $z^{b,i}, z^{\Delta,i} \sim U[0, 1]$, $\mu = 0.01$, $\lambda^y = 0.1$, $z^y \sim U[0, 1]$, $r = 0.01$, $\phi = 0.001$, $\alpha = 2$, $T = 10$. In the top panels, we set $S_t^b > \bar{S}$. In the bottom panels we set $S_t^b < \bar{S}$.

Finally, in Figure 3.18, we plot the optimal ‘lit’ and dark-pool strategies as functions of the bid price and the spread. The plots are to be read as follows:

Each surface represents the optimal posting in the venue specified in the title, for the time t specified in the legend, if the inventory at that particular time is 30,000. This is only to show the qualitative features of the optimal strategy, as a complete solution would also require an optimal posting for all levels of inventory at all times (we here only plot surfaces for one-second time intervals). We can see that roundtrips in dark pools are not necessarily beneficial, especially when adding features such as permanent impact and prices dynamics different from martingales. As a final consideration, we note that the posting in both venues increases—as maturity approaches—due to the terminal penalty α .

3.3.3.2 Geometric Lévy model

For the sake of completeness, we propose an exponential model so to ensure the positivity of the best bid price and the spread processes at every time $u \in [t, T]$. (We here shall further require $|z^{b,i}| < 1$, $z^{\Delta,1} > -1$ and $z^{\Delta,2} < 1$, almost surely). We let the best bid price be defined by Equation (3.13) and we let the market spread evolve according to

$$\frac{d\Delta_u}{\Delta_u} = (\bar{\mu}^\Delta + \mu\nu_u)du - dJ_u^{b,1} + dJ_u^{b,2} + dJ_u^{\Delta,1} - dJ_u^{\Delta,2}, \quad (3.28)$$

where we have set $\mu^\Delta(t, \Delta, v) = (\bar{\mu}^\Delta + \mu v)\Delta$, $h_i^\Delta(t, \Delta) = \Delta(\mathbb{1}_{\{i=1\}} - \mathbb{1}_{\{i=2\}})$ and $h_i^{b,\Delta}(t, s^b, \Delta) = \Delta(\mathbb{1}_{\{i=2\}} - \mathbb{1}_{\{i=1\}})$. In Figure 3.19 we plot a simulation of the best ask, the mid and the best bid prices. We keep the inventory and the cash dynamics as in Equations (3.16) and (3.25) respectively, and we consider the value function stated in Equation (3.26).

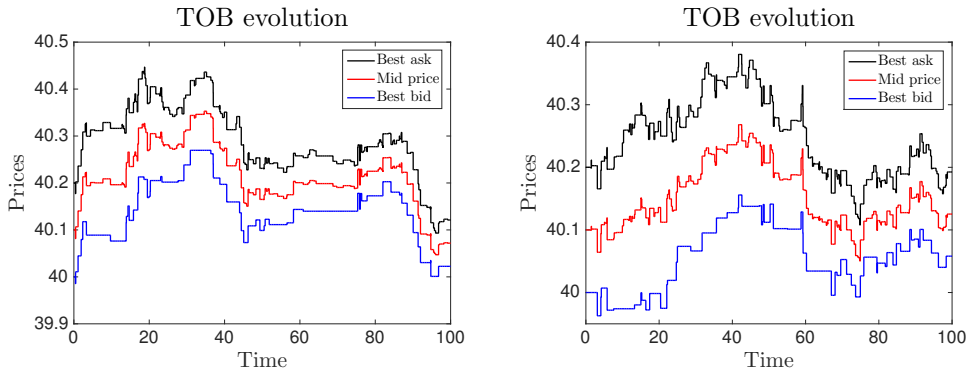


FIGURE 3.19: Simulation of Equations (3.13) and (3.28). We set $z^{b,i}, z^{\Delta,i} \sim U[0, 1]$, $\lambda^{b,1} = \lambda^{b,2} = 0.5$, $\lambda^{\Delta,1} = \lambda^{\Delta,2} = 0.6$, $\bar{\mu}^b = \bar{\mu}^\Delta = 0$, $\bar{S} = 40$, $S_t = 40$, $\Delta_t = 0.2$, $T = 100$.

The associated HJB PIDE is given by

$$\begin{aligned}
\sup_{v \in \mathcal{Z}} \left\{ \frac{\partial V}{\partial t}(t, \mathbf{x}) - rV(t, \mathbf{x}) - \phi x^2 + (\bar{\mu}^b - \mu v) s^b \frac{\partial V}{\partial s^b}(t, \mathbf{x}) \right. \\
+ (\bar{\mu}^\Delta + \mu v) \Delta \frac{\partial V}{\partial \Delta}(t, \mathbf{x}) + v(s^b - \beta v) \frac{\partial V}{\partial y}(t, \mathbf{x}) - v \frac{\partial V}{\partial x}(t, \mathbf{x}) \\
+ \lambda^y \mathbb{E}^{(z^y)} \left[V(t, x - nz^y, s^b, \Delta, y + nz^y(s^b + \Delta/2)) - V(t, \mathbf{x}) \right] \\
+ \lambda^{b,1} \mathbb{E}^{(z^{b,1})} \left[V(t, x, s^b(1 + z^{b,1}), \Delta(1 - z^{b,1}), y) - V(t, \mathbf{x}) \right] \\
+ \lambda^{b,2} \mathbb{E}^{(z^{b,2})} \left[V(t, x, s^b(1 - z^{b,2}), \Delta(1 + z^{b,2}), y) - V(t, \mathbf{x}) \right] \\
+ \lambda^{\Delta,1} \mathbb{E}^{(z^{\Delta,1})} \left[V(t, x, s^b, \Delta(1 + z^{\Delta,1}), y) - V(t, \mathbf{x}) \right] \\
\left. + \lambda^{\Delta,2} \mathbb{E}^{(z^{\Delta,2})} \left[V(t, x, s^b, \Delta(1 - z^{\Delta,2}), y) - V(t, \mathbf{x}) \right] \right\} = 0,
\end{aligned} \tag{3.29}$$

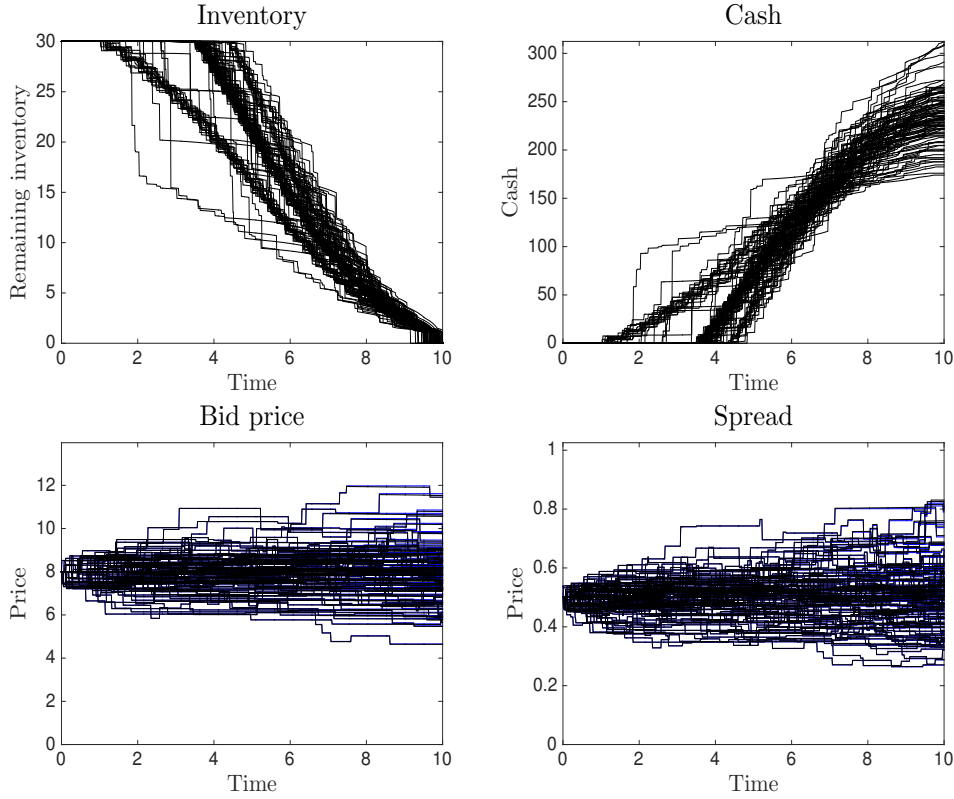


FIGURE 3.20: Simulation of Equations (3.16), (3.25), (3.13) and (3.28). We set $\beta = 0.001$, $\mu = 0.001$, $x = 30$, $s^b = 5$, $\Delta = 0.5$, $\lambda^{b,1} = \lambda^{b,2} = \lambda^{\Delta,1} = \lambda^{\Delta,2} = 0.5$, $z^{b,i}, z^{\Delta,i} \sim U[0, 1]$, $\lambda^y = 0.1$, $z^y \sim U[0, 1]$, $r = 0.02$, $T = 10$, $\phi = 0.001$, $\alpha = 2$, $\bar{\mu}^b = \bar{\mu}^\Delta = 0$. In the bottom panels, the black lines depict the impacted prices while the corresponding blue lines represent the theoretical unimpacted prices.

As we provided an extended analysis of the model parameters in Section 3.3.3.1,

we here only show the state-variables simulations and the optimal ‘lit’ and dark-pool strategies, in Figures 3.20 and 3.21 respectively. In the top panels of Figure 3.21, the spread and the best bid price are assumed to be supermartingales while in the bottom panels they are assumed to be submartingales. We note that the optimal quantity to be posted in both venues is smaller in the latter case compared to the former. Finally, we note that roundtrips are not necessarily beneficial.

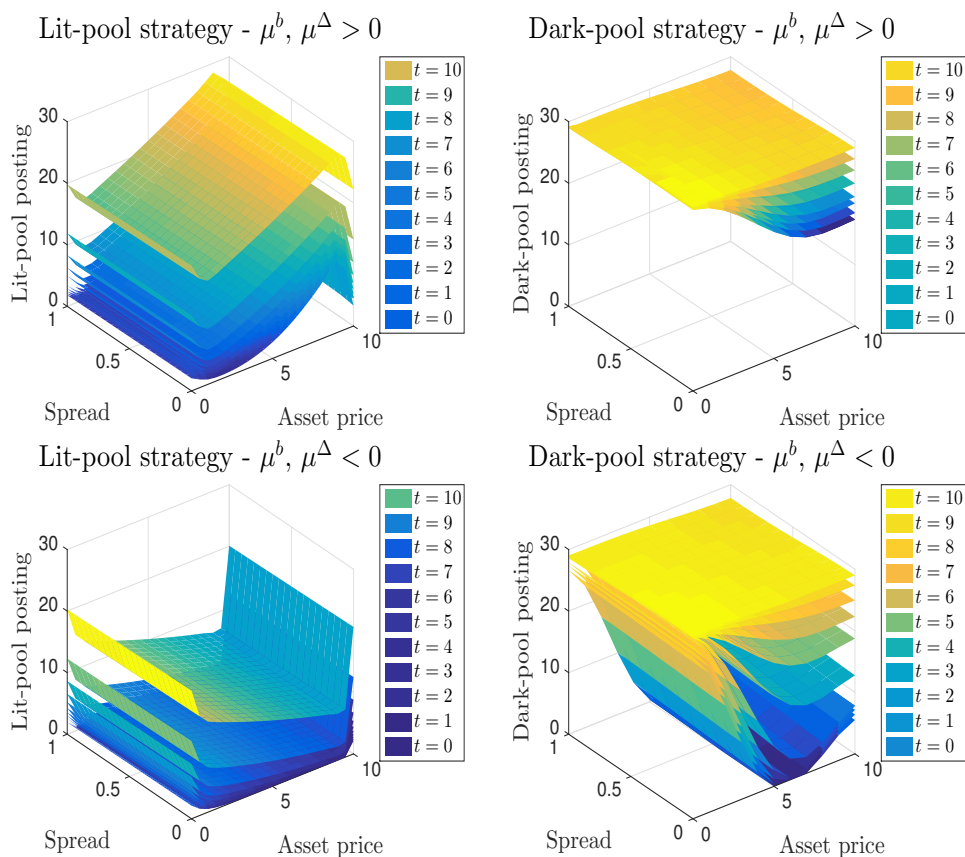


FIGURE 3.21: Optimal ‘lit’ and dark-pool strategies—found by solving the HJB equation (3.29)—for an inventory of 30 (left and right panels, respectively). We set $\beta = 0.01$, $x = 30$, $\lambda^{b,1} = \lambda^{b,2} = \lambda^{\Delta,1} = \lambda^{\Delta,2} = 0.2$, $z^{b,i}, z^{\Delta,i} \sim U[0, 1)$, $\mu = 0.01$, $\lambda^y = 0.1$, $z^y \sim U[0, 1]$, $r = 0.01$, $\phi = 0.001$, $\alpha = 2$, $T = 10$. In the left panel we set $\bar{\mu}^b = \bar{\mu}^\Delta = 0.001$. In the right panel we set $\bar{\mu}^b = \bar{\mu}^\Delta = -0.001$.

3.4 Conclusions

In this chapter we present a more sophisticated model than the one introduced in Chapter 2. First, we consider a class of models that can be adapted to the particular situation at hand. Next, we treat in details two explicit examples for

the dynamics of the bid-price and market-spread processes. Finally, we study the role of the model's parameters and plot the optimal strategy of the agent.

We note that the selling schedule crucially depends on both the price dynamics (the best bid) and the market's liquidity (the spread). We consider a mean-reverting model so to reproduce observed market features, and a geometric Lévy model so to ensure the positivity of the prices processes involved.

We take as main reference the papers by Kratz and Schöneborn [57] and Horst and Naujokat [52], and we here outline the main differences. Compared to Kratz and Schöneborn [57], we: (i) introduce an explicit model for the spread process, (ii) consider the permanent price impact for both the best bid price and the spread processes, (iii) consider processes other than martingales, (iv) allow for partial execution in the dark pool and (v) provide a general setup so to account for various modelling preferences. On the other hand, we consider continuous-time trading in the 'lit' pool as opposed to Horst and Naujokat [52], who consider discrete-time trading when crossing the spread. Points (iv) and (v) mentioned above are also a novelty compared to the work by Horst and Naujokat [52].

Chapter 4

The market-making problem in a customised liquidity pool

4.1 Overview of the chapter

Market makers are liquidity providers. They set bid and ask quotes and trade with impatient investors who seek to immediately buy or sell a certain quantity of a financial asset. A portion of the market-maker's P&L derives from the spread charged to the clients. On the other hand, holding a non-zero inventory carries an intrinsic risk associated with the unpredictable changes to which an asset price is subject. This risk is further increased by a potential information asymmetry due to which a market maker trades in the wrong direction.

We consider a financial entity that offers a dealer service to its clients. Such an entity may be a small financial shop, an individual trading desk of large institutions, as well as large firms which provide liquidity to a selected pool of clients. Among these, we find, e.g., investment banks,¹ hedge funds and high-frequency traders. In the industry, such financial entity is sometimes referred to as CLP¹. These bespoke liquidity pools share some characteristics with so-called dark pools, while *additionally* providing the dealer service. As such CLPs may be viewed as “grey pools”, that is, a kind of hybrid between a dark pool and a ‘lit’ pool. CLPs typically offer two-way prices to their clients while preserving their

¹The terminology ‘alternative liquidity pool’ is also used.

anonymity. Clients can compare prices from various dealers through internal GUI applications, but there is no centralised liquidity pool² that displays those prices, which are streamed directly to the clients in conditions of market opacity and confidentiality. CLPs thus offer for all practical purposes a market-making service, though they have no *obligation* to offer two-sided liquidity at any time. In the remainder of the paper, we use the terms “dealer activity” and “market making” interchangeably.

In the situation at hand the CLP (i) offers liquidity to its clients (who may be both buyers and sellers) and (ii) may post limit and market orders in a ‘lit’ exchange to control the level of its inventory. We emphasise that the work presented here has no particular asset class in mind, since the CLP may specialise in, e.g. stocks, commodities and foreign exchange trading.

While Section 2.3.2 already treats part of the original work included in this thesis, the model presented there is very limited in that (i) it does not allow the CLP to choose the prices it offers to clients, (ii) it only allows the CLP to post limit orders in the lit pool on top of the book and not deeper, (iii) the lit-pool spread is assumed to be constant, and (iv) the model is very specific, thus not allowing for much flexibility.

In what follows, we address the aforementioned four points by providing a more flexible and structured model. We start by presenting the trading strategies of the CLP for the purpose of inventory management. Next we formulate the optimisation problem and we provide some examples by numerically solving the associated HJB equation. This chapter is based on Crisafi & Macrina [31].

Throughout the present chapter we use standard finite difference methods to solve—backward in time—the HJB equations stated herein. We thus obtain and plot the numerical solution. The algorithm and techniques used are described in detail in Section 7.5.2. Furthermore, under each plot there are the values of the parameters used, for reproducibility purposes.

²In foreign exchange, examples of centralised liquidity pools include EBS, FXAll, Hotspot, Thomson Reuters, etc., and in equity we may mention LSE, NYSE, NASDAQ, etc.

4.2 Market making in CLPs

We consider a CLP that trades with buyers and sellers by being their counterparty. It executes incoming buy and sell orders by its clients over a finite period of time $t \leq u \leq T < \infty$ and may resort to the centralised exchange platform if its inventory becomes critically small or large.

We fix a filtered probability space $(\Omega, \mathcal{F}, \{\mathcal{F}_u\}_{t \leq u \leq T}, \mathbb{P})$ satisfying the usual conditions and we assume that: (i) the CLP mid-price is aligned with the standard exchange mid-price $\{S_u\}$, and (ii) the CLP chooses the spread it charges to clients. We define the LOB mid-price by

$$dS_u = \bar{k}_{M_u}^{\pm} dM_u, \quad (4.1)$$

where $\{M_u\}$ is a Poisson process with intensity λ^m and $\bar{k}_{M_u}^{\pm}$ is a collection of i.i.d. random variables valued in $\{-\bar{k}, \bar{k}\}$. We choose such simple dynamics in Equation (4.1)—i.e. the mid-price can only move a tick a.s.—because our intention is to focus on the market-making activity of the CLP, disregarding any potential market-view it may have, or sudden price moves. Along the lines of Guilbaud and Pham [47], we model the LOB bid-ask half spread by a continuous-time Markov chain $\{k_u\}_{t \leq u \leq T}$ with a discrete state space $\mathbb{K} := \{k_0, k_1, k_2, \dots, k_n\}$, where $k_0 < k_1 < k_2 < \dots < k_n$ are set so to reflect the granularity of the standard-exchange prices. In particular, for $j = 0, 1, 2, \dots, n-1$, we let $k_{j+1} - k_j = \bar{k} > 0$. The chain is generated by $\{Q\} = (r_{ij})$ such that $\mathbb{P}[k_{u+du} = k_j | k_u = k_i] = r_{ij} du + o(du)$ and $\mathbb{P}[k_{u+du} = k_i | k_u = k_i] = 1 + r_{ii} du + o(du)$, with $r_{ij} \geq 0$ for all $j \neq i$ and $r_{ii} = -\sum_{j \neq i} r_{ij}$. Such a choice has interesting financial justifications. Because the spread is a measure of the market liquidity, lower states in \mathbb{K} (e.g. k_0) may be associated with periods of higher liquidity compared to higher states (e.g. k_n). Also, by correctly choosing the transition probabilities, one can postulate the existence of a “normal” level of the spread—for each particular class of assets—from which deviations are unlikely to happen. Furthermore, the transition from one state to another can be associated with the submission of both aggressive and passive orders by market participants.

We remark that when we write k_u , we mean the level of the spread at time $u \in [t, T]$, whereas with the notation $k \in \mathbb{K}$ we refer to a particular state k_j , for $j = 0, 1, 2, \dots, n$.

At any time $u \in [t, T]$, the best LOB bid and ask prices are given by $S_u^b = S_u - k_u$ and $S_u^a = S_u + k_u$, respectively. In Figure 4.1 we provide two sample paths for the ‘lit’-pool TOB.

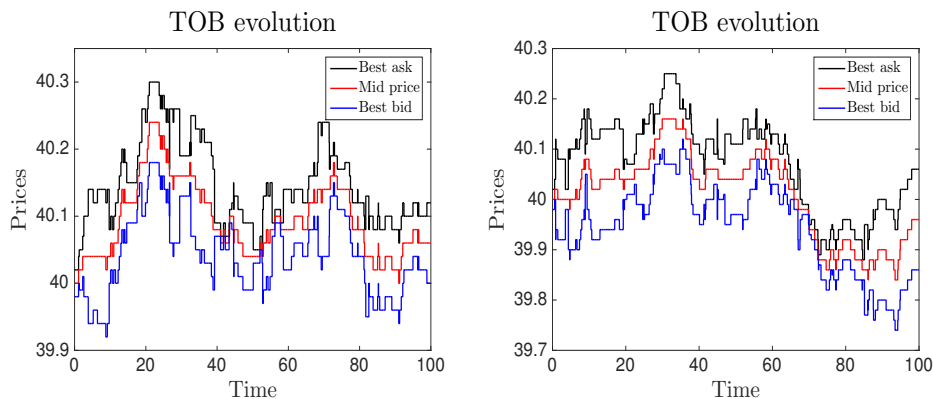


FIGURE 4.1: Sample paths for (4.1). We set $\bar{k} = 0.01$ and $\mathbb{K} = \{0.01, 0.02, \dots, 0.1\}$.

At each time $u \in [t, T]$, we consider three options for the inventory management: (i) the CLP’s order flow may be controlled by accordingly choosing the prices offered to its clients, (ii) a limit order—of which execution is uncertain—is posted to the standard exchange, or (iii) a costly market order is submitted to the standard exchange. Our goal is thus to obtain the critical levels of the inventory for which it is optimal to (i) skew the CLP prices, (ii) submit limit orders, and (iii) submit market orders.

4.2.1 Pricing strategy

We consider the processes δ_u^+, δ_u^- to be (i) the controls of the optimisation problem presented in Section 4.2.3 and (ii) part of the pricing strategy of the CLP. The CLP chooses the values of $\{\delta_u^\pm\}$. We denote by $S_u - \delta_u^-$ and $S_u + \delta_u^+$ the *base prices* and by $\delta_u^+ + \delta_u^-$ the *base spread* from which the CLP derives the prices offered to its clients, since the actual spread paid by the client to the CLP is also a function of the order-size of the client, see Equation (4.3). In order to

maintain competitiveness with respect to standard exchanges and other liquidity providers, we assume that the CLP base spread does not exceed the standard exchange spread under normal circumstances (i.e., acceptable inventory levels). Nonetheless, it may be skewed with respect to the ‘lit’-exchange spread on the protect side (e.g. the sell side when the CLP has a negative inventory), while we assume that the aggress side (e.g. the buy side when the CLP has a negative inventory) shall not cross the mid-price level. This last assumption is justified since crossing the mid-price leaks to buy-side agents very sensitive information regarding the CLP level of inventory. We thus suppose that δ_u^+ and δ_u^- are predictable processes valued in $[0, \bar{\delta}]$, where the upper bound is justified by practical considerations (N.B., an infinite spread results in an infinite price), as well as by the incentive for the CLP to maintain its quotes within a constant range.

The CLP flow of client orders can be affected by changing δ_u^+ and δ_u^- (that is, the arrival intensity of buyers and sellers is a function of the quotes posted by the market maker). We might assume for example that the CLP has a positive inventory at time $u \in [t, T]$. It can make trading more attractive to buyers rather than sellers, so to rebalance its inventory level. In particular, by lowering δ_u^+ and increasing δ_u^- , the CLP encourages buyers to place orders while sellers are discouraged to do so. We further assume that the CLP accepts clients’ orders at time u (i.e., it keeps streaming dealable prices to clients) only if the inventory at time u^- lies within $[-\bar{X}, \bar{X}]$, where $\bar{X} > 0$ so that, if either boundary is surpassed, the CLP may only trade in one direction. Such an assumption is supported by the following financial interpretation: the CLP is subject to regulatory constraints (e.g. internal risk-management) which do not allow to hold or short-sell a position bigger than a fixed authorised quantity. Throughout the market-making activity (i.e., between hedging times), we define the CLP inventory process $\{X_u\}$ by

$$dX_u = dJ_u^- \mathbb{1}_{\{X_{u^-} \leq \bar{X}\}} - dJ_u^+ \mathbb{1}_{\{X_{u^-} \geq -\bar{X}\}}, \quad (4.2)$$

where $J_u^\pm := \sum_{i=1}^{N_u^\pm} q_i^\pm$ and where the Cox processes $\{N_u^\pm\}$ have intensities $\lambda_\delta^\pm = \lambda^\pm(\delta_u^\pm)$. The random variables q_i^\pm are i.i.d. with support $\mathbb{Q} := \{0, q_1, \dots, q_N\}$

where these model the size of the trades executed by the CLP. At any time $u \in [t, T]$, we have $\text{sign}[X_u] = \{-1, 0, 1\}$ where we include short-selling for the case $\text{sign}[X_u] = -1$. We model the CLP cash process $\{Y_u\}$ by

$$dY_u = f(u, S_{u-}, \delta_u^+, q_u^+) dJ_u^+ \mathbb{1}_{\{X_{u-} \geq -\bar{x}\}} - f(u, S_{u-}, \delta_u^-, q_u^-) dJ_u^- \mathbb{1}_{\{X_{u-} \leq \bar{x}\}}, \quad (4.3)$$

where q_u^\pm is shorthand notation for $q_{N_u^\pm}^\pm$. The function f allows the CLP to offer a stream of prices related to the size of the client's order³. In particular the CLP offers tighter spreads for smaller sizes and wider spreads for larger sizes. The function f further allows for various ways to calculate P&L. We remark that Equations (4.2) and (4.3) are strongly coupled. For example, the arrival of a seller at time u increases the inventory X_{u-} by q_u^- and reduces the cash amount Y_{u-} by $f(u, S_{u-}, \delta_u^-, q_u^-) q_u^-$. The analogous holds for the arrival of buyers.

4.2.2 Hedging strategy

The CLP can resort to the standard exchange to liquidate (respectively refill) part of its inventory; we assume that it cannot post speculative orders. This means that at time $u \in [t, T]$ a buy order can be posted only if $X_u < 0$ while a sell order can be posted if $X_u > 0$. We refer to Remark 7.1 for the compact version of the equations treated in the present section.

4.2.2.1 Limit orders

The CLP can post a limit order by specifying a quantity η and a limit price $S \pm (k + \kappa)$, where κ is the optimal distance from the best price, at which it wants to buy or sell. We only consider IOC orders and we model their execution percentages by a $[0, 1]$ -valued sequence of i.i.d. random variables z_i , of which cumulative distribution function heavily depends on the limit-price chosen by

³We wish to remark that, within this context, the function f is fixed *a priori* by the market maker and is not the object of the optimisation.

the CLP. In particular, if a limit order is posted at time τ_i^ℓ , for $i = 1, 2, \dots$, then it impacts the inventory and the cash processes as follows:

$$X_{\tau_i^\ell} = \Gamma(\eta_i, X_{\tau_i^\ell-}, z_i), \quad Y_{\tau_i^\ell} = \chi(\eta_i, Y_{\tau_i^\ell-}, z_i, S_{\tau_i^\ell-}, k_{\tau_i^\ell-}, \kappa_i). \quad (4.4)$$

Since the CLP cannot post speculative orders in the ‘lit’ pool, it must hold $|\Gamma(\eta_i, X_{\tau_i^\ell-}, z_i)| \leq |X_{\tau_i^\ell-}|$, almost surely. For example a limit buy order, which if executed increases the inventory, can only be posted if the CLP holds a negative inventory, and vice versa. The cash process changes accordingly. We state these assumptions rigorously in Chapter 7. We let \mathcal{T}_{tT} be the set of stopping times valued in $[t, T]$, and $\mathcal{N} := [\min(0, -X_{\tau_i^\ell-}), \max(0, -X_{\tau_i^\ell-})]$ be the set of all admissible control actions. A limit-order strategy is a collection of stopping times and actions $L = (\tau_i^\ell, \eta_i, \kappa_i)_{i \geq 1} \in \mathcal{T}_{tT} \times \mathcal{N} \times \mathbb{K}^\ell$, where the elements in $\mathbb{K}^\ell \subset \mathbb{K}$ reflect the price-granularity of the ‘lit’ exchange.

4.2.2.2 Market orders

Alternatively, the CLP can submit a market order, which (i) is more expensive and (ii) benefits from sure execution as it is matched with existing limit orders. A market order of size ξ_i posted at a time τ_i^m impacts the inventory and cash processes as follows:

$$X_{\tau_i^m} = \Lambda(\xi_i, X_{\tau_i^m-}), \quad Y_{\tau_i^m} = c(\xi_i, Y_{\tau_i^m-}, S_{\tau_i^m-}, k_{\tau_i^m-}), \quad (4.5)$$

where $|\Lambda(\xi_i, X_{\tau_i^m-})| \leq |X_{\tau_i^m-}|$. A market-order strategy is a collection of stopping times and actions $M = (\tau_i^m, \xi_i)_{i \geq 1} \in \mathcal{T}_{tT} \times \mathcal{X}$, where the set \mathcal{X} is defined by $\mathcal{X} = [\min(0, -X_{\tau_i^m-}), \max(0, -X_{\tau_i^m-})]$.

The level of generality in the limit-order and the market-order impulses offers the flexibility to include various features. For example, there are different methods to compute the P&L. Furthermore, one may like to account for the fees paid to the exchange for using their services and for possible liquidity rebates for limit orders.

4.2.3 The value function

We consider the problem of maximising expected terminal cash subject to a terminal penalty for holding a non-zero inventory by the terminal date. In defining the objective function, we are led by Guilbaud and Pham [47] and we propose the following

$$V(t, x, y, s; k) = \sup_{D, L, M} \mathbb{E} \left[U(X_T, Y_T, S_T, k_T) + \int_t^T g(u, X_u) du - \sum_{t \leq \tau_i^m < T} \epsilon_m - \sum_{t \leq \tau_i^\ell < T} \epsilon_\ell \right], \quad (4.6)$$

where $D := (\delta_u^+, \delta_u^-)_{u \geq t}$, the function U is the utility derived from the cash and inventory holdings at time T , and g is a running penalty for the risk of holding the inventory. In the summations of Equation (4.6), we include the penalties ϵ_m and ϵ_ℓ for submitting market and limit orders in the standard exchange, where $\epsilon_m > \epsilon_\ell > 0$. Throughout the paper we have the vector of state variables $\mathbf{x} := [x, y, s] \in \mathcal{O} := [-\bar{X} - q_N, \bar{X} + q_N] \times \mathbb{R}^2$. Equation (4.6) satisfies the DPP, see Fleming and Soner [37]. That is, for all $\tau \in \mathcal{T}_{tT}$, we have

$$V(t, \mathbf{x}; k) = \sup_{D, L, M} \mathbb{E} \left[\int_t^\tau g(u, X_u) du - \sum_{t \leq \tau_i^m < \tau} \epsilon_m - \sum_{t \leq \tau_i^\ell < \tau} \epsilon_\ell + V(\tau, \mathbf{X}_\tau; k_\tau) \right]. \quad (4.7)$$

This is an optimal double-obstacle impulse control problem. We define the non-local operators \mathcal{L} and \mathcal{M} , for limit and market orders respectively, by

$$\mathcal{L}V(t, \mathbf{x}; k) = \sup_{\eta \in \mathcal{N}, \kappa \in \mathbb{K}^\ell} \mathbb{E}^{(z)} \left[V(t, \Gamma(\eta, x, z), \chi(\eta, y, z, s, k, \kappa), s; k) \right] - \epsilon_\ell, \quad (4.8)$$

where the expectation is taken with respect to the random variable z , and

$$\mathcal{M}V(t, \mathbf{x}; k) = \sup_{\xi \in \mathcal{X}} V(t, \Lambda(\xi, x), c(\xi, y, s, k), s; k) - \epsilon_m. \quad (4.9)$$

We introduce the operator $\bar{\mathcal{A}}$ defined by

$$\begin{aligned}
\bar{\mathcal{A}}(t, \mathbf{x}, k, p, \varphi, \delta^+, \delta^-) &= p + \sum_{k' \neq k} r_{kk'} [\varphi(t, \mathbf{x}; k') - \varphi(t, \mathbf{x}; k)] \\
&+ \lambda^m \mathbb{E}^{(\bar{k}^\pm)} \left[(\varphi(t, x, y, s + \bar{k}^\pm; k) - \varphi(t, \mathbf{x}; k)) \right] \\
&+ \lambda_\delta^+ \mathbb{E}^{(q^+)} \left[(\varphi(t, x - q^+, y + f(t, s, \delta^+, q^+)q^+, s; k) - \varphi(t, \mathbf{x}; k)) \right] \mathbb{1}_{\{x \geq -\bar{x}\}} \\
&+ \lambda_\delta^- \mathbb{E}^{(q^-)} \left[(\varphi(t, x + q^-, y - f(t, s, \delta^-, q^-)q^-, s; k) - \varphi(t, \mathbf{x}; k)) \right] \mathbb{1}_{\{x \leq \bar{x}\}},
\end{aligned} \tag{4.10}$$

where the expectations are taken with respect to the random variables \bar{k}^\pm , q^+ and q^- , respectively. Furthermore, we set

$$\mathcal{A}(t, \mathbf{x}, k, p, \varphi) = \sup_{\delta^\pm \in [0, \bar{\delta}]} \bar{\mathcal{A}}(t, \mathbf{x}, k, p, \varphi, \delta^+, \delta^-).$$

The value function $V(t, \mathbf{x}; k)$ satisfies the HJB system of QVIs⁴

$$\min \{-g(t, x) - \mathcal{A}(t, \mathbf{x}, k, \partial_t V, V); (V - \mathcal{M}V)(t, \mathbf{x}; k); (V - \mathcal{L}V)(t, \mathbf{x}; k)\} = 0, \tag{4.11}$$

on $[t, T) \times \mathcal{O} \times \mathbb{K}$, with terminal condition $V(T, x, y, s; k) = U(x, y, s, k)$. Equation (4.11) can be interpreted as follows: if $V - \mathcal{M}V > 0$ and $V - \mathcal{L}V > 0$, then the value function cannot be improved by an impulse and thus no orders are submitted to the standard exchange. As soon as $V - \mathcal{M}V < 0$ or $V - \mathcal{L}V < 0$, the value function is set to $V - \mathcal{M}V = 0$ or $V - \mathcal{L}V = 0$ and an impulse takes place. In the event $V - \mathcal{M}V < 0$ and $V - \mathcal{L}V < 0$, the value function is set to $V - \max\{\mathcal{M}V, \mathcal{L}V\} = 0$. We thus consider intervention times (τ_i^ℓ and τ_i^m) and impulses (η_i , κ_i and ξ_i) by which the CLP can control the evolution of the state variables X_u and Y_u . For this purpose, we define the continuation region (CR), the limit orders impulse region (LI) and the market orders impulse region (MI) by

$$\begin{aligned}
CR &:= \{(u, \mathbf{x}, k) \in [t, T) \times \mathcal{O} \times \mathbb{K} : V > \mathcal{L}V \ \& \ V > \mathcal{M}V\}, \\
LI &:= \{(u, \mathbf{x}, k) \in [t, T) \times \mathcal{O} \times \mathbb{K} : \mathcal{L}V = V \ \& \ \mathcal{L}V > \mathcal{M}V\}, \\
MI &:= \{(u, \mathbf{x}, k) \in [t, T) \times \mathcal{O} \times \mathbb{K} : \mathcal{M}V = V \ \& \ \mathcal{M}V > \mathcal{L}V\}.
\end{aligned} \tag{4.12}$$

⁴We refer to Section 7.1 for details on its derivation.

The system of QVIs introduced in Equation (4.11) is highly non-linear and somewhat similar to the one studied in Guilbaud and Pham [47], although in the present model two distinct impulses can take place. Some dimension reduction is possible if the mid-price is assumed to be a martingale (see e.g. Cartea and Jaimungal [20] and Guilbaud and Pham [47, 48]), since the optimal strategy in feedback-form will only be a function of the inventory. We make this assumption in the numerical section that follows, while keeping the general model presented in this section at a higher degree of generality. In the next section we provide some explicit examples of the model and we find numerically the optimal strategy by means of the solving algorithm proposed in Guilbaud and Pham [47, 48].

4.3 Explicit examples and numerical results

We started this chapter with the intention of addressing some of the shortcomings of the model presented in Section 2.3.2. In the previous section we presented a class of models which allows for various choices of the state variables dynamics, the control sets and the performance criterion. In the present section, we specifically consider the points mentioned in Section 4.1—i.e. (i) the CLP can choose optimally the prices it offers to clients, (ii) the CLP can post limit orders deep in the book, (iii) the lit-pool spread is not constant—and we provide numerical examples⁵ in which we progressively add such features to the model presented in Section 2.3.2. We briefly recall the state variables dynamics—though they are very similar to the ones in Section 2.3.2—for readability. Throughout this section, we assume that the mid-price is modelled by Equation (4.1) and that limit orders in the ‘lit’ exchange cannot be partially filled. This is not a strong assumption as long as we consider unit-sized orders posted in the standard exchange. In fact, the majority of the times, posting unit-sized orders in a ‘lit’ market serves as to reduce consistent price slippage deriving from the order-book imbalance. We assume that clients pay the “adjusted base spread” to the CLP, where in the latter the size of the client’s order is taken into account. We

⁵While it would obviously be desirable to base the analysis on CLPs real data, it does not come as a surprise that such sensitive information is strictly private and not shared outside firms.

thus assume that the inventory and the cash processes evolve according to

$$dX_u = dJ_u^- \mathbb{1}_{\{X_{u-} \leq \bar{x}\}} - dJ_u^+ \mathbb{1}_{\{X_{u-} \geq -\bar{x}\}},$$

$$dY_u = (S_{u-} + \delta_u^+(1+c)^{q_u^+}) dJ_u^+ \mathbb{1}_{\{X_{u-} \geq -\bar{x}\}} - (S_{u-} - \delta_u^-(1+c)^{q_u^-}) dJ_u^- \mathbb{1}_{\{X_{u-} \leq \bar{x}\}},$$

where we have set $f(t, s, \delta^\pm, q^\pm) = (s + \delta^\pm(1+c)^{q^\pm})$ and $0 < c < 1$ is a pre-determined fixed constant. The convexity of the non-linear function $(1+c)^{q^\pm}$ reflects the fact that for the CLP it is more expensive to hedge a larger order due to the price slippage in the exchange. Thus, the CLP charges more for each unit of such an order. Next, we introduce the possibility of submitting unit-sized market and limit orders in the standard exchange. At each time t_i , the CLP checks whether it is more convenient to (i) execute trades in the CLP only, (ii) submit a market order such that

$$X_{t_i} = X_{t_{i-}} + \xi_i, \quad Y_{t_i} = Y_{t_{i-}} - \xi_i (S_{t_{i-}} + \xi_i k_{t_{i-}}), \quad (4.13)$$

where $\xi_i \in \mathcal{X} := \{-\mathbb{1}_{\{x>0\}}, \mathbb{1}_{\{x<0\}}\}$, or (iii) submit a limit order such that

$$X_{t_i} = X_{t_{i-}} + \eta_i z_i, \quad Y_{t_i} = Y_{t_{i-}} - \eta_i (S_{t_{i-}} - (k_{t_{i-}} + \kappa_i) \eta_i) z_i, \quad (4.14)$$

where $\eta_i \in \mathcal{N} = \{-\mathbb{1}_{\{x>0\}}, \mathbb{1}_{\{x<0\}}\}$ and z_i are i.i.d. random variables supported in $\{0, 1\}$. In Equation (4.6) we set $U(x, y, s, k) = y + x(s - \alpha x)$ and $g(u, x) = -\phi x^2$, where $\phi > 0$. In order to thoroughly understand the marginal effects of the three changes mentioned above, we think it is better to add them *progressively* to the model. We thus start by considering a situation where the CLP can skew its prices but (i) it can only post limit orders on top of the book, and (ii) the lit pool spread is constant, only to remove them later in the discussion. The form of the terminal condition suggests we can use the ansatz (see, e.g., Cartea et al. [23]) $V(t, \mathbf{x}) = y + xs + h(t, x)$, which henceforth will be inserted in Equation (4.11).

4.3.1 Optimal dark-pool spread

We let the CLP choose between three possible scenarios.

(i) It can choose not to skew the prices and thus to let $\delta^+ = \delta^-$ and $\lambda^+ = \lambda^-$ (which we call *no skew*), (ii) it may skew the prices downward such that $\delta^+ < \delta^-$ and $\lambda^+ > \lambda^-$ (which we call *left* or *downward skew*), and (iii) it may skew the prices upward such that $\delta^+ > \delta^-$ and $\lambda^+ < \lambda^-$ (which we call *right* or *upward skew*). The upward skew penalises buyers over sellers while the opposite holds for the downward skew. Mathematically, the above reduces to assuming that the CLP optimally chooses the prices $(\delta^+, \delta^-) \in \mathcal{D} := \{(\delta_n^+, \delta_n^-), (\delta_r^+, \delta_r^-), (\delta_l^+, \delta_l^-)\}$ for the no skew, the right skew and the left skew scenarios, respectively. Associated to such prices, we assume arrival intensities of the form $(\lambda_\delta^+, \lambda_\delta^-) \in \mathcal{I} := \{(\lambda_n^+(\delta_n^+), \lambda_n^-(\delta_n^-)), (\lambda_r^+(\delta_r^+), \lambda_r^-(\delta_r^-)), (\lambda_l^+(\delta_l^+), \lambda_l^-(\delta_l^-))\}$. The QVI now reads:

$$\begin{aligned} \min \left\{ - \sup_{(\delta^+, \delta^-) \in \mathcal{D}} \left(\lambda_\delta^+ \mathbb{E}^{(q^+)} \left[\delta^+ q^+ (1+c)^{q^+} + h(t, x - q^+) - h(t, x) \right] \mathbb{1}_{\{x \geq -\bar{X}\}} \right. \right. \\ \left. \left. + \lambda_\delta^- \mathbb{E}^{(q^-)} \left[\delta^- q^- (1+c)^{q^-} + h(t, x + q^-) - h(t, x) \right] \mathbb{1}_{\{x \leq \bar{X}\}} \right) \right. \\ \left. \phi x^2 - \frac{\partial h(t, x)}{\partial t} - \lambda^m x \mathbb{E}^{(\bar{k}^\pm)} [\bar{k}^\pm]; h(t, x) - \sup_{\xi \in \mathcal{X}} \left[-k - \epsilon_m + h(t, x + \xi) \right]; \right. \\ \left. \left. h(t, x) - \sup_{\eta \in \mathcal{N}} \mathbb{E}^{(z)} \left[kz - \epsilon_\ell + h(t, x + \eta z) \right] \right\} = 0, \end{aligned} \quad (4.15)$$

with terminal condition $h(T, x) = -\alpha x^2$. We numerically solve (4.15) to find the optimal CLP pricing and hedging strategy. We expect to find additional boundaries to the one obtained in Section 2.3.2, since the CLP now has different pricing alternatives.

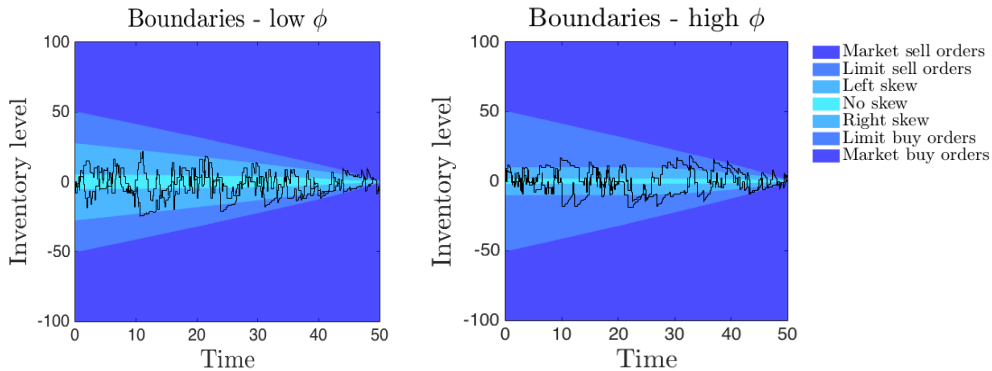


FIGURE 4.2: Optimal inventory thresholds found by solving the HJB equation (4.15). We set $\alpha = 2$, $\mathcal{D} := \{(0.5, 0.5), (0.3, 0.6), (0.6, 0.3)\}$, $\mathcal{I} := \{(0.5, 0.5), (0.6, 0.4), (0.4, 0.6)\}$, $\epsilon_\ell = 3$, $\epsilon_m = 6$, $c = 0.05$, $\lambda^m = 0.5$, $k = 1$, $q^\pm \sim U[1, 10]$, $z \sim U[0, 1]$, $s = 40$, $\mathbb{E}[\bar{k}^\pm] = 0$, $x = y = 0$, $\bar{X} = 100$. In the left panel we set $\phi = 0.01$. In the right panel we set $\phi = 0.0001$.

In Figure 4.2 we show two simulated inventory paths (relative to a unique stock-price path) and we plot them above the optimal boundaries found by solving Equation (4.15). We see that when the inventory is relatively small, it is optimal not to skew the prices so to receive on average an equal number of buy and sell orders (here we assume that no-skewing implies equal arrival intensities of buyers and sellers, which may not be the case in particular market conditions, e.g. new information is available to a number of clients which are incentivised to trade in the same direction). If the the inventory increases (resp. decreases), the CLP employs a left/downward (resp. right/upward) skew so to encourage buyers (resp. sellers). As in the toy model, there are inventory levels for which it is optimal to resort to the standard exchange. The critical inventory level at which the CLP begins placing orders in the standard exchange falls as the terminal liquidation date is approached. We plot the optimal boundaries for the case of moderate risk aversion (right panel) and high risk aversion (right panel). We notice that the hedging activity of the CLP is highly correlated to its degree of risk aversion. Indeed, for high values of ϕ , the CLP starts posting orders to the standard exchange for smaller inventory values and vice versa.

Remark 4.1. While the inventory thresholds shown are the optimal boundaries found numerically by solving the HJB equation (4.15), the (superimposed) simulated inventory paths are meant for illustration purposes only. In particular, they crucially depend on the partition of the time grid. For example, when the hedging boundaries are surpassed and the optimal strategy suggests that limit orders should be posted, the simulated paths only capture one limit order per time-grid point. If the grid points are, e.g., one second apart, the plot would show one limit order per second until the inventory is back within the market-making region. If instead the grid was finer and points were one millisecond apart, the paths would show one limit order per millisecond. Put it in another way, if the time grid had N points, then a maximum of $N - 1$ optimal stopping times could take place (we do not allow for an impulse at the terminal time). We wish to stress that the solution of (4.15) comprises of the optimal boundaries only, while the simulated paths are a visual aid to better understand the business of the CLP.

4.3.2 Optimal lit-pool posting

In the previous section we have included the option of skewing the prices that the CLP offers, but the model is still limited in that the hedging in the standard exchange by means of limit orders can only be done on top of the book. Here we modify this assumption and we allow the CLP to also post at the second best and third best prices. According to the LOB model presented in Section 4.2, we let the minimum price tick by \bar{k} , and thus allow the CLP to post limit sell orders at prices $s + k$, $s + k + \bar{k}$ and $s + k + 2\bar{k}$, while limit buy orders can be posted at prices $s - k$, $s - k - \bar{k}$ and $s - k - 2\bar{k}$. According to the notation used in Equation (4.14), we assume that the limit price at which the CLP posts in the standard exchange can be optimally chosen between $\kappa \in \mathbb{K}^\ell := \{0, \bar{k}, 2\bar{k}\}$.

By posting deeper in the book, the CLP earns a higher spread if its order gets executed, while the filling probability of such an order is reduced. In fact, for a deep limit order to be executed a market order that walks the book is needed, and the latter are quite rare. To reflect the fact that the filling-probability of a limit order depends on how far from the mid-price such an order is posted, we assume that $\mathbb{P}[z_i = 0] = \ell^\kappa(z_0)$ and $\mathbb{P}[z_i = 1] = \ell^\kappa(z_1) = 1 - \ell^\kappa(z_0)$. The associated QVI for the function $h(t, x)$ is

$$\begin{aligned} \min \left\{ - \sup_{(\delta^+, \delta^-) \in \mathcal{D}} \left(\lambda_\delta^+ \mathbb{E}^{(q^+)} \left[\delta^+ q^+ (1+c)^{q^+} + h(t, x - q^+) - h(t, x) \right] \mathbb{1}_{\{x \geq -\bar{x}\}} \right. \right. \\ \left. \left. + \lambda_\delta^- \mathbb{E}^{(q^-)} \left[\delta^- q^- (1+c)^{q^-} + h(t, x + q^-) - h(t, x) \right] \mathbb{1}_{\{x \leq \bar{x}\}} \right) \right. \\ \left. \phi x^2 - \frac{\partial h(t, x)}{\partial t} - \lambda^m x \mathbb{E}^{(\bar{k}^\pm)} [\bar{k}^\pm]; h(t, x) - \sup_{\xi \in \mathcal{X}} \left[-k - \epsilon_m + h(t, x + \xi) \right]; \right. \\ \left. \left. h(t, x) - \sup_{\eta \in \mathcal{N}, \kappa \in \mathbb{K}^\ell} \mathbb{E}^{(z)} \left[(k + \kappa) z - \epsilon_\ell + h(t, x + \eta z) \right] \right\} = 0. \end{aligned} \quad (4.16)$$

with terminal condition $h(T, x) = -\alpha x^2$. In Figure 4.3, the optimal strategy obtained by solving (4.16) is shown. We notice that after skewing the prices, the CLP should start submitting limit orders deep in the book and progressively

moves towards the top of the book. Shortly before the end of the trading period, it should resort to market orders. Again, we show the different strategies employed by a highly risk-averse and a moderately risk-averse CLP (in the left and right panels, respectively). In Figure 4.4 we show the different strategies for high and low values of the terminal-penalty parameter α . When the penalty for holding a non-zero inventory at T increases, we notice that the boundaries shrink dramatically, especially towards the end.

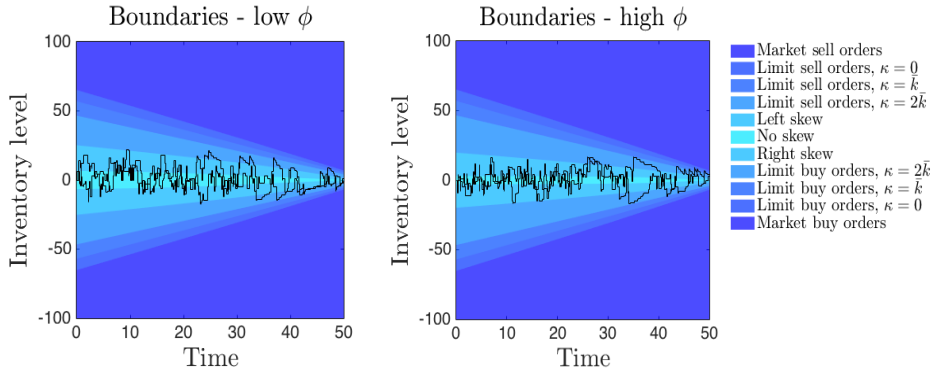


FIGURE 4.3: Optimal inventory thresholds found by solving the HJB equation (4.16). We set $\alpha = 2$, $\mathcal{D} := \{(0.5, 0.5), (0.3, 0.6), (0.6, 0.3)\}$, $\mathcal{I} := \{(0.5, 0.5), (0.6, 0.4), (0.4, 0.6)\}$, $\epsilon_\ell = 3$, $\epsilon_m = 6$, $c = 0.05$, $\lambda^m = 0.5$, $k = 1$, $q^\pm \sim U[1, 10]$, $z \sim U[0, 1]$, $s = 40$, $\mathbb{E}[\bar{k}^\pm] = 0$, $x = y = 0$, $\bar{X} = 100$, $\bar{k} = 0.01$, $\ell^{\kappa=0}(z_1) = 0.9$, $\ell^{\kappa=\bar{k}}(z_1) = 0.8$, $\ell^{\kappa=2\bar{k}}(z_1) = 0.6$. In the left panel we set $\phi = 0.01$. In the right panel we set $\phi = 0.0001$.

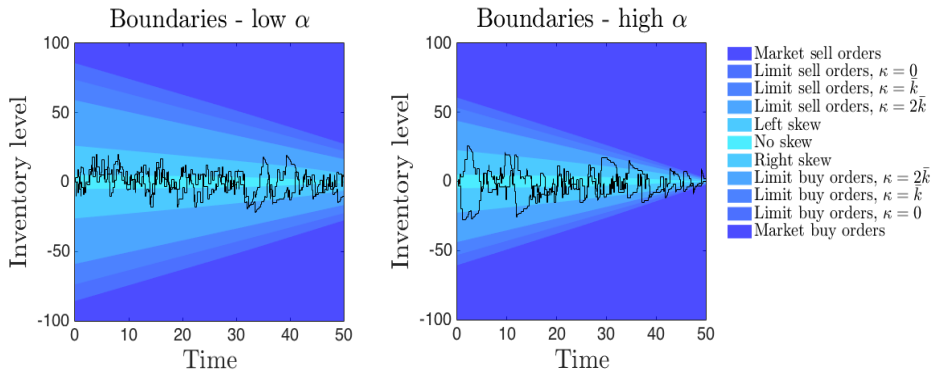


FIGURE 4.4: Optimal inventory thresholds found by solving the HJB equation (4.16). We set $\phi = 0.001$, $\mathcal{D} := \{(0.5, 0.5), (0.3, 0.6), (0.6, 0.3)\}$, $\mathcal{I} := \{(0.5, 0.5), (0.6, 0.4), (0.4, 0.6)\}$, $\epsilon_\ell = 3$, $\epsilon_m = 6$, $c = 0.05$, $\lambda^m = 0.5$, $k = 1$, $q^\pm \sim U[1, 10]$, $z \sim U[0, 1]$, $s = 40$, $\mathbb{E}[\bar{k}^\pm] = 0$, $x = y = 0$, $\bar{X} = 100$, $\bar{k} = 0.01$, $\ell^{\kappa=0}(z_1) = 0.9$, $\ell^{\kappa=\bar{k}}(z_1) = 0.8$, $\ell^{\kappa=2\bar{k}}(z_1) = 0.6$. In the left panel we set $\alpha = 6$. In the right panel we set $\alpha = 0.5$.

We emphasise that if the terminal preferred inventory level was non-zero, it would produce a shift in the optimal boundaries by an equal amount.

4.3.3 P&L distribution

Here we simulate the model described in Section 4.3.2 and we find numerically the terminal P&L distribution, calculated by $Y_T + X_T(S_T - \bar{k} \times \text{sign}[X_T])$, where we are assuming that the terminal inventory is liquidated via a market order. In Table 4.1 we list the values of the parameters we choose for the simulation, while in Figure 4.5 we show the empirical distribution of the terminal cash for different levels of the risk aversion of the CLP. We simulate five hundred paths for the stock price and a thousand paths for inventory, making a total of five hundred thousand different scenarios.

TABLE 4.1: Parameters value

S_0, X_0, Y_0	\bar{X}	δ_n^+	δ_n^-	δ_u^+	δ_u^-	δ_d^+	δ_d^-
40, 0, 0	100	0.5	0.5	0.3	0.6	0.6	0.3
$\kappa_0, \kappa_1, \kappa_2$	$\lambda^+(\delta_n^+)$	$\lambda^-(\delta_n^-)$	$\lambda^+(\delta_u^+)$	$\lambda^-(\delta_u^-)$	$\lambda^+(\delta_d^+)$	$\lambda^-(\delta_d^-)$	c
0, $\bar{k}, 2\bar{k}$	0.5	0.5	0.6	0.4	0.4	0.6	0.05
$\ell^{\kappa_0}, \ell^{\kappa_1}, \ell^{\kappa_2}$	k	$\epsilon_m, \epsilon_\ell$	λ^m	\bar{k}	q^\pm	\mathcal{N}	\mathcal{X}
0.9, 0.8, 0.6	1	6, 3	0.5	0.01	$U\{1, 10\}$	± 1	± 1

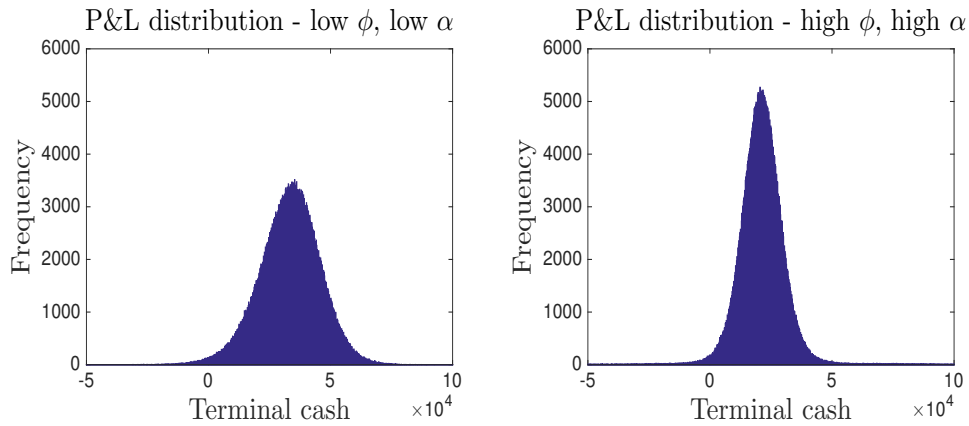


FIGURE 4.5: Terminal cash distribution as defined in Section 4.3.2. In the left panel we set $\alpha = 0.5$ and $\phi = 0.00001$. In the right panel we set $\alpha = 6$ and $\phi = 0.01$.

First, we notice that the activity is, on average, profitable and thus the CLP is incentivised to act as a market maker by offering a stream of prices to its clients. A unremarkably risk-averse CLP employs a less expensive hedging strategy and the average P&L is higher than the case of high risk aversion (in the plots above we have 28,384 versus 20,366 for the left and right panels, respectively). On the other hand, there is more dispersion around the mean, and the standard deviations are 13,813 and 9,182 for the left and right panels, respectively. As a matter of fact, the choice relies on the willingness to take risk specific to each CLP, which may be further conditioned by the regulations in place. A less risk-averse CLP holds its inventory for longer compared to a high risk averse, and hopes to liquidate its inventory by means of its market-making activity, rather than through hedging. On the other hand, such a CLP may be subject, from time to time, to larger losses caused by the price moving against its holdings.

4.3.4 Stochastic lit-pool spread

In the last simulation we relax assumption (d) and introduce a stochastic bid-ask spread. We let $\mathbb{K} := \{1, 2\}$, that is the market can be in a tight-spread regime and a wide-spread regime, depending on whether there is good or poor liquidity in the market, respectively. The generator matrix can be chosen in various ways, so to model the specific features of the market under consideration. For example, we could consider a “seasonal” pattern where transitions between regimes happen rarely and last for longer periods of time. Also, we could reproduce features similar to mean-reversion by choosing a “preferred” state by making reversion to that state very likely. The matrices Q_1 and Q_2 are examples of seasonal and mean-reverting patterns, respectively:

$$Q_1 = \begin{pmatrix} -r & r \\ r & -r \end{pmatrix}, \quad Q_2 = \begin{pmatrix} -r_{low} & r_{low} \\ r_{high} & -r_{high} \end{pmatrix}, \quad (4.17)$$

where $r, r_{low}, r_{high} > 0$. In Q_1 the lower r , the rarer the transition between states happens. In Q_2 , we choose $k = 1$ as the preferred state, and the higher r_{high} , compared to r_{low} , the higher is the transition rate to state 1. The two-dimensional system of QVIs now reads as

$$\begin{aligned}
\min \left\{ - \sup_{(\delta^+, \delta^-) \in \mathcal{D}} \left(\lambda_{\delta^+} \mathbb{E}^{(q^+)} \left[\delta^+ q^+ (1+c)^{q^+} + h_k(t, x - q^+) - h_k(t, x) \right] \mathbb{1}_{\{x \geq -\bar{X}\}} \right. \right. \\
+ \lambda_{\delta^-} \mathbb{E}^{(q^-)} \left[\delta^- q^- (1+c)^{q^-} + h_k(t, x + q^-) - h_k(t, x) \right] \mathbb{1}_{\{x \leq \bar{X}\}} \Big) \\
\phi x^2 - \frac{\partial h_k(t, x)}{\partial t} - \lambda^m x \mathbb{E}^{(\bar{k}^{\pm})} [\bar{k}^{\pm}] - \sum_{k' \neq k} r_{kk'} [h_{k'}(t, x) - h_k(t, x)]; \\
h_k(t, x) - \sup_{\xi \in \mathcal{X}} [-k - \epsilon_m + h_k(t, x + \xi)]; \\
\left. h_k(t, x) - \sup_{\eta \in \mathcal{N}, \kappa \in \mathbb{K}^\ell} \mathbb{E}^{(z)} [(k + \kappa) z - \epsilon_\ell + h_k(t, x + \eta z)] \right\} = 0,
\end{aligned} \tag{4.18}$$

with terminal condition $h_k(T, x) = -\alpha x^2$. In Equation (4.18) where we have used the ansatz $V(t, x, y, s; k) = y + xs + h_k(t, x)$. The subscript k indicates that we refer to the regime $k \in \mathbb{K}$. In Figures 4.6 and 4.7 we plot the optimal boundaries found by solving (4.18) for the case of seasonal and mean-reverting patterns, respectively.

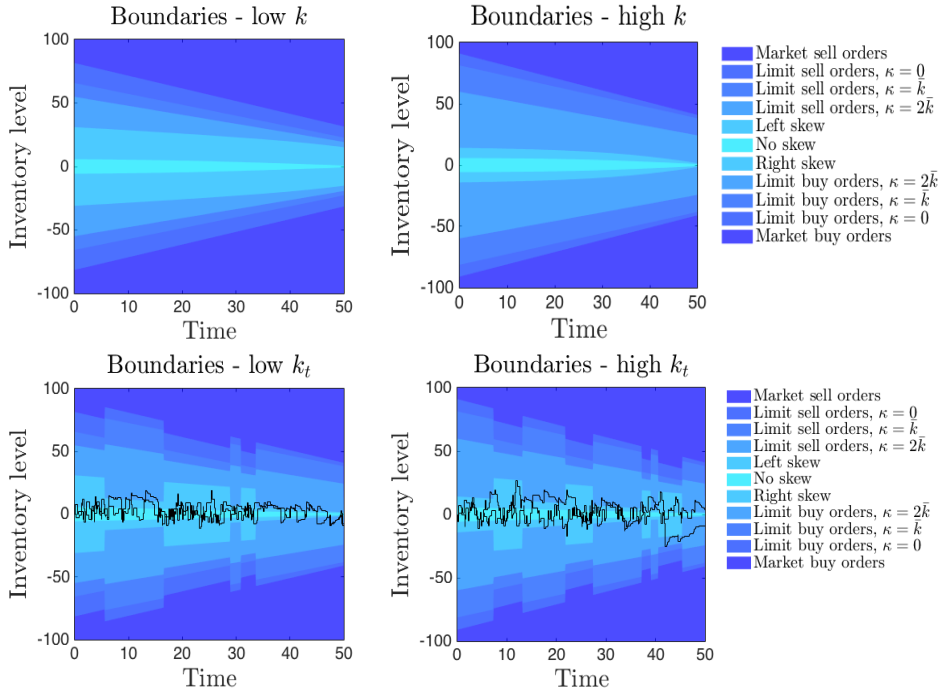


FIGURE 4.6: Optimal inventory thresholds found by solving the HJB equation (4.18). Seasonal pattern. We set $\alpha = 2$, $r = 1$, $\phi = 0.001$, $\mathcal{D} := \{(0.5, 0.5), (0.3, 0.6), (0.6, 0.3)\}$, $\mathcal{I} := \{(0.5, 0.5), (0.6, 0.4), (0.4, 0.6)\}$, $\epsilon_\ell = 3$, $\epsilon_m = 6$, $c = 0.05$, $\lambda^m = 0.5$, $k = 1$, $q^\pm \sim U[1, 10]$, $z \sim U[0, 1]$, $s = 40$, $\mathbb{E}[\bar{k}^\pm] = 0$, $x = y = 0$, $\bar{X} = 100$, $\bar{k} = 0.01$, $\ell^{\kappa=0}(z_1) = 0.9$, $\ell^{\kappa=\bar{k}}(z_1) = 0.8$, $\ell^{\kappa=2\bar{k}}(z_1) = 0.6$, $\mathbb{K} = \{1, 2\}$.

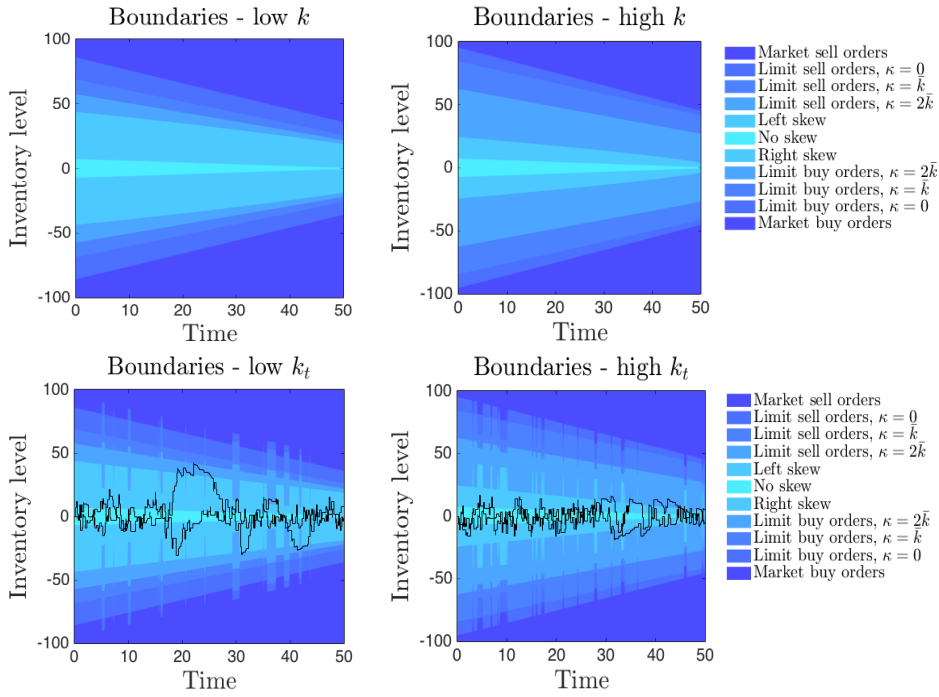


FIGURE 4.7: Optimal inventory thresholds found by solving the HJB equation (4.18). Mean-reverting pattern. We set $\alpha = 2$, $r_{high} = 6$, $r_{low} = 0.5$, $\phi = 0.001$, $\mathcal{D} := \{(0.5, 0.5), (0.3, 0.6), (0.6, 0.3)\}$, $\mathcal{I} := \{(0.5, 0.5), (0.6, 0.4), (0.4, 0.6)\}$, $\epsilon_\ell = 3$, $\epsilon_m = 6$, $c = 0.05$, $\lambda^m = 0.5$, $k = 1$, $q^\pm \sim U[1, 10]$, $z \sim U[0, 1]$, $s = 40$, $\mathbb{E}[\bar{k}^\pm] = 0$, $x = y = 0$, $\bar{X} = 100$, $\mathbb{K} = \{1, 2\}$, $\bar{k} = 0.01$, $\ell^{\kappa=0}(z_1) = 0.9$, $\ell^{\kappa=\bar{k}}(z_1) = 0.8$, $\ell^{\kappa=2\bar{k}}(z_1) = 0.6$.

We first note that in the case of high-spread regime in Figure 4.6, the CLP starts (i) earlier to submit limit orders and (ii) later to submit market orders, compared to the case of low-spread regime. The same shape is observable in Figure 4.7, although it is more evident since the return to the state of low-spread regime (preferred state) is highly likely. This behaviour has the following interpretation: when the spread is high, limit orders are more remunerative (or, better, cheaper if we also consider the penalty for posting in the standard exchange), while market orders are more expensive and thus their submission is postponed.

4.4 Conclusions

In the present work we study an optimal market-making problem faced by a CLP. The CLP earns the optimally selected spread by trading with its clients. Market participants, who consider trading via CLPs, may be of the view that it is desirable to take advantage of favourable prices offered by the CLPs and to benefit from avoiding price impact—to which they would be otherwise exposed—especially if forced to submit market orders in a ‘lit’ exchange.

A stream of two-way prices is offered to each client. Such prices are functions of the size traded by the client and the CLP holding. Throughout the activity the pool faces an inventory risk, which can be reduced (i) by controlling the width and the skew of the CLP spread, and (ii) by resorting to the standard exchange via both market and limit orders. Internal CLP transactions are preferred so to avoid information leakage. Such a feature is modelled via a fixed penalty incurred by the CLP whenever it submits an order to the ‘lit’ exchange. As confirmed by the numerical results, the CLP will refrain from placing orders in a standard exchange as long as the size of the inventory is small. Whenever the optimal boundary is exceeded, the CLP resorts to the standard exchange by means of limit orders. A limit order is cheaper though its execution is uncertain. The CLP can choose the limit price; we find that the more the inventory grows, the closer to the mid-price the CLP will post. This is reasonable since the filling probability of limit orders depends on how far from the mid-price they are posted. If the inventory becomes critically large, market orders will be preferred instead, which are costly but benefit from sure execution. When the end of the market-making activity approaches (which, e.g., might be thought of as the end of the trading day) the market-orders region in the ‘lit’ exchange widens while the CLP and limit-order regions in the standard exchange diminish. In fact, the market maker will incur in a higher penalty for holding a large inventory at the terminal date. These conclusions are obtained by formulating and numerically solving a double obstacle standard stochastic and impulse control problem, for which we provide four numerical examples with increasing complexity. Compared to the state-of-the-art literature on ‘lit’ pool market making (see e.g. Guéant et al. [45], Cartea et al. [24], and Guilbaud & Pham [47, 48]), adding a CLP to the model substantially modifies the “standard” ‘lit’ exchange market-making problem for the following reasons: (i) the prices offered to clients can be functions of the size traded (which would not be possible in a classic LOB), and (ii) there are no such things as minimum tick size, minimum quantities or queues in the CLP that may be assumed, and (iii) the standard exchange is only utilised as a hedging venue, while two-way prices are offered to clients and are not available to general market participants. This work provides a rather flexible setup for the management of a CLP inventory. The pricing and the hedging strategies are illustrated in detail.

Chapter 5

Market making: an application to the eFX spot market

5.1 Overview of the chapter

In this chapter we adapt the framework introduced in Chapter 4 to a broker-dealer firm that operates in the electronic foreign exchange (eFX) market. The academic literature on FX spot-trading has its main focus on empirical studies of aggregated data to evaluate trading strategies, to forecast short-term price movements, and to analyse the effects of information asymmetry on trading and price discovery. In this category we find, e.g., the work by Deng et al. [35] who employ multiple kernels learning and genetic algorithm to forecast future price movements and test their model on the USDJPY pair. We also find the work by Menkhoff et al. [66], who utilise ten years of aggregated daily data of fifteen different currency pairs, and show that the customers' order flow has significant predictive content. Such an order flow is also the object of the study carried out by Berger et al. [8] who confirm that, within electronic markets, such an order flow has predictive power for up to a minute. Next, Chen and Gau [27] utilise daily Electronic Broking Services (EBS) data to accept their hypothesis that the bid quote offers more price discovery compared to the ask quote. Gençai and Gradojevic [?] utilise EBS data of EURUSD, USDJPY and USDCHF to cluster patterns of informed traders and find that early morning and late afternoon

UTC (coordinated universal time) have the highest concentration of asymmetric information. Informed trading in FX markets has also been studied by Payne [71], who employs a vector autoregressive (VAR) model to quantify the effects of informed flow on market prices, and shows that the impact of such flow accounts for around 60% of the quoted spread. In this context, we further mention (i) the work by King et al. [55], who provide an extensive survey of the FX market microstructure literature, (ii) the seminal papers by Lyons [64, 65], who proposes discrete-time inventory-control models, and “hot-potato” models for inventory management, respectively, and (iii) the work by Evans and Lyons [36], in which the authors consider the predictive content of the order-flow for the first time in the literature.

Academic research more pertinent to the work presented in this chapter is very limited when it comes to the FX asset class. The work by Chaboud et al. [26] provides an in-depth econometric analysis of the effects of algorithmic and computerised trading on market efficiency. They find a substantial reduction of triangular arbitrage opportunities, which derives from a faster circulation of information. Kozhan et al. [56] modify the Lyons [36] framework to include limit and market orders, thus reproducing the features of an order-driven market. A structural VAR model is used by Schmidt [76] to describe a multi-dealer FX spot electronic order-driven market and find that the trading volume is the main source of market impact. An optimal market-making problem in the FX market has been proposed by Veraart [84], who considers a multi-dealer market in which a firm can optimise the quotes proposed to its customers and can reduce its inventory by trading with other dealers. They set up an optimisation problem in which the agent maximises the terminal value of the portfolio, while penalising for high-variance portfolios. The optimal strategy is found via numerical techniques. Veraart in [85] further analyses an optimal investment problem in the foreign exchange market, in which the investor aims to maximise the terminal value of a portfolio which consists of domestic and foreign currencies.

Impulse-control problems are primarily used, within the FX literature, to study central bank policy intervention. In this context we mention the works by Cadenillas and Zapatero [16], Bertola et al. [9], Mundaka and Øksendal [68], and

Kercheval and Moreno [54].

The present chapter is organised as follows. We first provide an introduction to the FX market and its specific features. We then explain in detail the dissimilarities among a standard market-making problem adaptable to general asset classes (e.g. equity) and an analogous problem specific to FX trading. Next, we consider a scenario where one currency pair is traded (EURUSD) and a joint service of brokerage and principal trading is offered by the firm to its clients. We assume that the firm can hedge its position via market orders in the standard exchange. We assume that—due to potential regulatory needs of producing a harmonised balance sheet to which the firm may be subject—the terminal P&L are calculated in a reference currency. We choose the latter to be USD and thus, at the end of the trading period, the terminal EUR inventory is converted to USD. Finally, we move to a three-currency-pair scenario (from which the generalisation to n currency pairs is trivial) and we consider the same problem of mixed principal/agency trade execution and hedging. The questions we aim to address in the present chapter are:

1. What is the optimal proportion of principal-versus-agency trading that the CLP should offer?
2. What is the optimal hedging strategy when trading specifically in the FX market?

To answer those questions, we modify the framework presented in Chapter 4 and we find the optimal trading strategy of the CLP.

5.1.1 The FX spot market

The FX market is mainly an OTC market, which at the present time is little-regulated. We take the perspective of a financial firm, such as a CLP, which has the technological means to offer its clients a competitive financial service in high-speed markets. The clients can also count on a network of trade counterparties provided by the firm, which we assume plays the role of a liquidity provider. CLPs have access to a number of ECNs (Electronic Communication Networks)

which provide a real-time facility for price discovery. An example of an ECN is EBS (ICAP Group) which provides services such as EBS Live (real-time prices delivered from the EBS matching platform direct to the CLP) and EBS Market (global trading platform). The CLPs access EBS Live via EBS Ai (a direct two-way interface with the EBS spot market). EBS updates the order book (available liquidity and prices) every 100ms.

The CLP takes into account the prices and liquidity shown in the ECNs when making a decision as to what price to offer to its client depending also on the “in-house” liquidity that the CLP can provide. Such considerations also influence the decision as to what percentage of the client’s order the CLP wishes to execute against its principal liquidity and what it will place in the ECN markets via its brokerage service.

The advantages for a market participant to place orders by utilising a CLP are: (i) anonymity (which mitigates the information leakage), (ii) no or limited market impact for the client, (iii) access to state-of-the-art trading technology offering a 24/7 trade service, (iv) reduction of latency, and (v) access to additional liquidity offered by the CLP (through principal trading) beyond what is available in ECNs or other markets.

5.1.2 Trading spot FX: the CLP perspective

The spot-FX pricing mechanism adopted by the CLP does not need to be dissimilar from the one of any other asset class. In fact the CLP can take the ECN’s printed prices as a reference to establish its own quotes. On the other hand, the hedging mechanism in foreign exchange is slightly different to the one in stock markets in that every currency can be exchanged with any other, while shares usually are exchanged (sold or bought) receiving cash in return (there are exceptions as in, e.g., exchange options where one share is “exchanged” for a share of another asset).

The above argument suggests that, when taking hedging decisions, the firm shall further choose between direct and/or cross hedging, depending on inventory

levels and market conditions. We refer to Section 5.3 for mathematical and numerical details.

We now provide an example to clarify the difference between direct and cross liquidation¹ (the underlying principle can be applied to direct and cross hedging).

1. Let us consider a stock market with three assets: A , B and C , where C is cash in, say, dollars. Assume that the price of asset A is S^A (\$) per share and S^B (\$) is the price per share of asset B . Assume further that we have a portfolio consisting of X^A units of stock A , X^B units of stock B and an amount X^C of dollars. *Liquidating the portfolio* is usually referred to as the actions of (i) buying/selling X^A shares of A in exchange for $X^A S^A$ (\$), and (ii) buying/selling X^B shares of B in exchange for $X^B S^B$ (\$). The terminal value of the portfolio is, therefore, $X^C + X^A S^A + X^B S^B$ (\$).

2. Let us now consider an FX market where three currencies are traded: € (EUR), £ (GBP), and \$ (USD). Assume further that our portfolio consists of $X^£$, $X^€$ and $X^\$$ units of GBP, EUR and USD, respectively. The current exchange rates are given by $S^{€\$}$ (EURUSD), $S^{£\$}$ (GBPUSD) and $S^{€£}$ (EURGBP). *Liquidating the portfolio*—be it to check the cumulative P&L or to decrease the risk for the exchange rates to move in an unfavourable direction with respect to our holdings—is referred to as the action of converting two of the inventories in what is considered being the reference currency. For this purpose, we choose the latter to be USD. We have the following three options for the conversion into USD:
 - (a) We can exchange both $X^£$ and $X^€$ for USD and calculate the P&L by the formula $X^\$ + X^€ S^{€\$} + X^£ S^{£\$}$, or
 - (b) we can first exchange $X^£$ for EUR and then exchange the updated EUR holding to USD, which gives a P&L of $X^\$ + (X^€ + X^£/S^{€£}) S^{€\$}$, and finally
 - (c) we can first exchange $X^€$ for GBP and then exchange the updated GBP holding to USD, which gives a P&L of $X^\$ + (X^€ S^{€£} + X^£) S^{£\$}$.

¹While people who are familiar with FX will find such an example trivial, we believe it is important to clarify the motivation behind the choice of such an asset class.

This is different from the first scenario in that we do not have the option of exchanging asset A for asset B , as there is not a quoted price (or, incidentally, “exchange rate”) S^{AB} .

If there is only one price available in the market for each currency pair, then the triangular arbitrage relation

$$S^{\text{€}\text{£}} = \frac{S^{\text{€}\text{¤}}}{S^{\text{£}\text{¤}}} \quad (5.1)$$

shall hold, and the liquidating options (a), (b) and (c) in the FX example (2.) are identical, regardless of the levels of $X^{\text{¤}}$, $X^{\text{€}}$ and $X^{\text{£}}$. On the contrary, when bid and ask prices are available for each currency pair, the above liquidation alternatives cease to be equivalent. Given the tedious calculations and the amount of algebra involved to formally show this result, we postpone such a discussion to Section 7.6 in the Appendix, at the end of the present work.

5.2 One currency pair

We start by considering a market where only one currency pair (EURUSD) is traded. While being less interesting than the three-currency-pair case, and similar to the analysis carried out in Chapter 4, we believe it is worth exploring for the following reason: we here consider a firm which offers a joint service of (i) providing principal liquidity to its clients as well as (ii) providing a brokerage service for a fee (which is a substantial difference from Chapter 4, where the CLP could only execute 100% of the orders principally). By looking at this simple case first, we have the opportunity to understand the structure of the model and the principal-versus-agency trading relationship before focusing on the hedging part.

5.2.1 Financial problem

Let us assume that a client (e.g. a pension fund) wishes to execute a sizeable order when both a ‘lit’ and a CLP are available.

From the client perspective, the situation is analogous to the one treated in Chapter 3 if the CLP activity is restricted to anonymous order-matching. On the other hand, if the CLP offers principal liquidity, the problem is slightly different in that (i) the execution in the CLP is fully guaranteed (except in rare circumstances when, e.g., the so-called “last look” is applied), and (ii) the principal prices offered by the CLP are commensurate to the size traded by the client. The latter point may incentivise the client to split such a sizeable order between the ‘lit’ and the dark venues, since the resulting cumulative trading conditions may be more favourable than the price offered only by the CLP on its own (this type of problem has been solved in, e.g., Laruelle et al [60]).

From the CLP perspective, the problem is different to the one treated in Chapter 4 for three main reasons. Firstly, the CLP can only offer principal liquidity, thus leaving the clients with no other choice but to resort to the lit pool by themselves, if they wished to trade in multiple venues. Secondly, by choosing the amount of principal liquidity offered, the CLP can implement a more efficient hedging strategy and inventory management. Thirdly by offering an optimal combination of principal liquidity and brokerage, the CLP has control on the amount sent to the ECN and on the resulting market impact, and can thus program its hedging strategy (along with its internalisation means) accordingly. Ultimately, we want to find the optimal ratio of principal vs ECN liquidity that the CLP should choose to offer to its clients.

5.2.2 Mathematical model

We consider a CLP which offers a market-making service for EURUSD. At each time $u \in [t, T]$ the CLP carries both EUR and USD inventories; in the spirit of Chapter 4, we find an analogy between the USD inventory and the cash process. In fact, being the reference currency, the USD inventory does not carry any risk, which can all be attributed to the EUR inventory. We assume that the currency pair is traded in the ECN at $\{S_u^{\text{€\$}} - \Delta_u^{\text{€\$}}/2, S_u^{\text{€\$}} + \Delta_u^{\text{€\$}}/2\}$, where $\{\Delta_u^{\text{€\$}}\}$ is the market spread for EURUSD. At each time $u \in [t, T]$, a portion $\alpha_u \in [0, 1]$ of principal liquidity for an order of random size q^+ is offered to buyers and a

portion $\beta_u \in [0, 1]$ of principal liquidity for an order of random size q^- is offered to sellers. The quotes set by the CLP should reflect the current ECN quotes, its EUR inventory position and the amount of principal liquidity offered. We denote the prices offered by the CLP by p_u^+ and p_u^- for buyers and sellers, respectively. We refer to Section 5.2.2.1 for an in-depth discussion on the pricing mechanism of the CLP. The remaining portions of clients' orders, i.e. $(1 - \alpha_u)q_u^+$ and $(1 - \beta_u)q_u^-$, are traded by the CLP in the ECN on behalf of the client. For the latter service, the CLP charges a commission $\eta > 0$ commensurate to the size of the order. The EUR inventory of the CLP thus evolves according to

$$dX_u^\epsilon = (\beta_u + (1 - \beta_u)\eta)dJ_u^- - (\alpha_u - (1 - \alpha_u)\eta)dJ_u^+, \quad (5.2)$$

where $X_t^\epsilon = x^\epsilon$. We define $J_u^\pm := \sum_{i=1}^{N_u^\pm} q_i^\pm$, where the Cox processes $\{N_u^\pm\}$ have intensities $\lambda_p^\pm = \lambda^\pm(p^\pm)$, and q_i^\pm , $i \geq 0$, are i.i.d. random variables which model the order size. When the Cox process $\{N_u^+\}$ jumps, the CLP sells $q_{N_u^+}^+$ EURUSD by offering $\alpha_u q_{N_u^+}^+$ principal liquidity and a brokerage service for $(1 - \alpha_u)q_{N_u^+}^+$. An analogous interpretation holds when the Poisson process $\{N_u^-\}$ jumps and the CLP buys EURUSD. The USD inventory thus evolves according to

$$dX_u^\$ = \alpha_u p_u^+ dJ_u^+ - \beta_u p_u^- dJ_u^-. \quad (5.3)$$

Trading in the ECN on behalf of the client causes a permanent impact on prices, which we model by $\gamma \in \mathbb{R}_+$. We consider such impact to affect both sides of the LOB, as it is well known that they are strongly correlated. The second and third term in Equation (5.4) serve this purpose for buyers and sellers, respectively. We assume that the ECN mid-price and spread processes satisfy

$$dS_u^{\epsilon\$} = \kappa(\bar{S} - S_{u^-}^{\epsilon\$})du + \sigma^{s,\epsilon\$}dW_u^{s,\epsilon\$} + \gamma(1 - \alpha_u)dJ_u^+ - \gamma(1 - \beta_u)dJ_u^- \quad (5.4)$$

and

$$d\Delta_u^{\text{€\$}} = \sigma^{\Delta, \text{€\$}} \Delta_u^{\text{€\$}} dW_u^{\Delta, \text{€\$}}, \quad (5.5)$$

respectively. In Equations (5.4) and (5.5) we let $S_t^{\text{€\$}} = s^{\text{€\$}}$, $\Delta_t^{\text{€\$}} = \Delta^{\text{€\$}}$, \bar{S} is the exchange-rate long-term mean, $\kappa \geq 0$ is the speed of mean reversion and $\sigma^{s, \text{€\$}}, \sigma^{\Delta, \text{€\$}} \in \mathbb{R}_+$. Furthermore $\{W_u^{s, \text{€\$}}\}$ and $\{W_u^{\Delta, \text{€\$}}\}$ are independent Brownian motions. We acknowledge that the model defined by Equation (5.4) may produce negative prices. On the other hand, it captures realistic features (such as mean reversion and random jumps) which are commonly observed in market data.

5.2.2.1 Pricing strategy

We here describe the pricing mechanism of the CLP. We believe that the CLP's quotes should depend on (i) the current ECN price, (ii) the sign of the risky (EUR) inventory, and (iii) the portion of principal liquidity offered to the clients. The pricing process of the CLP can thus be summarised as follows:

1. In order to be more competitive, the base spread offered by the CLP is tighter than the ECN one and set to $\xi_1 \Delta_{u^-}^{\text{€\$}}$, where ξ_1 is a constant in $[0, 1]$. The CLP's base quotes are, therefore, $S_{u^-}^{\text{€\$}} + \xi_1 \Delta_{u^-}^{\text{€\$}}/2$ and $S_{u^-}^{\text{€\$}} - \xi_1 \Delta_{u^-}^{\text{€\$}}/2$, respectively.
2. The CLP applies an inventory skew to its quotes. In particular, it skews the prices down when it is long EURUSD and skews its prices up when it is short EURUSD. We define the *position-adjusted* ask and bid prices by $S_{u^-}^{\text{€\$}} + \xi_1 \Delta_{u^-}^{\text{€\$}}/2 - \xi_2 \text{sign}[X_{u^-}^{\text{€}}]$ and $S_{u^-}^{\text{€\$}} - \xi_1 \Delta_{u^-}^{\text{€\$}}/2 - \xi_2 \text{sign}[X_{u^-}^{\text{€}}]$, respectively, where $\xi_2 \geq 0$.
3. The CLP widens its spread for larger portions of principal liquidity offered. This feature reflects both an increase in the risk of unfavourable price movements as well as an increase in the expected hedging costs the CLP is subject to when large orders are executed principally. We therefore set the final prices offered to clients at $p_u^+ = S_{u^-}^{\text{€\$}} + \xi_1 \Delta_{u^-}^{\text{€\$}}/2 - \xi_2 \text{sign}[X_{u^-}^{\text{€}}] + \xi_3 \alpha_u$ and $p_u^- = S_{u^-}^{\text{€\$}} - \xi_1 \Delta_{u^-}^{\text{€\$}}/2 - \xi_2 \text{sign}[X_{u^-}^{\text{€}}] - \xi_3 \beta_u$, respectively, where $\xi_3 \geq 0$.

We define the distance of the CLP prices from the ECN mid-price by $\delta_{CLP}^+ = \xi_1 \Delta_{u^-}^{\text{€\$}}/2 - \xi_2 \text{sign}[X_{u^-}^{\text{€}}] + \xi_3 \alpha_u$ and $\delta_{CLP}^- = \xi_1 \Delta_{u^-}^{\text{€\$}}/2 + \xi_2 \text{sign}[X_{u^-}^{\text{€}}] + \xi_3 \beta_u$. Furthermore, along the lines of Cartea et al. [23], we let $\lambda_p^\pm = \lambda^\pm e^{-c\delta_{CLP}^\pm}$, where $c \geq 0$.

5.2.2.2 Hedging strategy

When skewing the quotes offered by the CLP is not sufficient for reducing its EUR inventory, the firm resorts to the ECN for hedging purposes. Let us assume that it is optimal at time τ to reduce the magnitude of the EUR inventory by one unit² (by symmetry, this will also reduce the magnitude of the USD inventory). Analogously to Chapter 4, the EUR inventory is subject to the following impulse

$$X_\tau^{\text{€}} = X_{\tau^-}^{\text{€}} + \mathbb{1}_{\{X_{\tau^-}^{\text{€}} < 0\}} - \mathbb{1}_{\{X_{\tau^-}^{\text{€}} > 0\}}. \quad (5.6)$$

The USD inventory changes accordingly. In particular, if $X_{\tau^-}^{\text{€}} > 0$, the CLP is selling EURUSD at the current ECN bid, while if $X_{\tau^-}^{\text{€}} < 0$ it is buying EURUSD at the current ECN ask price. Therefore, for the USD inventory, we have

$$X_\tau^{\text{\$}} = X_{\tau^-}^{\text{\$}} - (S_{\tau^-}^{\text{€\$}} + \Delta_{\tau^-}^{\text{€\$}}/2) \mathbb{1}_{\{X_{\tau^-}^{\text{€}} < 0\}} + (S_{\tau^-}^{\text{€\$}} - \Delta_{\tau^-}^{\text{€\$}}/2) \mathbb{1}_{\{X_{\tau^-}^{\text{€}} > 0\}}.$$

The ECN mid-price is impacted similarly to Equation (5.4), that is

$$S_\tau^{\text{€\$}} = S_{\tau^-}^{\text{€\$}} + \gamma \mathbb{1}_{\{X_{\tau^-}^{\text{€}} < 0\}} - \gamma \mathbb{1}_{\{X_{\tau^-}^{\text{€}} > 0\}}. \quad (5.7)$$

Also, we consider a fixed cost the CLP sustains when crossing the spread. This can be seen as a fixed ECN fee as well as the cost of information leakage, which we model via a positive constant ϵ . The hedging strategy, as defined in this context, is a collection of stopping times $M : (\tau_i)_{i \geq 0}$ at which it is optimal to cross the spread in the ECN so to reduce the EUR position.

²A “unit” can be intended as a standard lot, which in FX can be of 10^5 or 10^6 of the left-hand side currency, depending on the specific ECN rules.

5.2.3 The value function

For simplicity, we write the control processes by $\alpha = \{\alpha_u\}$ and $\beta = \{\beta_u\}$, and the vector of state variables by $\mathbf{x} := \{x^\text{€}, x^\text{\$}, s^\text{€\$}, \Delta^\text{€\$}\}$. We define the value function of the CLP by

$$V(t, \mathbf{x}) = \max_{\alpha, \beta, M} \mathbb{E}_{t, \mathbf{x}} \left[\text{P\&L}_T - \hat{\alpha} (X_T^\text{€})^2 - \phi \int_t^T (X_u^\text{€})^2 du - \sum_{t \leq \tau_i < T} \epsilon \right], \quad (5.8)$$

where the term P\&L_T is the terminal theoretical cash of which components are derived from the USD inventory and the EUR inventory evaluated at the ECN mid-price. That is, $\text{P\&L}_T = X_T^\text{\$} + X_T^\text{€} S_T^\text{€\$}$. The terminal and the running penalties for holding a non zero inventory are parametrised by³ $\hat{\alpha} \geq 0$ and $\phi \geq 0$, as done in Chapters 3 and 4. The value function satisfies the following HJB quasi variational inequality⁴:

$$\min \left\{ \phi (x^\text{€})^2 - \kappa (\bar{S} - s^\text{€\$}) \frac{\partial V}{\partial s^\text{€\$}} - \frac{1}{2} (\sigma^{s, \text{€\$}})^2 \frac{\partial^2 V}{(\partial s^\text{€\$})^2} - \frac{1}{2} (\sigma^{\Delta, \text{€\$}} \Delta^\text{€\$})^2 \frac{\partial^2 V}{(\partial \Delta^\text{€\$})^2} - \frac{\partial V}{\partial t} - \mathcal{L}^- V(t, \mathbf{x}) - \mathcal{L}^+ V(t, \mathbf{x}); V(t, \mathbf{x}) - \mathcal{M} V(t, \mathbf{x}) \right\} = 0, \quad (5.9)$$

where the operators \mathcal{L}^- , \mathcal{L}^+ and \mathcal{M} are defined by

$$\begin{aligned} \mathcal{L}^+ V(t, \mathbf{x}) &= \sup_{\alpha} \lambda_p^+ \\ \mathbb{E}^{(q^+)} [V(x^\text{€} - (\alpha - (1 - \alpha)\eta)q^+, x^\text{\$} + \alpha p^+ q^+, s^\text{€\$} + \gamma(1 - \alpha)q^+, \Delta^\text{€\$}) - V(t, \mathbf{x})], \end{aligned}$$

$$\begin{aligned} \mathcal{L}^- V(t, \mathbf{x}) &= \sup_{\beta} \lambda_p^- \\ \mathbb{E}^{(q^-)} [V(x^\text{€} + (\beta + (1 - \beta)\eta)q^-, x^\text{\$} - \beta p^- q^-, s^\text{€\$} - \gamma(1 - \beta)q^-, \Delta^\text{€\$}) - V(t, \mathbf{x})], \end{aligned}$$

³To keep consistency with the previous chapters, we here call the terminal penalty $\hat{\alpha}$. The latter shall not be confused with the portion of principal liquidity offered to sellers, i.e. $\{\alpha_u\}$.

⁴We refer to Section 7.1 for details on its derivation.

and

$$\mathcal{MV}(t, \mathbf{x}) = V(x^{\text{€}} + \mathbb{X}^{\text{€}}, x^{\text{§}} + \mathbb{X}^{\text{§}}, s^{\text{€§}} + \mathbb{S}^{\text{€§}}, \Delta^{\text{€§}}) - \epsilon, \quad (5.10)$$

respectively. In Equation (5.10) we define $\mathbb{X}^{\text{€}} = \mathbb{1}_{\{x^{\text{€}} < 0\}} - \mathbb{1}_{\{x^{\text{€}} > 0\}}$, $\mathbb{X}^{\text{§}} = (s^{\text{€§}} - \Delta^{\text{€§}}/2)\mathbb{1}_{\{x^{\text{€}} > 0\}} - (s^{\text{€§}} + \Delta^{\text{€§}}/2)\mathbb{1}_{\{x^{\text{€}} < 0\}}$ and $\mathbb{S}^{\text{€§}} = \gamma\mathbb{1}_{\{x^{\text{€}} < 0\}} - \gamma\mathbb{1}_{\{x^{\text{€}} > 0\}}$. Next we solve numerically the QVI in Equation (5.9) and discuss the optimal pricing and hedging strategy of the CLP.

5.2.4 Numerical results

In this section we explore some features of the model. For convenience, if the inventory is positive, we define α to be the *aggress liquidity* and β the *protect liquidity*. This is because α helps to reduce the inventory and thus the CLP wants to be more aggressive on α and more conservative on β . On the other hand, if the inventory is negative, for analogous reasons we define α to be the *protect liquidity* and β the *aggress liquidity*. For simplicity, we first assume that the EURUSD exchange rate is a martingale, i.e., there is no mean reversion ($\kappa = 0$) and no permanent price impact ($\gamma = 0$). Thereafter, we include such features and show how the optimal strategy changes as a function of the FX rate.

We numerically approximate the solution of Equation (5.9) by an explicit—backward in time—finite difference scheme. Within this section, we consider an equally-spaced time grid valued in $[0, 100]$ with increments of 0.1, an equally-spaced inventory grid ($x^{\text{€}}$) valued in $[-50, 50]$ with increments of 0.1, an equally spaced price grid ($s^{\text{€§}}$) values in $[1.07, 1.08]$ with increments of 0.01 and an equally spaced spread grid ($\Delta^{\text{€§}}$) valued in $[0, 0.0002]$ with increments of 0.0001. The random variables q^{\pm} can take values in $\{0, 1, 2, \dots, 20\}$ with equal probability of $\frac{1}{21}$ and the controls α and β can take values in $\{0, 0.1, \dots, 1\}$. At every node, we check which combination of α and β is optimal (i.e. maximises the value function) and we store the values, which we plot below. At every time, and for each node, we further check whether a hedging action improves the value function, and we store the inventory level at which it is optimal to cross the spread and reduce the firm's holdings. The solving algorithm we use is very

similar to the one used for Chapter 4 and described in Section (7.5.2). Finally, as noted in Chapters 2 and 4, when $s^{\text{€\$}}$ or $\Delta^{\text{€\$}}$ are martingales, we can use the usual ansatz (see Cartea et al. [23] for details) and reduce the number of state variables. Such reduction benefits the computational speed.

5.2.4.1 Martingale property of the FX rate

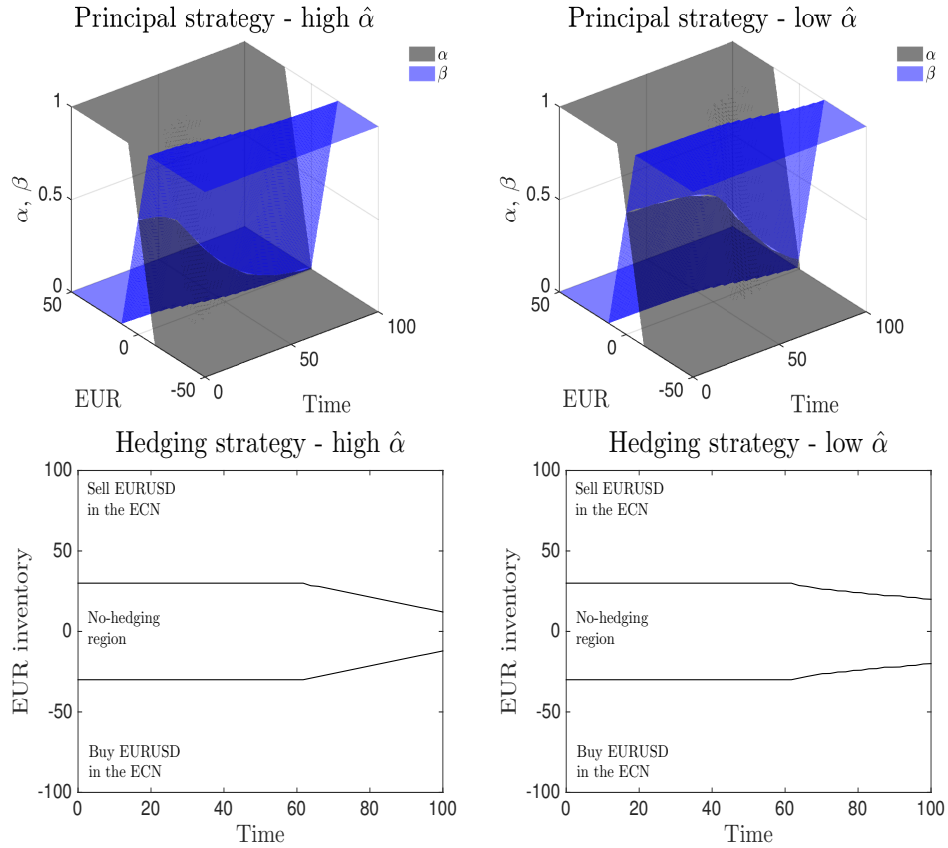


FIGURE 5.1: Optimal principal-liquidity strategy (top panels) and hedging strategy (bottom panels)—displayed as a function of time and inventory—found by solving the HJB equation (5.9). We set $\lambda^{\pm} = 0.5$, $q^{\pm} \sim U[0, 20]$, $\eta = 25 \times 10^{-6}$, $\phi = 0.05$, $\gamma = \kappa = 0$, $\xi_1 = 0.5$, $\xi_2 = 0.5$ pips, $\xi_3 = 0.001$, $\epsilon = 5$, $s^{\text{€\$}} = 1.075$, $\Delta^{\text{€\$}} = 2$ pips. In the left panels we set $\hat{\alpha} = 6$. In the right panels we set $\hat{\alpha} = 0.5$.

If we neglect both (i) the permanent impact of the brokerage and hedging activities on the mid-price, and (ii) the mean-reversion property of the mid-price, we can reduce the dimensionality of the problem. The optimal strategy α , β and M now only depends on the time and the inventory level. In Figure 5.1 we show the principal strategy α and β (top panels) and the hedging strategy (bottom panels) for different values of the terminal penalty $\hat{\alpha}$. A higher terminal

penalty (cf. left panels) discourages the firm from offering high percentages of principal liquidity, towards maturity, on the protect side compared to a lower terminal penalty. Furthermore the optimal hedging boundaries tighten towards maturity compared to low values of the terminal penalty. We further note that the hedging strategy is less aggressive than the one featured in Chapter 4. The reason is that, towards maturity, very little principal liquidity is offered on the protect side, while it is mainly offered on the aggress side.

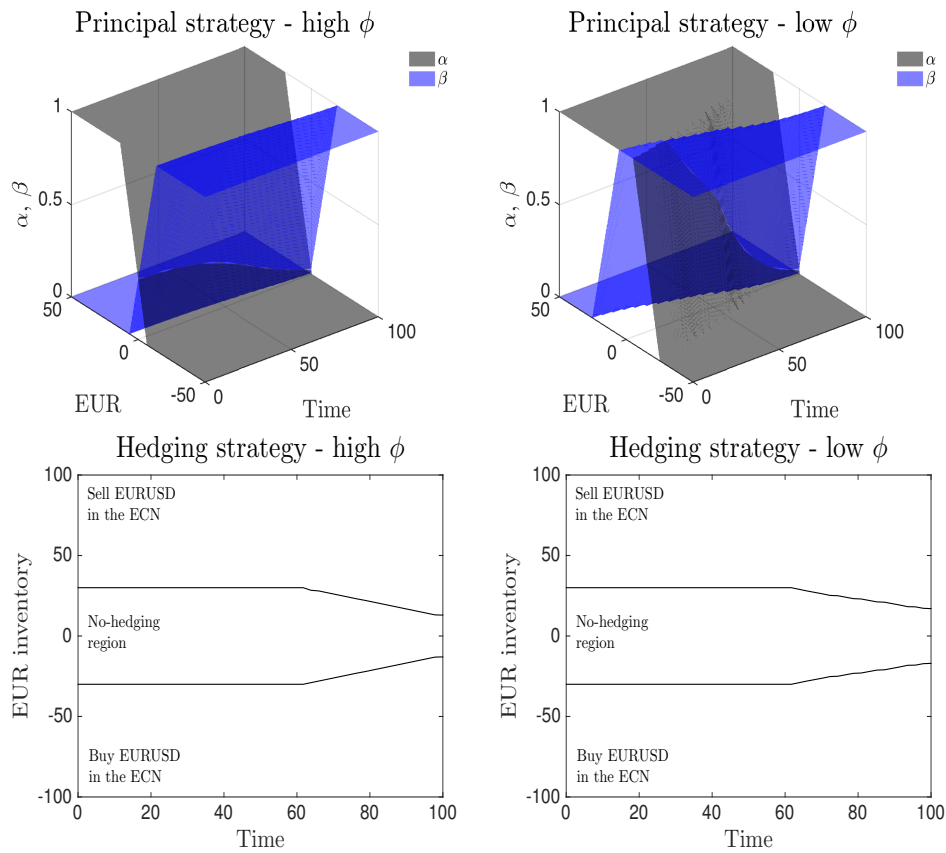


FIGURE 5.2: Optimal principal-liquidity strategy (top panels) and hedging strategy (bottom panels)—displayed as a function of time and inventory—found by solving the HJB equation (5.9). We set $\lambda^\pm = 0.5$, $q^\pm \sim U[0, 20]$, $\eta = 25 \times 10^{-6}$, $\hat{\alpha} = 2$, $\gamma = \kappa = 0$, $\xi_1 = 0.5$, $\xi_2 = 0.5$ pips, $\xi_3 = 0.001$, $\epsilon = 5$, $s^{\text{€\$}} = 1.075$, $\Delta^{\text{€\$}} = 2$ pips. In the left panels we set $\phi = 0.1$. In the right panels we set $\phi = 0.001$.

In Figure 5.2 we show the optimal principal-liquidity (top panels) and hedging strategies (bottom panels) for high and low values of the running penalty. High values of ϕ reduce the percentage of principal liquidity offered to clients throughout the period and tighten the hedging boundaries, while low values of ϕ increase

the percentage of principal liquidity and widen the hedging boundaries. Such results are in agreement with the ones shown in Chapter 4.

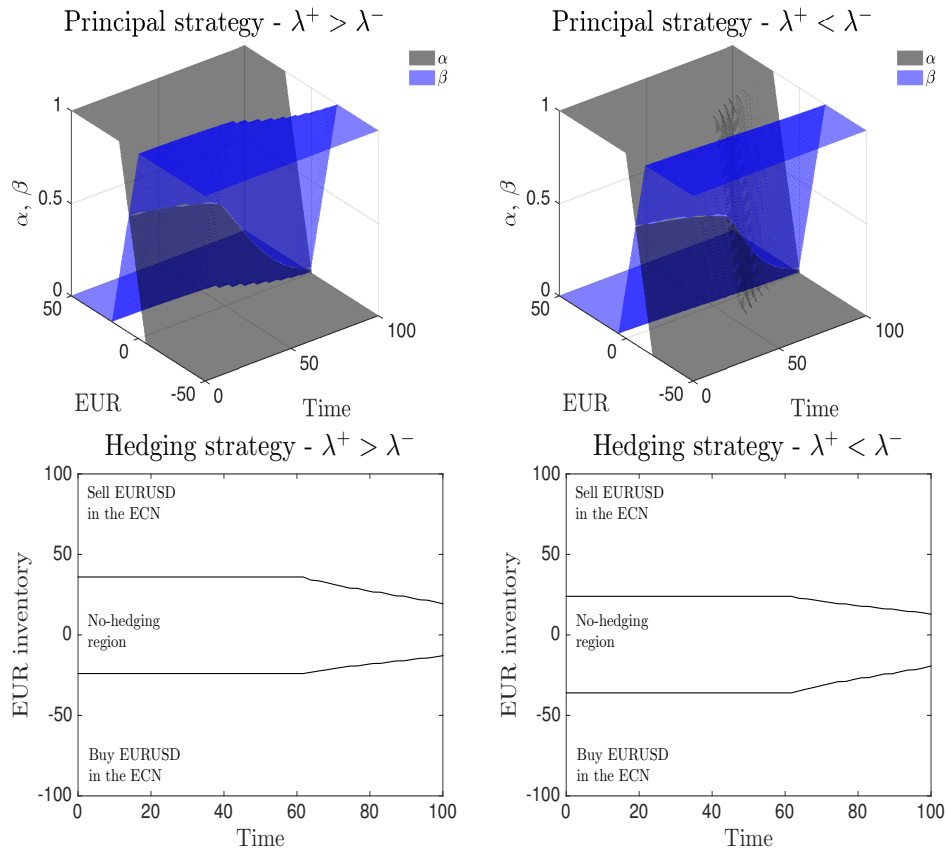


FIGURE 5.3: Optimal principal-liquidity strategy (top panels) and hedging strategy (bottom panels)—displayed as a function of time and inventory—found by solving the HJB equation (5.9). We set $q^\pm \sim U[0, 20]$, $\eta = 25 \times 10^{-6}$, $\hat{\alpha} = 2$, $\phi = 0.05$, $\gamma = \kappa = 0$, $\xi_1 = 0.5$, $\xi_2 = 0.5$ pips, $\xi_3 = 0.001$, $\epsilon = 5$, $s^{\text{€\$}} = 1.075$, $\Delta^{\text{€\$}} = 2$ pips. In the left panels we set $\lambda^+ = 0.7$ and $\lambda^- = 0.3$. In the right panels we set $\lambda^+ = 0.3$ and $\lambda^- = 0.7$.

In Figure 5.3 we show the effect of different expectations regarding the client's arrival-flow. When the CLP is confident that buyers arrive at a higher frequency than sellers, (i.e. $\lambda^+ > \lambda^-$), its inventory is expected to decrease and thus more principal liquidity is offered to sellers (higher β compared to α). On the hedging side, the optimal boundaries are skewed upward. That is, the CLP starts hedging sooner when it holds a negative inventory compared to a positive one. The opposite holds when the arrival-flow of sellers is higher than the one of buyers.

5.2.4.2 Permanent price impact

The addition of a permanent price impact adds interesting features to the optimal strategy.

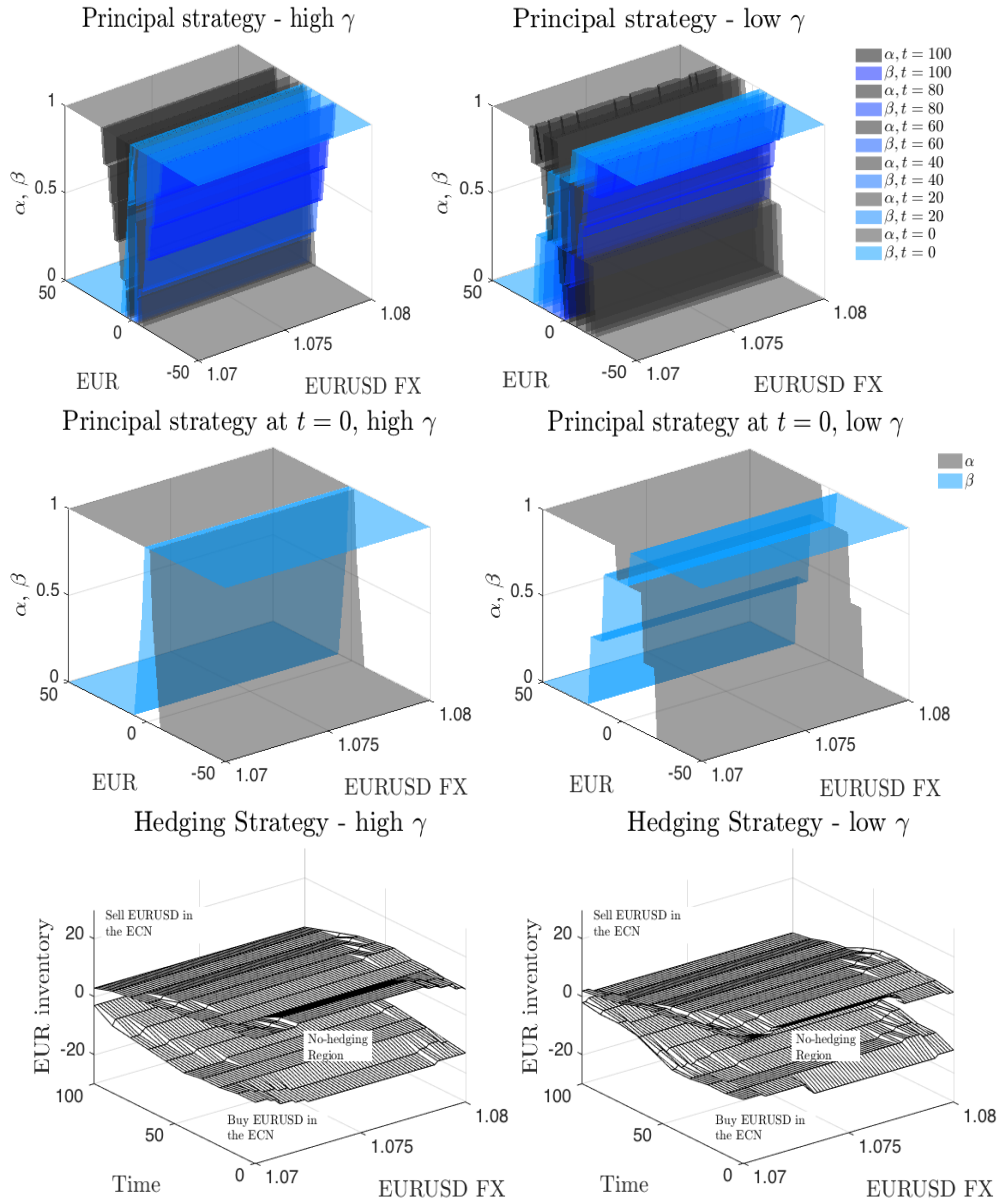


FIGURE 5.4: Optimal principal-liquidity strategy (top panels) and hedging strategy (bottom panels)—displayed as a function of time and inventory—found by solving the HJB equation (5.9). We set $q^\pm \sim U[0, 20]$, $\eta = 25 \times 10^{-6}$, $\hat{\alpha} = 2$, $\phi = 0.05$, $\lambda^\pm = 0.5$, $\kappa = 0$, $\xi_1 = 0.5$, $\xi_2 = 0.5$ pips, $\xi_3 = 0.001$, $\epsilon = 5$, $s^{\text{€\$}} = 1.075$, $\Delta^{\text{€\$}} = 2$ pips. In the left panels we set $\gamma = 0.01$. In the right panels we set $\gamma = 0.0001$.

In Figure 5.4, we show the optimal principal strategy through time (top panels), the optimal principal strategy at the initial time (central panels) and the hedging

strategy (bottom panels). In the left panels we consider a high price impact while in the right panels a low price impact is considered. It is interesting to note that while a high price impact implies less principal liquidity being offered to clients on the protect side, when we are at time 0 and for a neutral position, more principal liquidity is offered for higher permanent impact. The financial justification of such a feature is as follows. The CLP accepts a higher inventory risk (when starting from a neutral position) so to avoid unfavourable impact on the market price through its brokerage activity and relies on its internalisation means.

5.2.4.3 Mean-reversion

When the FX rate mean-reverts to its long-term mean \bar{S} , both principal and hedging decisions are made on the basis of the value of the current price with respect to \bar{S} .

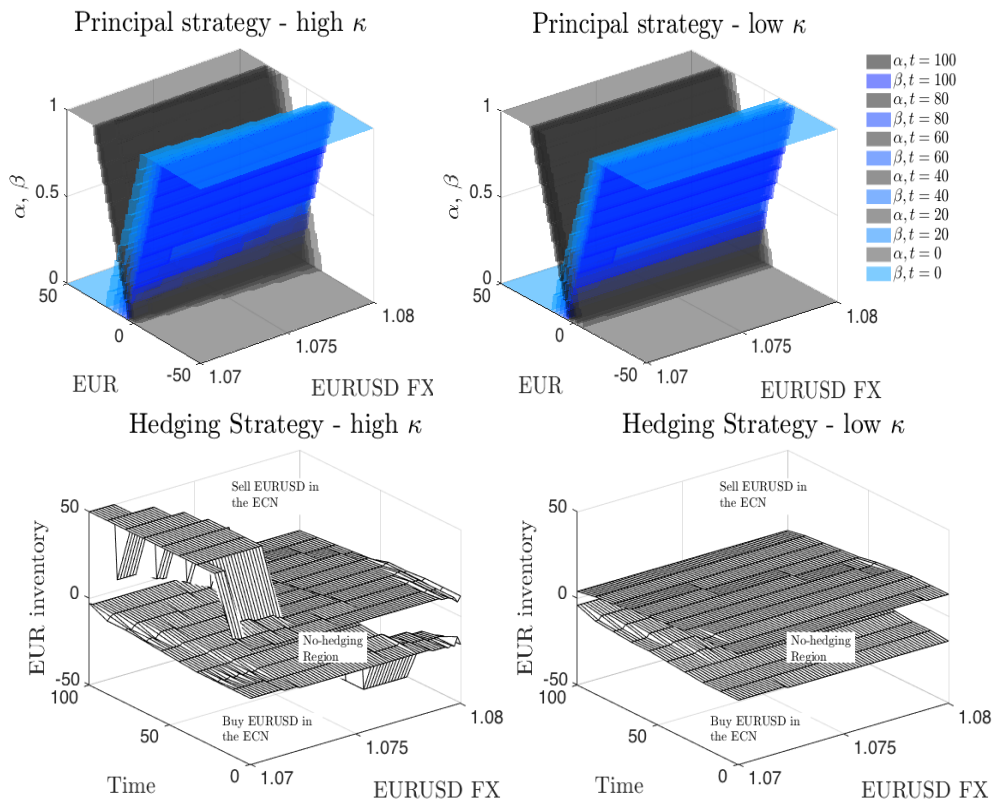


FIGURE 5.5: Optimal principal-liquidity strategy (top panels) and hedging strategy (bottom panels)—displayed as a function of time and inventory—found by solving the HJB equation (5.9). We set $q^\pm \sim U[0, 20]$, $\eta = 25 \times 10^{-6}$, $\hat{\alpha} = 2$, $\phi = 0.05$, $\bar{S} = 1.075$, $\lambda^\pm = 0.5$, $\gamma = 0$, $\xi_1 = 0.5$, $\xi_2 = 0.5$ pips, $\xi_3 = 0.001$, $\epsilon = 5$, $\Delta^{\text{€\$}} = 2$ pips.

In the left panels we set $\kappa = 0.05$. In the right panels we set $\kappa = 0.005$.

In Figure 5.5, we note that when the FX rate is below its long-term mean, more principal liquidity is offered to sellers than buyers. On the other hand, when the FX rate is above its long-term mean, more principal liquidity is offered to buyers. Such a feature is more evident when the speed of mean reversion κ is high (top-left panel). This can be justified by the intention of the CLP to exploit a short-lived opportunity of a market mis-pricing. On the hedging side, we notice that for a high mean-reversion speed, hedging is postponed when the price is unfavourably high or low (for a negative and positive inventory, respectively).

5.2.5 Price and inventory simulation

We here plot two distinct simulations (left and right panels) of the typical activity of the CLP.

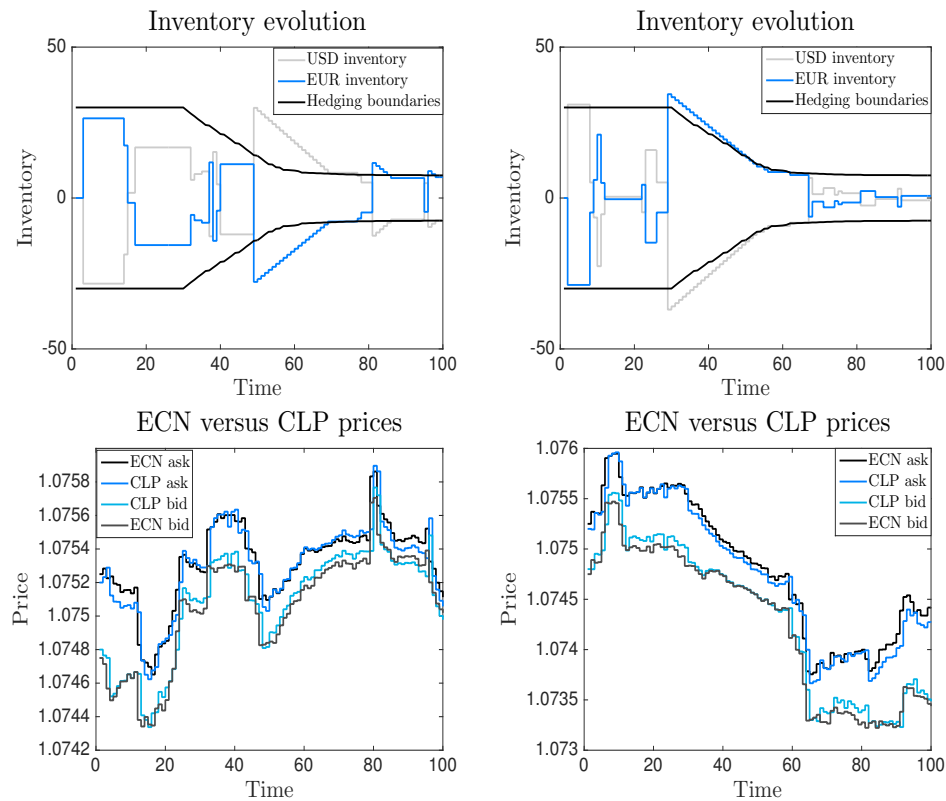


FIGURE 5.6: Inventory simulation (top panels) and prices simulation (bottom panels). We set $q^\pm \sim U[0, 50]$, $\eta = 25 \times 10^{-6}$, $\hat{\alpha} = 2$, $\phi = 0.05$, $\bar{S} = 1.075$, $\lambda^\pm = 0.5$, $\gamma = 0$, $\xi_1 = 0.5$, $\xi_2 = 0.5$ pips, $\xi_3 = 0.001$, $\epsilon = 5$, $\Delta^{\text{€\$}} = 2$ pips, $\kappa = 0.005$.

In the top panels of Figure 5.6 we plot the EUR and USD inventory, and superimpose the hedging boundaries. In the bottom panels we simulate the ECN and

the CLP prices. We notice that the CLP spread is, as expected, tighter than the ECN one. When the inventory skew is applied, the aggress price is closer to the mid-price, while the protect side may be less advantageous than the ECN one. In the price simulation we further include the mean-reversion of prices and the permanent impact of trades. Around time $t = 50$, in the top-left panel, we notice that the CLP is short EURUSD to the point it needs to resort to the ECN for hedging. Buying EURUSD in the centralised market causes a market impact which is evident in the bottom left panel, where prices have a clear increasing trend around the same time. On the other hand, in the top-right panel around time $t = 30$, the CLP is long EURUSD. The bottom-right panel shows indeed the consistent slippage (starting around the same time), which is caused by the CLP through its hedging activity.

5.3 Three currency pairs

In this section we assume that the CLP offers liquidity for three currency pairs, two of which are direct pairs (i.e. EURUSD and GBPUSD) and one is a cross pair (EURGBP), and that it hedges its positions in a single ECN (which may be a synthetic ECN constructed via aggregation of the books belonging to different ECNs). When we refer to *direct pairs*, we mean that one of the legs is USD and by *cross pair* we indicate those currency pairs of which neither leg is USD. Typically direct pairs are more liquid (i.e. have tighter spreads) than cross pairs.

The CLP activity can be summarised as follows:

1. **On the pricing side**, the CLP receives orders from buyers and sellers for each of the currency pairs. It provides principal liquidity for a portion of such orders, while the remainder is traded in the ECN on behalf of the client, and it is executed at the market price. Analogously to Section 5.2.2, the CLP chooses the prices at which it offers principal liquidity, and it charges a commission fee for the brokerage service.
2. **On the hedging side**, the CLP needs to manage the risk of holding the inventories deriving from offering principal liquidity to clients. Its options

are as follows: (i) the CLP skews its prices and/or reduces the portion of principal liquidity on the protect side (while increasing the proportion of principal liquidity on the aggress side), and (ii) it can post market orders in the ECN. In the latter option, as briefly mentioned in Section 5.1.2, the CLP has the choice of hedging via direct and/or cross pairs. As it is typically more expensive to hedge via the cross-pair, we would expect the hedging to happen through the direct pairs. Nonetheless, there may be circumstances which make the cross-pair hedging optimal, as we shall see in Section 5.3.3.

In the remainder of the chapter, we assume that

- EURUSD is traded at $\{S_u^{\text{€\$}} - \Delta_u^{\text{€\$}}/2, S_u^{\text{€\$}} + \Delta_u^{\text{€\$}}/2\}$,
- GBPUSD is traded at $\{S_u^{\text{£\$}} - \Delta_u^{\text{£\$}}/2, S_u^{\text{£\$}} + \Delta_u^{\text{£\$}}/2\}$,
- EURGBP is traded at $\{S_u^{\text{€£}} - \Delta_u^{\text{€£}}/2, S_u^{\text{€£}} + \Delta_u^{\text{€£}}/2\}$,

where $\{\Delta_u^{\text{€\$}}\}$, $\{\Delta_u^{\text{£\$}}\}$, $\{\Delta_u^{\text{€£}}\}$ are the bid/ask spreads for EURUSD, GBPUSD and EURGBP, respectively. By means of standard arguments we can derive the triangular arbitrage relations, given by

$$\frac{S_u^{\text{€\$}} - \Delta_u^{\text{€\$}}/2}{(S_u^{\text{€£}} + \Delta_u^{\text{€£}}/2)(S_u^{\text{£\$}} + \Delta_u^{\text{£\$}}/2)} \leq 1, \quad (5.11)$$

and

$$\frac{(S_u^{\text{£\$}} - \Delta_u^{\text{£\$}}/2)(S_u^{\text{€£}} - \Delta_u^{\text{€£}}/2)}{S_u^{\text{€\$}} + \Delta_u^{\text{€\$}}/2} \leq 1; \quad (5.12)$$

which shall hold at any time $u \in [t, T]$.

We note that Equation (5.1) implies both (5.11) and (5.12). For simplicity, we assume that Equation (5.1) holds and that the EURGBP spread is given by $\Delta_u^{\text{€£}} = k(\Delta_u^{\text{€\$}} + \Delta_u^{\text{£\$}})$, where $k > 0$. As a byproduct of the above assumptions, we have two fewer processes to model.

5.3.1 A revision of the state-variables dynamic

For notational simplicity, we write the state variables dynamics as a seven-dimensional vector. In particular, we let $\mathbf{X}_u := (S_u^{\text{€\$}}, S_u^{\text{£\$}}, \Delta_u^{\text{€\$}}, \Delta_u^{\text{£\$}}, X_u^{\text{€}}, X_u^{\text{£}}, X_u^{\text{\$}})$, with initial value given by $\mathbf{x} := (s^{\text{€\$}}, s^{\text{£\$}}, \Delta^{\text{€\$}}, \Delta^{\text{£\$}}, x^{\text{€}}, x^{\text{£}}, x^{\text{\$}})$.

The first two components of the vector \mathbf{X}_u are the mid-prices for the EURUSD and GBPUSD exchange rates, respectively. The third and fourth elements are the market spreads for the EURUSD and GBPUSD, respectively. Finally, the last three components are the EUR, GBP and USD inventories, respectively.

We also define the vector of principal-liquidity controls by $\boldsymbol{\alpha}_u := (\alpha_u^{\text{€\$}}, \alpha_u^{\text{£\$}}, \alpha_u^{\text{€£}})$ and $\boldsymbol{\beta}_u := (\beta_u^{\text{€\$}}, \beta_u^{\text{£\$}}, \beta_u^{\text{€£}})$. Each component of the above controls is the principal-liquidity portion of orders offered to clients who: (i) buy EURUSD ($\alpha_u^{\text{€\$}}$), (ii) buy GBPUSD ($\alpha_u^{\text{£\$}}$), (iii) buy EURGBP ($\alpha_u^{\text{€£}}$), (iv) sell EURUSD ($\beta_u^{\text{€\$}}$), (v) sell GBPUSD ($\beta_u^{\text{£\$}}$), and (vi) sell EURGBP ($\beta_u^{\text{€£}}$). The stochastic process \mathbf{X}_u satisfies the following stochastic differential equation:

$$d\mathbf{X}_u = \boldsymbol{\sigma}(u, \mathbf{X}_u)d\mathbf{W}_u + \mathbf{h}(u, \mathbf{X}_u, \boldsymbol{\alpha}_u, \boldsymbol{\beta}_u, \mathbf{q}_u)d\mathbf{N}_u, \quad (5.13)$$

where $\{\mathbf{W}_u\} := (\{W_u^{s, \text{€\$}}\}, \{W_u^{s, \text{£\$}}\}, \{W_u^{\Delta, \text{€\$}}\}, \{W_u^{\Delta, \text{£\$}}\})'$ is a 4-dimensional Brownian motion and the 6-dimensional jump process is defined by $\{\mathbf{N}_u\} := (\{N_u^{+, \text{€\$}}\}, \{N_u^{+, \text{£\$}}\}, \{N_u^{+, \text{€£}}\}, \{N_u^{-, \text{€\$}}\}, \{N_u^{-, \text{£\$}}\}, \{N_u^{-, \text{€£}}\})'$. The elements of both the diffusion and the jump vectors are assumed to be independent. Also, for $i = \text{€\$}, \text{£\$}, \text{€£}$, each element of the jump vector is a Cox processes $\{N_u^{\pm, i}\}$ with intensity $\lambda_p^{\pm, i} = \lambda^{\pm}(p^{\pm, i})$ and $q^{\pm, i}$ are i.i.d. random variables which model the order size. Furthermore, we have $\boldsymbol{\sigma} : [t, T] \times \mathbb{R}^7 \rightarrow \mathbb{R}^{7 \times 4}$, and $\mathbf{h} : [t, T] \times \mathbb{R}^7 \times [0, 1]^3 \times [0, 1]^3 \times [0, \bar{q}]^7 \rightarrow \mathbb{R}^{7 \times 6}$, where $\bar{q} > 0$. In particular, we let

$$\boldsymbol{\sigma}(u, \mathbf{X}_u) = \begin{bmatrix} \sigma^{s, \text{€\$}} S_u^{\text{€\$}} & 0 & 0 & 0 & 0 & 0 & 0 \\ 0 & \sigma^{s, \text{£\$}} S_u^{\text{£\$}} & 0 & 0 & 0 & 0 & 0 \\ 0 & 0 & \sigma^{\Delta, \text{€\$}} \Delta_u^{\text{€\$}} & 0 & 0 & 0 & 0 \\ 0 & 0 & 0 & \sigma^{\Delta, \text{£\$}} \Delta_u^{\text{£\$}} & 0 & 0 & 0 \end{bmatrix}',$$

and

$$h(u, \mathbf{X}_u, \boldsymbol{\alpha}_u, \boldsymbol{\beta}_u, \mathbf{q}_u) =$$

$$\begin{bmatrix} h^{+, \text{€\$}}, h^{+, \text{£\$}}, h^{+, \text{€£}}, h^{-, \text{€\$}}, h^{-, \text{£\$}}, h^{-, \text{€£}} \end{bmatrix} =$$

$$\begin{bmatrix} 0 & 0 & 0 & 0 & 0 & 0 \\ 0 & 0 & 0 & 0 & 0 & 0 \\ 0 & 0 & 0 & 0 & 0 & 0 \\ 0 & 0 & 0 & 0 & 0 & 0 \\ 0 & 0 & 0 & 0 & 0 & 0 \\ 0 & 0 & 0 & 0 & 0 & 0 \end{bmatrix}'$$

In analogy with the pricing method described in Section 5.2.2.1, we define $p_u^{+,j\$} = S_{u-}^{j\$} + \xi_1 \Delta_{u-}^{j\$} / 2 - \xi_2 \text{sign}[X_{u-}^j] + \xi_3 \alpha_u^{j\$}$ and $p_u^{-,j\$} = S_{u-}^{j\$} - \xi_1 \Delta_{u-}^{j\$} / 2 - \xi_2 \text{sign}[X_{u-}^j] - \xi_3 \beta_u^{j\$}$ for direct pairs, i.e. where $j = \text{€}, \text{£}$. For the cross pair, we shall make the following consideration for the inventory skew. If the CLP is long EURUSD and short GBPUSD (which is similar to being long EURGBP) then it should skew its prices down as incoming trades from buyers of EURGBP are 100% risk-decreasing. Analogously, when the CLP is short EURUSD and long GBPUSD, then it should skew its prices up so to encourage sellers of EURGBP. Assume, on the other hand, that the CLP is long in both EURUSD and GBPUSD. An upward skew would be aimed at reducing the GBP inventory (risk decreasing) and increase the EUR inventory (risk increasing). Analogously, a downward skew would be aimed at reducing the EUR inventory (risk decreasing) and increase the GBP inventory (risk increasing). The same considerations hold when the CLP is short in both EURUSD and GBPUSD. We therefore believe that, on such occasions, no inventory skew should be applied to the EURGBP quotes as there is no such thing as a ‘preferred’ trade direction. The last scenario we can encounter is being neutral on one inventory and not so in the other. We believe that in such a case the preferred trade direction should be the one that rebalances the non-neutral inventory, as a trade in the opposite direction would be 100% risk increasing. In view of the above thoughts, we shall define

$p_u^{+, \text{€}\text{£}} = S_{u^-}^{\text{€}\text{£}} + \xi_1 \Delta_{u^-}^{\text{€}\text{£}}/2 - \xi_2 \text{sign}[X_{u^-}^{\text{€}}] + \xi_2 \text{sign}[X_{u^-}^{\text{£}}] + \xi_3 \alpha_u^{\text{€}\text{£}}$ and $p_u^{-, \text{€}\text{£}} = S_{u^-}^{\text{€}\text{£}} - \xi_1 \Delta_{u^-}^{\text{€}\text{£}}/2 - \xi_2 \text{sign}[X_{u^-}^{\text{€}}] + \xi_2 \text{sign}[X_{u^-}^{\text{£}}] - \xi_3 \beta_u^{\text{€}\text{£}}$. It is easy to see that when the EUR and GBP inventories have the same sign, the skews cancel each other out. When one of the positions is neutral, the prices are moderately skewed. Finally, when the two inventories have opposite signs, the prices are highly skewed. We define $\delta_{CLP}^{\pm, i}$ in the same fashion we did in Section 5.2.2.1 and we let $\lambda_p^{\pm, i} = \lambda^{\pm, i} e^{-c \delta_{CLP}^{\pm, i}}$.

When the risk associated with holding the EUR and/or GBP inventories increases, the CLP may consider crossing the spread in the ECN by submitting market orders. Assuming that at time τ an hedging action is optimal, the CLP has the following alternatives: It can trade EURUSD by

$$\begin{aligned} X_\tau^{\text{€}} &= X_{\tau^-}^{\text{€}} + \mathbb{1}\{X_{\tau^-}^{\text{€}} < 0\} - \mathbb{1}\{X_{\tau^-}^{\text{€}} > 0\}, \\ X_\tau^{\text{£}} &= X_{\tau^-}^{\text{£}} - (S_{\tau^-}^{\text{€}\text{£}} + \Delta_{\tau^-}^{\text{€}\text{£}}/2) \mathbb{1}\{X_{\tau^-}^{\text{€}} < 0\} + (S_{\tau^-}^{\text{€}\text{£}} - \Delta_{\tau^-}^{\text{€}\text{£}}/2) \mathbb{1}\{X_{\tau^-}^{\text{€}} > 0\}, \end{aligned}$$

Alternatively, it can trade GBPUSD by

$$\begin{aligned} X_\tau^{\text{£}} &= X_{\tau^-}^{\text{£}} + \mathbb{1}\{X_{\tau^-}^{\text{£}} < 0\} - \mathbb{1}\{X_{\tau^-}^{\text{£}} > 0\}, \\ X_\tau^{\text{€}} &= X_{\tau^-}^{\text{€}} - (S_{\tau^-}^{\text{£}\text{€}} + \Delta_{\tau^-}^{\text{£}\text{€}}/2) \mathbb{1}\{X_{\tau^-}^{\text{£}} < 0\} + (S_{\tau^-}^{\text{£}\text{€}} - \Delta_{\tau^-}^{\text{£}\text{€}}/2) \mathbb{1}\{X_{\tau^-}^{\text{£}} > 0\}, \end{aligned}$$

Finally, it can trade EURGBP by

$$\begin{aligned} X_\tau^{\text{€}} &= X_{\tau^-}^{\text{€}} + \mathbb{1}\{X_{\tau^-}^{\text{€}} < 0, X_{\tau^-}^{\text{£}} > 0\} - \mathbb{1}\{X_{\tau^-}^{\text{€}} > 0, X_{\tau^-}^{\text{£}} < 0\}, \\ X_\tau^{\text{£}} &= X_{\tau^-}^{\text{£}} - (S_{\tau^-}^{\text{€}\text{£}} + \Delta_{\tau^-}^{\text{€}\text{£}}/2) \mathbb{1}\{X_{\tau^-}^{\text{€}} < 0, X_{\tau^-}^{\text{£}} > 0\} + (S_{\tau^-}^{\text{€}\text{£}} - \Delta_{\tau^-}^{\text{€}\text{£}}/2) \mathbb{1}\{X_{\tau^-}^{\text{€}} > 0, X_{\tau^-}^{\text{£}} < 0\}. \end{aligned}$$

The hedging strategy is thus a collection of stopping times and currency pairs, i.e. $M : (\tau_\ell, y_\ell)_{\ell \geq 0}$, where $y_\ell \in \{\text{€}\text{£}, \text{£}\text{€}, \text{€}\text{€}\}$, for which it is optimal to submit a market order for that specific pair. Furthermore, every time the CLP posts a market order in the ECN, it is subject to a fixed penalty given by $\epsilon^y > 0$. We assume that $\epsilon^{\text{€}\text{£}} = \epsilon^{\text{£}\text{€}} < \epsilon^{\text{€}\text{€}}$.

The reasoning behind this last assumption is that hedging through cross pairs is typically more expensive and it is done only when reducing the risk of *both* inventories. This gives to other market participants more information on the CLP current inventories and such leakage comes with a cost. The impulse part can be rewritten, in matrix notation, as $\mathbf{X}_\tau = \mathbf{X}_{\tau^-} + m^y(\tau, \mathbf{X}_{\tau^-})$, where $m(\tau, \mathbf{X}_{\tau^-})$ is defined by

$$m(\tau, \mathbf{X}_u) =$$

$$\begin{bmatrix} m^{\text{€\$}}, m^{\text{£\$}}, m^{\text{€£}} \end{bmatrix} = \begin{bmatrix} 0 & 0 & 0 & 0 & -\left(S_{\tau^-}^{\text{€\$}} + \Delta_{\tau^-}^{\text{€\$}}/2\right) \mathbb{1}_{\{X_{\tau^-}^{\text{€€}} < 0\}} & 0 & +\left(S_{\tau^-}^{\text{€\$}} - \Delta_{\tau^-}^{\text{€\$}}/2\right) \mathbb{1}_{\{X_{\tau^-}^{\text{€€}} > 0\}} \\ 0 & 0 & 0 & 0 & 0 & \mathbb{1}_{\{X_{\tau^-}^{\text{££}} < 0\}} & -\left(S_{\tau^-}^{\text{£\$}} + \Delta_{\tau^-}^{\text{£\$}}/2\right) \mathbb{1}_{\{X_{\tau^-}^{\text{££}} < 0\}} \\ 0 & 0 & 0 & 0 & 0 & -\mathbb{1}_{\{X_{\tau^-}^{\text{££}} > 0\}} & +\left(S_{\tau^-}^{\text{£\$}} - \Delta_{\tau^-}^{\text{£\$}}/2\right) \mathbb{1}_{\{X_{\tau^-}^{\text{££}} > 0\}} \\ 0 & 0 & 0 & 0 & \mathbb{1}_{\{X_{\tau^-}^{\text{€€}} < 0, X_{\tau^-}^{\text{££}} > 0\}} & -\left(S_{\tau^-}^{\text{€£}} + \Delta_{\tau^-}^{\text{€£}}/2\right) \mathbb{1}_{\{X_{\tau^-}^{\text{€€}} < 0, X_{\tau^-}^{\text{££}} > 0\}} & 0 \\ 0 & 0 & 0 & 0 & -\mathbb{1}_{\{X_{\tau^-}^{\text{€€}} > 0, X_{\tau^-}^{\text{££}} < 0\}} & +\left(S_{\tau^-}^{\text{€£}} - \Delta_{\tau^-}^{\text{€£}}/2\right) \mathbb{1}_{\{X_{\tau^-}^{\text{€€}} > 0, X_{\tau^-}^{\text{££}} < 0\}} & 0 \end{bmatrix}'.$$

5.3.2 The value function

We here define the value function and the associated HJB equation, while in the next section we show the optimal strategy, which we obtain numerically. We define the value function by

$$\begin{aligned} V(t, \mathbf{x}) = \sup_{\alpha, \beta, M} \mathbb{E}_{t, \mathbf{x}} \left[X_T^{\text{€}} + X_T^{\text{£}} (S_T^{\text{€£}} - \hat{\alpha} X_T^{\text{€}}) + X_T^{\text{£}} (S_T^{\text{££}} - \hat{\alpha} X_T^{\text{£}}) \right. \\ \left. - \phi \int_t^T \left((X_u^{\text{€}})^2 + (X_u^{\text{£}})^2 \right) du - \sum_{y \in \{\text{€£}, \text{££}, \text{€£}\}} \sum_{t \leq \tau_i^y < T} \epsilon_i^y \right]. \end{aligned} \quad (5.14)$$

By making use of the same notation employed by Pham [74, 75] and Øksendal and Sulem [70], we can write the HJB equation as follows

$$\min \left\{ -\frac{1}{2} \text{tr}(\boldsymbol{\sigma} \boldsymbol{\sigma}' D_{\mathbf{x}}^2 V) - \sup_{\alpha, \beta} \sum_{\substack{i=\text{€}\$, \text{£}\$, \text{€}\text{£} \\ j=+, -}} \lambda_p^{j,i} \mathbb{E}^{(q^{j,i})} [V(t, \mathbf{x} + h^{j,i}) - V(t, \mathbf{x})] \right. \\ \left. \phi(x^{\text{€}})^2 + \phi(x^{\text{£}})^2; V(t, \mathbf{x}) - \sup_{y \in \{\text{€}\$, \text{£}\$, \text{€}\text{£}\}} \left(V(t, \mathbf{x} + \mathbf{m}(t, \mathbf{x})) - \epsilon^y \right) \right\} = 0, \quad (5.15)$$

where $D_{\mathbf{x}}^2 V$ denotes the Hessian matrix of the function V . In Equation (5.15) the part containing the impulse has to be interpreted as follows: if $\arg \max V(t, \mathbf{x} + \mathbf{m}(t, \mathbf{x})) - \epsilon^y = \text{€}\$$, the CLP crosses the spread by trading EURUSD in the ECN and the value function becomes $V(t, \mathbf{x} + \mathbf{m}^{\text{€}\$}(t, \mathbf{x})) - \epsilon^{\text{€}\$}$. The direction of such trade is chosen according to the sign of the EUR inventory (sell if the latter is positive and buy if it is negative). In financial terms, assuming that a hedging action is optimal, the CLP needs to decide which is the best currency to trade in the ECN by considering both: (i) risk reduction, and (ii) cost of trading.

5.3.3 Numerical results

Below we show the optimal strategy found by numerically solving the HJB in Equation (5.15). In Figure 5.7 we show the principal strategy employed by the CLP for the three currency pairs. In the left panels we show the strategy for $t = 0$, while in the right panels we have $t \rightarrow T$. We notice that the principal liquidity offered on the protect side is reduced as we approach the terminal time. The large proportion of cross liquidity offered (bottom-left panel) is due to the larger spread earned when trading the cross pair. Such increased reward is nonetheless offset by a doubly increased risk (starting from a neutral position). We further notice that the principal strategy is analogous to the one-currency-pair case. The new information provided by the current setting is given by the hedging strategy, which we plot in Figures 5.8 and 5.9. The numerical technique is analogous to the one described in Section 5.2.4.

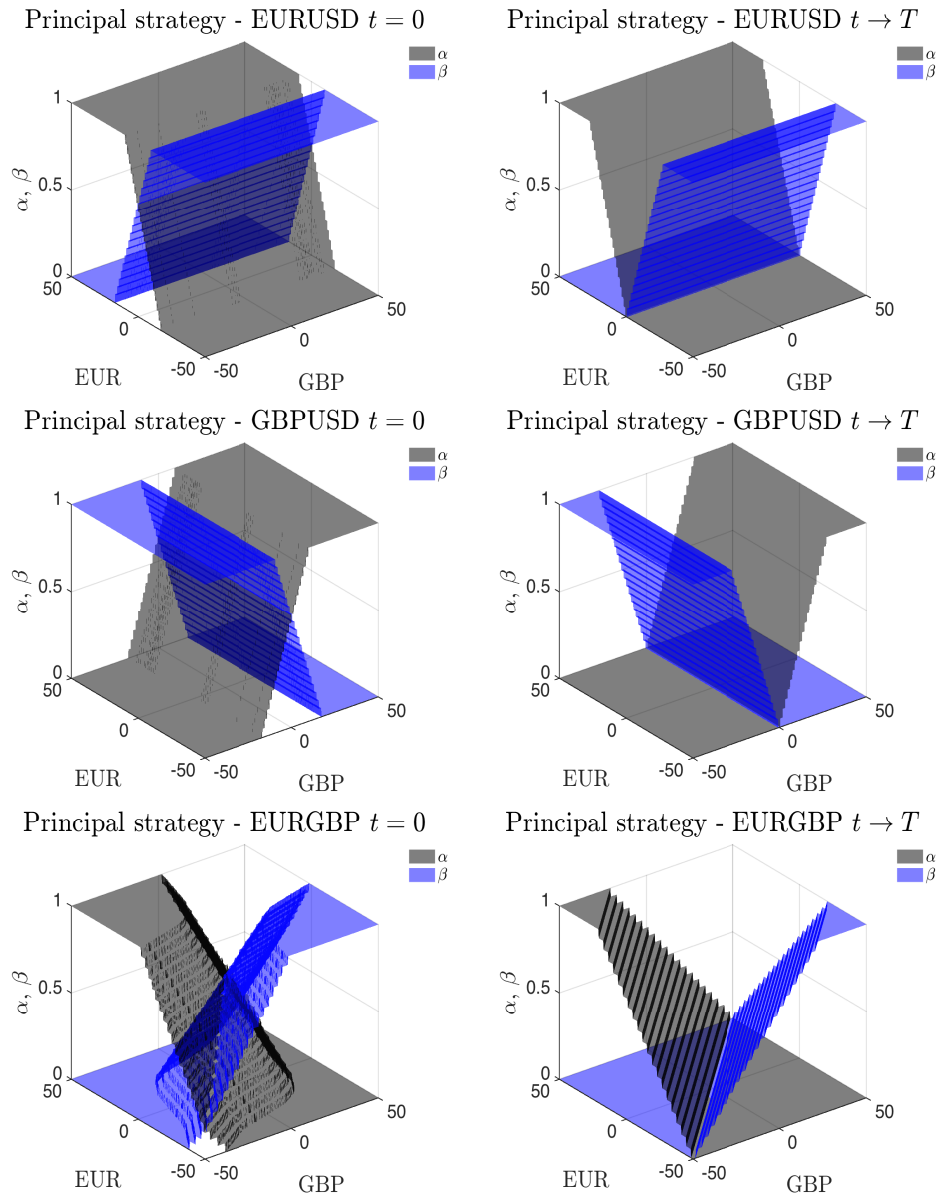


FIGURE 5.7: Optimal principal-liquidity strategy found by solving the HJB equation (5.15). We set $q^\pm \sim U[0, 20]$, $\eta = 25 \times 10^{-6}$, $\hat{\alpha} = 2$, $\phi = 0.05$, $\lambda^\pm = 0.5$, $\xi_1 = 0.5$, $\xi_2 = 0.5$ pips, $\xi_3 = 0.001$, $\epsilon^{\text{€}\$, \text{£}\$} = 5$, $\epsilon^{\text{€}\text{£}} = 10$, $\Delta^{\text{€}\$} = \Delta^{\text{£}\$} = 2$ pips, $\Delta^{\text{€}\text{£}} = 3$ pips.

In each of the twelve plots in Figures 5.8 and 5.9, the grey area defines the region of the plane (i.e. the EUR and GBP inventory levels) for which it is optimal to hedge through the pair specified in the figure. In Figure 5.8 we plot the hedging strategy for low values of the EURGBP spread. We notice that the cross-pair hedging regions are wider than the ones shown in Figure 5.9 (right, top and bottom panels). This reflects the tradeoff between the cost of the hedging strategy and the benefit of reducing both inventories at once.

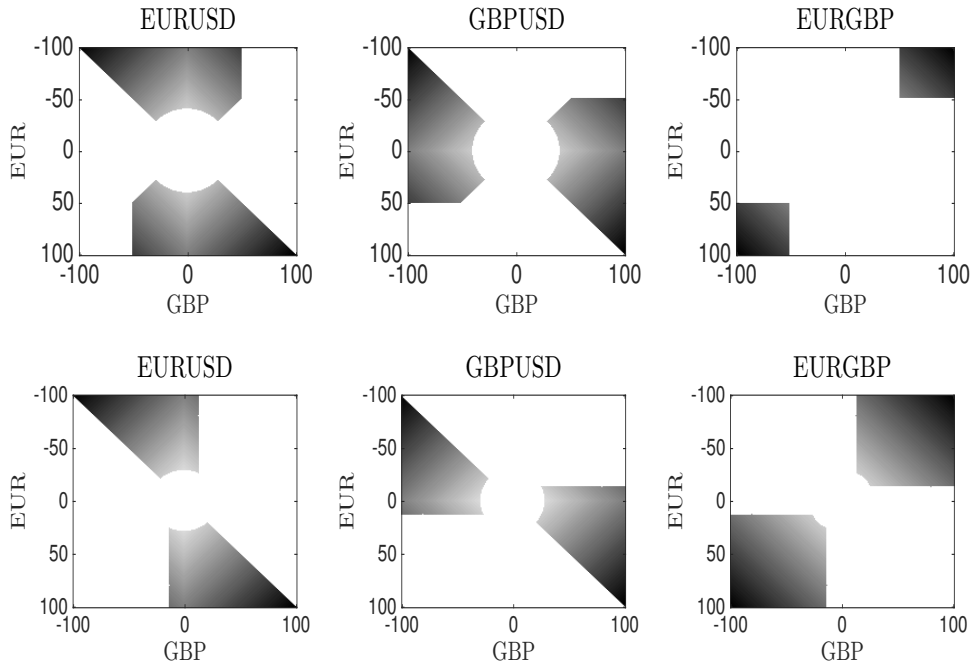
Hedging strategy - low $\Delta^{\text{€}\text{£}}$ 

FIGURE 5.8: Optimal hedging strategy found by solving the HJB equation (5.15).
Top panels: $t = 0$. Bottom panels: $t \rightarrow T$.

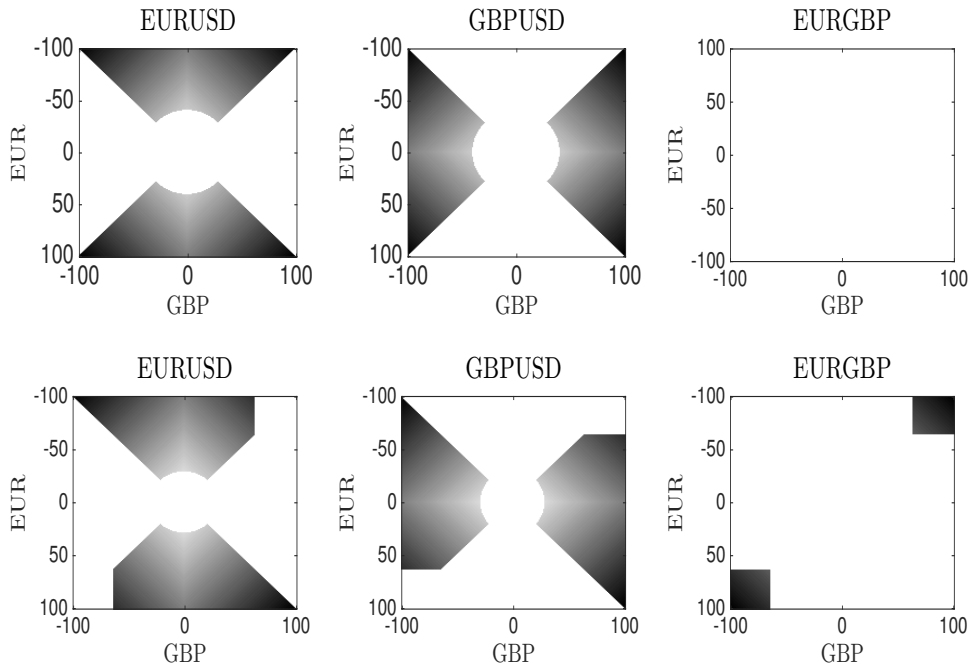
Hedging strategy - high $\Delta^{\text{€}\text{£}}$ 

FIGURE 5.9: Optimal hedging strategy found by solving the HJB equation (5.15).
Top panels: $t = 0$. Bottom panels: $t \rightarrow T$.

5.3.4 Price and inventory simulation

In Figure 5.10 we show the qualitative features of the CLP activity. In the top and bottom-left panels we plot the ECN and CLP prices.

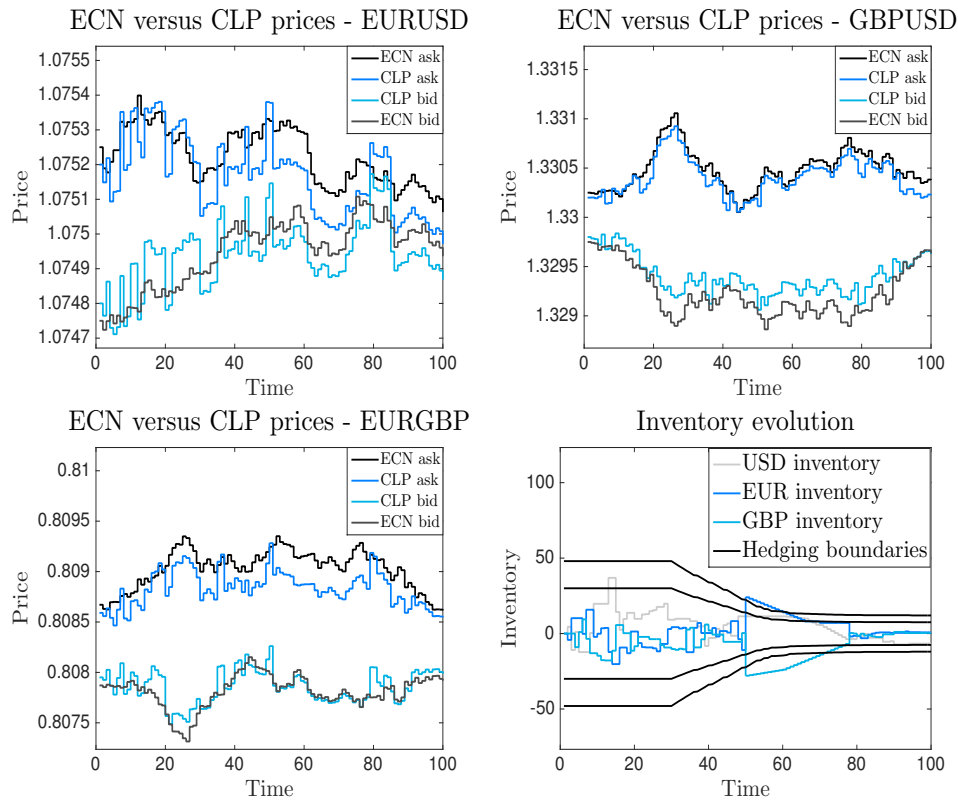


FIGURE 5.10: Price simulation (top panels and bottom-left panel) and inventory simulation (bottom-right panel).

In the bottom-right panel we plot the EUR, GBP and USD inventories and superimpose the direct and cross-pair mean hedging boundaries. Such boundaries have to be interpreted as follows. If the interior boundaries are surpassed by either the EUR or GBP inventories, then the CLP starts hedging via EURUSD or GBPUSD, respectively. The only exception to the above occurs when the exterior boundaries are surpassed by both the EUR and GBP inventories, and they do so in opposite directions. For example, if the upper exterior boundary is surpassed by the EUR inventory while the lower exterior boundary is surpassed by the GBP inventory, then the CLP is long EURGBP and it is optimal to hedge in the ECN by selling EURGBP. The opposite holds when the CLP is severely short EURGBP, i.e. the upper exterior boundary is surpassed by the GBP inventory and the lower exterior boundary is surpassed by the EUR inventory. In

the latter case, the CLP should hedge by buying EURGBP. In the simulation provided in Figure 5.10, such an occurrence happens at around time $t = 50$, when the CLP is long EURGBP. We can further notice that, around the same time, the prices offered by the CLP to its clients are set according to its position. In the top-left panel, the prices are skewed down due to the CLP being long EUR. In the top-right panel the prices are skewed up due to the CLP being short GBP. Finally, in the bottom-left panel, the prices are skewed down so to encourage buyers of EURGBP.

5.4 Conclusions

In this chapter we study the activity of a CLP which offers a joint service of principal and agency trading to its clients by streaming tailored two-way prices and by executing orders while preserving the counterparty's anonymity. The CLP earns a commission from the brokerage service while a spread is earned through principal trading. During the activity the CLP is subject to an inventory risk which is mitigated by skewing its prices, as well as by crossing the spread in the 'lit' market. We focus on the foreign exchange market and we consider both one-currency-pair and three-currency-pair cases.

When only one currency pair is traded, and thus we have fewer state variables to model, we can study the effects of mean-reversion and permanent price impact. If the FX rate mean reverts, the principal liquidity offered depends on where the current price is in its mean-reversion cycle. For example, when the FX rate is below its long-term mean, more principal liquidity should be offered to sellers. We further analyse the effect of the permanent price impact when trading in the ECN and show that for a neutral position, the CLP should offer more principal liquidity when the price impact is high. The financial interpretation of such a feature is that the CLP tries to avoid unfavourably impacting the market price at which it may need to hedge its new position in the case it fails to internalise the received flow.

Finally we present the case where three currency pairs are available for trading and gain insights on the hedging strategy the CLP should offer. We assume

that the cross pair is less liquid and thus a higher spread (compared to direct pairs) is earned when trading with clients. Such benefit is nevertheless offset by a higher risk accepted by the CLP (we are referring to the cases of: (i) a neutral position held by the CLP, and (ii) short—or long—positions are held by the CLP in both direct pairs). With regards to the hedging strategy, the CLP refrains from hedging through the cross pair unless the benefit of doing so, i.e. the simultaneous reduction of both inventories, counterbalances the higher spread paid in the ECN.

Chapter 6

Final conclusions

6.1 Summary of main results and contributions

In the present work we go through some of the typical situations that agents and firms face when trading in electronic markets. Nowadays most venues have limit order books and market participants trade among each other in a supply and demand setting. Various considerations should be made before trading. In particular we refer to present market conditions, terminal goal, market impact, et cetera.

Today more than ever, and especially in high-speed markets, such considerations need to be made in advance by planning for potential future scenarios and by constructing algorithms which take the current market situation as an input and output the best strategy. Real-time market data are in fact processed by high powered machines which then take trading decisions accordingly.

In a nutshell, we propose models that can be used when trading in electronic markets. It is worth emphasising that they can be applied to many distinct situations. For example, nothing prevents us from taking the optimal execution model presented in Chapter 3 and integrating it in the model shown in Chapter 4, thus solving an optimal liquidation problem every time the CLP starts its hedging procedures.

In this work we answer various questions:

1. How shall an agent execute a large trade in an order-driven market?
2. What changes when the agent can simultaneously trade in a dark pool?
3. How shall a firm, which provides liquidity to clients, set its prices and hedge its position?
4. How shall a firm choose the ratio of principal versus agency liquidity when providing a hybrid execution service within the FX market?

The first two questions have been addressed elsewhere, too. We contribute to the current literature by adding and explaining important financial features to the governing system of SDEs (e.g. permanent price impact when trading in the standard exchange). As such, when trading in a less liquid market, our model should provide a more accurate approximation of the optimal strategy compared to models in which the price is assumed to be a martingale and the permanent price impact is neglected. Questions 3 and 4 are a novelty in the literature. While market-making problems have been extensively studied, the specific behaviour of firms trading with clients in a protected pool and hedging in an order-driven market have not. The mathematics applied therein is analogous to the ones used to solve standard market-making problems à la Cartea et al. [23]. However the contribution of the present work lies in the development of financial models which (i) allow for transparent interpretations, and (ii) to a great extent are ready for applications in the financial industry.

There are various financial features that come into play in both the optimal-liquidation and the optimal market-making problems. First, there is the risk caused by uncertain future price movements. On the other hand, liquidating the position faster has two main drawbacks: (i) price impact, and (ii) adverse selection. We do not treat the latter in this thesis, but we mention it in Section 6.2 when giving directions for possible future work. The optimal strategy depends on the trade-off between exploiting market opportunities (as in the case of mean reversion) while trying to minimise unfavourable market disruption, such as price slippage.

The shape of the optimal policy is determined, among other things, by the risk appetite of the agents or firms. We find that a strongly risk-averse player

should always choose early execution, whether this is in the form of liquidation or hedging. On the other hand, slightly more risk-prone agents are willing to bear price and time uncertainty in the hope to achieve a better final outcome. As we show in Chapter 4, Section 4.3.3, the market maker faces a trade-off between accepting a higher risk (measured via the variance of the performance) in favour of higher expected returns. Unfortunately risk preferences, which are agent-specific, are difficult to quantify and estimate, especially when they are also subject to legal and compliance requirements.

6.2 Future work

There is a number of directions that future research on these topics may take. For example, it would be appropriate to include some adverse-selection measure in our models. The main idea behind adverse-selection within this context can be illustrated as follows. Assume that a limit sell order is executed. This implies a potential increase in the best ask price, which would make the posting agent regret their trading decision as now the price has moved in what would have been their favour. Such a feature could be included in the context of a firm hedging its inventory in the ‘lit’ pool.

Another modification which could be done to the hedging strategy of the firm would be to consider a model à la optimal-liquidation framework to be integrated in the optimal market-making setting. As of now, in the models presented in Chapters 4 and 5, the firm may only hedge one unit or one lot at any given time, through an impulse in the model. It would be interesting to have, at each time the firm enters in a position which requires hedging, a liquidation schedule based on more sophisticated models, rather than the current setting, which can be assimilated to the constant-liquidation-rate strategy.

When it comes to FX e-trading, the future directions the research may take are many. We here mention the two which we believe would have the greatest impact in both academic research and industry practice. First, it is worth extending the framework treated in Chapter 6 to N currency pairs, including the synthetic ones. When we refer to *synthetic* currency pairs, we indicate those pairs for which

there is no quoted price in the ECN. An example of such pairs is TRYDKK. There is no price for Turkish lira and Danish krone, while there are quoted prices for USDTRY and EURDKK and, of course, EURUSD. The TRYDKK pair can not be traded directly in the ECN. Nevertheless one can, for example, buy USDTRY, sell EURDKK and buy EURUSD in order to sell TRYDKK. A client may occasionally want to see such a pair directly quoted by the firm, without having to work through multiple transactions. On the firm's side, this would require an algorithm which aggregates the information available on pairs directly traded in the ECN and outputs a reasonable spread for such a synthetic pair, further considering its potential hedging needs.

Another interesting extension we consider includes the modelling of multiple competing firms which offer liquidity within the same pool of clients and try to win the business. Typically, clients have their own algorithms which aggregate the various sources of liquidity and trade with the most convenient one at every point in time. A reasonable assumption is that every firm has access to the same pool of ECNs and thus starts with the same information set. Analysing the competition among liquidity providers requires assumptions on the pricing mechanisms of multiple firms and some ambiguity measure to take into account the potential errors in the modelling assumptions. This would answer questions like: Assuming a client is allowed to trade with multiple firms sequentially, which price should be offered so that our firm is on top of the queue, while still making the trade profitable? How would the hedging strategy change, given that other firms may be hedging at the same time in the same direction? Would trading within firms (for hedging purposes, as opposed to cross the spread in the ECN) be preferable?

These are the types of projects which are being pursued in ongoing research.

Chapter 7

Viscosity solutions and numerical procedures

The objectives of this chapter are as follows:

1. We state—as a reference—the DPP for a mixed optimal stochastic and impulse-control problem;
2. We show that the value functions resulting from the models presented in this thesis are the unique viscosity solutions of the associated HJB equations;
3. We provide a description of the numerical schemes used to obtain the results shown in Chapters 3 and 4. The numerical scheme used in Chapter 5 is analogous to the one used in Chapter 4.

The proofs detailed in this chapter are based on already existing mathematical results and therefore, although they are adapted to the specific models presented in this thesis, we do not wish to include them in the original work presented herein. We refer to Shreve [78, 79] and Steele [82] for an introductory overview on stochastic calculus, which is the main mathematical tool used throughout this thesis.

7.1 Background material

7.1.1 Dynamic programming and HJB equation

We intentionally keep the tone of this section general, so to accommodate the various cases presented in Chapters 3, 4 and 5. In particular, we state the DPP for a mixed optimal stochastic and impulse-control problem. Let us assume we have a well-defined \mathbb{R}^n -valued process, starting at a value $\mathbf{x} \in \mathbb{R}^n$,

$$d\mathbf{X}_u = \mathbf{b}(u, \mathbf{X}_u, \mathbf{v}_u)du + \boldsymbol{\sigma}(u, \mathbf{X}_u, \mathbf{v}_u)d\mathbf{B}_u + \boldsymbol{\gamma}(u, \mathbf{X}_{u-}, \mathbf{v}_u)d\mathbf{J}_u \quad (7.1)$$

that has a unique and strong solution, and where $\{\mathbf{v}_u\}$ is valued in the set \mathcal{U} of admissible processes. We let $\mathbf{b} : [0, T] \times \mathbb{R}^n \rightarrow \mathbb{R}^n$, $\boldsymbol{\sigma} : [0, T] \times \mathbb{R}^n \rightarrow \mathbb{R}^{n \times m}$, $\boldsymbol{\gamma} : [0, T] \times \mathbb{R}^n \times \mathbb{R}^\ell \rightarrow \mathbb{R}^{n \times \ell}$. The process $\{\mathbf{B}_u\}$ is an m -dimensional Brownian motion and \mathbf{J}_u is an ℓ -dimensional compound Poisson process. The components of such multidimensional processes are assumed to be independent. Furthermore, let us consider a continuous time Markov chain \mathbf{k} , with discrete state space \mathbb{K} , generated by $\{Q\} = (r_{ij})$.

Discrete impulses can take place at a cost $\Phi(u, \mathbf{x}, \zeta)$ to shift the process to a new value $\Psi(u, \mathbf{x}, \mathbf{k}, \zeta)$, where $\zeta \in \Upsilon$ is the action decision. That is, if at time τ an impulse takes place, we have

$$\mathbf{X}_\tau = \Psi(\tau, \mathbf{X}_{\tau-}, \mathbf{k}_{\tau-}, \zeta_\tau) = \mathbf{X}_{\tau-} + \bar{\Psi}(\tau, \mathbf{k}_{\tau-}, \zeta_\tau). \quad (7.2)$$

Remark 7.1. Following the notation in Davis et al. [33], we wish to mention that Equations (7.1) and (7.2) can be compactly written by

$$d\mathbf{X}_u = \mathbf{b}(u, \mathbf{X}_u, \mathbf{v}_u)du + \boldsymbol{\sigma}(u, \mathbf{X}_u, \mathbf{v}_u)d\mathbf{B}_u + \boldsymbol{\gamma}(u, \mathbf{X}_{u-}, \mathbf{v}_u)d\mathbf{J}_u + \sum_i \delta(u - \tau_i) \bar{\Psi}(\tau_i, \mathbf{k}_{\tau_i-}, \zeta_{\tau_i}), \quad (7.3)$$

where $\delta(\cdot)$ denotes the Dirac delta function. A third alternative is to follow the notation employed by Horst and Naujokat [52], who define a non-decreasing counting càdlàg process M_u and write the state-variable dynamics by

$$\begin{aligned} d\mathbf{X}_u = & \mathbf{b}(u, \mathbf{X}_u, \mathbf{v}_u)du + \boldsymbol{\sigma}(u, \mathbf{X}_u, \mathbf{v}_u)d\mathbf{B}_u + \boldsymbol{\gamma}(u, \mathbf{X}_{u-}, \mathbf{v}_u)d\mathbf{J}_u \\ & + \bar{\Psi}(u, \mathbf{k}_{u-}, \zeta_u)dM_u, \end{aligned} \quad (7.4)$$

where the process $\{M_u\}$ jumps every time the agent gives an impulse to the system. The three dynamics mentioned allow for an impulse of size $\bar{\Psi}(\tau_i, \mathbf{k}_{\tau_i-}, \zeta_{\tau_i})$ to take place at the discretion of the agent and thus have the same meaning. Throughout the present work we prefer to adopt the non-compact notation, i.e. Equations (7.1) and (7.2), in line with most of the literature relevant to this thesis (e.g. Seydel [77] and Cartea et al. [23] and the references therein).

The value function is defined by

$$\begin{aligned} V(t, \mathbf{x}; \mathbf{k}) = & \sup_{\{\mathbf{v}_u\}_{t \leq u \leq \hat{T}, (\tau_i, \xi_i)_{i \geq 0}}} \mathbb{E}_{t, \mathbf{x}, \mathbf{k}} \left[\int_t^{\hat{T}} \vartheta(u, \mathbf{X}_u, \mathbf{v}_u)du + \varrho(\mathbf{X}_{\hat{T}}, \mathbf{k}_{\hat{T}}) \right. \\ & \left. - \sum_{\tau_i \in [t, \hat{T})} \Phi(\tau_i, \mathbf{X}_{\tau_i-}, \zeta_i) \right], \end{aligned} \quad (7.5)$$

where $\hat{T} := \inf(u < t | \mathbf{x} \notin \mathcal{O}) \wedge T$, where $\mathcal{O} \subseteq \mathbb{R}^n$ is the domain of the state variable \mathbf{X}_u . The above is a stochastic/impulse control problem for controlled jump diffusions with regime switching (given by the Markov chain \mathbf{k}). In absence of impulses, let $\boldsymbol{\nu}^*$ denote the optimal control. For $\theta \in [t, T]$, we define the control $\hat{\boldsymbol{\nu}}_u$ by

$$\hat{\boldsymbol{\nu}}_u := \begin{cases} \boldsymbol{\nu}_u, & u \in [t, \theta] \\ \boldsymbol{\nu}_u^*, & \text{otherwise.} \end{cases}$$

We can let τ_r be the first time the regime switches from its initial state. For all $\theta \leq \tau_r$ we can rewrite the value function by

$$\begin{aligned}
V(t, \mathbf{x}; \mathbf{k}) &= \sup_{\{\mathbf{v}_u\}_{t \leq u \leq \theta}} \mathbb{E}_{t, \mathbf{x}, \mathbf{k}} \left[\int_t^\theta \vartheta(u, \mathbf{X}_u, \mathbf{v}_u) du + \int_\theta^{\hat{T}} \vartheta(u, \mathbf{X}_u, \mathbf{v}_u^*) du \right. \\
&\quad \left. + \varrho(\mathbf{X}_{\hat{T}}, \mathbf{k}_{\hat{T}}) \right], \\
&= \sup_{\{\mathbf{v}_u\}_{t \leq u \leq \theta}} \mathbb{E}_{t, \mathbf{x}, \mathbf{k}} \left[\int_t^\theta \vartheta(u, \mathbf{X}_u, \mathbf{v}_u) du + \mathbb{E}_{\theta, \mathbf{X}_\theta, \mathbf{k}_\theta} \left[\int_\theta^{\hat{T}} \vartheta(u, \mathbf{X}_u, \mathbf{v}_u^*) du \right. \right. \\
&\quad \left. \left. + \varrho(\mathbf{X}_{\hat{T}}, \mathbf{k}_{\hat{T}}) \right] \right], \\
&= \sup_{\{\mathbf{v}_u\}_{t \leq u \leq \theta}} \mathbb{E}_{t, \mathbf{x}, \mathbf{k}} \left[\int_t^\theta \vartheta(u, \mathbf{X}_u, \mathbf{v}_u) du + V(\theta, \mathbf{X}_\theta; \mathbf{k}_\theta) \right], \\
&= V(t, \mathbf{x}; \mathbf{k}) + \sup_{\{\mathbf{v}_u\}_{t \leq u \leq \theta}} \mathbb{E}_{t, \mathbf{x}} \left[\int_t^\theta \vartheta(u, \mathbf{X}_u, \mathbf{v}_u) + \left(\frac{\partial}{\partial t} + \mathcal{L} \right) V(u, \mathbf{X}_u; \mathbf{k}_u) du \right],
\end{aligned}$$

where the last inequality comes from an application of Dynkin's formula to the function V and \mathcal{L} is the infinitesimal generator of the processes $\{\mathbf{X}_u, \mathbf{k}_u\}$, given by

$$\begin{aligned}
\mathcal{L}V(t, \mathbf{x}; \mathbf{k}) &= \sum_{i=1}^n (b)^i \frac{\partial V}{\partial x_i} + \frac{1}{2} \sum_{i=1}^n \sum_{j=1}^n (\sigma \sigma^T)^{ij} \frac{\partial^2 V}{\partial x_i \partial x_j} \\
&\quad + \sum_{\mathbf{k}' \neq \mathbf{k}} r_{\mathbf{k}\mathbf{k}'} \left[V(t, \mathbf{x}; \mathbf{k}') - V(t, \mathbf{x}; \mathbf{k}) \right]; \\
&\quad + \sum_{i=1}^{\ell} \lambda^i \mathbb{E} [V(t, \mathbf{x} + (\gamma)^i z_i; \mathbf{k}) - V(t, \mathbf{x}; \mathbf{k})],
\end{aligned}$$

where $(b)^i$ is the i -th component of the vector \mathbf{b} in Equation (7.1), $(\sigma \sigma^T)^{ij}$ is the entry on the i -th row and j -th column in the matrix $\sigma \sigma^T$ and $(\gamma)^i$ is the i -th column of the matrix γ . By letting $\theta = t + h \wedge \tau_r$, dividing by h and letting $h \rightarrow 0$ we obtain

$$\sup_{\mathbf{v}} \left\{ \vartheta(t, \mathbf{x}, \mathbf{v}) + \left(\frac{\partial}{\partial t} + \mathcal{L} \right) V(t, \mathbf{x}; \mathbf{k}) \right\} = 0. \quad (7.6)$$

If a discount factor is present, we have

$$\begin{aligned}
V(t, \mathbf{x}; \mathbf{k}) &= \sup_{\{\mathbf{v}_u\}_{t \leq u \leq \theta}} \mathbb{E}_{t, \mathbf{x}, \mathbf{k}} \left[\int_t^\theta e^{-r(u-t)} \vartheta(u, \mathbf{X}_u, \mathbf{v}_u) du + e^{-r(\theta-t)} V(\theta, \mathbf{X}_\theta; \mathbf{k}_\theta) \right], \\
&= V(t, \mathbf{x}; \mathbf{k}) \\
&+ \sup_{\{\mathbf{v}_u\}_{t \leq u \leq \theta}} \mathbb{E}_{t, \mathbf{x}, \mathbf{k}} \left[\int_t^\theta e^{-r(u-t)} \left(\vartheta(u, \mathbf{X}_u, \mathbf{v}_u) + \left(\frac{\partial}{\partial t} - r + \mathcal{L} \right) V(u, \mathbf{X}_u; \mathbf{k}_u) \right) du \right],
\end{aligned}$$

By letting $\theta = t + h \wedge \tau_r$, dividing by h and letting $h \rightarrow 0$ we obtain

$$\sup_{\mathbf{v}} \left\{ \vartheta(t, \mathbf{x}, \mathbf{v}) + \left(\frac{\partial}{\partial t} - r + \mathcal{L} \right) V(t, \mathbf{x}; \mathbf{k}) \right\} = 0. \quad (7.7)$$

When we add the possibility of having impulses, we follow the same approach but with $\theta = t + h \wedge \tau_r \wedge \tau_1$, where τ_1 is the first time an impulse takes place. When we let $h \rightarrow 0$ we face two distinct possibilities: (i) $\tau_1 > t$, and (ii) $\tau_1 = t$. If $\tau_1 > t$, then (7.6) holds. If, on the other hand, $\tau_1 = t$, the value function is subject to the following impulse

$$\mathcal{M}V(t, \mathbf{x}; \mathbf{k}) = \sup_{\zeta \in \Upsilon} V(t, \Psi(t, \mathbf{x}, \mathbf{k}, \zeta); \mathbf{k}) - \Phi(t, \mathbf{x}, \zeta).$$

We can thus conclude that $V(t, \mathbf{x}; \mathbf{k})$ satisfies the following system of quasi variational inequalities (QVI)

$$\begin{cases} \min \left\{ -\frac{\partial V}{\partial t} - \sup_{\mathbf{v}} \{ \mathcal{L}V(t, \mathbf{x}; \mathbf{k}) + \vartheta(t, \mathbf{x}, \mathbf{v}) \}; V(t, \mathbf{x}; \mathbf{k}) - \mathcal{M}V(t, \mathbf{x}; \mathbf{k}) \right\} = 0 \\ \hspace{15em} \text{on } [t, T) \times \mathcal{O} \\ V(t, \mathbf{x}; \mathbf{k}) = \varrho(\mathbf{x}, \mathbf{k}) \quad \text{on } T \times \partial\mathcal{O}. \end{cases} \quad (7.8)$$

Remark 7.2. A QVI is referred as to an inequality since, on $[t, T) \times \mathcal{O} \times \mathbb{K}$, Equation (7.8) is a compact version of the three following conditions, which shall

hold simultaneously:

$$\begin{cases} -\frac{\partial V}{\partial t} - \sup_v \{\mathcal{L}V(t, \mathbf{x}; \mathbf{k}) + \vartheta(t, \mathbf{x}, \mathbf{v})\} \geq 0, \\ V(t, \mathbf{x}; \mathbf{k}) - \mathcal{M}V(t, \mathbf{x}; \mathbf{k}) \geq 0, \\ \left(-\frac{\partial V}{\partial t} - \sup_v \{\mathcal{L}V(t, \mathbf{x}; \mathbf{k}) + \vartheta(t, \mathbf{x}, \mathbf{v})\} \right) \left(V(t, \mathbf{x}; \mathbf{k}) - \mathcal{M}V(t, \mathbf{x}; \mathbf{k}) \right) = 0. \end{cases}$$

Equation (7.8) is meaningful only if the function $V(t, \mathbf{x}; \mathbf{k})$ is sufficiently smooth, but this does not need to be the case. We thus make use of the weaker notion of viscosity solutions, which do not require the smoothness of the value function, so to ensure the convergence of the numerical scheme. In fact, convergence results for numerical schemes have been proved starting from the characterisation of the value function by the unique viscosity solution to the associated dynamic programming equation (see, e.g., Fleming and Soner [37]). Loosely speaking, Barles and Souganidis [6] prove that, provided a comparison result is proved for a viscosity solution, any monotone, stable and consistent numerical scheme converges to the correct solution.

7.1.2 Viscosity solutions

Viscosity solution theory is a powerful tool when it comes to HJB equations, since proving the regularity and smoothness of the value function may not be an easy task. Viscosity solutions are defined for both continuous and discontinuous functions, depending on whether the continuity of the value function wants to be shown as a separate result, or it comes as a byproduct of the strong comparison result which guarantees uniqueness of the viscosity solution. For the sake of generality, we here report the definitions of viscosity solution for discontinuous functions. First, for each \mathbf{k} , we need to define the lower and the upper semi-continuous envelopes (l.s.c. and u.s.c. envelopes, respectively) of the function $V(t, \mathbf{x}; \mathbf{k})$, given by

$$V^*(t, \mathbf{x}; \mathbf{k}) = \limsup_{t' \rightarrow t, \mathbf{x}' \rightarrow \mathbf{x}} V(t', \mathbf{x}'; \mathbf{k}), \quad V_*(t, \mathbf{x}; \mathbf{k}) = \liminf_{t' \rightarrow t, \mathbf{x}' \rightarrow \mathbf{x}} V(t', \mathbf{x}'; \mathbf{k}).$$

$$W^* \leq V_* \quad \text{and} \quad V^* \leq W_*.$$

Since, by construction, we already have that $W_* \leq W^*$ and $V_* \leq V^*$, we have the following equality

$$W_* = W^* = V_* = V^*.$$

As a byproduct, we obtain the continuity of the value function, since a function that is both u.s.c. and l.s.c. is continuous.

7.2 Reconciliation of notation

In this section we show that the models in Chapters 2, 3, and 4 are special cases of Equations (7.1) and (7.5). Therefore, the derivation of HJB (7.8) applies to the models presented in the main body of the thesis¹. The notation is kept consistent with the relevant sections of the thesis.

7.2.1 Chapter 2

In Chapter 2 we consider: (i) optimal liquidation, and (ii) optimal market-making problems. While the former has no impulse, the latter has some. We here aim to show that all such models are special cases of the general model described in Section 7.1. We note that we don't have any Markov chain in Chapter 2, hence we drop the dependence on \mathbf{k} .

7.2.1.1 Optimal liquidation

We here look at the models described in Sections 2.2.1.1 and 2.3.1.1.

¹We do not include Chapter 5 since its notation is already in line with Equations (7.1) and (7.5) and therefore it is straightforward to see that it is a special case.

1. Section 2.2.1.1;

The controlled process \mathbf{X}_u in (7.1) is here given by setting $\mathbf{X}_u = (X_u, S_u^b)$, where $\boldsymbol{\gamma} \equiv 0$, $\mathbf{b} = [-\nu_u, -\mu\nu_u]'$, $\boldsymbol{\sigma} = [0, \sigma]'$, $\mathbf{B}_u = [W_u]$ and $\mathbf{J}_u = 0$.

The value function in Equation (7.5) is here given by setting $\vartheta(u, \mathbf{x}, \boldsymbol{\nu}) = \hat{s}^b \nu - \phi x^2$ and $\varrho(\mathbf{x}) = (s^b - \alpha x)x$.

2. Section 2.3.1.1;

The controlled process \mathbf{X}_u in (7.1) is here given by setting $\mathbf{X}_u = (X_u, Y_u, S_u)$, where $\boldsymbol{\gamma} = [-\eta_u, \eta_u S_u, 0]'$, $\mathbf{b} = [-\nu_u, \nu_u \hat{S}_u, 0]'$, $\boldsymbol{\sigma} = [0, 0, \sigma]'$, $\mathbf{B}_u = [W_u]$, and $\mathbf{J}_u = [N_u]$. Furthermore, the jumps here are assumed to be one-sized, hence the compound Poisson process (\mathbf{J}_u) is a simple Poisson process (N_u).

The value function in Equation (7.5) is here given by setting $\vartheta(u, \mathbf{x}, \boldsymbol{\nu}) = -\phi x^2$ and $\varrho(\mathbf{x}) = y + (s - \alpha x)x$.

7.2.1.2 Optimal market making

We here look at the models described in Sections 2.2.2.1 and 2.3.2.1.

1. Section 2.2.2.1;

The controlled process \mathbf{X}_u in (7.1) is here given by setting $\mathbf{X}_u = (X_u, Y_u, S_u)$, where $\mathbf{b} \equiv 0$ and $\boldsymbol{\sigma} = [0, 0, \sigma]'$, $\mathbf{B}_u = [W_u]$, $\mathbf{J}_u = [N_u^-, N_u^+]'$ and

$$\boldsymbol{\gamma} = \begin{bmatrix} 1 & -1 \\ -S_u + k & S_u + k \\ 0 & 0 \end{bmatrix}.$$

For the impulse part, we have $\Phi(u, \mathbf{x}, \zeta) = \epsilon$ and $\Psi(u, \mathbf{x}, \zeta) = [x + \zeta, y - \zeta(s + k\zeta), 0]'$.

The value function in Equation (7.5) is here given by setting $\vartheta(u, \mathbf{x}, \boldsymbol{\nu}) = -\phi x^2$ and $\varrho(\mathbf{x}) = y + (s^b - \alpha x)x$.

2. Section 2.3.2.1;

The controlled process \mathbf{X}_u in (7.1) is here given by setting $\mathbf{X}_u = (X_u, Y_u, S_u)$, where $\mathbf{b} \equiv 0$ and $\boldsymbol{\sigma} = [0, 0, \sigma]'$, $\mathbf{B}_u = [W_u]$, $\mathbf{J}_u = [N_u^-, N_u^+]'$ and

$$\gamma = \begin{bmatrix} 1 & -1 \\ -S_u + k & S_u + k \\ 0 & 0 \end{bmatrix}.$$

For the impulse part, we have $\Phi(u, \mathbf{x}, \zeta) = \epsilon^m \mathbb{1}_{\{if\ market\}} + \epsilon^\ell \mathbb{1}_{\{if\ limit\}}$ and $\Psi(u, \mathbf{x}, \zeta) = [x + \zeta, y - \zeta(s + k\zeta), 0]' \mathbb{1}_{\{if\ market\}} + [x + \zeta z, y - \zeta(s - k\zeta)z, 0]' \mathbb{1}_{\{if\ limit\}}$.

The value function in Equation (7.5) is here given by setting $\vartheta(u, \mathbf{x}, \boldsymbol{\nu}) = -\phi x^2$ and $\varrho(\mathbf{x}) = y + (s^b - \alpha x)x$.

7.2.2 Chapter 3

In Chapter 3 we discuss two general models for optimal liquidation. The first one—Section 3.2—treats optimal liquidation when only the ‘lit’ pool is available to the agent. The second one—Section 3.3—treats optimal liquidation when both ‘lit’ and dark pools are available to the agent. We here show that both models are special cases of the general model described in Section 7.1. We note that we don’t have any Markov chain in Chapter 3, hence we drop the dependence on \mathbf{k} .

Section 3.2;

The controlled process \mathbf{X}_u in (7.1) is here given by setting $\mathbf{X}_u = (X_u, S_u^b, Y_u)$, where $\mathbf{b} = [-\nu_u, \mu^b(u, S_u^b, \nu_u) - \sum_{i=1}^2 \lambda^{b,i} u \mathbb{E}[z^{b,i}], \mu^y(u, S_u^b, \nu_u)]'$, $\mathbf{B}_u = 0$,

$$\gamma = \begin{bmatrix} 0 & 0 \\ h_1^b(u, S_u^b) & h_2^b(u, S_u^b) \\ 0 & 0 \end{bmatrix}.$$

$\boldsymbol{\sigma} \equiv 0$, and $\mathbf{J}_u = [J_u^{b,1}, J_u^{b,2}]'$.

The value function in Equation (7.5) is here given by setting $\vartheta(u, \mathbf{x}, \boldsymbol{\nu}) = f(u, \mathbf{x}, \nu)$ and $\varrho(\mathbf{x}) = g(\mathbf{x})$.

Section 3.3;

The controlled process \mathbf{X}_u in (7.1) is here given by setting $\mathbf{X}_u = (X_u, S_u^b, \Delta_u, Y_u)$, where $\mathbf{B}_u = 0$, $\boldsymbol{\sigma} \equiv 0$, $\mathbf{J}_u = [J_u^{b,1}, J_u^{b,2}, J_u^{\Delta,1}, J_u^{\Delta,2}, J_u^y]$, and

$$\mathbf{b} = \begin{bmatrix} -\nu_u, \mu^b(u, S_u^b, \nu_u) - \sum_{i=1}^2 \lambda^{b,i} u \mathbb{E}[z^{b,i}], \\ \mu^\Delta(u, \Delta_u, \nu_u) - \sum_{i=1}^2 \lambda^{b,i} u \mathbb{E}[z^{b,i}] - \sum_{i=1}^2 \lambda^{\Delta,i} u \mathbb{E}[z^{\Delta,i}], \mu^y(u, S_u^b, \nu_u) \end{bmatrix}'$$

$$\boldsymbol{\gamma} = \begin{bmatrix} 0 & 0 & 0 & 0 & -\eta_u \\ h_1^b(u, S_u^b) & h_2^b(u, S_u^b) & 0 & 0 & 0 \\ h_1^{b,\Delta}(u, S_u^b, \Delta_u) & h_2^{b,\Delta}(u, S_u^b, \Delta_u) & h_1^\Delta(u, \Delta_u) & h_2^\Delta(u, \Delta_u) & 0 \\ 0 & 0 & 0 & 0 & h^y(u, S_u^b, \Delta_u, \eta_u) \end{bmatrix}.$$

The value function in Equation (7.5) is here given by setting $\vartheta(u, \mathbf{x}, \boldsymbol{\nu}) = f_1(u, \mathbf{x}, \boldsymbol{\nu})$ and $\varrho(\mathbf{x}) = g_1(\mathbf{x})$.

7.2.3 Chapter 4

In Chapter 4 we outline one general model in Section 4.2. We here show that such a model is a special case of the general model described in Section 7.1.

The controlled process \mathbf{X}_u in (7.1) is here given by setting $\mathbf{X}_u = (X_u, Y_u, S_u)$, where $\mathbf{b} \equiv 0$, $\mathbf{B}_u = 0$, $\boldsymbol{\sigma} \equiv 0$, $\mathbf{J}_u = [J_u^-, J_u^+, M_u]$, where M_u is a Poisson process, and

$$\boldsymbol{\gamma} = \begin{bmatrix} \mathbb{1}_{\{X_{u-} \leq \bar{x}\}} & -\mathbb{1}_{\{X_{u-} \geq -\bar{x}\}} & 0 \\ -f(u, S_u, \delta_u^-, q_u^-) \mathbb{1}_{\{X_{u-} \leq \bar{x}\}} & f(u, S_u, \delta_u^+, q_u^+) \mathbb{1}_{\{X_{u-} \geq -\bar{x}\}} & 0 \\ 0 & 0 & \bar{k}_u^\pm \end{bmatrix}.$$

For the impulse part, we have $\Phi(u, \mathbf{x}, \zeta) = \epsilon^m \mathbb{1}_{\{if \text{ market}\}} + \epsilon^\ell \mathbb{1}_{\{if \text{ limit}\}}$ and

$$\begin{aligned} \Psi(u, \mathbf{x}, \mathbf{k}, \zeta) = & [\Delta(\zeta, x), c(\zeta, y, s, k), 0]' \mathbb{1}_{\{if \text{ market}\}} \\ & + [\Gamma(\eta, x, \zeta), \chi(\eta, y, z, s, k, \kappa), 0]' \mathbb{1}_{\{if \text{ limit}\}}. \end{aligned}$$

The value function in Equation (7.5) is here given by setting $\vartheta(u, \mathbf{x}, \boldsymbol{\nu}) = g(u, \mathbf{x})$ and $\varrho(\mathbf{x}, \mathbf{k}) = U(\mathbf{x}, \mathbf{k})$.

7.3 Proofs for Chapter 3

In this section we show that the value function of the optimal control problem presented in Chapter 3 is the unique continuous viscosity solution of the HJB PIDE given by Equation (3.22).

7.3.1 Dark pool optimal control problem

We adapt the definitions given in the previous section to the particular problem at hand.

Definition 7.6. *A continuous function $V : [0, T] \times \mathcal{O} \rightarrow \mathbb{R}$ is a viscosity subsolution (resp. supersolution) of the HJB Equation (3.22) if*

$$r\phi(\bar{t}, \bar{\mathbf{x}}) - \frac{\partial \phi}{\partial t}(\bar{t}, \bar{\mathbf{x}}) - \mathcal{H}_1(\bar{t}, \bar{\mathbf{x}}, D_{\mathbf{x}}\phi) - \mathcal{B}_{b,\Delta}(\bar{t}, \bar{\mathbf{x}}, \phi) - \mathcal{B}_{\Delta}(\bar{t}, \bar{\mathbf{x}}, \phi) - \mathcal{B}_y(\bar{t}, \bar{\mathbf{x}}, \phi) \leq 0$$

(resp. ≥ 0) for each $\phi \in \mathcal{C}^{1,1}([0, T] \times \mathcal{O}) \cap \mathcal{PB}$ such that $V(t, \mathbf{x}) - \phi(t, \mathbf{x})$ attains its maximum (resp. minimum) at $(\bar{t}, \bar{\mathbf{x}}) \in [0, T] \times \mathcal{O}$. A continuous function is a viscosity solution if it is both a viscosity subsolution and a viscosity supersolution.

We here assume that all the real-valued functions defined in this paper satisfy the Lipschitz continuity and the linear growth conditions, uniformly in the control variables. We assume that the real value functions $\psi(t, \mathbf{y}, \mathbf{v})$ defined by

$$\psi(t, \mathbf{y}, \mathbf{v}) \in \left\{ \mu^b(\cdot), h_{1,2}^b(\cdot), \mu^{\Delta}(\cdot), h_{1,2}^{\Delta}(\cdot), h_{1,2}^{b,\Delta}(\cdot), \mu^y(\cdot), h^y(\cdot), f(\cdot), g(\cdot), \right. \\ \left. f_1(\cdot), g_1(\cdot) \right\},$$

such that

$$|\psi(t_1, \mathbf{y}_1, \mathbf{v}) - \psi(t_2, \mathbf{y}_2, \mathbf{v})| \leq C(|t_1 - t_2| + \|\mathbf{y}_1 - \mathbf{y}_2\|)$$

and

$$|\psi(t_1, \mathbf{y}_1, \mathbf{v})| \leq C(1 + |t_1| + \|\mathbf{y}_1\|),$$

where $\mathbf{y}_{1,2}$ is the vector of state variables and \mathbf{v} is the vector of controls associated to every function (the latter may also be empty). Standard results—see, e.g., Ikeda and Watanabe [53]—ensure that there exists a strong and path-wise unique solution of the price, the spread and the wealth models defined by Equations (3.2), (3.15) and (3.17).

7.3.2 Moments estimates

We now provide some moments estimates of S_u^b . We note that both the following proposition and its proof, are analogous for Δ_u , X_u and Y_u . In the remainder of the paper, we write $\mathbf{X}_{t,\mathbf{x}}(u)$ for the state variables at time u with initial values (t, \mathbf{x}) since we need the initial conditions explicitly.

Proposition 7.7. *Fix $p = 1, 2$ and let $S_{t,s^b}^b(u)$ be the random variable at a fixed time $u \in [t, T]$ with initial values $(t, s^b) \in [0, T] \times \mathbb{R}_+$. Then, for any $v \in \mathcal{V}$ and for any stopping time $\tau_0 \leq h \in [0, T]$ there exists a constant $K = K(p, C, T) > 0$ such that*

$$\begin{aligned} \mathbb{E} \left[|S_{t,s^b}^b(\tau_0)|^p \right] &\leq K \left(1 + |s^b|^p \right), \\ \mathbb{E} \left[|S_{t,s_1^b}^b(\tau_0) - S_{t,s_2^b}^b(\tau_0)|^p \right] &\leq K \left(|s_1^b - s_2^b|^p \right), \\ \mathbb{E} \left[|S_{t,s^b}^b(\tau_0) - s^b|^p \right] &\leq K \left(1 + |s^b|^p \right) (h - t)^{\frac{p}{2}}, \\ \mathbb{E} \left[\sup_{0 \leq u \leq h} |S_{t,s^b}^b(u) - s^b|^p \right] &\leq K \left(1 + |s^b|^p \right) (h - t)^{\frac{p}{2}}. \end{aligned} \tag{7.11}$$

Proof. We adapt the proof in Pham [75] to the present work and indeed we shall consider the proof only for $p = 2$ as it suffices to ensure the relation for $p = 1$, according to Hölder's inequality. In order to reduce notation, here K is a generic positive constant which may take different values in different places. Define \mathcal{T}_h as the set of all stopping times smaller than $h \in [0, T]$. By the optional sampling

theorem and the Lévy-Itô isometry, we have

$$\begin{aligned} \mathbb{E} \left[|S_{t,s^b}^b(\tau_0)|^2 \right] &\leq K \mathbb{E} \left[|s^b|^2 + \int_t^{\tau_0} \left| \mu^b(u, S_{t,s^b}^b(u), \nu_u) \right|^2 du \right. \\ &\quad \left. + \sum_{i=1}^2 \lambda^{b,i} \mathbb{E} \left[|z_1^{b,i}|^2 \right] \int_t^{\tau_0} \left| h_i^b(u, S_{t,s^b}^b(u)) \right|^2 du \right], \end{aligned}$$

for $\tau_0 \in \mathcal{T}_h$. By the linear growth conditions on μ^b , h_1^b , h_2^b , we have

$$\mathbb{E} \left[|S_{t,s^b}^b(\tau_0)|^2 \right] \leq K \left[1 + |s^b|^2 + \mathbb{E} \int_t^{\tau_0} |S_{t,s^b}^b(u)|^2 du \right]. \quad (7.12)$$

As noted in Pham (1998), if τ_0 were a deterministic time, (7.12) would yield

$$\mathbb{E} \left[|S_{t,s^b}^b(\tau_0)|^2 \right] \leq K \left[1 + |s^b|^2 \right].$$

By definition of \mathcal{T}_h , we note that

$$\mathbb{E} \left[\int_t^{\tau_0} |S_{t,s^b}^b(u)|^2 du \right] \leq \mathbb{E} \left[\int_t^h |S_{t,s^b}^b(u)|^2 du \right].$$

Thus, by applying Fubini's theorem to exchange the order of integration and by Gronwall's lemma,

$$\mathbb{E} \left[|S_{t,s^b}^b(\tau_0)|^2 \right] \leq K \left[1 + |s^b|^2 + \int_t^h \mathbb{E} \left[|S_{t,s^b}^b(u)|^2 \right] du \right] \leq K \left[1 + |s^b|^2 \right], \quad (7.13)$$

for a suitable constant $K = K(p, C, M, T)$. Define the process Z_u by $Z_u = S_{t,s_1^b}^b(u) - S_{t,s_2^b}^b(u)$. Then by an application of Itô's formula to $|Z_u|^2$, we have

$$\begin{aligned} \mathbb{E} \left[|Z_{\tau_0}|^2 \right] &= \mathbb{E} \left[|s_1^b - s_2^b|^2 + \int_t^{\tau_0} 2Z_u \left(\mu^b(u, S_{t,s_1^b}^b(u), \nu_u) - \mu^b(u, S_{t,s_2^b}^b(u), \nu_u) \right) du \right. \\ &\quad \left. + \sum_{i=1}^2 \lambda^{b,i} \mathbb{E} \left[|z_1^{b,i}|^2 \right] \int_t^{\tau_0} \left| h_i^b(u, S_{t,s_1^b}^b(u)) - h_i^b(u, S_{t,s_2^b}^b(u)) \right|^2 du \right]. \end{aligned}$$

From the Lipschitz condition on μ^b , h_1^b and h_2^b , it follows that

$$\mathbb{E} \left[|Z_{\tau_0}|^2 \right] \leq K \mathbb{E} \left[|s_1^b - s_2^b|^2 + \int_t^{\tau_0} |S_{t,s_1^b}^b(u) - S_{t,s_2^b}^b(u)|^2 du \right].$$

By making use of Fubini's Theorem and Gronwall's lemma we get

$$\mathbb{E} \left[\left| S_{t, s_1^b}^b(\tau_0) - S_{t, s_2^b}^b(\tau_0) \right|^2 \right] \leq K \mathbb{E} \left[\left| s_1^b - s_2^b \right|^2 + \int_t^h |Z_u|^2 du \right] \leq K \left| s_1^b - s_2^b \right|^2,$$

for a suitable constant $K = K(p, C, T)$. For the third moment estimate, we make use of the first moment estimate in (7.11) to obtain

$$\mathbb{E} \left[\left| S_{t, s^b}^b(\tau_0) - s^b \right|^2 \right] \leq K \left[\int_t^{\tau_0} \left(1 + \mathbb{E} \left[\left| S_{t, s^b}^b(u) \right|^2 \right] \right) du \right] \leq K \left(1 + \left| s^b \right|^2 \right) (h-t).$$

The fourth moment estimate in (7.11) follows from the third moment estimate, Doob's maximal inequality, and the fact that the constant K does not depend on the control process. \square

7.3.3 Viscosity solution

In what follows, we note that it suffices to show the viscosity property for the model presented in Section 3.3, since the model discussed in Section 3.2 is a special case.

Proposition 7.8. *The value function $V : [0, T] \times \mathcal{O} \rightarrow \mathbb{R}$ defined in (3.18) is continuous on $[0, T] \times \mathcal{O}$. Furthermore, for $K > 0$ and $\forall \mathbf{x} \in \mathcal{O}$, it satisfies*

$$V(t, \mathbf{x}) \leq K(1 + \|\mathbf{x}\|_1). \quad (7.14)$$

Proof. We proceed in two steps. We first show that the value function is Lipschitz continuous in \mathbf{x} , uniformly in t . Next we show that it is continuous in t . We take $\mathbf{x}, \mathbf{y} \in \mathcal{O}$ and since $|\sup(A) - \sup(B)| \leq \sup|A - B|$, we have that

$$\begin{aligned} |V(t, \mathbf{x}) - V(t, \mathbf{y})| &= \\ & \left| \sup_{\nu \in \mathcal{Z}} \mathbb{E} \left[\int_t^\tau e^{-r(u-t)} f_1(u, \mathbf{X}_{t, \mathbf{x}}(u), \nu_u) du + e^{-r(\tau-t)} g_1(\mathbf{X}_{t, \mathbf{x}}(\tau)) \right] \right. \\ & \quad \left. - \sup_{\nu \in \mathcal{Z}} \mathbb{E} \left[\int_t^\tau e^{-r(u-t)} f_1(u, \mathbf{X}_{t, \mathbf{y}}(u), \nu_u) du + e^{-r(\tau-t)} g_1(\mathbf{X}_{t, \mathbf{y}}(\tau)) \right] \right| \\ & \leq \sup_{\nu \in \mathcal{Z}} \left| \mathbb{E} \left[\int_t^\tau e^{-r(u-t)} \left(f_1(u, \mathbf{X}_{t, \mathbf{x}}(u), \nu_u) - f_1(u, \mathbf{X}_{t, \mathbf{y}}(u), \nu_u) \right) du \right. \right. \\ & \quad \left. \left. + e^{-r(\tau-t)} \left(g_1(\mathbf{X}_{t, \mathbf{x}}(\tau)) - g_1(\mathbf{X}_{t, \mathbf{y}}(\tau)) \right) \right] \right|. \end{aligned}$$

The Lipschitz continuity of f_1 and g_1 give

$$\begin{aligned}
& |V(t, \mathbf{x}) - V(t, \mathbf{y})| \\
& \leq \sup_{\nu \in \mathcal{Z}} \mathbb{E} \left[\int_t^\tau e^{-r(u-t)} K \|\mathbf{X}_{t, \mathbf{x}}(u) - \mathbf{X}_{t, \mathbf{y}}(u)\|_1 du \right. \\
& \qquad \qquad \qquad \left. + e^{-r(\tau-t)} K \|\mathbf{X}_{t, \mathbf{x}}(\tau) - \mathbf{X}_{t, \mathbf{y}}(\tau)\|_1 \right] \\
& \leq K \|\mathbf{x} - \mathbf{y}\|_1,
\end{aligned}$$

where the last inequality is justified by the moments estimates in Proposition 7.7. We note that an analogous calculation will produce Equation (7.14). We now take $0 \leq t_1 < t_2 < T$ and we apply the DPP to obtain

$$\begin{aligned}
|V(t_1, \mathbf{x}) - V(t_2, \mathbf{x})| = & \left| \sup_{\nu \in \mathcal{Z}} \mathbb{E} \left[\int_{t_1}^{t_2 \wedge \tau} e^{-r(u-t_1)} f_1(u, \mathbf{X}_{t_1, \mathbf{x}}(u), \nu_u) du \right. \right. \\
& \left. \left. + e^{-r(t_2-t_1)} V(t_2, \mathbf{X}_{t_1, \mathbf{x}}(t_2)) \mathbb{1}_{\{\tau \geq t_2\}} + e^{-r(\tau-t_1)} g_1(\mathbf{X}_{t_1, \mathbf{x}}(\tau)) \mathbb{1}_{\{\tau < t_2\}} \right] - V(t_2, \mathbf{x}) \right|.
\end{aligned}$$

We can add and subtract the quantity

$$\mathbb{1}_{\{\tau < t_2\}} e^{-r(\tau-t_1)} (g_1(\mathbf{x}) + V(t_2, \mathbf{x})) + \mathbb{1}_{\{\tau \geq t_2\}} e^{-r(t_2-t_1)} V(t_2, \mathbf{x}),$$

to obtain

$$\begin{aligned}
|V(t_1, \mathbf{x}) - V(t_2, \mathbf{x})| \leq & \sup_{\nu \in \mathcal{Z}} \mathbb{E} \left[\int_{t_1}^{t_2 \wedge \tau} e^{-r(u-t_1)} |f_1(u, \mathbf{X}_{t_1, \mathbf{x}}(u), \nu_u)| du \right. \\
& + \mathbb{1}_{\{\tau \geq t_2\}} e^{-r(t_2-t_1)} |V(t_2, \mathbf{X}_{t_1, \mathbf{x}}(t_2)) - V(t_2, \mathbf{x})| \\
& + \mathbb{1}_{\{\tau < t_2\}} e^{-r(\tau-t_1)} |g_1(\mathbf{X}_{t_1, \mathbf{x}}(\tau)) - g_1(\mathbf{x})| \\
& + \mathbb{1}_{\{\tau < t_2\}} e^{-r(\tau-t_1)} |g_1(\mathbf{x}) - V(t_2, \mathbf{x})| \\
& + \mathbb{1}_{\{\tau < t_2\}} |(e^{-r(\tau-t_1)} - 1)V(t_2, \mathbf{x})| \\
& \left. + \mathbb{1}_{\{\tau \geq t_2\}} |(e^{-r(t_2-t_1)} - 1)V(t_2, \mathbf{x})| \right] \\
& \leq K |t_2 - t_1| (1 + \|\mathbf{x}\|_1),
\end{aligned}$$

where the last inequality is justified by: (i) the linear growth of f_1 , g_1 and V , the Lipschitz continuity of g_1 and of V in \mathbf{x} uniformly in t , and the moment

estimates in Proposition 7.7. Thus, we can conclude that

$$|V(t_1, \mathbf{x}) - V(t_2, \mathbf{y})| \leq K(|t_2 - t_1|(1 + \|\mathbf{x}\|_1) + \|\mathbf{x} - \mathbf{y}\|_1). \quad \square$$

Proposition 7.9. *The value function V defined by Equation (3.18) is a viscosity solution of the HJB PIDE (3.22).*

Proof. We show that $V(t, \mathbf{x})$ is a continuous viscosity solution of (3.22) by proving that it is both a supersolution and a subsolution. We proceed along the same lines of Øksendal and Sulem [70] and we first show the supersolution property. We define a test function $\phi : [0, T] \times \mathcal{O} \rightarrow \mathbb{R}$ such that $\phi \in \mathcal{C}^{1,1}([0, T] \times \mathcal{O}) \cap \mathcal{PB}$ and, without loss of generality, we assume that $V - \phi$ reaches its minimum at $(\bar{t}, \bar{\mathbf{x}})$, such that

$$V(\bar{t}, \bar{\mathbf{x}}) - \phi(\bar{t}, \bar{\mathbf{x}}) = 0. \quad (7.15)$$

We let τ_1 be a stopping time defined by $\tau_1 = \inf \{u > \bar{t} \mid \mathbf{X}_{\bar{t}, \bar{\mathbf{x}}}(u) \notin B_\epsilon(\bar{\mathbf{x}})\}$, where $B_\epsilon(\bar{\mathbf{x}})$ is the ball of radius ϵ centred in $\bar{\mathbf{x}}$. Then we define the stopping time $\tau^* = \tau_1 \wedge (\bar{t} + h)$ for $0 < h < T - \bar{t}$ and note that $\bar{\gamma} := \mathbb{E}_{\bar{t}, \bar{\mathbf{x}}}[\tau^* - \bar{t}] > 0$. From the first part of DPP and the definition of ϕ , it follows that, $\forall \nu \in \mathcal{Z}$,

$$V(\bar{t}, \bar{\mathbf{x}}) \geq \mathbb{E} \left[\int_{\bar{t}}^{\tau^*} e^{-r(u-\bar{t})} f_1(u, \mathbf{X}_{\bar{t}, \bar{\mathbf{x}}}^\nu(u), \nu_u) du + e^{-r(\tau^*-\bar{t})} \phi(\tau^*, \mathbf{X}_{\bar{t}, \bar{\mathbf{x}}}^\nu(\tau^*)) \right].$$

By applying Dynkin's formula to $e^{-r(\tau^*-\bar{t})} \phi(\tau^*, \mathbf{X}_{\bar{t}, \bar{\mathbf{x}}}^\nu(\tau^*))$ at $(\bar{t}, \bar{\mathbf{x}})$, we get

$$\begin{aligned} \mathbb{E} \left[\int_{\bar{t}}^{\tau^*} \left(e^{-r(u-\bar{t})} f_1(u, \mathbf{X}_{\bar{t}, \bar{\mathbf{x}}}^\nu(u), \nu_u) - e^{-r(u-\bar{t})} \left\{ r\phi(u, \mathbf{X}_{\bar{t}, \bar{\mathbf{x}}}^\nu(u)) \right. \right. \right. \\ \left. \left. - \frac{\partial \phi}{\partial t}(u, \mathbf{X}_{\bar{t}, \bar{\mathbf{x}}}^\nu(u)) - \bar{\mathcal{H}}_1(u, \mathbf{X}_{\bar{t}, \bar{\mathbf{x}}}^\nu(u), D_{\mathbf{x}}\phi, \nu_u) - \mathcal{B}_{b, \Delta}(u, \mathbf{X}_{\bar{t}, \bar{\mathbf{x}}}^\nu(u), \phi) \right. \right. \\ \left. \left. \left. - \mathcal{B}_\Delta(u, \mathbf{X}_{\bar{t}, \bar{\mathbf{x}}}^\nu(u), \phi) - \bar{\mathcal{B}}_y(u, \mathbf{X}_{\bar{t}, \bar{\mathbf{x}}}^\nu(u), \phi, \eta_u) \right\} \right) du \right] \leq 0, \end{aligned}$$

where $\bar{\mathcal{H}}_1$ and $\bar{\mathcal{B}}_y$ are defined respectively by

$$\bar{\mathcal{H}}_1(t, \mathbf{x}, \mathbf{p}, v) = -vp_1 + \mu^b(t, s^b, v)p_2 + \mu^\Delta(t, \Delta, v)p_3 + \mu^y(t, s^b, \Delta, v)p_4, \text{ and}$$

$$\bar{\mathcal{B}}_y(t, \mathbf{x}, \varphi, n) = \lambda^y \mathbb{E}^{(z^y)} \left[\varphi(t, x - nz^y, s^b, \Delta, y + h^y(t, s^b, \Delta, n)z^y) - \varphi(t, \mathbf{x}) \right].$$

We divide both sides by $-\bar{\gamma}$ and let $h \rightarrow 0$, resulting in

$$\begin{aligned} r\phi(\bar{t}, \bar{\mathbf{x}}) - \frac{\partial\phi}{\partial t}(\bar{t}, \bar{\mathbf{x}}) - \bar{\mathcal{H}}_1(\bar{t}, \bar{\mathbf{x}}, D_{\mathbf{x}}\phi, v) - f_1(\bar{t}, \bar{\mathbf{x}}, v) - \mathcal{B}_{b,\Delta}(\bar{t}, \bar{\mathbf{x}}, \phi) \\ - \mathcal{B}_{\Delta}(\bar{t}, \bar{\mathbf{x}}, \phi) - \bar{\mathcal{B}}_y(\bar{t}, \bar{\mathbf{x}}, \phi, \eta) \geq 0. \end{aligned}$$

Due to the arbitrariness of \mathbf{v} , we can rewrite the above as

$$r\phi(\bar{t}, \bar{\mathbf{x}}) - \frac{\partial\phi}{\partial t}(\bar{t}, \bar{\mathbf{x}}) - \mathcal{H}_1(\bar{t}, \bar{\mathbf{x}}, D_{\mathbf{x}}\phi) - \mathcal{B}_{b,\Delta}(\bar{t}, \bar{\mathbf{x}}, \phi) - \mathcal{B}_{\Delta}(\bar{t}, \bar{\mathbf{x}}, \phi) - \mathcal{B}_y(\bar{t}, \bar{\mathbf{x}}, \phi) \geq 0,$$

which proves the supersolution inequality. We now prove the subsolution inequality. We let ϕ be a smooth and polynomially-bounded test function such that $V - \phi$ has its maximum at $(\bar{t}, \bar{\mathbf{x}})$. Without loss of generality, we assume $V(\bar{t}, \bar{\mathbf{x}}) - \phi(\bar{t}, \bar{\mathbf{x}}) = 0$. We shall show that

$$r\phi(\bar{t}, \bar{\mathbf{x}}) - \frac{\partial\phi}{\partial t}(\bar{t}, \bar{\mathbf{x}}) - \mathcal{H}_1(\bar{t}, \bar{\mathbf{x}}, D_{\mathbf{x}}\phi) - \mathcal{B}_{b,\Delta}(\bar{t}, \bar{\mathbf{x}}, \phi) - \mathcal{B}_{\Delta}(\bar{t}, \bar{\mathbf{x}}, \phi) - \mathcal{B}_y(\bar{t}, \bar{\mathbf{x}}, \phi) \leq 0.$$

Let us assume by contradiction that

$$e^{-rT} \left(r\phi(\bar{t}, \bar{\mathbf{x}}) - \frac{\partial\phi}{\partial t}(\bar{t}, \bar{\mathbf{x}}) - \mathcal{H}_1(\bar{t}, \bar{\mathbf{x}}, D_{\mathbf{x}}\phi) - \mathcal{B}_{b,\Delta}(\bar{t}, \bar{\mathbf{x}}, \phi) - \mathcal{B}_{\Delta}(\bar{t}, \bar{\mathbf{x}}, \phi) - \mathcal{B}_y(\bar{t}, \bar{\mathbf{x}}, \phi) \right) > \delta, \quad (7.16)$$

for $\delta > 0$ and $\mathbf{X}_{\bar{t}, \bar{\mathbf{x}}}(u) \in B_{\epsilon}(\bar{t}, \bar{\mathbf{x}})$. We define $\tau_1 = \inf \{u > \bar{t} \mid (u, \mathbf{X}_{\bar{t}, \bar{\mathbf{x}}}(u)) \notin B_{\epsilon}(\bar{t}, \bar{\mathbf{x}})\}$ and we define the stopping time $\tau^* = \tau_1 \wedge (\bar{t} + h)$. By the DPP, there exists a control $\nu^* \in \mathcal{Z}$ such that, for all $\delta > 0$, we have

$$V(\bar{t}, \bar{\mathbf{x}}) \leq \mathbb{E} \left[\int_{\bar{t}}^{\tau^*} e^{-r(u-\bar{t})} f_1(u, \mathbf{X}_{\bar{t}, \bar{\mathbf{x}}}^{\nu^*}(u), \nu_u^*) du + e^{-r(\tau^*-\bar{t})} \phi(\tau^*, \mathbf{X}_{\bar{t}, \bar{\mathbf{x}}}^{\nu^*}(\tau^*)) \right] + \frac{\delta\bar{\gamma}}{2}.$$

We divide both sides by $-\bar{\gamma}$ and get

$$\begin{aligned} \frac{1}{\bar{\gamma}} \mathbb{E} \left[\int_{\bar{t}}^{\tau^*} - \left(e^{-r(u-\bar{t})} f_1(u, \mathbf{X}_{\bar{t}, \bar{\mathbf{x}}}^{\nu^*}(u), \nu_u^*) - e^{-r(u-\bar{t})} \left\{ r\phi(u, \mathbf{X}_{\bar{t}, \bar{\mathbf{x}}}^{\nu^*}(u)) \right. \right. \right. \\ \left. \left. - \frac{\partial\phi}{\partial t}(u, \mathbf{X}_{\bar{t}, \bar{\mathbf{x}}}^{\nu^*}(u)) - \bar{\mathcal{H}}_1(u, \mathbf{X}_{\bar{t}, \bar{\mathbf{x}}}^{\nu^*}(u), D_{\mathbf{x}}\phi, \nu_u^*) - \mathcal{B}_{b,\Delta}(u, \mathbf{X}_{\bar{t}, \bar{\mathbf{x}}}^{\nu^*}(u), \phi) \right. \right. \\ \left. \left. - \mathcal{B}_{\Delta}(u, \mathbf{X}_{\bar{t}, \bar{\mathbf{x}}}^{\nu^*}(u), \phi) - \bar{\mathcal{B}}_y(u, \mathbf{X}_{\bar{t}, \bar{\mathbf{x}}}^{\nu^*}(u), \phi, \eta_u^*) \right\} \right) du \right] \leq \frac{\delta}{2}. \quad (7.17) \end{aligned}$$

By substituting Equation (7.16) in Equation (7.17) we obtain the desired contradiction (i.e. $\delta/2 < 0$). \square

Proposition 7.10. *Let U (resp. V) be a viscosity subsolution (resp. supersolution) of (3.22). If $U(T, \mathbf{x}) \leq V(T, \mathbf{x})$ on \mathcal{O} , then $U \leq V$ on $[0, T] \times \mathcal{O}$.*

Proof. Let U be a subsolution and V be a supersolution. Since $U, V \in \mathcal{PB}$, then there exists a $p > 1$ such that

$$\frac{|U(t, \mathbf{x})| + |V(t, \mathbf{x})|}{(1 + \|\mathbf{x}\|_p^p)} < \infty, \quad (7.18)$$

where the operator $\|\cdot\|_p^p$ is the L_p -norm raised to the p -th power. Let $\tilde{V}^\epsilon(t, \mathbf{x}) := V(t, \mathbf{x}) + \epsilon\kappa(t, \mathbf{x})$, where $\epsilon > 0$ and $\kappa(t, \mathbf{x}) = e^{-\zeta t}(1 + \|\mathbf{x}\|_{2p}^{2p})$, for $\zeta > 0$. Then \tilde{V}^ϵ is a supersolution of (3.22). Indeed, let $\phi(t, \mathbf{x})$ be the test function for \tilde{V}^ϵ , then the test function for V is $\phi(t, \mathbf{x}) - \epsilon\kappa(t, \mathbf{x})$. First note that we have

$$\begin{aligned} r\epsilon\kappa(t, \mathbf{x}) - \frac{\partial\epsilon\kappa}{\partial t}(t, \mathbf{x}) - \sup_{\mathbf{v} \in \mathcal{Z}} \bar{\mathcal{H}}_1(t, \mathbf{x}, D_{\mathbf{x}}\epsilon\kappa, \mathbf{v}) - \mathcal{B}_{b,\Delta}(t, \mathbf{x}, \epsilon\kappa) \\ - \mathcal{B}_\Delta(t, \mathbf{x}, \epsilon\kappa) - \mathcal{B}_y(t, \mathbf{x}, \epsilon\kappa) \geq 0, \end{aligned}$$

for ζ sufficiently large. By the supersolution property of V , we have

$$\begin{aligned} r(\phi - \epsilon\kappa)(t, \mathbf{x}) - \frac{\partial(\phi - \epsilon\kappa)}{\partial t}(t, \mathbf{x}) - \mathcal{H}_1(t, \mathbf{x}, D_{\mathbf{x}}(\phi - \epsilon\kappa)) - \mathcal{B}_{b,\Delta}(t, \mathbf{x}, \phi - \epsilon\kappa) \\ - \mathcal{B}_\Delta(t, \mathbf{x}, \phi - \epsilon\kappa) - \mathcal{B}_y(t, \mathbf{x}, \phi - \epsilon\kappa) \geq 0, \end{aligned}$$

and recalling that $\sup(A + B) \leq \sup A + \sup B$, we have

$$\begin{aligned} r\phi(t, \mathbf{x}) - \frac{\partial\phi}{\partial t}(t, \mathbf{x}) - \mathcal{H}_1(t, \mathbf{x}, D_{\mathbf{x}}\phi) - \mathcal{B}_{b,\Delta}(t, \mathbf{x}, \phi) - \mathcal{B}_\Delta(t, \mathbf{x}, \phi) - \mathcal{B}_y(t, \mathbf{x}, \phi) \geq \\ r\epsilon\kappa(t, \mathbf{x}) - \frac{\partial\epsilon\kappa}{\partial t}(t, \mathbf{x}) - \sup_{\mathbf{v} \in \mathcal{Z}} \bar{\mathcal{H}}_1(t, \mathbf{x}, D_{\mathbf{x}}\epsilon\kappa, \mathbf{v}) - \mathcal{B}_{b,\Delta}(t, \mathbf{x}, \epsilon\kappa) \\ - \mathcal{B}_\Delta(t, \mathbf{x}, \epsilon\kappa) - \mathcal{B}_y(t, \mathbf{x}, \epsilon\kappa) \geq 0. \end{aligned}$$

Since by (7.18) $\lim_{\mathbf{x} \rightarrow \pm\infty} \sup_{[0, T]} (U - \tilde{V}^\epsilon)(t, \mathbf{x}) = -\infty$, we can assume w.l.o.g. that

$$\mathcal{M} := \max_{[0, T] \times \mathcal{O}} (U(t, \mathbf{x}) - V(t, \mathbf{x})),$$

is attained at $(\bar{t}, \bar{\mathbf{x}}) \in [0, T] \times \Sigma$, where $\Sigma \subset \mathcal{O}$ is a compact set. In order to prove Proposition 7.10, it suffices to show that $\mathcal{M} < 0$. Suppose by contradiction that there exists a $(\bar{t}, \bar{\mathbf{x}}) \in [0, T) \times \Sigma$ such that $\mathcal{M} > 0$. For $\epsilon > 0$, we define

the function Ψ^ϵ by $\Psi^\epsilon(t_1, t_2, \mathbf{x}_1, \mathbf{x}_2) = U(t_1, \mathbf{x}_1) - V(t_2, \mathbf{x}_2) - \psi^\epsilon(t_1, t_2, \mathbf{x}_1, \mathbf{x}_2)$, where

$$\psi^\epsilon(t_1, t_2, \mathbf{x}_1, \mathbf{x}_2) := \frac{1}{2\epsilon} (|t_1 - t_2|^2 + \|\mathbf{x}_1 - \mathbf{x}_2\|_2^2).$$

The function Ψ^ϵ is continuous and admits a maximum point \mathcal{M}^ϵ , where $\mathcal{M} \leq \mathcal{M}^\epsilon$, at $m = (t_1^\epsilon, t_2^\epsilon, \mathbf{x}_1^\epsilon, \mathbf{x}_2^\epsilon)$. That is, the function $U(t_1, \mathbf{x}_1) - \psi^\epsilon(t_1, t_2, \mathbf{x}_1, \mathbf{x}_2)$ has a local maximum at m and $V(t_2, \mathbf{x}_2) - (-\psi^\epsilon(t_1, t_2, \mathbf{x}_1, \mathbf{x}_2))$ has a local minimum at m . Also, formally $\lim_{\epsilon \rightarrow 0} (t_1^\epsilon, t_2^\epsilon, \mathbf{x}_1^\epsilon, \mathbf{x}_2^\epsilon)$ converges, up to a subsequence, to $(\bar{t}, \bar{t}, \bar{\mathbf{x}}, \bar{\mathbf{x}})$ (see Crandall et al. [29] for details). We let $o^\epsilon = (t_1 - t_2)/\epsilon$, and define the vector \mathbf{p}^ϵ by

$$\mathbf{p}^\epsilon = (p_1^\epsilon, p_2^\epsilon, p_3^\epsilon, p_4^\epsilon) = \left(\frac{1}{\epsilon}(x_1^\epsilon - x_2^\epsilon), \frac{1}{\epsilon}(s_1^{b,\epsilon} - s_2^{b,\epsilon}), \frac{1}{\epsilon}(\Delta_1^\epsilon - \Delta_2^\epsilon), \frac{1}{\epsilon}(y_1^\epsilon - y_2^\epsilon) \right).$$

We can apply the viscosity subsolution and supersolution properties at the point m to obtain, with a slight abuse of notation², the following inequalities:

$$\begin{aligned} rU(t_1^\epsilon, \mathbf{x}_1^\epsilon) - o^\epsilon - \mathcal{H}_1(t_1^\epsilon, \mathbf{x}_1^\epsilon, \mathbf{p}^\epsilon) - \mathcal{B}_{b,\Delta}(t_1^\epsilon, \mathbf{x}_1^\epsilon, U, p_2^\epsilon, p_3^\epsilon) - \mathcal{B}_\Delta(t_1^\epsilon, \mathbf{x}_1^\epsilon, U, p_3^\epsilon) \\ - \mathcal{B}_y(t_1^\epsilon, \mathbf{x}_1^\epsilon, U) \leq 0, \end{aligned}$$

$$\begin{aligned} rV(t_2^\epsilon, \mathbf{x}_2^\epsilon) - o^\epsilon - \mathcal{H}_1(t_2^\epsilon, \mathbf{x}_2^\epsilon, \mathbf{p}^\epsilon) - \mathcal{B}_{b,\Delta}(t_2^\epsilon, \mathbf{x}_2^\epsilon, V, p_2^\epsilon, p_3^\epsilon) - \mathcal{B}_\Delta(t_2^\epsilon, \mathbf{x}_2^\epsilon, V, p_3^\epsilon) \\ - \mathcal{B}_y(t_2^\epsilon, \mathbf{x}_2^\epsilon, V) \geq 0, \end{aligned}$$

where, for $\phi \in \mathcal{PB}$, we have

$$\begin{aligned} \mathcal{B}_{b,\Delta}(t, \mathbf{x}, \phi, p, q) = \\ \sum_{i=1}^2 \lambda^{b,i} \mathbb{E}^{(z^{b,i})} \left[\phi(t, x, s^b + h_i^b(t, s^b) z^{b,i}, \Delta + h_i^{b,\Delta}(t, s^b, \Delta) z^{b,i}, y) - \phi(t, \mathbf{x}) \right. \\ \left. - h_i^b(t, s^b) z^{b,i} p - h_i^{b,\Delta}(t, s^b, \Delta) z^{b,i} q \right], \end{aligned}$$

$$\begin{aligned} \mathcal{B}_\Delta(t, \mathbf{x}, \phi, q) = \sum_{i=1}^2 \lambda^{\Delta,i} \mathbb{E}^{(z^{\Delta,i})} \left[\phi(t, x, s^b, \Delta + h_i^\Delta(t, \Delta) z^{\Delta,i}, y) \right. \\ \left. - \phi(t, \mathbf{x}) - h_i^\Delta(t, \Delta) z^{\Delta,i} q \right]. \end{aligned}$$

²The equivalence of the two different definitions of viscosity solution has been discussed extensively in, e.g., Pham [74] and Seydel [77].

We can subtract the two inequalities and take the limit for $\epsilon \rightarrow 0$ to get $r[U(\bar{t}, \bar{x}) - V(\bar{t}, \bar{x})] \leq 0$, which concludes the proof. \square

7.4 Proofs for Chapter 4

7.4.1 Assumption

We state all the standing assumptions which are introduced in the modelling setup presented in Chapter 4.

1. The real-valued functions f , U and g satisfy Lipschitz continuity and the linear growth conditions.
2. $\Gamma : \mathcal{N} \times [-\bar{X} - q_N, \bar{X} + q_N] \times [0, 1] \rightarrow \mathbb{R}$ and $\chi : \mathcal{N} \times \mathbb{R} \times [0, 1] \times \mathbb{R} \times \mathbb{K} \times \mathbb{K}^\ell \rightarrow \mathbb{R}$ are Lipschitz continuous functions satisfying

$$|x|^2 - \mathbb{E}^{(z)}[|\Gamma(\eta, x, z)|^2] > 1, \quad |y|^2 - \mathbb{E}^{(z)}[|\chi(\eta, y, z, s, k, \kappa)|^2] > 1,$$

for all $\eta \in \mathcal{N}$, $z \in [0, 1]$ and $x, y, s \in \mathcal{O}$.

3. $\Lambda : \mathcal{X} \times [-\bar{X} - q_N, \bar{X} + q_N] \rightarrow \mathbb{R}$ and $c : \mathcal{X} \times \mathbb{R}^2 \times \mathbb{K} \rightarrow \mathbb{R}$ are Lipschitz continuous functions satisfying, for $M > 0$, the following properties:

$$|x|^2 - |\Lambda(\xi, x)|^2 > 1, \quad |y|^2 - |c(\xi, y, s, k)|^2 > 1,$$

for all $\xi \in \mathcal{X}$ and $x, y, s \in \mathcal{O}$.

7.4.2 Viscosity solution

Definition 7.1. *A system of functions $V : [0, T) \times \mathcal{O} \times \mathbb{K} \rightarrow \mathbb{R}$ is a viscosity subsolution, (resp. supersolution), of (4.11) if*

$$\min \left\{ -g(\bar{t}, \bar{x}) - \mathcal{A}(\bar{t}, \bar{x}, \hat{k}, \partial_t \phi, \phi); (V^* - \mathcal{M}V^*)(\bar{t}, \bar{x}; \hat{k}); (V^* - \mathcal{L}V^*)(\bar{t}, \bar{x}; \hat{k}) \right\} \leq 0, \quad (7.19)$$

$$\left(\begin{array}{l} \text{resp.} \\ \min \left\{ -g(\bar{t}, \bar{x}) - \mathcal{A}(\bar{t}, \bar{x}, \hat{k}, \partial_t \phi, \phi); (V_* - \mathcal{M}V_*)(\bar{t}, \bar{x}; \hat{k}); (V_* - \mathcal{L}V_*)(\bar{t}, \bar{x}; \hat{k}) \right\} \geq 0 \end{array} \right), \quad (7.20)$$

where $\phi \in \mathcal{C}^{1,0,0}([0, T] \times \mathcal{O} \times \mathbb{K})$ is such that $V^*(t, \mathbf{x}; k) - \phi(t, \mathbf{x}; k)$ (resp. $V_*(t, \mathbf{x}; k) - \phi(t, \mathbf{x}; k)$) attains its maximum (resp. minimum) at $(\bar{t}, \bar{x}, \hat{k}) \subset [t, T] \times \mathcal{O} \times \mathbb{K}$.

Proposition 7.11. (Existence) *The system of functions $V(t, \mathbf{x}; k)$ is a viscosity solution of the QVI (4.11).*

Proof. We use definition 7.1 and we show that the system of functions $V(t, \mathbf{x}; k)$ is a viscosity solution by proving that it is both a supersolution and a subsolution. First we note that we have $V(T, \mathbf{x}; k) = U(\mathbf{x}; k)$ on $\{T\} \times \mathcal{O} \times \mathbb{K}$, thus we need to prove the viscosity property only on $[t, T] \times \mathcal{O} \times \mathbb{K}$. Results in, e.g., Ly Vath et al. [63] ensure that $\mathcal{M}V_* \leq (\mathcal{M}V)_*$ and $\mathcal{L}V_* \leq (\mathcal{L}V)_*$. By definition of the value function, we have $V \geq \mathcal{M}V$ and $V \geq \mathcal{L}V$ for all $(u, \mathbf{x}) \in [t, T] \times \mathcal{O}$. It follows that $V_* \geq (\mathcal{M}V)_* \geq \mathcal{M}V_*$ and $V_* \geq (\mathcal{L}V)_* \geq \mathcal{L}V_*$. That is, to prove the supersolution property, it suffices to show that

$$-g(\bar{t}, \bar{x}) - \mathcal{A}(\bar{t}, \bar{x}, \hat{k}, \partial_t \phi, \phi) \geq 0. \quad (7.21)$$

Let $(V_* - \phi)(\bar{t}, \bar{x}; \hat{k}) = 0$, where $(\bar{t}, \bar{x}, \hat{k}) = \arg \min (V_* - \phi)(t, \mathbf{x}; k)$. By definition of V_* , there exists a sequence $(t_m, \mathbf{x}_m) \rightarrow (\bar{t}, \bar{x})$ such that $V_*(t_m, \mathbf{x}_m; \hat{k}) \rightarrow V_*(\bar{t}, \bar{x}; \hat{k})$ as $m \rightarrow \infty$. We define the stopping time

$$\theta_m = \inf \{u > t_m \mid \mathbf{X}_{t_m, \mathbf{x}_m}(u) \notin B_\epsilon(t_m, \mathbf{x}_m)\}, \quad (7.22)$$

where $B_\epsilon(t_m, \mathbf{x}_m)$ is the open ball of radius ϵ centred in (t_m, \mathbf{x}_m) . We choose a strictly positive sequence $h_m \rightarrow 0$ as $m \rightarrow \infty$ and let the stopping time $\theta_m^* := \theta_m \wedge (t_m + h_m) \wedge \theta^* \wedge \tau_i$, where θ^* is the first time the regime switches from its initial value \bar{k} and where τ_i is the first time an impulse takes place. By the DPP and the definition of the function ϕ , we have for any admissible control strategy

$$V(t_m, \mathbf{x}_m; \hat{k}) \geq \mathbb{E} \left[\int_{t_m}^{\theta_m^*} g(u, X_{t_m, \mathbf{x}_m}(u)) du + \phi(\theta_m^*, \mathbf{X}_{t_m, \mathbf{x}_m}(\theta_m^*); k_{\theta_m^*}) \right]. \quad (7.23)$$

An application of Itô's formula to ϕ between t_m and θ_m^* yields

$$\begin{aligned} (V_* - \phi)(t_m, \mathbf{x}_m; \hat{k}) &\geq \\ \mathbb{E} \left[\int_{t_m}^{\theta_m^*} \left[g(u, X_{t_m, \mathbf{x}_m}(u)) + \bar{\mathcal{A}}(u, \mathbf{X}_{t_m, \mathbf{x}_m}(u), \hat{k}, \partial_t \phi, \phi, \delta_u^+, \delta_u^-) \right] du \right], & \quad (7.24) \end{aligned}$$

We can divide by $-h_m$, then let $m \rightarrow \infty$ and apply the mean value theorem. Finally, the result follows from the arbitrariness of the control variable.

First note that if $V^* = \mathcal{M}V^*$ or $V^* = \mathcal{L}V^*$, the subsolution property is immediately satisfied. We assume therefore that $V^* > \mathcal{M}V^*$ and $V^* > \mathcal{L}V^*$; we then need to show that

$$-g(\bar{t}, \bar{\mathbf{x}}) - \mathcal{A}(\bar{t}, \bar{\mathbf{x}}, \hat{k}, \partial_t \phi, \phi) \leq 0. \quad (7.25)$$

By continuity of the mapping in (7.25), we assume on the contrary that there exists a $\epsilon_1 > 0$ and an $\epsilon_2 > 0$ such that $-g(\bar{t}, \bar{\mathbf{x}}) - \mathcal{A}(\bar{t}, \bar{\mathbf{x}}, \hat{k}, \partial_t \phi, \phi) \geq \epsilon_1$, for all $\mathbf{X}_{\bar{t}, \bar{\mathbf{x}}}(u) \in B_{\epsilon_2}(\bar{t}, \bar{\mathbf{x}})$. We take the sequences $h_m \rightarrow 0$ and $(t_m, \mathbf{x}_m) \rightarrow (\bar{t}, \bar{\mathbf{x}})$, as $m \rightarrow \infty$, valued in $B_{\epsilon_2}(\bar{t}, \bar{\mathbf{x}})$ and we define the stopping times θ_m by (7.22) with $\epsilon < \epsilon_2$ and $\theta_m^* := \theta_m \wedge (t_m + h_m) \wedge \theta^* \wedge \tau_i$. By Itô's formula and the DPP, there exists an admissible control strategy $(\delta_u^{+, *}, \delta_u^{-, *})$ for which

$$\mathbb{E} \left[\int_{t_m}^{\theta_m^*} \left[g(u, X_{t_m, x_m}(u)) + \bar{A}(u, \mathbf{X}_{t_m, x_m}(u), \hat{k}, \partial_t \phi, \phi, \delta_u^{+,*}, \delta_u^{-,*}) \right] du \right], \quad (7.26)$$

$$\gamma_m - \frac{\epsilon_1 h_m}{2} \leq$$

where $\gamma_m = (V^* - \phi)(t_m, \mathbf{x}_m; \hat{k})$. Dividing by $-h_m$, we find that

$$0 \geq \frac{\gamma_m}{h_m} - \frac{\epsilon_1}{2} + \frac{\epsilon_1}{h_m} \mathbb{E}[\theta_m^* - t_m]. \quad (7.27)$$

Since $\mathbb{E}[\theta_m^* - t_m]/h_m \rightarrow 1$ as $m \rightarrow \infty$, we get $\epsilon_1/2 \leq 0$, which contradicts $\epsilon_1 > 0$. \square

Proposition 7.2. (*Strong Comparison Principle*) *Let v and u be a supersolution and a subsolution respectively of the QVI (4.11). Then $u^* \leq v_*$ on $[0, T] \times \mathcal{O} \times \mathbb{K}$.*

We write v and u in place of v_* and u^* for simplicity. We first prove that there exists a ζ -strict supersolution. We refer to, e.g., Seydel [77] for technical details. We consider the function $v^\zeta(t, \mathbf{x}; k) = v(t, \mathbf{x}; k) + \zeta e^{\beta(T-t)}(1 + \|\mathbf{x}\|_{2p}^{2p})$, where $\beta > 0$ and $p > 1$ are to be determined later. Then we have:

$$\begin{aligned} & v^\zeta(t, \mathbf{x}; k) - \mathcal{M}v^\zeta(t, \mathbf{x}; k) \geq \\ & v(t, \mathbf{x}; k) + \zeta e^{\beta(T-t)}(|x|^{2p} + |y|^{2p}) - \mathcal{M}v(t, \mathbf{x}; k) \\ & - \sup_{\xi \in \mathcal{X}} \left[\zeta e^{\beta(T-t)} (|\Lambda(\xi, x)|^{2p}) \right] - \sup_{\xi \in \mathcal{X}} \left[\zeta e^{\beta(T-t)} (|c(\xi, y, s, k)|^{2p}) \right] + \epsilon_m \geq \\ & \zeta e^{\beta(T-t)} \left[|x|^{2p} - \sup_{\xi \in \mathcal{X}} (|\Lambda(\xi, x)|^{2p}) \right] \\ & + \zeta e^{\beta(T-t)} \left[|y|^{2p} - \sup_{\xi \in \mathcal{X}} (|c(\xi, y, s, k)|^{2p}) \right] + \epsilon_m > \zeta, \end{aligned} \quad (7.28)$$

where the second-to-last inequality follows from the supersolution property of the function v , while the last inequality follows from assumption (3) and the fact that $|a| > |b| \Rightarrow |a|^p > |b|^p \forall p > 1$. Analogously, we have:

$$\begin{aligned}
v^\zeta(t, \mathbf{x}; k) - \mathcal{L}v^\zeta(t, \mathbf{x}; k) &\geq \zeta e^{\beta(T-t)} \left[|x|^{2p} - \sup_{\eta \in \mathcal{N}, \kappa \in \mathbb{K}^\ell} \mathbb{E}^{(z)} \left[(|\Gamma(\eta, x, z)|^{2p}) \right] \right] \\
&\quad + \zeta e^{\beta(T-t)} \left[|y|^{2p} - \sup_{\eta \in \mathcal{N}, \kappa \in \mathbb{K}^\ell} \mathbb{E}^{(z)} \left[(|\chi(\eta, y, z, s, k, \kappa)|^{2p}) \right] \right] + \epsilon_\ell \\
&> \zeta.
\end{aligned}$$

Finally we take into consideration the PIDE part. We let ϕ^ζ be the test function for v^ζ . Then $\phi := \phi^\zeta - \zeta e^{\beta(T-t)} (1 + \|\mathbf{x}\|_{2p}^{2p})$ is the test function for v . We therefore have:

$$\begin{aligned}
&-g(t, x) - \mathcal{A}(t, \mathbf{x}, k, \partial_t \phi^\zeta, v^\zeta) \\
&\geq \\
&-g(t, x) - \mathcal{A}(t, \mathbf{x}, k, \partial_t \phi, v) + \beta \zeta e^{\beta(T-t)} (1 + \|\mathbf{x}\|_{2p}^{2p}) \\
&\quad - \lambda^m \mathbb{E}^{(\bar{k}^\pm)} \left[\zeta e^{\beta(T-t)} (|s + \bar{k}^\pm|^{2p} - |s|^{2p}) \right] \\
&- \sup_{\delta^+ \in [0, \bar{\delta}]} \lambda_\delta^+ \mathbb{E}^{(q^+)} \left[\zeta e^{\beta(T-t)} (|x - q^+|^{2p} + |y + f(t, s, \delta^+, q^+)q^+|^{2p} - |x|^{2p} - |y|^{2p}) \right. \\
&\quad \left. \mathbb{1}_{\{x \geq -\bar{X}\}} \right] \\
&- \sup_{\delta^- \in [0, \bar{\delta}]} \lambda_\delta^- \mathbb{E}^{(q^-)} \left[\zeta e^{\beta(T-t)} (|x + q^-|^{2p} + |y - f(t, s, \delta^-, q^-)q^-|^{2p} - |x|^{2p} - |y|^{2p}) \right. \\
&\quad \left. \mathbb{1}_{\{x \leq \bar{X}\}} \right] \\
&\geq \\
&\quad + \beta \zeta e^{\beta(T-t)} (1 + \|\mathbf{x}\|_{2p}^{2p}) - \lambda^m \mathbb{E}^{(\bar{k}^\pm)} \left[\zeta e^{\beta(T-t)} (|s + \bar{k}^\pm|^{2p} - |s|^{2p}) \right] \\
&- \sup_{\delta^+ \in [0, \bar{\delta}]} \lambda_\delta^+ \mathbb{E}^{(q^+)} \left[\zeta e^{\beta(T-t)} (|x - q^+|^{2p} + |y + f(t, s, \delta^+, q^+)q^+|^{2p} - |x|^{2p} - |y|^{2p}) \right. \\
&\quad \left. \mathbb{1}_{\{x \geq -\bar{X}\}} \right] \\
&- \sup_{\delta^- \in [0, \bar{\delta}]} \lambda_\delta^- \mathbb{E}^{(q^-)} \left[\zeta e^{\beta(T-t)} (|x + q^-|^{2p} + |y - f(t, s, \delta^-, q^-)q^-|^{2p} - |x|^{2p} - |y|^{2p}) \right. \\
&\quad \left. \mathbb{1}_{\{x \leq \bar{X}\}} \right] \\
&\geq \zeta,
\end{aligned}$$

for β sufficiently large. Now we set

$$v_m = \left(1 - \frac{1}{m}\right)v + \frac{1}{m}v^\zeta, \quad u_m = \left(1 + \frac{1}{m}\right)u - \frac{1}{m}v^\zeta. \quad (7.29)$$

Using Definition 7.1, one can prove that

$$\begin{aligned} \min \left\{ -g(t, x) - \mathcal{A}(t, \mathbf{x}, k, \partial_t \phi_m, \phi_m); (v_m - \mathcal{M}v_m)(t, \mathbf{x}; k); (v_m - \mathcal{L}v_m)(t, \mathbf{x}; k) \right\} \\ \geq \frac{\zeta}{m}. \end{aligned} \quad (7.30)$$

where $\phi^m := \phi + \frac{1}{m}\zeta e^{\beta(T-t)}(1 + \|\mathbf{x}\|_{2p}^{2p})$ is the test function for v_m and ϕ is the test function for v and

$$\begin{aligned} \min \left\{ -g(t, x) - \mathcal{A}(t, \mathbf{x}, k, \partial_t \varphi_m, \varphi_m); (u_m - \mathcal{M}u_m)(t, \mathbf{x}; k); (u_m - \mathcal{L}u_m)(t, \mathbf{x}; k) \right\} \\ \leq -\frac{\zeta}{m}, \end{aligned} \quad (7.31)$$

where $\varphi_m := \frac{m+1}{m}\varphi - \frac{1}{m}\phi - \frac{1}{m}\zeta e^{\beta(T-t)}(1 + \|\mathbf{x}\|_{2p}^{2p})$ is the test function for u_m and φ is the test function for u . We further note that u and v are polynomially bounded (see e.g. Crisafi & Macrina [20], Proposition 6.3, for details). Thus, we have for each $k \in \mathbb{K}$

$$\begin{aligned} \lim_{\mathbf{x} \rightarrow \pm\infty} (u_m - v_m)(t, \mathbf{x}; k) &= \lim_{\mathbf{x} \rightarrow \pm\infty} \left(1 + \frac{1}{m}\right)(u - v)(t, \mathbf{x}; k) \\ &\quad - \frac{2}{m}\zeta e^{\beta(T-t)}(1 + \|\mathbf{x}\|_{2p}^{2p}) \\ &= -\infty, \end{aligned} \quad (7.32)$$

where we set p larger than the degree of the bounding polynomial of u and v . Thus the supremum is attained in a bounded set. Since $u_m - v_m$ is upper semicontinuous, it attains a maximum over a compact set. Next we show that, for all m large, we have

$$M := \max_{t, \mathbf{x}, k} (u_m(t, \mathbf{x}; k) - v_m(t, \mathbf{x}; k)) \leq 0, \quad (7.33)$$

where $(\bar{t}, \bar{\mathbf{x}}, \hat{k}) = \arg \max(u_m(t, \mathbf{x}; k) - v_m(t, \mathbf{x}; k))$. We define the auxiliary function Ψ^ϵ by

$$\Psi^\epsilon(t_1, t_2, \mathbf{x}_1, \mathbf{x}_2; k) := u_m(t_1, \mathbf{x}_1; k) - v_m(t_2, \mathbf{x}_2; k) - \frac{1}{2\epsilon} (|t_1 - t_2|^2 + \|\mathbf{x}_1 - \mathbf{x}_2\|_2^2), \quad (7.34)$$

For each $k \in \mathbb{K}$, Ψ^ϵ is upper semicontinuous and therefore it admits a maximum $M^{\epsilon, k}$ at $(t_1^{k, \epsilon}, t_2^{k, \epsilon}, \mathbf{x}_1^{k, \epsilon}, \mathbf{x}_2^{k, \epsilon})$. Let M^ϵ be defined by $M^\epsilon = \max_{k \in \mathbb{K}} M^{\epsilon, k}$, attained at the point $(t_1^\epsilon, t_2^\epsilon, \mathbf{x}_1^\epsilon, \mathbf{x}_2^\epsilon, k^\epsilon) \rightarrow (\bar{t}, \bar{t}, \bar{\mathbf{x}}, \bar{\mathbf{x}}, \hat{k})$ as $\epsilon \rightarrow 0$. Furthermore, we have that $M^\epsilon \geq M$ and $M^\epsilon \rightarrow M$ as $\epsilon \rightarrow 0$. We now wish to prove that $M \leq 0$. Let us assume on the contrary that $M^\epsilon > 0$. We go through the various cases. Let

$$(u_m - \mathcal{M}u_m)(t_1^\epsilon, \mathbf{x}_1^\epsilon; k^\epsilon) \leq 0. \quad (7.35)$$

By the supersolution property of v_m and by subtracting the two inequalities, we have

$$(u_m - \mathcal{M}u_m)(t_1^\epsilon, \mathbf{x}_1^\epsilon; k^\epsilon) - (v_m - \mathcal{M}v_m)(t_2^\epsilon, \mathbf{x}_2^\epsilon; k^\epsilon) + \frac{\zeta}{m} \leq 0. \quad (7.36)$$

We can now develop a contradiction argument since

$$\begin{aligned} M &= \lim_{\epsilon \rightarrow 0} u_m(t_1^\epsilon, \mathbf{x}_1^\epsilon; k^\epsilon) - v_m(t_2^\epsilon, \mathbf{x}_2^\epsilon; k^\epsilon) \\ &\leq \lim_{\epsilon \rightarrow 0} \mathcal{M}u_m(t_1^\epsilon, \mathbf{x}_1^\epsilon; k^\epsilon) - \mathcal{M}v_m(t_2^\epsilon, \mathbf{x}_2^\epsilon; k^\epsilon) - \frac{\zeta}{m} \leq M - \frac{\zeta}{m}. \end{aligned} \quad (7.37)$$

The second case arises when $(u_m - \mathcal{L}u_m)(t_1^\epsilon, \mathbf{x}_1^\epsilon; k^\epsilon) \leq 0$. We follow the same procedure to show that

$$\begin{aligned} M &= \lim_{\epsilon \rightarrow 0} u_m(t_1^\epsilon, \mathbf{x}_1^\epsilon; k^\epsilon) - v_m(t_2^\epsilon, \mathbf{x}_2^\epsilon; k^\epsilon) \\ &\leq \lim_{\epsilon \rightarrow 0} \mathcal{L}u_m(t_1^\epsilon, \mathbf{x}_1^\epsilon; k^\epsilon) - \mathcal{L}v_m(t_2^\epsilon, \mathbf{x}_2^\epsilon; k^\epsilon) - \frac{\zeta}{m} \leq M - \frac{\zeta}{m}. \end{aligned} \quad (7.38)$$

Next we consider the PIDE part. We subtract the argument of the subsolution from the argument of the supersolution and obtain

$$\begin{aligned} g(t_1^\epsilon, x_1^\epsilon) + \mathcal{A}(t_1^\epsilon, \mathbf{x}_1^\epsilon, k^\epsilon, \frac{1}{\epsilon}(t_1^\epsilon - t_2^\epsilon), u_m) - g(t_2^\epsilon, x_2^\epsilon) \\ - \mathcal{A}(t_2^\epsilon, \mathbf{x}_2^\epsilon, k^\epsilon, \frac{1}{\epsilon}(t_1^\epsilon - t_2^\epsilon), v_m) \geq \frac{\zeta}{m}. \end{aligned}$$

Since we assumed $M^\epsilon > 0$, we can choose a $\varrho > 0$ and we have

$$\begin{aligned} 0 < \varrho M^\epsilon &= \varrho \left(u_m(t_1^\epsilon, \mathbf{x}_1^\epsilon; k^\epsilon) - v_m(t_2^\epsilon, \mathbf{x}_2^\epsilon; k^\epsilon) - \frac{1}{2\epsilon} (|t_1^\epsilon - t_2^\epsilon|^2 + \|\mathbf{x}_1^\epsilon - \mathbf{x}_2^\epsilon\|_2^2) \right) \\ &\leq g(t_1^\epsilon, x_1^\epsilon) + \mathcal{A}(t_1^\epsilon, \mathbf{x}_1^\epsilon, k^\epsilon, \frac{1}{\epsilon}(t_1^\epsilon - t_2^\epsilon), u_m) - g(t_2^\epsilon, x_2^\epsilon) \\ &\quad - \mathcal{A}(t_2^\epsilon, \mathbf{x}_2^\epsilon, k^\epsilon, \frac{1}{\epsilon}(t_1^\epsilon - t_2^\epsilon), v_m). \end{aligned}$$

We can now analyse every component in detail. First we note that, due to Assumption (4),

$$g(t_1^\epsilon, x_1^\epsilon) - g(t_2^\epsilon, x_2^\epsilon) \leq |g(t_1^\epsilon, x_1^\epsilon) - g(t_2^\epsilon, x_2^\epsilon)| \leq C (|t_1^\epsilon - t_2^\epsilon| + |x_1^\epsilon - x_2^\epsilon|) \rightarrow 0 \quad (7.39)$$

as $\epsilon \rightarrow 0$. For the remaining parts, let us rewrite

$$\begin{aligned} \mathcal{B}_s^k(t, \mathbf{x}, \psi) &:= \mathbb{E}^{(\bar{k}^\pm)} \left[(\psi(t, x, y, s + \bar{k}^\pm; k) - \psi(t, \mathbf{x}; k)) \right], \\ \mathcal{B}_+^k(t, \mathbf{x}, \psi) &:= \sup_{\delta^+ \in [0, \bar{\delta}]} \lambda_\delta^+ \mathbb{E}^{(q^+)} \left[(\psi(t, x - q^+, y + f(t, s, \delta^+, q^+)q^+, s; k) \right. \\ &\quad \left. - \psi(t, \mathbf{x}; k)) \mathbb{1}_{\{x \geq -\bar{X}\}} \right], \\ \mathcal{B}_-^k(t, \mathbf{x}, \psi) &:= \sup_{\delta^- \in [0, \bar{\delta}]} \lambda_\delta^- \mathbb{E}^{(q^-)} \left[(\psi(t, x + q^-, y - f(t, s, \delta^-, q^-)q^-, s; k) \right. \\ &\quad \left. - \psi(t, \mathbf{x}; k)) \mathbb{1}_{\{x \leq \bar{X}\}} \right], \end{aligned}$$

and

$$\mathcal{Q}\psi(t, \mathbf{x}; k) := \sum_{k' \neq k} r_{kk'} [\psi(t, \mathbf{x}; k') - \psi(t, \mathbf{x}; k)].$$

We analyse $\mathcal{B}_+^{k^\epsilon}(t_1^\epsilon, \mathbf{x}_1^\epsilon, u_m) - \mathcal{B}_+^{k^\epsilon}(t_2^\epsilon, \mathbf{x}_2^\epsilon, v_m)$ as the other integrals can be treated analogously. After some manipulation, we find:

$$\begin{aligned} \mathcal{B}_+^{k^\epsilon}(t_1^\epsilon, \mathbf{x}_1^\epsilon, u_m) - \mathcal{B}_+^{k^\epsilon}(t_2^\epsilon, \mathbf{x}_2^\epsilon, v_m) &\leq \sup_{\delta^+ \in [0, \bar{\delta}]} \lambda_\delta^+ \mathbb{E}^{(q^+)} \left[\left(\Psi^\epsilon(t_1^\epsilon, t_2^\epsilon, x_1^\epsilon - q^+, x_2^\epsilon - q^+, \right. \right. \\ &y_1^\epsilon + f(t_1^\epsilon, s_1^\epsilon, \delta^+, q^+)q^+, y_2^\epsilon + f(t_2^\epsilon, s_2^\epsilon, \delta^+, q^+)q^+, s_1^\epsilon, s_2^\epsilon; k^\epsilon) - \Psi^\epsilon(t_1^\epsilon, t_2^\epsilon, \mathbf{x}_1^\epsilon, \mathbf{x}_2^\epsilon; k^\epsilon) \\ &+ \frac{1}{2\epsilon} \left(|y_1^\epsilon + f(t_1^\epsilon, s_1^\epsilon, \delta^+, q^+)q^+ - y_2^\epsilon - f(t_2^\epsilon, s_2^\epsilon, \delta^+, q^+)q^+|^2 - |y_1^\epsilon - y_2^\epsilon| \right) \mathbb{1}_{\{x_1^\epsilon \leq \bar{X}\}} \left. \right] \\ &+ \sup_{\delta^+ \in [0, \bar{\delta}]} \lambda_\delta^+ \mathbb{E}^{(q^+)} \left[\left(v_m(t_2^\epsilon, x_2^\epsilon - q^+, y_2^\epsilon + f(t_2^\epsilon, s_2^\epsilon, \delta^+, q^+)q^+, s_2^\epsilon; k^\epsilon) \right. \right. \\ &\left. \left. - v_m(t_2^\epsilon, \mathbf{x}_2^\epsilon; k^\epsilon) \right) \mathbb{1}_{\{x_1^\epsilon \leq \bar{X}\}} \right] \\ &- \sup_{\delta^+ \in [0, \bar{\delta}]} \lambda_\delta^+ \mathbb{E}^{(q^+)} \left[\left(v_m(t_2^\epsilon, x_2^\epsilon - q^+, y_2^\epsilon + f(t_2^\epsilon, s_2^\epsilon, \delta^+, q^+)q^+, s_2^\epsilon; k^\epsilon) \right. \right. \\ &\left. \left. - v_m(t_2^\epsilon, \mathbf{x}_2^\epsilon; k^\epsilon) \right) \mathbb{1}_{\{x_2^\epsilon \leq \bar{X}\}} \right]. \end{aligned}$$

Since the function Ψ^ϵ attains its maximum at $(t_1^\epsilon, t_2^\epsilon, \mathbf{x}_1^\epsilon, \mathbf{x}_2^\epsilon; k^\epsilon)$, we have

$$\begin{aligned} \mathcal{B}_+^{k^\epsilon}(t_1^\epsilon, \mathbf{x}_1^\epsilon, u_m) - \mathcal{B}_+^{k^\epsilon}(t_2^\epsilon, \mathbf{x}_2^\epsilon, v_m) &\leq \sup_{\delta^+ \in [0, \bar{\delta}]} \lambda_\delta^+ \mathbb{E}^{(q^+)} \left[\frac{1}{2\epsilon} \left(|y_1^\epsilon + f(t_1^\epsilon, s_1^\epsilon, \delta^+, q^+)q^+ - y_2^\epsilon - f(t_2^\epsilon, s_2^\epsilon, \delta^+, q^+)q^+|^2 \right. \right. \\ &\left. \left. - |y_1^\epsilon - y_2^\epsilon|^2 \right) \mathbb{1}_{\{x_1^\epsilon \leq \bar{X}\}} \right] \\ &+ \sup_{\delta^+ \in [0, \bar{\delta}]} \lambda_\delta^+ \mathbb{E}^{(q^+)} \left[\left(v_m(t_2^\epsilon, x_2^\epsilon - q^+, y_2^\epsilon + f(t_2^\epsilon, s_2^\epsilon, \delta^+, q^+)q^+, s_2^\epsilon; k^\epsilon) \right. \right. \\ &\left. \left. - v_m(t_2^\epsilon, \mathbf{x}_2^\epsilon; k^\epsilon) \right) \mathbb{1}_{\{x_1^\epsilon \leq \bar{X}\}} \right] \\ &- \sup_{\delta^+ \in [0, \bar{\delta}]} \lambda_\delta^+ \mathbb{E}^{(q^+)} \left[\left(v_m(t_2^\epsilon, x_2^\epsilon - q^+, y_2^\epsilon + f(t_2^\epsilon, s_2^\epsilon, \delta^+, q^+)q^+, s_2^\epsilon; k^\epsilon) \right. \right. \\ &\left. \left. - v_m(t_2^\epsilon, \mathbf{x}_2^\epsilon; k^\epsilon) \right) \mathbb{1}_{\{x_2^\epsilon \leq \bar{X}\}} \right] \end{aligned}$$

First we note that, when we let $\epsilon \rightarrow 0$, we have $x_1^\epsilon, x_2^\epsilon \rightarrow \bar{x}$. Thus the two last terms of the previous inequality offset each other. Since the first term tends to

zero as $\epsilon \rightarrow 0$, we have that

$$\lim_{\epsilon \rightarrow 0} \mathcal{B}_+^{k^\epsilon}(t_1^\epsilon, \mathbf{x}_1^\epsilon, u_m) - \mathcal{B}_+^{k^\epsilon}(t_2^\epsilon, \mathbf{x}_2^\epsilon, v_m) \leq 0. \quad (7.40)$$

Finally, we have

$$\mathcal{Q}\left(u_m(t_1^\epsilon, \mathbf{x}_1^\epsilon, k^\epsilon) - v_m(t_2^\epsilon, \mathbf{x}_2^\epsilon, k^\epsilon)\right) \leq 0 \quad (7.41)$$

since the maximum is attained at k^ϵ . Thus, by letting $\epsilon \rightarrow 0$, we get $\rho M \leq 0$, which is a contradiction since $\rho > 0$. Therefore $M \leq 0$. Furthermore, since we have proved that $u^* \leq v_*$, the value function is continuous as it is both upper and lower semicontinuous. \square

7.5 Numerical procedures

In this section we briefly show the numerical schemes adopted to find the optimal strategy. These are similar to the one proposed by Guilbaud and Pham [47] and Bian et al. [11], and adapted to the particular models at hand. Such a scheme has proved to be monotone, stable and consistent in Guilbaud and Pham [47]. We provide pseudocodes for Chapters 3 and 4, since the numerical scheme used in Chapter 5 is a combination of both of the above.

7.5.1 Chapter 3

We create an equally-spaced grid for (i) the time axis such that $t_{i+1} - t_i = \delta t$, $\forall i = 0, 1, 2, \dots, n-1$, (ii) the inventory where $x_{j+1} - x_j = \delta x$ $\forall j = 0, 1, 2, \dots, m-1$, (iii) the price where $s_{k+1} - s_k = \delta s$ $\forall k = 0, 1, 2, \dots, p-1$, (iv) the spread where $\Delta_{\ell+1} - \Delta_\ell = \delta \Delta$ $\forall \ell = 0, 1, 2, \dots, q-1$, and (v) the cash process where $y_{u+1} - y_u = \delta y$ $\forall u = 0, 1, 2, \dots, o-1$. We write $V^{i,j,k,\ell,u} = V(t_i, x_j, s_k, \Delta_\ell, y_u)$ and define the following numerical derivatives:

$$\begin{aligned} V_{(t)}^{i,j,k,\ell,u} &:= \frac{V^{i+1,j,k,\ell,u} - V^{i,j,k,\ell,u}}{\delta t}, & V_{(x)}^{i,j,k,\ell,u} &:= \frac{V^{i,j+1,k,\ell,u} - V^{i,j,k,\ell,u}}{\delta x}, \\ V_{(s)}^{i,j,k,\ell,u} &:= \frac{V^{i,j,k+1,\ell,u} - V^{i,j,k,\ell,u}}{\delta s}, & V_{(\Delta)}^{i,j,k,\ell,u} &:= \frac{V^{i,j,k,\ell+1,u} - V^{i,j,k,\ell,u}}{\delta \Delta}, \end{aligned}$$

$$V_{(y)}^{i,j,k,\ell,u} := \frac{V^{i,j,k,\ell,u+1} - V^{i,j,k,\ell,u}}{\delta y}.$$

The pseudocode we use to approximate the solution of Equation (3.27) is as follows:

Algorithm 1 Pseudocode for PIDE (3.27)

```

1: for all  $j, k, \ell, u$ 
2:   Set  $V^{n,j,k,\ell,u} = e^{-r(t_n-t_0)}(y_u + x_j(s_k - \alpha x_j))$ .
3: end
4: for  $i=n-1, n-2, \dots, 0$ 
5:   for all  $j \in \mathbb{X}, k \in \mathbb{S}, \ell \in \mathbb{D}, u \in \mathbb{Y}$ 
6:
7:     * Compute the optimal rate of trading (by applying first order conditions)
8:
9:     
$$v^* = \frac{s_k V_{(y)}^{i+1,j,k,\ell,u} - \mu V_{(s)}^{i+1,j,k,\ell,u} - V_{(x)}^{i+1,j,k,\ell,u} + \mu V_{(\Delta)}^{i+1,j,k,\ell,u}}{2\beta V_{(y)}^{i+1,j,k,\ell,u}}.$$

10:    * Compute
11:    
$$V^{i,j,k,\ell,u} = (1 - r\delta t)V^{i+1,j,k,\ell,u} + \delta t \left( -\phi x_j^2 \right.$$

12:      
$$+ (\kappa^b(\bar{S} - s_k) - \mu v^*)V_{(s)}^{i+1,j,k,\ell,u} - v^*V_{(x)}^{i+1,j,k,\ell,u}$$

13:      
$$+ (\kappa^\Delta(\bar{\Delta} - \Delta_\ell) + \mu v^*)V_{(\Delta)}^{i+1,j,k,\ell,u} + v^*(s_k - \beta v^*)V_{(y)}^{i+1,j,k,\ell,u}$$

14:      
$$+ \lambda^y \sup_{\eta \in [0, x_j]} \sum_{\iota} p(z_\iota^y) \left[ V^{i+1,j-\zeta_{1,\iota},k,\ell,u+\zeta_{2,\iota}} - V^{i+1,j,k,\ell,u} \right]$$

15:      
$$+ \lambda^{b,1} \sum_{\iota} p(z_\iota^{b,1}) \left[ V^{i+1,j,k+z_\iota^{b,1},\ell-z_\iota^{b,1},u} - V^{i+1,j,k,\ell,u} \right]$$

16:      
$$+ \lambda^{b,2} \sum_{\iota} p(z_\iota^{b,2}) \left[ V^{i+1,j,k-z_\iota^{b,2},\ell+z_\iota^{b,2},u} - V^{i+1,j,k,\ell,u} \right]$$

17:      
$$+ \lambda^{\Delta,1} \sum_{\iota} p(z_\iota^{\Delta,1}) \left[ V^{i+1,j,k,\ell+z_\iota^{\Delta,1},u} - V^{i+1,j,k,\ell,u} \right]$$

18:      
$$+ \lambda^{\Delta,2} \sum_{\iota} p(z_\iota^{\Delta,2}) \left[ V^{i+1,j,k,\ell-z_\iota^{\Delta,2},u} - V^{i+1,j,k,\ell,u} \right] \Big),$$

19:
20:    where  $\zeta_{1,\iota} := \arg \min_{\xi=0,1,2,\dots,m-j} |x_\xi - \eta z_\iota^y|$ ,
21:    and  $\zeta_{2,\iota} := \arg \min_{\xi=0,1,2,\dots,o-u} |y_\xi - \eta z_\iota^y(s_k + \Delta_\ell/2)|$ .
22:
23:    * Store the arg max  $(v^*, \eta^*)(t_i, x_j, s_k, \Delta_\ell, y_u)$ .
24:  end
25:  * Compute  $V^{i,j,k,\ell,u}$  for  $k = 0, 1, \dots, \bar{z} - 1, k = p - \bar{z} + 1, \dots, p$ ,
26:   $\ell = 0, 1, \dots, \bar{z} - 1, \ell = q - \bar{z} + 1, \dots, q$ ,
27:   $u = 0, 1, \dots, \bar{y} - 1, u = o - \bar{y} + 1, \dots, o$  by interpolation.
28: end

```

In the above algorithm, we discretise the distribution of $\{z^{b,1}, z^{b,2}, z^{\Delta,1}, z^{\Delta,2}\}$ such that they are all supported in a finite set, say, $I = 0, 1, 2, \dots, \bar{z}$, which denotes the number of nodes the price and the spread move with probability $p(z_\iota)$, where $\iota \in I$, associated with every state. We thus reduce the space grids of s^b and Δ , of which indices are in the sets $\mathbb{S} := \bar{z}, \bar{z}+1, \dots, p-\bar{z}$ and $\mathbb{D} := \bar{z}, \bar{z}+1, \dots, q-\bar{z}$, respectively. We further reduce the space grid y to be $\mathbb{Y} := \bar{y}, \bar{y} + 1, \dots, o - \bar{y}$, where $\bar{y} := \arg \min_{\xi=0,1,2,\dots,o} |y_\xi - x_m(s_p - \alpha x_m)|$. We provide the pseudocode for the mean-reverting model—the one for the geometric Lévy model is analogous.

Throughout Chapter 3, we set an equally-spaced time grid $[0,10]$ with intervals of 0.01, an equally-spaced price grid $[0,10]$ with intervals of 0.1, an equally-spaced spread grid $[0.1,1]$ with intervals of 0.1 and an equally-spaced inventory grid $[0, 30]$, with intervals of 1. The random variables $z^{b,i}$ and $z^{\Delta,i}$ can take values in $[0, 0.9]$ with intervals of 0.1 and probability associated to each state of 0.1. The random variables z^y can take values in $[0, 1]$ with intervals of 0.1 and probability associated to each state of $\frac{1}{11}$.

7.5.2 Chapter 4

We present here the stylised numerical scheme used to solve the QVI (4.18). The previous examples (including the ones in Chapter 2) can be derived as a special case. We create an equally-spaced time grid $0 = t_0, t_1, t_2, \dots, t_n = T$, where $T > 0$ and $t_{i+1} - t_i = \Delta t$, $\forall i = 0, 2, \dots, n - 1$ and an equally-spaced space grid $-X = x_0, x_1, x_2, \dots, x_m = X$, where $X > 0$ and $x_{j+1} - x_j = \Delta x$, such that $1/\Delta x \in \mathbb{N}$. To simplify the notation, we write $h_k^{i,j} = h_k(t_i, x_j)$, where $i = 0, 1, \dots, n - 1$, $j \in \mathbb{J} := 1/\Delta x, 1/\Delta x + 1, \dots, m - 1/\Delta x$ and $k \in \mathbb{K}$. Here we further assume that $\mathbb{E}[\bar{k}^\pm] = 0$. For the random variables q^+ , q^- and z^κ we discretise the sample space and associate to each state ι a probability $p(q_\iota^+)$, $p(q_\iota^-)$ and $p(z_\iota^\kappa)$. In particular, throughout Chapter 4, we set an equally-spaced time grid $[0,50]$ with intervals of 1 and an equally-spaced inventory grid $[-100, 100]$, with intervals of 0.1. The random variable z can take values in $[0, 1]$ with intervals of 0.1 and probability associated to each state of 0.1. The random variables q^\pm can take values in $[0, 10]$ with intervals of 0.1 and probability of $\frac{1}{101}$.

Algorithm 2 Pseudocode for QVI (4.18)

```

1: for all  $k \in \mathbb{K}$  and  $j=0,1,\dots,m$ 
2:   Set  $h_k^{n,j} = -\alpha x_j^2$ .
3: end
4: for  $i=n-1,n-2,\dots,0$ 
5:   for all  $k \in \mathbb{K}$  and  $j \in \mathbb{J}$ 
6:     * Compute
7:
8:      $\mathcal{T}h_k^{i,j} = h_k^{i+1,j} + \Delta t \left( -\phi x_j^2 + \sum_{k' \neq k} r_{kk'} (h_{k'}^{i+1,j} - h_k^{i+1,j}) \right)$ 
9:
10:     $+ \sup_{\delta \pm \in \mathcal{D}} \left[ \sum_l p(q_l^+) \lambda_\delta^+ \left( \delta^+ q_l^+ (1+c)^{q_l^+} + h_k^{i+1,j-q_l^+/\Delta x} - h_k^{i+1,j} \right) \right.$ 
11:     $\left. + \sum_l p(q_l^-) \lambda_\delta^- \left( \delta^- q_l^- (1+c)^{q_l^-} + h_k^{i+1,j+q_l^-/\Delta x} - h_k^{i+1,j} \right) \right]$ ,
12:    and store the arg max  $(\delta^{+,*}, \delta^{-,*})(t_i, x_j)$ .
13:    * Compute  $\mathcal{M}h_k^{i,j} = \sup_{\xi = \pm 1/\Delta x} \left[ -k + h_k^{i+1,j+\xi} \right] - \epsilon_m$ ,
14:    and store the arg max  $\xi_i^*(t_i, x_j)$ .
15:
16:    * Compute
17:     $\mathcal{L}h_k^{i,j} = \sup_{\eta = \pm 1/\Delta x, \kappa \in \mathcal{K}} \left[ \sum_l p(z_l^\kappa) \left( z_l^\kappa (k + \kappa) + h_k^{i+1,j+\eta z_l^\kappa} \right) \right] - \epsilon_\ell$ ,
18:    and store the arg max  $(\eta_i^*, \kappa_i^*)(t_i, x_j)$ .
19:
20:    * Set  $h_k^{i,j} = \max \left( \mathcal{T}h_k^{i,j}, \mathcal{M}h_k^{i,j}, \mathcal{L}h_k^{i,j} \right)$  and store the relative policy.
21:  end
22:  * Compute  $h_k^{i,j}$  for  $j = 0, 1, \dots, 1/\Delta x - 1$  and  $j = m - 1/\Delta x, \dots, m$ 
23:  by interpolation.
24: end

```

7.6 Non-equivalence of liquidation strategies

Firstly, we need to redefine the strategies in terms of the bid and ask quotes and we note that we have four different cases, depending on the sign of the inventories. Eventually, we want the conditions to be independent on the specific sizes of X^ϵ and X^ℓ .

1. If $X^{\text{€}} > 0$ and $X^{\text{£}} > 0$, then the three liquidation alternatives are

$$\begin{aligned}
\text{(a)} \quad & X^{\text{£}} + X^{\text{€}}(S^{\text{€£}} - \Delta^{\text{€£}}/2) + X^{\text{£}}(S^{\text{££}} - \Delta^{\text{££}}/2), \\
\text{(b)} \quad & X^{\text{£}} + (X^{\text{€}}(S^{\text{€£}} - \Delta^{\text{€£}}/2) + X^{\text{£}})(S^{\text{££}} - \Delta^{\text{££}}/2), \\
\text{(c)} \quad & X^{\text{£}} + \left(X^{\text{€}} + \frac{X^{\text{£}}}{S^{\text{€£}} + \Delta^{\text{€£}}/2} \right) (S^{\text{€£}} - \Delta^{\text{€£}}/2).
\end{aligned} \tag{7.42}$$

The three strategies are equivalent if we have

$$\begin{aligned}
\text{(i)} \quad & (S^{\text{€£}} - \Delta^{\text{€£}}/2) = (S^{\text{€£}} - \Delta^{\text{€£}}/2)(S^{\text{££}} - \Delta^{\text{££}}/2) \\
\text{(ii)} \quad & \frac{S^{\text{€£}} - \Delta^{\text{€£}}/2}{S^{\text{€£}} + \Delta^{\text{€£}}/2} = (S^{\text{££}} - \Delta^{\text{££}}/2) \\
\Rightarrow \quad & S^{\text{€£}} - \Delta^{\text{€£}}/2 = (S^{\text{€£}} + \Delta^{\text{€£}}/2)(S^{\text{££}} - \Delta^{\text{££}}/2).
\end{aligned} \tag{7.43}$$

The above conditions hold true simultaneously if and only if $\Delta^{\text{€£}}/2 = 0$, which contradicts the hypothesis of the existence of bid and ask quotes for all three currency pairs.

2. If $X^{\text{€}} < 0$ and $X^{\text{£}} < 0$, then the three liquidation alternatives are

$$\begin{aligned}
\text{(a)} \quad & X^{\text{£}} + X^{\text{€}}(S^{\text{€£}} + \Delta^{\text{€£}}/2) + X^{\text{£}}(S^{\text{££}} + \Delta^{\text{££}}/2), \\
\text{(b)} \quad & X^{\text{£}} + (X^{\text{€}}(S^{\text{€£}} + \Delta^{\text{€£}}/2) + X^{\text{£}})(S^{\text{££}} + \Delta^{\text{££}}/2), \\
\text{(c)} \quad & X^{\text{£}} + \left(X^{\text{€}} + \frac{X^{\text{£}}}{S^{\text{€£}} - \Delta^{\text{€£}}/2} \right) (S^{\text{€£}} + \Delta^{\text{€£}}/2).
\end{aligned} \tag{7.44}$$

The three strategies are equivalent if simultaneously we have

$$\begin{aligned}
\text{(i)} \quad & (S^{\text{€£}} + \Delta^{\text{€£}}/2) = (S^{\text{€£}} + \Delta^{\text{€£}}/2)(S^{\text{££}} + \Delta^{\text{££}}/2) \\
\text{(ii)} \quad & \frac{S^{\text{€£}} + \Delta^{\text{€£}}/2}{S^{\text{€£}} - \Delta^{\text{€£}}/2} = (S^{\text{££}} + \Delta^{\text{££}}/2) \\
\Rightarrow \quad & S^{\text{€£}} + \Delta^{\text{€£}}/2 = (S^{\text{€£}} - \Delta^{\text{€£}}/2)(S^{\text{££}} + \Delta^{\text{££}}/2).
\end{aligned} \tag{7.45}$$

The above conditions hold true if and only if $\Delta^{\text{€£}}/2 = 0$, which contradicts the hypothesis of the existence of bid and ask quotes for all three currency pairs.

3. If $X^{\text{€}} > 0$ and $X^{\text{£}} < 0$, then the three liquidation alternatives are

$$\begin{aligned}
& \text{(a)} \quad X^{\text{£}} + X^{\text{€}}(S^{\text{€£}} - \Delta^{\text{€£}}/2) + X^{\text{£}}(S^{\text{££}} + \Delta^{\text{££}}/2), \\
& \text{(b)} \\
& \text{(b1)} \quad X^{\text{£}} + \overbrace{\left(X^{\text{€}}(S^{\text{€£}} - \Delta^{\text{€£}}/2) + X^{\text{£}} \right)}^{>0} (S^{\text{££}} - \Delta^{\text{££}}/2), \\
& \text{(b2)} \quad X^{\text{£}} + \overbrace{\left(X^{\text{€}}(S^{\text{€£}} - \Delta^{\text{€£}}/2) + X^{\text{£}} \right)}^{<0} (S^{\text{££}} + \Delta^{\text{££}}/2), \tag{7.46} \\
& \text{(c)} \\
& \text{(c1)} \quad X^{\text{£}} + \underbrace{\left(X^{\text{€}} + \frac{X^{\text{£}}}{S^{\text{€£}} - \Delta^{\text{€£}}/2} \right)}_{>0} (S^{\text{€£}} - \Delta^{\text{€£}}/2), \\
& \text{(c2)} \quad X^{\text{£}} + \underbrace{\left(X^{\text{€}} + \frac{X^{\text{£}}}{S^{\text{€£}} - \Delta^{\text{€£}}/2} \right)}_{<0} (S^{\text{€£}} + \Delta^{\text{€£}}/2).
\end{aligned}$$

First, we note that condition (b1) can only happen together with condition (c1) and, analogously, (b2) with condition (c2). We start by considering the triplet (a), (b1) and (c1) and we get

$$\begin{aligned}
& \text{(i)} \quad S^{\text{€£}} - \Delta^{\text{€£}}/2 = (S^{\text{€£}} - \Delta^{\text{€£}}/2)(S^{\text{££}} + \Delta^{\text{££}}/2) \\
& \text{(ii)} \quad X^{\text{€}}(S^{\text{€£}} - \Delta^{\text{€£}}/2)(S^{\text{££}} - \Delta^{\text{££}}/2) + X^{\text{£}}(S^{\text{££}} - \Delta^{\text{££}}/2) \tag{7.47} \\
& \quad = X^{\text{€}}(S^{\text{€£}} - \Delta^{\text{€£}}/2) + X^{\text{£}} \frac{S^{\text{€£}} - \Delta^{\text{€£}}/2}{S^{\text{€£}} - \Delta^{\text{€£}}/2}
\end{aligned}$$

In condition (ii) we can compare coefficients since we want the conditions to be independent of the specific levels of the inventories $X^{\text{€}}$ and $X^{\text{£}}$. Condition (ii) thus reduces to

$$(S^{\text{€£}} - \Delta^{\text{€£}}/2)(S^{\text{££}} - \Delta^{\text{££}}/2) = (S^{\text{€£}} - \Delta^{\text{€£}}/2). \tag{7.48}$$

Conditions (i) and (ii) hold simultaneously if $\Delta^{\text{££}}/2 = 0$. For the triplet (a), (b2) and (c2) analogous considerations hold and the three alternatives are equivalent if $\Delta^{\text{€£}}/2 = 0$.

4. If $X^{\text{€}} < 0$ and $X^{\text{£}} > 0$, then the three liquidation alternatives are

$$\begin{aligned}
& \text{(a)} \quad X^{\text{£}} + X^{\text{€}}(S^{\text{€£}} + \Delta^{\text{€£}}/2) + X^{\text{£}}(S^{\text{££}} - \Delta^{\text{££}}/2), \\
& \text{(b)} \\
& \text{(b1)} \quad X^{\text{£}} + \overbrace{\left(X^{\text{€}}(S^{\text{€£}} + \Delta^{\text{€£}}/2) + X^{\text{£}} \right)}^{>0} (S^{\text{££}} - \Delta^{\text{££}}/2), \\
& \text{(b2)} \quad X^{\text{£}} + \overbrace{\left(X^{\text{€}}(S^{\text{€£}} + \Delta^{\text{€£}}/2) + X^{\text{£}} \right)}^{<0} (S^{\text{££}} + \Delta^{\text{££}}/2), \tag{7.49} \\
& \text{(c)} \\
& \text{(c1)} \quad X^{\text{£}} + \underbrace{\left(X^{\text{€}} + \frac{X^{\text{£}}}{S^{\text{€£}} + \Delta^{\text{€£}}/2} \right)}_{>0} (S^{\text{€£}} - \Delta^{\text{€£}}/2), \\
& \text{(c2)} \quad X^{\text{£}} + \underbrace{\left(X^{\text{€}} + \frac{X^{\text{£}}}{S^{\text{€£}} + \Delta^{\text{€£}}/2} \right)}_{<0} (S^{\text{€£}} + \Delta^{\text{€£}}/2).
\end{aligned}$$

We can proceed as in point 3 to find analogous results on $\Delta^{\text{££}}/2$ and $\Delta^{\text{€£}}/2$.

Wrapping up, we can state that if $\Delta^{\text{€£}}/2$, $\Delta^{\text{££}}/2$ and $\Delta^{\text{€£}}/2$ are strictly positive, than the three alternatives need not to be identical.

Bibliography

- [1] ALFONSI A., FRUTH A., SCHIED A. (2009): Optimal execution strategies in limit order books with general shape functions, *Quantitative Finance* **10**(2), 143-157.
- [2] ALMGREN R., CHRISS N. (2001): Optimal execution of portfolio transactions, *Journal of Risk* **3**, 5-39.
- [3] AMIHUD Y., MENDELSON H. (1980): Dealership Market: Market-Making with Inventory, *Journal of Financial Economics* **8**, 31-53.
- [4] AMIHUD Y., MENDELSON H. (1986): Asset pricing and the bid-ask spread, *Journal of Financial Economics* **17**(2), 223-249.
- [5] AVELLANEDA M., STOIKOV S. (2008): High-frequency trading in a limit order book, *Quantitative Finance* **8**(3), 217-224.
- [6] BARLES G., SOUGANIDIS P. E. (1991): Convergence of Approximation Schemes for Fully Nonlinear Second Order Equations, *Asymptotic Analysis* **4**(3), 2347-2349.
- [7] BAYRAKTART E., LUDKOVSKY M. (2012): Liquidation in limit order books with controlled intensity, *Mathematical Finance* **24**(4), 627-650.
- [8] BERGER D. W., CHABOUD A. P., CHERNENKO S. V., HOWORKA E., WRIGHT J. H. (2008): Order flow and exchange rate dynamics in electronic brokerage system data, *Journal of International Economics* **75**, 93-109.

-
- [9] BERTOLA G., RUNGGLADIER W. J., YASUDA K. (2016): On Classical and Restricted Impulse Stochastic Control for the Exchange Rate, *Applied Mathematics & Optimization* **74**(2), 423-454.
- [10] BERTSIMAS D., LO A. W. (1998): Optimal control of execution costs, *Journal of Financial Markets* **1**(1), 1-50.
- [11] BIAN B., WU N., ZHENG H. (2016): Optimal Liquidation in a Finite Time Regime Switching Model with Permanent and Temporary Pricing Impact, *Discrete and Continuous Dynamical Systems (Series B)* **21**, 1401-1420.
- [12] BRIGO D., DI GRAZIANO G. (2014): Optimal trade execution under displaced diffusions dynamics across different risk criteria, *Journal of Financial Engineering* **1**(2), DOI: 10.1142/S2345768614500184.
- [13] BRUGLER J. (2015): Into the light: dark pool trading and intraday market quality on the primary exchange, *Staff Working Paper, Bank of England* **545**.
- [14] BUTI S., RINDI R., WERNER I. M. (2011): Dark Pool Trading Strategies, *IGIER Working Paper Series* **421**.
- [15] BUTI S., RINDI R., WERNER I. M. (2015): Dynamic Dark Pool Trading Strategies in Limit Order Markets, SSRN: 1571416.
- [16] CADENILLAS Á., ZAPATERO F. (1999): Optimal Central Bank Intervention in the Foreign Exchange Market, *Journal of Economic Theory* **87**(1), 218-242.
- [17] CARMONA R., WEBSTER K. (2012): High frequency market making, arXiv:1210.5781.
- [18] CARTEA Á., DONNELLY R., JAIMUNGAL S. (2014): Algorithmic Trading with Model Uncertainty, SSRN: 2310645.
- [19] CARTEA Á., JAIMUNGAL S. (2013): Modelling Asset Prices for Algorithmic and High-Frequency Trading, *Applied Mathematical Finance* **20**(6), 512-547.

-
- [20] CARTEA Á., JAIMUNGAL S. (2015): Risk Metrics and Fine Tuning of High Frequency Trading Strategies, *Mathematical Finance* **25**(3), 576-611.
- [21] CARTEA Á., JAIMUNGAL S. (2015): A Closed-Form Execution Strategy to Target VWAP, SSRN: 2542314.
- [22] CARTEA Á., JAIMUNGAL S., KINZEBULATOV D. (2016): Algorithmic Trading with Learning, *International Journal of Theoretical and Applied Finance* **19**(4), DOI: 10.1142/S021902491650028X.
- [23] CARTEA Á., JAIMUNGAL S., PENALVA J. (2016): Algorithmic and High Frequency Trading, *Cambridge University Press*.
- [24] CARTEA Á., JAIMUNGAL S., RICCI J. (2014): Buy Low Sell High: a High Frequency Trading Perspective, *SIAM Journal on Financial Mathematics* **5**(1), 415-444.
- [25] CARTEA Á., PENALVA J. (2012): Where is the Value in High Frequency Trading?, *The Quarterly Journal of Finance* **13**(1), 1-46.
- [26] CHABOUD A. P., CHIQUOINE B., HJALMARSSON E., VEGA C. (2014): Rise of the Machines: Algorithmic Trading in the Foreign Exchange Market, *The Journal of Finance* **69**(5), 2045-2084.
- [27] CHEN Y. L., GAU Y. F. (2014): Asymmetric responses of ask and bid quotes to information in the foreign exchange market, *Journal of Banking & Finance* **38**, 194-204.
- [28] CONT R., KUKANOV A. STOIKOV S. (2013): The Price Impact of Order Book Events, *The Journal of Financial Econometrics* **12**(1), 47-88.
- [29] CRANDALL M. G., ISHII H., LIONS P. L. (1984): Some properties of viscosity solutions of Hamilton-Jacobi equations, *Transactions of the American Mathematical Society* **282**(2), 487-502.
- [30] CRISAFI M. A., MACRINA A. (2016): Simultaneous Trading in 'Lit' and Dark Pools, *International Journal of Theoretical and Applied Finance* **19**(8), 1650055 (33 pages).

-
- [31] CRISAFI M. A., MACRINA A. (2017): Inventory Management in Customised Liquidity Pools, *Cogent Mathematics* **4**, 1281594.
- [32] DANIËLS T. R., DÖNGES J., HEINEMANN F. (2013): Crossing network versus dealer market: Unique equilibrium in the allocation of order flow, *European Economic Review* **62**, 41-57.
- [33] DAVIS M. H. A., GUO X., WU G. (2010): Impulse Control of Multidimensional Jump Diffusions, *SIAM Journal on Control and Optimization* **48**(8), 5276-5293.
- [34] DEGRYSE H., VAN ACHTER M., WUYTS G. (2009): Dynamic order submission strategies with competition between a dealer market and a crossing network, *Journal of Financial Economics* **91**, 319-338.
- [35] DENG S., YOSHIYAMA K., MITSUBUCHI T., SAKURAI A. (2015): Hybrid Method of Multiple Kernel Learning and Genetic Algorithm for Forecasting Short-Term Foreign Exchange Rates, *Computational Economics* **45**(1), 49-89.
- [36] EVANS M., LYONS R. (2002): Order flow and exchange rate dynamics, *Journal of Political Economy* **110**(1), 170-180.
- [37] FLEMING W. H., SONER H. M. (2006): Controlled Markov Processes and Viscosity Solutions, *Springer*.
- [38] FODRA P., PHAM H (2015): High frequency trading and asymptotics for small risk aversion in a Markov renewal model, *SIAM Journal on Financial Mathematics* **6**(1), 656-684.
- [39] FREI C., WESTRAY N. (2013): Optimal execution of a VWAP order: A stochastic control approach, *Mathematical Finance* **25**(3), 457-672.
- [40] GARMAN M.B. (1976): Market microstructure, *Journal of Financial Economics* **3**(3), 257-275.
- [41] GATHERAL J., SCHIED A. (2011): Optimal Trade Execution under Geometric Brownian Motion in the Almgren and Chriss Framework, *International Journal of Theoretical and Applied Finance* **14**(3), 353-368.

-
- [42] GENÇAY R. GRADOJEVIC N. (2013): Private information and its origins in an electronic foreign exchange market, *Economic Modelling* **33**, 86-93.
- [43] GUÉANT O. (2016): The Financial Mathematics of Market Liquidity: From Optimal Execution to Market Making, *Chapman and Hall/CRC Financial Mathematics Series*.
- [44] GUÉANT O., LEHALLE C. A., TAPIA J. F. (2012): Optimal Portfolio Liquidation with Limit Orders, *SIAM Journal on Financial Mathematics* **3**(1), 740-764.
- [45] GUÉANT O., LEHALLE C. A., TAPIA J. F. (2013): Dealing with the inventory risk: a solution to the market making problem, *Mathematics and Financial Economics* **7**(4), 477-507.
- [46] GUÉANT O., ROYER G. (2014): VWAP execution and guaranteed VWAP, *SIAM Journal on Financial Mathematics* **5**(1), 445-471.
- [47] GUILBAUD F., PHAM H. (2013): Optimal High-Frequency Trading with Limit and Market Orders, *Quantitative Finance* **13**(1), 79-94.
- [48] GUILBAUD F., PHAM H. (2015): Optimal high-frequency trading in a pro rata microstructure with predictive information, *Mathematical Finance* **25**(3), 545-575.
- [49] HAWKES A. J. (1971): Point Spectra of Some Mutually Exciting Point Processes, *Journal of the Royal Statistical Society. Series B (Methodological)* **33**(3), 438-443.
- [50] HENDERSHOTT T., MENDELSON H. (2000): Crossing Networks and Dealer Markets: Competition and Performance, *The Journal of Finance* **55**(5), 2071-2115.
- [51] HO T., STOLL H. R. (1981): Optimal Dealer Pricing Under Transactions and Return Uncertainty, *Journal of Financial Economics* **9**, 47-73.
- [52] HORST U., NAUJOKAT F. (2014): When to Cross the Spread? Trading in Two-Sided Limit Order Books, *SIAM Journal on Financial Mathematics* **5**(1), 278-315.

-
- [53] IKEDA N., WATANABE S. (1989): Stochastic Differential Equations and Diffusion Processes 2nd ed., *North-Holland Mathematical Library*.
- [54] KERCHEVAL A. N., MORENO J. F. (2011): Optimal intervention in the foreign exchange market when interventions affect market dynamics, arXiv:0909.1142.
- [55] KING M. R., OSLER C. L., RIME D. (2009): The market microstructure approach to foreign exchange: Looking back and looking forward, *Journal of International Money and Finance* **38**, 95-119.
- [56] KOZHAN R., MOORE M., PAYNE R. (2015): Market Order Flows, Limit Order Flows and Exchange Rate Dynamics, SSRN:2695705.
- [57] KRATZ P., SCHÖNEBORN T. (2013): Portfolio Liquidation in Dark Pools in Continuous Time, *Mathematical Finance* **25**(3), 496-544.
- [58] KRATZ P., SCHÖNEBORN T. (2016): Optimal Liquidation and Adverse Selection in Dark Pools, *Mathematical Finance*, DOI:10.1111/mafi.12126.
- [59] KYLE A. S. (1985): Continuous Auctions and Insider Trading, *Econometrica* **53**(6), 1315-1335.
- [60] LARUELLE S., LEHALLE C. A., PAGÉS G. (2011): Optimal Split of Orders Across Liquidity Pools: A Stochastic Algorithm Approach, *SIAM Journal on Financial Mathematics* **2**(1), 1042-1076.
- [61] LORENZ J. ALMGREN R. (2011): Mean-Variance Optimal Adaptive Execution, *Applied Mathematical Finance* **18**(5), 395-422.
- [62] LØKKA A. (2013): Optimal liquidation in a limit order book for a risk-averse investor, *Mathematical Finance* **24**(4), 696-727.
- [63] LY VATH V., MNIF M., PHAM H. (2007): A Model of Optimal Portfolio Selection under Liquidity Risk and Price Impact, *Finance and Stochastic* **4**, 579-603.
- [64] LYONS R. K. (1995): Tests of microstructural hypotheses in the foreign exchange market, *Journal of International Money and Finance* **39**, 321-351.

-
- [65] LYONS R. K. (1997): A simultaneous trade model of the foreign exchange hot potato, *Journal of International Economics* **42**, 275-298.
- [66] MENKHOFF L., SARNO L., SCHMELING M., SCHRIMPF A. (2016): Information Flows in Foreign Exchange Markets: Dissecting Customer Currency Trades, *The Journal of Finance* **71**(2), 601-634.
- [67] MOAZENI S., COLEMAN T. F., LI Y. (2013): Optimal execution under jump models for uncertain price impact, *Journal of Computational Finance* **16**(4), 35-78.
- [68] MUNDAKA G., ØKSENDAL B. (1998): Optimal stochastic intervention control with application to the exchange rate, *Journal of Mathematical Economics* **29**(2), 225-243.
- [69] OBIZHAEVA A., WANG J. (2013): Optimal Trading Strategy and Supply/Demand Dynamics, *Journal of Financial Markets* **16**(1), 1-32.
- [70] ØKSENDAL B., SULEM A. (2006): Applied Stochastic Control of Jump Diffusions. *Springer Berlin Heidelberg*.
- [71] PAYNE R. (2003): Informed trade in spot foreign exchange markets: an empirical investigation, *Journal of International Economics* **61**(2), 307-329.
- [72] PEMY M., ZHANG Q. (2006): Optimal stock liquidation in a regime switching model with finite time horizon, *Journal of Mathematical Analysis and Applications* **321**, 537-552.
- [73] PEMY M., ZHANG Q., YIN G.G. (2008): Liquidation of a Large Block of Stock with Regime Switching, *Mathematical Finance* **18**(4), 629-648.
- [74] PHAM H. (1998): Optimal Stopping of Controlled Jump Diffusion Processes: A Viscosity Solution Approach, *Journal of Mathematical Systems, Estimation and Control* **8**(1), 1-27.
- [75] PHAM H. (2009): Continuous-time Stochastic Control and Optimization with Financial Applications, *Springer*.

-
- [76] SCHMIDT A. B. (2016): Impact of Trading in the Multi-Dealer Spot Foreign Exchange, *The Journal of Trading* **11**(1), 68-75.
- [77] SEYDEL R. C. (2009): Existence and uniqueness of viscosity solutions for QVI associated with impulse control of jump-diffusions, *Stochastic Processes and their Applications* **119**(10), 3719-3748.
- [78] SHREVE S. E. (2005): Stochastic Calculus for Finance I: The Binomial Asset Pricing Model, *Springer*.
- [79] SHREVE S. E. (2013): Stochastic Calculus for Finance II: Continuous-Time Models, *Springer*.
- [80] SKELLAM J. G. (1946): The frequency distribution of the difference between two Poisson variates belonging to different populations, *Journal of the Royal Statistical Society, series A* **109**(3), 296.
- [81] SONER H. M. (1978): Jump Markov processes and viscosity solutions, *The Journal of Finance* **33**(4), 1133-1151.
- [82] STEELE J. M. (2010): Stochastic Calculus and Financial Applications, *Springer*.
- [83] STOLL H. R. (1986): The supply of dealer services in securities markets, *The Journal of Finance* **33**(4), 1133-1151.
- [84] VERAART L. A. M. (2010): Optimal Market Making in the Foreign Exchange Market, *Applied Mathematical Finance* **17**(4), 359-337.
- [85] VERAART L. A. M. (2011): Optimal investment in the foreign exchange market with proportional transaction costs, *Quantitative Finance* **11**(4), 631-640.
- [86] YE M. (2011): A Glimpse into the Dark: Price Formation, Transaction Cost and Market Share of the Crossing Network, SSRN:1521494.
- [87] ZHU H. (2013): Do Dark Pools Harm Price Discovery?, *Review of Financial Studies* **27**(3), 747-789.